



Final Report

Comparative Analyses of High-Altitude Lakes and Catchments in the Sierra Nevada: Susceptibility to Acidification

Principal Investigators

John M. Melack, James O. Sickman and Al Leydecker

Contributing Scientist

David Marrett

**Marine Science Institute and Institute for Computational Earth System
Science, University of California Santa Barbara, California 93106**

January 23, 1998

**Prepared for the California Air Resources Board
Contract A032-188**



Abstract

The atmospheric deposition and surface-water chemistry of 8 seasonally snow-covered catchments in the Sierra Nevada was measured from 1983 through 1994 to assess watershed susceptibility to acidic atmospheric deposition. Catchments and years included the following: Emerald Lake, 1983-1994; Pear Lake, 1986-1993; Topaz Lake, 1986-1993; Ruby Lake, 1986-1994; Crystal Lake, 1986-1993; Spuller Lake, 1989-1994; Topaz Lake, 1986-1993 and the Marble Fork of the Kaweah River, 1992-1994. The catchments are located in the alpine and subalpine zones of the Sierra Nevada of California, and their geographic locations span a majority of the north-south extent of the range. Four of the watersheds are located along the eastern slope of the range (Ruby Lake, Crystal Lake, Spuller Lake, Lost Lake), and the remainder are situated along the western slope (Emerald Lake, Pear Lake, Topaz Lake and the Marble Fork of Kaweah River). Seven of the catchments are glacial cirques, ranging in size from 25 to 441 ha, that contain lakes. The upper Marble Fork drains the Tokopah Valley of Sequoia National Park, a glacially carved basin of 1,900 ha which includes, within its boundaries, the watersheds for Emerald, Pear, and Topaz lakes along with several other small lakes and ponds.

Atmospheric deposition of water and solutes was determined by collections of non-winter precipitation (April through October) and by sampling the snowpack in the spring. Lakes and outflow streams in these catchments were sampled for chemistry year-round. Outflow samples were collected on a biweekly to daily basis during snowmelt runoff and lakes were sampled ca. 6 times per year. Outflow discharge was gauged continuously. All major solutes in atmospheric deposition and runoff (pH, ammonium, calcium, magnesium, sodium, potassium, chloride, nitrate, sulfate and acid neutralizing capacity (ANC)) were measured. A rigorous quality assurance - quality control protocol was followed. Meteorological conditions were monitored in two of the catchments (Emerald and Spuller).

The quantity and timing of snowmelt affected annual and interannual variability of surface-water chemistry in seasonally snow-covered catchments in the Sierra Nevada. General patterns of surface-water chemistry were identified using statistical analysis, however; there was considerable variation in these patterns among the watersheds. In most cases, pH decreased as runoff increased, reaching a minimum near the peak of snowmelt runoff. Several other pH patterns were observed: (1) pH increased as discharge increased, (2) pH reached a maximum at peak runoff, (3) pH changes were unrelated to changes in discharge and (4) pH remained fairly constant despite large changes in discharge.

Temporal changes for most other solutes demonstrated one of three different patterns: dilution, pulse/dilution or pulse/depletion. Acid anions such as nitrate and sulfate often increased in concentration in early snowmelt, with nitrate becoming depleted (i.e., analytically undetectable) and sulfate declining at peak runoff. In most catchments, nitrate peaks of between 5 and 15 $\mu\text{Eq L}^{-1}$ were common; in nitrogen limited lakes, e.g., Crystal and Lost, nitrate peaks during snowmelt were usually less than 2 $\mu\text{Eq L}^{-1}$. However, nitrate concentrations in the Topaz Lake catchment, were often highest in the winter, prior to snowmelt, and declined as runoff increased in the spring. Sulfate patterns were qualitatively similar to nitrate, but the magnitude of the changes were smaller. Differences

in sulfate maxima and minima were less than 1 to 2 $\mu\text{Eq L}^{-1}$ in most cases. In catchments with considerable groundwater and sulfur bearing bedrock, i.e., Spuller and Ruby lakes, sulfate declined by 10 to 20 $\mu\text{Eq L}^{-1}$ over the course of snowmelt.

Base cations and ANC most commonly exhibited a dilution pattern: concentrations declined as snowmelt runoff increased, with minima occurring near peak runoff. Depressions of ANC usually began in the early stages of melt. Outflow ANC, declined by 25% - 80% over the course of the spring; the average decline was about 50%. ANC minimums ranged from ca. 15 to 30 $\mu\text{Eq L}^{-1}$; Lost and Pear lakes had the lowest minima while ANC minima at Ruby and Crystal lakes were highest. In all catchments, ANC depression was greatest during years with deep snowpacks and high snowmelt runoff.

No long-term trends in pH or ANC were identified in surface waters of the Sierra Nevada during the period of 1983 through 1994. Trends were detected in other solutes which suggest that Sierran ecosystems are potentially sensitive to increased nutrient loading and climatic perturbations. Drought conditions in the Sierra Nevada probably were responsible for increasing the proportion of runoff derived from shallow groundwater in the Ruby Lake basin as evidenced by an increase in sulfate concentrations from ca. 6 to 12 $\mu\text{Eq L}^{-1}$ during the period of 1987 through 1994. Drought may also be partially responsible for increased retention of N in the Emerald Lake catchment. Long-term monitoring has revealed a 25 to 50% reduction in annual nitrate maxima and minima at Emerald Lake, with a concomitant shift of the lake's phytoplankton community from phosphorus limitation towards nitrogen limitation. These findings support recent evidence that N uptake in alpine catchments may increase due to climate warming and runs counter to the recent shift of Lake Tahoe to P limitation of phytoplankton. At Emerald Lake, decreases in nitrate represent a shift from Stage 2 to Stage 1 of nitrogen saturation and is a counter example to lakes and streams in the Front Range of the Rocky Mountains. Based on nitrate peaks during snowmelt and nitrate levels in snow, most of the catchments in our study are experiencing Stage 1 symptoms of N-saturation.

Dilution was the primary factor in ANC depression in surface waters during our study. The lakes could be divided into two classes based on their response to snowmelt: shallow, short residence-time (i.e., rapidly flushed) lakes where acidification accounted for <10% of the ANC decrease (Lost, Topaz, and Spuller); and lakes where acidification caused 25 to 35% of the depression due to larger lake volumes or lower snowmelt rates (Emerald, Pear, Ruby and Crystal). In lakes where acidification was important, nitrate and sulfate contributed equally during the first half of snowmelt, while sulfate dominated in the latter half.

The relationship between minimum and fall-overtake ANC for the lakes in this study was linear ($r^2 = 0.84$), and the equation remained unchanged as additional data from earlier synoptic surveys were added. This linear model, applied to Western Lakes Survey data for the Sierra Nevada, estimated that no lakes are currently acidified by snowmelt. However, the model's confidence limits allow for the possibility that up to 1.8% (~38) of Sierra Nevada lakes undergo snowmelt ANC depressions slightly below 0 $\mu\text{Eq L}^{-1}$.

The hydrology of high elevation catchments in the Sierra Nevada is dominated by the accumulation and melting of the winter snowpack. The majority of catchment outflow occurs during the annual snowmelt period which begins as early as late March following dry winters in the western Sierra, but may not start until early May in the eastern Sierra

Nevada when snowpacks are deep. Peak runoff occurred in early to mid June when winter snowfall was light and during late June and early July in wet years (e.g., 1993). At some catchments, peak outflow discharge following a wet winter was much greater than in dry years (e.g., Lost and Topaz lakes) while in others the range of peak flows was relatively small (e.g., Ruby and Crystal lakes).

Snowmelt from seasonally snow-covered catchments in the Sierra Nevada was often punctuated by periods of low discharge caused by spring snowstorms that cooled air temperatures and lowered the rate of snowmelt for several days at a stretch. Following peak discharge, runoff receded gradually during the summer and autumn. However, groundwater storage and release in the Ruby Lake basin are partly responsible for maintaining year-round outflow. In most catchments, outflow streams went dry by September when snow-cover was gone indicating that little water is stored in most Sierran watersheds. With the exception of the Crystal Lake basin, the catchments in the study lost little water via subsurface flow and were hydrologically tight. Winter runoff at all catchments was very low. At basins without groundwater inputs, winter streamflow was primarily the result of displacement of lake water by snowfall and, to a lesser extent, from winter snowmelt from south-facing slopes.

Only a small percentage of the settled snowpack is lost to evaporation in the Sierra Nevada. The typical evaporative loss from snow varies from 80 to 100 mm of water, approximately 6% of the average maximum accumulation. In drought years the loss is less, but represents a greater percentage of the maximum accumulation, 9 to 13%. During peak snow years the loss decreases to about 4%, although the extended length of the snow season somewhat increases the actual amount lost. Most of the loss occurs during the period of snow accumulation when vapor pressure differences are usually favorable for evaporation and conditions of atmospheric instability are often found. Even so, low vapor pressure differences between the air and the snow surface, the result of cold temperatures and the prior transit of the over-passing air over extensive snow-covered distances (which increase humidity and decrease the capacity to absorb additional moisture), limit total evaporation to relatively small quantities.

During snowmelt, stable atmospheric conditions and reduced vapor pressure differences, due to the higher vapor content of the warming spring air, reduce evaporation from snow to negligible amounts. Often near the end of this period, snowpack evaporation losses are exceeded by gains from condensation. Total evaporation from the snowpack during snowmelt is typically around 15 mm of water: 2 to 3% of the maximum accumulation during drought years, less than 1% for above normal snow years.

Snow chemistry was dilute and similar among the eight study catchments. Samples from the spring snowpack had pH levels typically between 5.3 and 5.6, with an overall mean value of 5.42. After hydrogen-ion, the most abundant ions in solution were compounds of nitrogen, ammonium and nitrate, with mean concentrations of 2.7 and 2.4 $\mu\text{Eq L}^{-1}$, respectively. Sulfate concentrations in winter snow were slightly lower: 1.0 to 3.0 $\mu\text{Eq L}^{-1}$ (overall mean, 2.0 $\mu\text{Eq L}^{-1}$). Of the remaining solutes, only calcium and sodium were found in levels much above the detection limit (mean values: 1.7 and 1.3 $\mu\text{Eq L}^{-1}$, respectively). Organic anions (acetate and formate) were difficult to measure in snow and were usually found at low concentrations (mean concentrations ca. 0.5 $\mu\text{Eq L}^{-1}$). The solutes that showed the most variability among years and among sites were potassium and

the organic anions. The most consistent solutes in snow during the study were hydrogen-ion and sulfate. Mean annual snowfall during the study was 1027 mm of water equivalence.

Non-winter precipitation (i.e., rain and snow from ca. April through November) varied considerably with respect to chemistry and quantity. Solute concentrations ranged from near detection limits to tens of microequivalents per liter. Most of the variability was due to the timing of the precipitation: spring and autumn storms were the most dilute and summer rains were relatively enriched with solutes. Thus, the annual volume-weighted mean concentration of non-winter precipitation depended on the mix of samples obtained. The mean pH of non-winter precipitation in the study was 4.93. Ammonium and nitrate concentrations were 8 to 9 times greater in non-winter precipitation than in winter snowfall (mean values, 23.4 and 20.7 $\mu\text{Eq L}^{-1}$, respectively). Ammonium levels were usually higher than nitrate, with both nitrogen ions exceeding the mean concentration of sulfate (15.1 $\mu\text{Eq L}^{-1}$). The mean chloride level measured in non-winter precipitation was 4.2 $\mu\text{Eq L}^{-1}$ which was only slightly higher than the mean concentration in winter snowfall. After ammonium and hydrogen-ion the next most abundant cations in non-winter precipitation were calcium (mean, 10.4 $\mu\text{Eq L}^{-1}$) and sodium (4.6 $\mu\text{Eq L}^{-1}$). In contrast to winter snow, organic anions were abundant in non-winter precipitation. Mean values for acetate and formate were on the order of 7 to 9 $\mu\text{Eq L}^{-1}$. The average annual input of water during non-winter periods of our study was 117 mm.

Precipitation intercepted by Sierran catchments is greatly altered by geochemical processes before exiting the catchments as streamflow. High rates of nitrogen deposition were measured in the study catchments (mean annual nitrogen deposition was 95.6 Eq ha^{-1}). Biological processes and other sinks within the watersheds consumed the large majority of these nutrient inputs. Ammonium was rarely found at detectable levels in outflow streams in our study. Nitrate concentrations were typically higher, but in most cases the input-output budgets showed a net retention of nitrate in the catchments. During most years, the majority of nitrogen deposition occurred during non-winter periods.

Hydrogen-ion deposition was also substantial in these catchments and winter snowfall was the main contributor. These inputs were effectively neutralized by the catchments and, on average, the basins consumed 87% of the hydrogen-ions deposited in them. Catchments in the eastern Sierra Nevada had significantly ($p < 0.05$) higher outflow ANC and neutralized a higher percentage of acid inputs than did basins in the Tokopah Valley or the Lost Lake watershed. These findings suggest that watersheds along the eastern slope of the Sierra Nevada may be less susceptible to harm from acid deposition than catchments along the western slope. Processes, principally mineral weathering and biological uptake of nitrogen, changed the chemical make-up of precipitation so that streamwaters exiting the catchments were a solution composed primarily of ANC (i.e., HCO_3^- or bicarbonate), calcium and dissolved silica.

Acknowledgments

Many dedicated and hard working individuals contributed their efforts to this project over the years. Without these people the research would never have been conducted. We would like to thank the following people for their efforts in the field:

Louis Andalero	Steve Hamilton	David Paradysz
Todd Anderson	Helen Hardenbergh	Rick Puskar
Darcy Aston	Darla Heil	Karl Roland
Leon Barmuta	Nina Hemphill	Sage Root
Sue Birac	Judith Hildinger	Scott Roripah
Jim Black	Robert Holmes	Mark Rowney
Aaron Brown	Pam Hopkins	Paul Schwarz
L. Compton	Anne Howatt	Frank Setaro
Scott Cooper	Rick Kattelmann	Rebecca Shaw
Dave Clow	Pete Kirchner	Suzanne Sippel
Gayle Dana	Roland Knapp	Richard Skeen
Dan Dawson	Kim Kratz	Kevin Skeen
John Dittlee	David Kushner	Bill Smith
Dennis Divins	Kevin Leary	Chad Soiseth
Jeff Dozier	Delores Lucero	Glenn Spindel
Robert Durand	Danny Marks	John Stoddard
Chris Dwyer	Annie McMillan	Monica Stormo
Lee Dyer	Lisa Meeker	Tom Suk
Kelly Elder	Hanna Merrill	Kathy Tonnessen
Valerie Ellis	Mignon Moskowitz	Mary Theime
Mike Embury	Linda Much	Sheila Weisman
Rand Erway	Warren Myers	Jane Weisenberger
Doug Erwin	Avis Newell	Michael Williams
Anne Esperanza	Sherry Nolen	Mark Williams
Nancy Fiddler	Randall Osterhuber	Amy Workinger
Patti Hagerty	Vilis Ozolins	Mike Zika
Jim Thorne	Tom Meixner	Nobu Ote

From the list above we would like to single out Pete Kirchner, Kevin Skeen, Sage Root, Glen Spindel and Vilis Ozolins for their efforts over a number of years.

Laboratory analyses were a major part of this research. During the course of the project, tens of thousands of samples were processed in the UCSB analytical laboratories and at field labs in Sequoia National Park and at the Sierra Nevada Aquatic Research Laboratory. Our thanks go to Frank Setaro for his dedication in performing chemical analyses and managing the QA/QC program over many years. Others who performed chemical analyses for this project include: Dan Dawson, Steve Hamilton, Helen Hardenbergh, Mignon Moskowitz, Marilyn Morrison, John Stoddard, Mark Williams and Michael Williams.

We would like to thank Delores Lucero for her many years of effort in this project. Delores performed countless chemical analyses, entered and organized vast amounts of data on the computer, assisted with field work and basically helped the project run smoothly and efficiently.

Dan Dawson, in addition to helping in the field, organized much of the operations in the eastern Sierra Nevada. Dan was also instrumental in attaining permission to work in the Inyo National Forest.

The cooperation of the National Park Service is greatly appreciated. We thank David Parsons, Anne Esperanza, David Graber, Tom Stohlgren, Harold Werner and Jack Vance for providing support to our project. We would also like to thank the following Lodgepole Rangers for their assistance: Richard Perelli, Gloria Silva, Lo Lyness, Tim Simonds, and Frieda Sherburne.

Many of the research sites in this report are in areas under the jurisdiction of the U.S. Forest Service. We would like to thank, Andrea Holland, Tom Heller, Bill Bramlette, Neil Berg, Gordon Peregun and Keith Waterfall for their cooperation and assistance.

We would like to thank David Groeneveld for aerial photographs of the watersheds, Mark Whiting for the bathymetric map of Ruby Lake and Mike Zika for the original design of the automated gauging stations. Bob Petty provided many analytical services during the course of the project. We would like to thank John Stoddard for invaluable assistance in many facets of this project. We are grateful to Mike Colee for digitizing the soils and vegetation field maps and for preparing the final maps in the report.

We would like to thank John Holmes, Steve Brown and Mary Bergen of the California Air Resources Board for their guidance and support over the years. Special thanks go to Kathy Tonnessen for her unflagging enthusiasm and energy without which this research would never have started.

We would like to acknowledge the many graduate students, who worked on this project, for their intellectual contributions. These students include: Kim Kratz, Mark Williams, Rick Kattelmann, Pam Hopkins, Helen Hardenbergh, Michael Williams, Mary Thieme, Lisa Meeker, Leon Barmuta, Steve Hamilton, Chad Soiseth, Diana Engle and Clifford Ochs. Several professors at UCSB and other universities who assisted and advised us include: Jeff Dozier, Robert Holmes, Lance Lesack, Thomas Fisher, John Harte and Scott Cooper.

This report is submitted in fulfillment of ARB Contract A032-188 (Comparative Analyses of High-Altitude Lakes and Catchments in the Sierra Nevada) by the Marine Science Institute and Institute for Computational Earth System Science of the University of California, Santa Barbara under the sponsorship of the California Air Resources Board. Additional support was provided by the National Aeronautics and Space Administration's EOS program.

Disclaimer

The statements and conclusions in this report are those of the contractor and not necessarily those of the California Air Resources Board. The mention of commercial products, their sources or their use in connection with the material reported herein is not to be construed as either an actual or implied endorsement of such products.

TABLE OF CONTENTS

ABSTRACT.....	i
ACKNOWLEDGMENTS.....	v
TABLE OF CONTENTS.....	vii
SUMMARY AND CONCLUSIONS.....	ix
RECOMMENDATIONS.....	16

CHAPTER ONE:

ANNUAL AND LONG-TERM VARIABILITY OF SURFACE WATER CHEMISTRY IN THE SIERRA NEVADA

1.1. INTRODUCTION.....	1-10
1.2. WATERSHED DESCRIPTIONS.....	1-12
1.3. METHODS.....	1-19
1.4. RESULTS AND DISCUSSION.....	1-28
1.5. CONCLUSIONS.....	1-48
1.6. REFERENCES.....	1-50

CHAPTER TWO:

ANNUAL WATER BALANCES OF EIGHT HIGH ELEVATION CATCHMENTS IN THE SIERRA NEVADA

2.1. INTRODUCTION.....	2-6
2.2. METHODS.....	2-7
2.3. RESULTS AND DISCUSSION.....	2-23
2.4. CONCLUSIONS.....	2-35
2.5. REFERENCES.....	2-37

CHAPTER THREE:

SOLUTE BALANCES FOR EIGHT HIGH ELEVATION CATCHMENTS IN THE SIERRA NEVADA

3.1. INTRODUCTION.....	3-7
3.2. METHODS.....	3-8
3.3. RESULTS AND DISCUSSION.....	3-13
3.4. CONCLUSIONS.....	3-44
3.5. REFERENCES.....	3-47

CHAPTER FOUR:

EVAPORATION IN SEASONALLY SNOW-COVERED CATCHMENTS OF THE SIERRA NEVADA

4.1. AN INTRODUCTION TO EVAPORATION FROM SNOW.....	4-5
4.2. THE CRAE MODEL.....	4-10
4.3. THE MEAN PROFILE MODEL.....	4-25
4.4. CONCLUSIONS.....	4-35
4.5. REFERENCES.....	4-39

APPENDIX ONE:

SOIL SURVEY OF SEASONALLY SNOW-COVERED CATCHMENTS OF THE
SIERRA NEVADA

A.1. INTRODUCTION	A-3
A.2. BACKGROUND AND METHODS.....	A-3
A.3. RESULTS	A-6
A.4. DISCUSSION	A-52
A.5. SUMMARY	A-53
A.6. REFERENCES.....	A-55

Summary and Conclusions

1. Background

Lakes and streams in the higher elevations of the Sierra Nevada mountains are some of the most dilute, weakly buffered waters in the United States. The catchments that supply runoff to these waters are underlain, predominantly, by granitic rocks, have poorly developed, thin soils and sparse vegetation. The hydrologic cycle of these watersheds is dominated by the annual accumulation and melting of a dilute, mildly acidic (pH ca. 5.5) snowpack (Melack et al. 1995). These conditions indicate that aquatic ecosystems in the Sierra Nevada may be adversely affected by anthropogenic acid deposition.

In this report we present results from regional studies of Sierra Nevada watersheds. The period of record runs from water year 1990 (October 1989 through September 1990) through water year 1994. The major objectives are:

1. Measure the major inputs and losses of water and solutes to high-elevation catchments of the Sierra Nevada.
2. Quantify the link between acid deposition and chemical changes in surface water chemistry.
3. Determine if there are trends and patterns in surface water chemistry and wet deposition (rain and snow) in the watersheds.
4. Provide data to be used in hydrologic and hydrochemical models of Sierran watersheds. These data include measurements of climatic conditions, evaporation, surface water chemistry, discharge and surveys of snow, soils and vegetation.

Answering these objectives allowed us to assess the year-round and long-term susceptibility of a variety of Sierran Lakes to acidic atmospheric-deposition. Overall, the investigations in this report were designed to provide information on the current status of high-altitude catchments in the Sierra Nevada which will be used by the California Air Resources Board in evaluating the need for acid deposition standards in the Sierra Nevada region.

1.1. Study Sites

The eight study sites in this report are located in the alpine and subalpine zones of the Sierra Nevada of California. Their geographic locations span a majority of the north-south extent of the Sierran range. Four of the watersheds are located along the eastern slope of the range (Ruby Lake, Crystal Lake, Spuller Lake, Lost Lake) and the remainder are situated along the western slope (Emerald Lake, Pear Lake, Topaz Lake and Marble Fork of Kaweah River). Seven of the catchments are glacial cirques, ranging in size from 25 to 441 ha, that contain lakes. The upper Marble Fork drains the Tokopah Valley of Sequoia National Park, a glacially carved basin of 1,900 ha which includes, within its boundaries, the watersheds for Emerald, Pear, and Topaz lakes along with several other small lakes and ponds.

2. General Approach

The atmospheric deposition and surface-water chemistry of 8 seasonally snow-covered catchments in the Sierra Nevada was measured from 1983 through 1994. Catchments and years included the following: Emerald Lake, 1983-1994; Pear Lake, 1986-1993; Topaz Lake, 1986-1993; Ruby Lake, 1986-1994; Crystal Lake, 1986-1993; Spuller Lake, 1989-1994; Topaz Lake, 1986-1993 and the Marble Fork of the Kaweah River, 1992-1994.

Lakes and surface waters in these catchments were sampled for chemistry year-round. Outflow samples were collected on a biweekly to daily basis during snowmelt runoff and lakes were sampled ca. 6 times per year. From 1983 through 1987, Emerald Lake was sampled biweekly during the ice-free seasons and monthly during the winter. Samples for chemical analyses were collected from three or four depths in the lakes. Inflows were sampled during snowmelt when they were free of snow. Prior to water year 1993, samples were collected by hand (grab sample) in polyethylene bottles. Beginning in water year 1993, automated samplers (ISCO) were used to collect outflow samples at some catchments.

Precipitation quantity and chemistry were measured year-round. Samples of the snowpack were obtained by digging pits to the ground and collecting duplicate, contiguous, vertical sections every 40 cm using a PVC tube (5 cm diameter, 50 cm long, with a sharp, beveled cutting edge). Along with snow chemistry, snow depth, snow density and snow-covered area were determined throughout each basin. Snow density was determined in vertical 10 cm intervals in each sampling pit using a wedge shaped, stainless-steel cutter. Snow depth was determined along transects (using graduated probes) from the lakes' edge to the boundaries of the watersheds; approximately 200-300 depth measurements were made at each basin. Snow-covered area was estimated from aerial photographs taken near the time of the survey (± 10 days). The timing of the snowpack sampling coincided with the period of maximum snow accumulation which usually occurred during late March or early April and yielded an accurate measure of winter precipitation and solute loading.

During the snow-free seasons, precipitation quantity was measured at each lake using a tipping-bucket rain-gauge connected to a solid-state data logger. Precipitation samples were collected in polyethylene buckets installed in an Aerochemetrics rain collector during the months of ca. June through October. Snowboards and shallow snowpits were used to measure snow that fell after the maximum accumulation surveys. For some watersheds during some years, precipitation quantities were estimated from records collected at nearby catchments or weather stations.

At each lake an automatic gauging station was established, consisting of an datalogger powered by a durable, weather-proof battery pack or solar panel. Stream stage was continuously monitored using pressure transducers, installed in the stream bed and recorded on the loggers. A thorough calibration of the transducers was done using various estimates of discharge. Weirs were installed in the outlet channels of Emerald and Spuller lakes.

Water balances were calculated for all basins. The inputs to the watersheds were rain and snow; the losses were lake outflow and evaporation. The evaporation term included sublimation of snow, lake evaporation and evapotranspiration.

Water balance
 $R_{in} + SNOW = outflow + evap.$

Solute balances were calculated for each watershed and consisted of two components: loading of solutes by wet, atmospheric deposition and outflow solute losses. Loading was divided into two types: snow and non-winter precipitation which were calculated separately. Solute loading by snow was calculated from the volume-weighted mean concentration of each solute multiplied by the total volume of snow at maximum accumulation divided by catchment area. The solute flux for non-winter precipitation was calculated by multiplying the volume-weighted mean concentration for this precipitation by its total volume and dividing by catchment area. Solute flux in the outflow of each lake was calculated from periodic outflow chemistry and daily outflow discharge normalized to catchment area so that fluxes could be compared among the watersheds. Using solute balances, the yield of solutes from the watersheds were computed as the difference between solute inputs and losses. Yield is expressed as equivalents per hectare per year. A positive yield indicated that the loss of the ion from the watershed was greater than the supply; a negative yield indicated that the loss of the ion was less than the supply.

To improve the accuracy of the water and mass balance calculations for the catchments, water lost through evapotranspiration was accounted for. To estimate these losses, meteorological stations were installed and operated at some of the catchments. For other sites, data from pre-existing weather stations ^{was} used.

Soils were mapped in all lake basins with the exception of Emerald Lake which had previously been mapped. The only portions of the Marble Fork watershed mapped were the Pear Lake, Topaz Lake and Emerald Lake watersheds which together make up about 23% of the Marble Fork drainage. In contrast to more traditional classification schemes, an alternative approach was used to map the soils. This approach was specifically designed to aid biogeochemical and hydrological investigations. Hand drawn maps produced from the soil inventories described above were converted to digital form using Arc/Info, a Geographic Information System (GIS). Aerial photographs were used to produce vegetation maps and GIS coverages.

3. Major Findings

3.1. Patterns of pH During Snowmelt

In contrast to other solutes, it was difficult to describe a consistent pattern of pH variation among the catchments or among water years. The most common pattern was one of declining pH as discharge increased, with lowest pH's occurring sometime near the peak of runoff. This pattern was often punctuated with transient pH increases or decreases that appear unrelated to discharge. Several other patterns of outflow pH were observed: (1) pH increased as discharge increased (e.g., Pear and Topaz lakes, 1991), (2) pH reaches maximum at the peak of snowmelt runoff, (3) pH exhibits a pattern seemingly independent of discharge, (4) pH remains fairly constant despite large changes in runoff (e.g., Ruby Lake, 1990). Based on the Friedman ANOVA, there was no statistically significant difference in pH during the first 75% of snowmelt runoff, but during the last 25% of runoff, pH increased significantly.

3.2. Patterns of ANC During Snowmelt.

The dominant pattern of ANC during snowmelt runoff is ANC decline as discharge increases with minimum ANC occurring at or near peak runoff. Near the end of snowmelt, ANC recovered but did not usually match pre-melt levels. This generalized pattern is supported by the statistical analysis which shows significantly lower ANC during stages peak runoff; ANC in during the first 25% of snowmelt runoff was significantly higher ($p < 0.1$) than in the last 25% of runoff. A pattern of increasing ANC with increasing runoff was also observed in few a cases, but these examples were most likely the result of infrequent sampling and poor resolution of the ANC time-series.

Depression of ANC caused by runoff often began in the early stages of snowmelt. Outflow ANC declined by 25% to 80% as a result of snowmelt; the most frequently observed change was a decline of about 50% from premelt conditions. Minimum outflow ANCs observed during the study were typically in the range of 15 to 30 $\mu\text{Eq L}^{-1}$. The lowest values were usually observed in the Lost Lake and Pear Lake watersheds (i.e., 10 to 15 $\mu\text{Eq L}^{-1}$) and highest values were measured at Crystal Lake (i.e., 50 to 65 $\mu\text{Eq L}^{-1}$). The greatest absolute ANC change was observed in the Spuller and Ruby lake watersheds (declines of 70 to 90 $\mu\text{Eq L}^{-1}$ and 40 to 60 $\mu\text{Eq L}^{-1}$, respectively). At Crystal Lake, snowmelt induced changes were on the order of 20 $\mu\text{Eq L}^{-1}$ or a depression of about 25% from premelt conditions. At all catchments ANC depression tended to be greater during years with high runoff compared to drought years. The annual pattern of ANC in high-elevation catchments of the Sierra Nevada indicates that dilution of streamwaters with snowmelt is a major cause of ANC depression during the runoff season.

3.3. Patterns of Nitrate During Snowmelt.

Nitrate had several patterns during snowmelt runoff. In some catchments nitrate concentrations declined throughout the snowmelt period. Results from the Friedman ANOVA on ranks support this pattern for the data set as a whole. A second pattern where a nitrate pulse occurred during Stage 2 of snowmelt (i.e., 25-50% of cumulative runoff) was seen during some years at nearly all catchments (Topaz Lake was the exception). The ANOVA on ranks for Emerald and Ruby lakes showed significantly higher nitrate concentrations during stage two than in Stages one (0-25% of cumulative runoff) or three (50-75% of cumulative runoff). Mechanistically, the pattern appears to be the result of a pulse of nitrate during the early stages of melt followed by depletion of nitrate caused by biological uptake in later stages, which we called the Pulse/Depletion pattern.

At Topaz Lake during water years 1988, 1991 and 1993, unusually high nitrate concentrations were measured during the winter and in the spring prior to snowmelt. Levels were on the order of 40 to 175 $\mu\text{Eq L}^{-1}$, much higher than peak nitrate values of less than 20 $\mu\text{Eq L}^{-1}$ observed at other catchments. High nitrate concentrations at Topaz Lake were not associated with nitrate-rich precipitation events. These data suggest that biological processes exert a large degree of control on the accumulation and release of nitrate in the Topaz Lake catchment.

Peak nitrate concentrations in catchment outflow during snowmelt varied by as much as ten-fold among the study catchments. Significantly lower ($p < 0.01$) concentrations were observed at Lost and Crystal lakes where peak values ranged from

about 0.5 to 2.0 $\mu\text{Eq L}^{-1}$, despite inflowing waters commonly having nitrate levels greater than 5 $\mu\text{Eq L}^{-1}$. The Emerald Lake and Marble Fork drainages had nitrate maximums of between 6 and 8 $\mu\text{Eq L}^{-1}$ during most years. At Pear and Ruby lakes peak nitrate levels ranged from 7 to 12 $\mu\text{Eq L}^{-1}$ during snowmelt. Highest snowmelt nitrate levels were observed in the outflow from Spuller Lake. Peak concentrations were consistent from year to year, i.e., $13 \pm 3 \mu\text{Eq L}^{-1}$.

3.4. Patterns of Sulfate During Snowmelt.

Patterns in sulfate concentration were qualitatively similar to nitrate patterns but the magnitude of the changes were smaller. Sulfate, on some occasions, exhibited a Pulse/Dilution pattern similar to nitrate, however, changes in sulfate concentration during the course of snowmelt were smaller. In other cases dilution throughout snowmelt was the observed pattern and this was the overall pattern identified from the statistical analysis. However, the magnitude of sulfate decline varied considerably among the watersheds and reductions of less than 1 to 2 $\mu\text{Eq L}^{-1}$ were observed in many cases. In these situations, sulfate declined by less than 30% from concentrations prior to snowmelt. Sulfate dilution was less, in both absolute and relative terms, than dilution of ANC, base cation or silicate in most cases. These findings suggest there is some biogeochemical process(es) in the catchments regulating sulfate concentrations.

3.5. Patterns of Base Cations and Silicate During Snowmelt.

The dominant pattern of base cations (i.e., sum of calcium, magnesium, sodium and potassium) and dissolved silica in outflow was dilution caused by snowmelt. All of these solutes declined substantially during snowmelt, reaching minima at or near the time of peak runoff; a pattern confirmed by results from the statistical analysis of snowmelt chemistry. Base cations were significantly lower ($p < 0.05$) during stage three (highest daily discharge) than stages one and two; SBC in stage four was significantly higher ($p < 0.1$) than in stage 3 but less than in stage one, indicating an incomplete recovery of base cation at the end of snowmelt. Silicate showed a similar pattern but there was no statistical difference between stages two and three.

3.6. Long-term Trends in pH and ANC

No trend in pH or ANC was found at Emerald Lake or its outflow during the period of 1983 through 1994. Annual maximum and minimum values of pH and ANC were variable over this period but do not trend either up or down. Because of lower sampling frequency in water years 1988 through 1994, solute chemistry in Emerald Lake exhibits less variability than in earlier years (1983-1987). Annual minimum and maximum values in Emerald Lake are less extreme than in the outflow owing to lower sampling frequency for the lake.

In the other catchments there was no identifiable trend in ANC or pH in the outflows from 1987 through 1994 nor any trend in VWM lake chemistry. In general, the annual ANC minimum at each lake was higher than that found in the outflow (the major exception is Topaz Lake where the minima are nearly identical). Examination of the autumn-survey data shows there is considerable inter-annual variability in ANC at most lakes with differences of 25 to 100% common. Fall overturn pH was also variable with

differences of ± 0.5 pH typical. This variability casts some doubt on the utility of autumn lake-surveys as a tool for detecting long-term trends in chemistry and suggests many decades of data will be required. No long-term trends in pH or ANC are identifiable for the period of 1981 to 1995 for any of these lakes, or for autumn samples of Emerald Lake which are included for purposes of comparison. Based on these observations, we conclude that surface waters in high-elevation regions of the Sierra Nevada have not undergone measurable acidification since 1981. In addition, based on a pH history estimated from diatom assemblages in Emerald Lake sediment, there has been no increase in acidity or decrease of ANC in Emerald Lake from 1825 to 1982 (Melack et al. 1989, Holmes et al. 1989). Thus, we conclude that the acid-neutralizing ability of the Emerald Lake watershed has not measurably changed during the last 180 years.

3.7. Long-term Trends in Other Solutes

From the time-series plots of lake and outflow chemistry only two catchments had long-term trends in surface water chemistry. At Ruby Lake, there was an increase in sulfate and base cations (lake only) in surface waters of the catchment from 1987 to 1994. There was also a lowering of annual maxima and minima of nitrate in the Emerald Lake basin during the period of 1983 through 1994.

From October 1987 through April 1994, sulfate concentrations increased from about $6 \mu\text{Eq L}^{-1}$ to ca. $12 \mu\text{Eq L}^{-1}$ in Ruby Lake and its outflow. The upward trend in sulfate ended early in 1994 when levels began to decline. Subsequent samples of the Ruby Lake outflow from 1995 and 1996 showed a continued decline in sulfate concentration (data not presented in this report). Low precipitation associated with the 1987-1992 drought caused the increase in sulfate concentration in surface waters of the Ruby Lake basin. That changes in sulfate were not measured until the following water year suggests a time-lag in the hydrologic system of the basin. The mechanism through which precipitation quantity affects sulfate chemistry in the Ruby Lake basin is unknown but is unique among the study sites as evidenced by the absence of sulfate trends elsewhere. Several, morphological characteristics set the Ruby Lake basin apart from the other study sites including its large size and high-elevation, substantial storage and release of groundwater within the basin (see Chapter Two) and the presence of rock glaciers. In addition, much of the Ruby Lake basin is underlain by granites that are high in sulfide minerals (e.g., FeS_2).

The other observable trend in surface water chemistry during the last 12 years was the decline of nitrate in the Emerald Lake watershed. From 1983 through 1987, peak concentrations in the lake and outflow were above $10 \mu\text{Eq L}^{-1}$ in nearly all years. Peak concentrations during water years 1990 through 1994 were less than $5 \mu\text{Eq L}^{-1}$ in the lake and $8\text{-}9 \mu\text{Eq L}^{-1}$ in the outflow. Prior to 1986, nitrate levels never fell below $1 \mu\text{Eq L}^{-1}$ in the outflow or less than $0.5 \mu\text{Eq L}^{-1}$ in the lake; during later years nitrate regularly declined to below the detection limit in both the lake and outflow stream. The decrease in the magnitude of nitrate maxima and minima at Emerald Lake was not an artifact of sampling procedures and analysis. Increased biological demand for nitrate is a possible explanation for the decline of nitrate in Emerald Lake. Since there was no identifiable trend in atmospheric phosphorus or nitrogen loading to the Emerald Lake, we conclude that biogeochemical processes within Emerald Lake or its catchment are probably the

cause of the change in trophic status observed. Interestingly, Williams and Melack (1997) also measured a decline in nitrate concentration in Log Creek which was contemporaneous with changes seen in Emerald Lake. This stream drains a small (50 ha), mixed conifer catchment (elevation 2067 m) located within 15 km of the Emerald Lake basin. Prior to 1990, nitrate concentrations ranged from the detection limit to 1.0 μM ; after 1990 levels were nearly always below the detection limit. The correspondence of temporal changes in nitrate concentrations between Emerald Lake and Log Creek supports the hypothesis that N dynamics in the Sierra Nevada are susceptible to climatic forcings.

3.8. Water Balances

Overall, precipitation in high-elevation catchments of the Sierra Nevada occurs primarily during the months of December through April. From 80 to over 90% of annual deposition of water to these basins is in the form of snow. The highest percentage of snow deposition occurs during infrequent wet winters with percentages as great as 95% or more.

During the period of our study drought conditions prevailed in California. Annual snow deposition at our catchments was typically from 500 to 700 mm of snow-water equivalence (SWE) during dry years and from 1200 to 2000 mm for wet winters. During 10 years of study at Emerald Lake, dry winters occurred 6 times, near-normal snow deposition occurred during two years (1985 and 1991) and there were two wet winters: 1986 and 1993.

Similarly, non-winter precipitation varied considerably. The summer season can have frequent afternoon thunderstorms (as in 1992) or can be almost completely rainless. Large spring and autumn storms occur in some years (i.e., 1987, 1993, 1994) but frequently these periods had little precipitation.

The hydrology of high-elevation catchments in the Sierra Nevada is dominated by the accumulation and melting of the winter snowpack. The majority of water efflux from the catchments occurs during the annual snowmelt period which begins as early as late March in dry winters in the western Sierra, but may not start until early May in the eastern Sierra Nevada when snowpacks are deep. Peak runoff occurs during early to mid June following dry winters and during late June and early July in wet years. At some sites, peak outflow discharge following a wet winter was much greater than in dry years (e.g., Lost, Topaz lakes) while in others the range of peak flows was relatively small (e.g., Ruby and Crystal lakes).

Following wet or dry winters, the shape of the melt hydrograph is often punctuated by periods of low discharge caused by spring snowstorms that cool air temperatures and lower the rate of snowmelt for several days at a stretch. Following peak runoff, the snowmelt hydrograph receded gradually during the summer and autumn. At most lakes, the outflow streams were dry by early September but, at others, groundwater inputs and melt from snow-fields on north-facing slopes kept the outlets flowing through the autumn and into winter. Winter runoff at all sites was very low. At catchments without groundwater inputs, winter streamflow was primarily the result of displacement of lake water by snowfall and to a lesser extent from winter snowmelt from south-facing slopes.

Non-winter precipitation comprised a small percentage of the annual water budgets. Small to modest groundwater storage and release were identified at two of the seven lakes' basins and in the Marble Fork drainage but appeared to be a significant source of water only in the autumn after snowmelt runoff had ended. However, groundwater storage and release in the Ruby Lake basin are partly responsible for the attenuation and lengthening of discharge from the basin.

3.9. Precipitation Chemistry

Snow chemistry was similar among the four years of study and among the sampling stations. Samples from the April 1 snowpack had pH levels typically between 5.3 and 5.5. After hydrogen the most abundant ions in solution were compounds of nitrogen (ammonium and nitrate) with concentrations usually between 1.5 to 4.5 $\mu\text{Eq L}^{-1}$. Sulfate concentrations (ca. 1.0 to 3.0 $\mu\text{Eq L}^{-1}$) in Sierran snow tended to be slightly less than nitrate and ammonium levels and higher than chloride. Of the remaining solutes, only calcium and sodium were found to have concentrations much above the detection limit. Organic anions (acetate and formate) were difficult to measure in the Sierran snowpack and were usually found in low concentrations. Snow chemistry from stations in the southern Sierra had slightly higher solute concentrations although the differences were not statistically significant.

Non-winter precipitation chemistry was variable, with solute concentrations ranging from near the detection limits to levels in the tens of microequivalents per liter. Most of the variability was due to the timing of the precipitation; spring and autumn storms being most dilute and summer rains being enriched with solutes. The annual volume-weighted mean concentration of non-winter precipitation depended on the mix of samples (i.e., spring, summer or autumn) obtained. Spring and autumn precipitation derived from large-scale Pacific weather systems and from localized thunderstorms. Summer rains were derived exclusively from local air masses during afternoon convective storms.

The mean pH of non-winter precipitation in the study was 4.93. Ammonium and nitrate concentrations were 8 to 9 times greater in non-winter precipitation than in winter snowfall (mean values, 23.4 and 20.7 $\mu\text{Eq L}^{-1}$, respectively). Ammonium levels were usually higher than nitrate, with both nitrogen compounds exceeding the mean concentration of sulfate (15.1 $\mu\text{Eq L}^{-1}$). The mean chloride level measured in non-winter precipitation was 4.2 $\mu\text{Eq L}^{-1}$ which is only slightly higher than concentrations in winter snowfall. After ammonium and hydrogen the next most abundant cations in non-winter precipitation were calcium (mean, 10.4 $\mu\text{Eq L}^{-1}$) and sodium (4.6 $\mu\text{Eq L}^{-1}$). In contrast to winter snow, organic anions were abundant in non-winter precipitation. Mean values for acetate and formate were on the order of 8 $\mu\text{Eq L}^{-1}$. The average annual flux of water during non-winter periods of our study was 117 mm

3.10. Volume-weighted Mean Chemistry

The mean pH for outlet streamflow during the 36 water years of record was 6.05 and ranged from 5.6 to 6.7. The catchment with the lowest pH was Lost Lake and the catchments with the highest pH were Ruby and Spuller lakes. With respect to VWM ANC, the catchments fell into three categories: low, modest and high. Catchments in the

lowest ANC category, i.e., 15 to 30 $\mu\text{Eq L}^{-1}$, were Lost Lake, Pear Lake and Emerald Lake basins. Watersheds with ANC in the range of 30 to 50 $\mu\text{Eq L}^{-1}$ would be classified as having modest ANC and would include the Topaz Lake, Spuller Lake and Marble Fork basins. In the highest category, with greater than 50 $\mu\text{Eq L}^{-1}$ of ANC on an annual basis, are the Crystal Lake and Ruby Lake watersheds. The average VWM ANC measured for the 36 water years studied was 36.2 $\mu\text{Eq L}^{-1}$.

Of the solutes measured, sulfate was the most consistent among the catchments and water years studied. The mean annual sulfate measured for the eight catchments in our study was 7.4 $\mu\text{Eq L}^{-1}$. With the exception of Ruby and Spuller lakes, sulfate concentrations on an annual basis ranged from 5 to 7 $\mu\text{Eq L}^{-1}$. Ruby Lake and Spuller Lake basins had sulfate levels from 8 to 10 $\mu\text{Eq L}^{-1}$.

3.11. Solute Balances

The eight watersheds in this study effectively neutralized acid deposition from winter and non-winter precipitation. Annual deposition of hydrogen ion during the study ranged from 23 to 128 Eq ha^{-1} . At Emerald Lake, hydrogen deposition varied by a factor of ca. 5 during the period of 1985 through 1994. The average annual deposition for the 36 water years of record (all catchments) was 52 Eq ha^{-1} .

Hydrogen-ion deposition was also substantial in these catchments and winter snowfall was the main contributor. These inputs were effectively neutralized by the catchments and, on average, the basins consumed 87% of the hydrogen-ions deposited in them. Catchments in the eastern Sierra Nevada had significantly ($p < 0.05$) higher outflow ANC and neutralized a higher percentage of acid inputs than did basins in the Tokopah Valley or the Lost Lake watershed. These findings suggest that watersheds along the eastern slope of the Sierra Nevada may be less susceptible to harm from acid deposition than catchments along the western slope. Processes, principally mineral weathering and biological uptake of nitrogen, changed the chemical make-up of precipitation so that streamwaters exiting the catchments were a solution composed primarily of ANC (i.e., HCO_3^- or bicarbonate), calcium and dissolved silica.

The majority of hydrogen deposition in high-elevation catchments of the Sierra Nevada occurs during winter months. A comparison of winter and non-winter loading of H^+ during the years of 1990 through 1993 shows that from 67% to 92% of annual deposition is from winter snowfall. The percentage of hydrogen deposition from winter loading (including dryfall onto snow) is directly related to the quantity of snow which falls. Hydrogen deposition from non-winter periods comprised a higher percentage of annual loading during years with low winter snowfall.

Based on input-output budgets of hydrogen ion, the catchments best able to neutralize acidic inputs were Ruby and Crystal lakes. The mean percentage of hydrogen consumed in these catchments during water years 1990 through 1994 was 94% (i.e., outflow flux divided by loading). With the exception of Lost Lake, the remaining catchments neutralized from 80 to 90 percent of hydrogen deposition on an annual basis. On an areal basis, the amount of hydrogen neutralized averaged 45 Eq ha^{-1} .

The eight watersheds in this study exported about 100 to 600 Eq ha^{-1} of ANC annually (mean, 250 Eq ha^{-1}). At all sites the export of ANC was related to the quantity of runoff and was greatest in years with large snowpacks.

High rates of base cation export were a conspicuous feature of the solute balances for the catchments in this study. The major cations exported from the catchments were calcium and sodium. The mean and range of yields for calcium were 171 Eq h and 42.7 to 407 Eq ha⁻¹, respectively. The same parameters for sodium were 66 Eq ha⁻¹ and 24.5 to 154 Eq ha⁻¹, respectively.

A large amount of nitrogen deposition was measured in the catchments in this study. Annual ammonium deposition usually exceeded nitrate deposition, ranging from 20.8 to 140 Eq ha⁻¹ and a mean value of 50.8 Eq ha⁻¹. Nitrate loading varied from 26.8 to 116 Eq ha⁻¹ and had a mean rate of 44.9 Eq ha⁻¹ per year in the 36 water years of record. For both ions the maximum loading rates were measured at Emerald Lake during water year 1987.

Most of the nitrogen intercepted by the Sierra Nevada mountains is utilized by terrestrial and aquatic ecosystems within the range. Based on the input-output budgets for ammonium and nitrate, biological demand for nitrogen is high in the Sierra Nevada. During the study, utilization of ammonium from wet deposition averaged greater than 96% on an annual basis. At some catchments, such as Crystal and Lost, nitrate utilization was in the range of 85% to 95% on an annual basis, but overall, uptake was typically on the order of 20 to 60%. Nitrate utilization tended to decline in wet years like 1993.

Non-winter precipitation is the major contributor of nitrogen during drought years. For the period of 1990 through 1992, well over half of the annual deposition of ammonium and nitrate took place during the months of ca. April through November. Similar patterns of nitrogen deposition were also seen in water years 1985 through 1987 at Emerald Lake. Moreover, even in relatively wet years such as 1993, deposition from non-winter precipitation was ca. 22% of annual loading.

There was a high degree of correspondence between winter snowfall quantity and winter solute deposition in the Sierra Nevada. For the 36 annual records, there were significant ($P < 0.01$, Pearson product moment correlation), positive correlations between all measured constituents (with the exception of formate) and snow-water equivalence (SWE).

At Emerald Lake and the other catchments, runoff of water explained 98% of the variability of the annual yield of ANC from the catchment. At Emerald, the relationship between runoff and ANC yield remained constant over a nearly fourfold range in runoff and a fivefold range in hydrogen ion deposition. These findings suggests that the acid-neutralizing capacity of the Emerald Lake watershed is not being challenged by current levels of acid deposition.

Base cations in surface waters of the Sierra Nevada are primarily the result of weathering of granitic minerals. In addition, a strong relationship between ANC and base cations in these waters has demonstrated that mineral weathering is the dominant pathway for neutralization of acids in the Sierra Nevada. At all eight catchments the predominant cations in outflows were calcium and sodium.

3.12. Episodic Acidification

Dilution was the primary factor in ANC depression in surface waters during our study. The study lakes could be divided into two classes based on their response to snowmelt: shallow, short residence-time (i.e., rapidly flushed) lakes where acidification

accounted for <10% of the ANC decrease; and lakes where acidification caused 25 to 35% of the depression due to larger lake volumes or lower snowmelt rates. In lakes where acidification was important, nitrate and sulfate contributed equally during the first half of snowmelt, while sulfate dominated in the latter half. Traditional analysis, examining the change in ANC, base cation and anion concentrations between minimum ANC and an index period, failed to capture the importance of nitrate and sulfate because their variation over the snowmelt pulse was fundamentally different from that of ANC and base cations; an analysis examining changes in concentrations over time was required to fully evaluate acidification.

The relationship between minimum and fall-overturn ANC for the lakes in this study was linear ($r^2 = 0.84$) and the equation remained unchanged as additional data from earlier synoptic surveys were added. This linear model, applied to Western Lakes Survey data for the Sierra Nevada, estimated that no lakes are currently acidified by snowmelt. However, the model's confidence limits allow for the possibility that up to 1.8% (~38) of Sierra Nevada lakes undergo snowmelt ANC depressions slightly below $0 \mu\text{Eq L}^{-1}$.

We used a simple prediction model to estimate the impact of increases in acid deposition of 50, 100 and 150 %: approximately 6, 9 and 14 %, respectively, of Sierra Nevada lakes (approximately 135, 185 and 290 lakes) became episodically acidified in these scenarios, i.e., $\text{ANC} < 0 \mu\text{Eq}\cdot\text{L}^{-1}$, but no lakes experienced chronic acidification ($\text{ANC} < 0$ at fall-overturn).

3.13. Evaporation Studies

Evaporation was estimated for the eight study sites in order to calculate complete and accurate water balances. Only a small percentage of the settled snowpack is lost to evaporation in the Central Sierra Nevada. Typically evaporative loss will vary from 80 to 100 mm of water, approximately 6 percent of the maximum accumulation during an average snow year. During drought years the loss is less, but represents a greater percentage of the maximum accumulation, 9 to 13 percent. During peak snow years the loss decreases to about 4 percent, although the extended length of the snow season somewhat increases the actual amount lost. Most of the loss occurs during the period of snow accumulation when vapor pressure gradients are usually favorable for evaporation, and conditions of atmospheric instability are often found. Even so, low vapor pressure differences between the air and the snow surface (the result of cold temperatures and the prior transit of the over-passing air over extensive snow-covered distances, which serve to increase its humidity and decrease its capacity to absorb additional moisture) limit the total evaporative loss to relatively small quantities.

During the snowmelt season, increasing atmospheric stability, and the reduction of the vapor pressure gradient due to the higher vapor content of the warming spring air, reduce evaporative losses from the snow to negligible amounts. Often near the end of this period, snowpack losses from evaporation are exceeded by gains from condensation. Total losses from the snowpack during the melt season are typically around 15 mm of water, representing 2 to 3 percent of the maximum accumulation during drought years, less than one percent for above normal snowpacks. Studies, such as this one, where the annual accounting and analysis of the water balance begins with the measurement of the

maximum accumulation at the start of spring snowmelt, can neglect evaporative loss from the snow.

However, the *total* evaporation from alpine and subalpine areas is not negligible or low. As the snowmelt season progresses, evaporation from saturated soil and free water surfaces becomes appreciable. The warming of wet soils and standing water, as their lower albedo increasingly absorbs radiation, generates high vapor pressures and conditions of local instability, enhancing evaporative losses. These snow-free surfaces also warm the over-passing air and increase the transport of sensible heat to the remaining snowpack, accelerating snowmelt and further increasing the availability of free water and saturated soils. Only as the availability of water diminishes, with the gradual drying of the basin, does the rate of evaporation decrease.

3.14. Soil and Vegetation Surveys

Soil and vegetation surveys were conducted in the Pear, Topaz, Ruby, Crystal, Spuller and Lost lake watersheds. Mapping of soils and vegetation in the Emerald Lake watershed were completed as part of the Integrated Watershed Study in the 1980's and have been reported to the ARB previously (Huntington and Akesson 1987, Rundel et al. 1988). Surveys of the Marble Fork drainage only include area within the Emerald, Pear and Topaz lake catchments. These areas represent 23% of the Marble Fork drainage and are representative of the entire drainage.

There were two reasons for conducting the soil and vegetation surveys. First, these data were needed as input parameters to ARB funded hydrologic (Elder 1995) and hydrochemical models (Wolford et al. 1996, Wolford and Bales 1996). Second, the surveys will be used for future analyses of Sierran biogeochemistry. The approach taken in the soil survey was original and designed for use by researchers from a variety of disciplines with particular emphasis on hydrology and biogeochemistry. The survey was essentially a semi-quantitative model of soil-landscape patterns on an areal basis, designed to be periodically improved with additions of quantitative data.

This soil survey used few soils and mapping units to emphasize major relationships in the soil-landscape continuum. Simple non-technical terminology facilitates use by general scientific audiences. The soil maps contain great cartographic detail in places. This detail was used in complex soil-landscapes to express some of the observed soil variability that otherwise would have been lost with less intensive mapping. Maps of these complex areas can be simplified for specific users.

Recommendations

We recommend that monitoring of surface water and precipitation chemistry be continued in the Tokopah Valley of Sequoia National Park. A design for this monitoring program is contained in Engle and Melack (1997). The catchments in this area (Emerald Lake, Pear Lake, Topaz Lake and Marble Fork of the Kaweah River) were among the most sensitive to acid deposition in our study. Maintaining the long-term data set from the Emerald Lake watershed should be the top priority of any additional work. This data set will be valuable in monitoring future environmental change due to climate change and increased urbanization of the San Joaquin Valley and Sierra foothill region.

Chapter One

Annual and Long-term Variability of Surface Water Chemistry in the Sierra Nevada

by

James O. Sickman, Al Leydecker and John M. Melack

Chapter One

TABLE OF CONTENTS

1.1. INTRODUCTION	1-10
1.2. WATERSHED DESCRIPTIONS	1-12
1.2.1. Crystal Lake Watershed	1-13
1.2.2. Emerald Lake Watershed	1-14
1.2.3. Lost Lake Watershed	1-15
1.2.4. Pear Lake Watershed	1-15
1.2.5. Ruby Lake Watershed	1-16
1.2.6. Spuller Lake Watershed	1-17
1.2.7. Topaz Lake Watershed	1-17
1.2.8. Marble Fork of the Kaweah River	1-18
1.3. METHODS	1-19
1.3.1. Lake and Stream Monitoring	1-19
1.3.2. Precipitation Sampling	1-20
1.3.3. Outflow Gauging	1-21
1.3.4. Water Balance	1-21
1.3.5. Watershed Solute Balance	1-22
1.3.6. Meteorological Measurements	1-22
1.3.7. Soil Surveys	1-22
1.3.8. Geographic Information Systems (GIS) and Vegetation Mapping	1-23
1.3.9. Quality Assurance and Control Procedures	1-24
1.3.9.1. QA/QC Results	1-25
1.4. RESULTS AND DISCUSSION	1-28
1.4.1. Annual Variability of Outflow Chemistry	1-28
1.4.1.1. Patterns of pH During Snowmelt.	1-29
1.4.1.2. Patterns of ANC During Snowmelt.	1-29
1.4.1.3. Patterns of Nitrate During Snowmelt.	1-30
1.4.1.4. Patterns of Sulfate During Snowmelt.	1-31
1.4.1.5. Patterns of Base Cations and Silicate During Snowmelt.	1-32
1.4.2. Long-term Trends in Lake and Outflow Chemistry	1-33
1.4.2.1. Long-term Trends in pH and ANC	1-34
1.4.2.2. Long-term Trends in Other Solutes	1-35
1.4.3. Mechanisms for ANC Depression During Snowmelt	1-38
1.4.3.1. The d-value Analysis	1-38
1.4.3.2. The Superposition Analysis	1-40
1.4.3.3. The Minimum ANC vs. Index ANC Relationship	1-42
1.4.3.4. The Eshleman, Acidification and Predictive Models	1-44
1.4.3.5. Future Acidification in the Sierra Nevada	1-46
1.5. CONCLUSIONS	1-48
1.6. REFERENCES	1-50

LIST OF TABLES

Table I-1. Summary of basin and lake characteristics.	1-55
Table I-2. Summary of water and solute balances.	1-56
Table I-3. Summary of quality assurance data for chemical analyses.....	1-57
Table I-4. Statistical analysis of temporal changes in solute chemistry during snowmelt.	1-58
Table I-5. Fall-overturn d-values for the eight study basins.	1-59
Table I-6. Pre-snowmelt d-values for the eight study basins.	1-60
Table I-7. Comparison of the d-values for the eight study basins based on two index periods...	1-61
Table I-8. Percent of the snowmelt ANC depression caused by dilution and by acidification.	1-62
Table I-9. Base-flow SBC/ANC ratios (R) for the study lakes.	1-63
Table I-10. Average index and episodic anion concentrations for the eight study basins.	1-64
Table I-11. Study lake ANC predictions from an acidification model.	1-65

LIST OF FIGURES

Figure I-1. Map of California with study locations.....	1-75
Figure I-2. Map of Upper Marble Fork of Kaweah River (Tokopah Valley.....	1-76
Figure I-3. Hypsographic curve and winter ice-depths from Crystal Lake.....	1-77
Figure I-4. Time-series of temperature and oxygen from Crystal Lake.....	1-78
Figure I-5. Topographic map of the Crystal Lake watershed.....	1-79
Figure I-6. Vegetation map of the Crystal Lake watershed.....	1-80
Figure I-7. Soil map of the Crystal Lake watershed.....	1-81
Figure I-8. Hypsographic curve and winter ice-depths from Emerald Lake.....	1-82
Figure I-9. Time-series of temperature and oxygen from Emerald Lake.....	1-83
Figure I-10. Hypsographic curve and winter ice-depths from Lost Lake.....	1-84
Figure I-11. Time-series of temperature and oxygen from Lost Lake.....	1-85
Figure I-12. Topographic map of the Lost Lake watershed.....	1-86
Figure I-13. Vegetation map of the Lost Lake watershed.....	1-87
Figure I-14. Soil map of the Lost Lake watershed.....	1-88
Figure I-15. Hypsographic curve and winter ice-depths from Pear Lake.....	1-89
Figure I-16. Time-series of temperature and oxygen from Pear Lake.....	1-90
Figure I-17. Topographic map of the Pear Lake watershed.....	1-91
Figure I-18. Vegetation map of the Pear Lake watershed.....	1-92
Figure I-19. Soil map of the Pear Lake watershed.....	1-93
Figure I-20. Hypsographic curve and winter ice-depths from Ruby Lake.....	1-94
Figure I-21. Time-series of temperature and oxygen from Ruby Lake.....	1-95
Figure I-22. Topographic map of the Ruby Lake watershed.....	1-96
Figure I-23. Vegetation map of the Ruby Lake watershed.....	1-97
Figure I-24. Soil map of the Ruby Lake watershed.....	1-98
Figure I-25. Hypsographic curve and winter ice-depths from Spuller Lake.....	1-99
Figure I-26. Time-series of temperature and oxygen from Spuller Lake.....	1-100
Figure I-27. Topographic map of the Spuller Lake watershed.....	1-101
Figure I-28. Vegetation map of the Spuller Lake watershed.....	1-102
Figure I-29. Soil map of the Spuller Lake watershed.....	1-103
Figure I-30. Hypsographic curve and winter ice-depths from Topaz Lake.....	1-104
Figure I-31. Time-series of temperature and oxygen from Topaz Lake.....	1-105

Figure I-32. Topographic map of the Topaz Lake watershed.....	1-106
Figure I-33. Vegetation map of the Topaz Lake watershed.....	1-107
Figure I-34. Soil map of the Topaz Lake watershed.....	1-108
Figure I-35. Frequency histograms of % Ion Difference and theoretical/measured conductance for lake and stream samples.....	1-109
Figure I-36. Scatter-plot of theoretical conductance/ measured conductance vs % Ion Difference, and histogram of difference between cations and anions in lake and stream samples.....	1-110
Figure I-37. Outflow discharge and pH in the Crystal Lake watershed during the snowmelt periods of 1990 through 1993.....	1-111
Figure I-38. Outflow discharge and pH in the Emerald Lake watershed during the snowmelt periods of 1990 through 1994.....	1-112
Figure I-39. Outflow discharge and pH in the Lost Lake watershed during the snowmelt periods of 1990 through 1993.....	1-113
Figure I-40. Outflow discharge and pH in the Upper Marble Fork watershed during the snowmelt periods of 1993 and 1994.....	1-114
Figure I-41. Outflow discharge and pH in the Pear Lake watershed during the snowmelt periods of 1990 through 1993.....	1-115
Figure I-42. Outflow discharge and pH in the Ruby Lake watershed during the snowmelt periods of 1990 through 1993.....	1-116
Figure I-43. Outflow discharge and pH in the Spuller Lake watershed during the snowmelt periods of 1990 through 1993.....	1-117
Figure I-44. Outflow discharge and pH in the Topaz Lake watershed during the snowmelt periods of 1990 through 1993.....	1-118
Figure I-45. Outflow discharge and ANC in the Crystal Lake watershed during the snowmelt periods of 1990 through 1993.....	1-119
Figure I-46. Outflow discharge and ANC in the Emerald Lake watershed during the snowmelt periods of 1990 through 1994.....	1-120
Figure I-47. Outflow discharge and ANC in the Lost Lake watershed during the snowmelt periods of 1990 through 1993.....	1-121
Figure I-48. Outflow discharge and ANC in the Upper Marble Fork watershed during the snowmelt periods of 1993 and 1994.....	1-122
Figure I-49. Outflow discharge and ANC in the Pear Lake watershed during the snowmelt periods of 1990 through 1993.....	1-123
Figure I-50. Outflow discharge and ANC in the Ruby Lake watershed during the snowmelt periods of 1990 through 1993.....	1-124
Figure I-51. Outflow discharge and ANC in the Spuller Lake watershed during the snowmelt periods of 1990 through 1993.....	1-125
Figure I-52. Outflow discharge and ANC in the Topaz Lake watershed during the snowmelt periods of 1990 through 1993.....	1-126

Figure I-53. Outflow discharge and nitrate in the Crystal Lake watershed during the snowmelt periods of 1990 through 1993.....	1-127
Figure I-54. Outflow discharge and nitrate in the Emerald Lake watershed during the snowmelt periods of 1990 through 1994.....	1-128
Figure I-55. Outflow discharge and nitrate in the Lost Lake watershed during the snowmelt periods of 1990 through 1993.....	1-129
Figure I-56. Outflow discharge and nitrate in the Upper Marble Fork watershed during the snowmelt periods of 1993 and 1994.	1-130
Figure I-57. Outflow discharge and nitrate in the Pear Lake watershed during the snowmelt periods of 1990 through 1993.....	1-131
Figure I-58. Outflow discharge and nitrate in the Ruby Lake watershed during the snowmelt periods of 1990 through 1993.....	1-132
Figure I-59. Outflow discharge and nitrate in the Spuller Lake watershed during the snowmelt periods of 1990 through 1993.....	1-133
Figure I-60. Outflow discharge and nitrate in the Topaz Lake watershed during the snowmelt periods of 1990 through 1993.....	1-134
Figure I-61. Outflow discharge and sulfate in the Crystal Lake watershed during the snowmelt periods of 1990 through 1993.....	1-135
Figure I-62. Outflow discharge and sulfate in the Emerald Lake watershed during the snowmelt periods of 1990 through 1994.....	1-136
Figure I-63. Outflow discharge and sulfate in the Lost Lake watershed during the snowmelt periods of 1990 through 1993.....	1-137
Figure I-64. Outflow discharge and sulfate in the Upper Marble Fork watershed during the snowmelt periods of 1993 and 1994.	1-138
Figure I-65. Outflow discharge and sulfate in the Pear Lake watershed during the snowmelt periods of 1990 through 1993.....	1-139
Figure I-66. Outflow discharge and sulfate in the Ruby Lake watershed during the snowmelt periods of 1990 through 1993.....	1-140
Figure I-67. Outflow discharge and sulfate in the Spuller Lake watershed during the snowmelt periods of 1990 through 1993.....	1-141
Figure I-68. Outflow discharge and sulfate in the Topaz Lake watershed during the snowmelt periods of 1990 through 1993.....	1-142
Figure I-69. Outflow discharge and the sum of calcium, magnesium, sodium and potassium in the Crystal Lake watershed during the snowmelt periods of 1990 through 1993.	1-143
Figure I-70. Outflow discharge and the sum of calcium, magnesium, sodium and potassium in the Emerald Lake watershed during the snowmelt periods of 1990 through 1994.....	1-144
Figure I-71. Outflow discharge and the sum of calcium, magnesium, sodium and potassium in the Lost Lake watershed during the snowmelt periods of 1990 through 1993.....	1-145
Figure I-72. Outflow discharge and the sum of calcium, magnesium, sodium and potassium in the Upper Marble Fork watershed during the snowmelt periods of 1993 and 1994.	1-146

Figure I-73. Outflow discharge and the sum of calcium, magnesium, sodium and potassium in the Pear Lake watershed during the snowmelt periods of 1990 through 1993.	1-147
Figure I-74. Outflow discharge and the sum of calcium, magnesium, sodium and potassium in the Ruby Lake watershed during the snowmelt periods of 1990 through 1993.	1-148
Figure I-75. Outflow discharge and the sum of calcium, magnesium, sodium and potassium in the Spuller Lake watershed during the snowmelt periods of 1990 through 1993.	1-149
Figure I-76. Outflow discharge and the sum of calcium, magnesium, sodium and potassium in the Topaz Lake watershed during the snowmelt periods of 1990 through 1993.	1-150
Figure I-77. Outflow discharge and silicate in the Crystal Lake watershed during the snowmelt periods of 1990 through 1993.	1-151
Figure I-78. Outflow discharge and silicate in the Emerald Lake watershed during the snowmelt periods of 1990 through 1994.	1-152
Figure I-79. Outflow discharge and silicate in the Lost Lake watershed during the snowmelt periods of 1990 through 1993.	1-153
Figure I-80. Outflow discharge and silicate in the Upper Marble Fork watershed during the snowmelt periods of 1993 and 1994.	1-154
Figure I-81. Outflow discharge and silicate in the Pear Lake watershed during the snowmelt periods of 1990 through 1993.	1-155
Figure I-82. Outflow discharge and silicate in the Ruby Lake watershed during the snowmelt periods of 1990 through 1993. Solid lines are discharge and solid lines with circles are outflow chemistry (symbols denote individual chemical samples).	1-156
Figure I-83. Outflow discharge and silicate in the Spuller Lake watershed during the snowmelt periods of 1990 through 1993. Solid lines are discharge and solid lines with circles are outflow chemistry (symbols denote individual chemical samples).	1-157
Figure I-84. Outflow discharge and silicate in the Topaz Lake watershed during the snowmelt periods of 1990 through 1993. Solid lines are discharge and solid lines with circles are outflow chemistry (symbols denote individual chemical samples).	1-158
Figure I-85. Generalized patterns of solute concentration during snowmelt runoff period. Solid lines are concentration, dashed lines are generalized discharge. Y-axes show relative solute concentration without scale. X-axes simulate the period of snowmelt which typically begins in April and continues through July.	1-159
Figure I-86. Time-series of outflow pH and ANC from the Crystal Lake watershed, 1990-1993.	1-160
Figure I-87. Time-series of outflow nitrate and sulfate from the Crystal Lake watershed, 1990-1993.	1-161
Figure I-88. Time-series of outflow sum of base cations and silicate from the Crystal Lake watershed, 1990-1993.	1-162
Figure I-89. Time-series of outflow pH and ANC from the Emerald Lake watershed, 1983-1994.	1-163
Figure I-90. Time-series of outflow nitrate and sulfate from the Emerald Lake watershed, 1983-1994.	1-164

Figure I-91. Time series of outflow chloride and ammonium from the Emerald Lake watershed, 1983-1994.....	1-165
Figure I-92. Time-series of outflow sum of base cations and silicate from the Emerald Lake watershed, 1983-1994.....	1-166
Figure I-93. Time-series of outflow pH and ANC from the Lost Lake watershed, 1990-1993.....	1-167
Figure I-94. Time-series of outflow nitrate and sulfate from the Lost Lake watershed, 1990-1993.....	1-168
Figure I-95. Time-series of outflow sum of base cations and silicate from the Lost Lake watershed, 1990-1993.....	1-169
Figure I-96. Time-series of outflow pH and ANC from the Pear Lake watershed, 1987-1994.....	1-170
Figure I-97. Time-series of outflow nitrate and sulfate from the Pear Lake watershed, 1987-1994.....	1-171
Figure I-98. Time-series of outflow sum of base cations and silicate from the Pear Lake watershed, 1987-1994.....	1-172
Figure I-99. Time-series of outflow pH and ANC from the Ruby Lake watershed, 1987-1994.....	1-173
Figure I-100. Time-series of outflow nitrate and sulfate from the Ruby Lake watershed, 1987-1994.....	1-174
Figure I-101. Time-series of outflow sum of base cations and silicate from the Ruby Lake watershed, 1987-1994.....	1-175
Figure I-102. Time-series of outflow pH and ANC from the Spuller Lake watershed, 1990-1994.....	1-176
Figure I-103. Time-series of outflow nitrate and sulfate from the Spuller Lake watershed, 1990-1994.....	1-177
Figure I-104. Time-series of outflow sum of base cations and silicate from the Spuller Lake watershed, 1990-1994.....	1-178
Figure I-105. Time-series of outflow pH and ANC from the Topaz Lake watershed, 1987-1994.....	1-179
Figure I-106. Time-series of outflow nitrate and sulfate from the Topaz Lake watershed, 1987-1994.....	1-180
Figure I-107. Time-series of outflow sum of base cations and silicate from the Topaz Lake watershed, 1987-1994.....	1-181
Figure I-108. Time-series of volume-weighted mean pH and ANC in Crystal Lake, 1986 - 1994.....	1-182
Figure I-109. Time-series of volume-weighted mean nitrate and sulfate in Crystal Lake, 1986-1994.....	1-183
Figure I-110. Time-series of volume-weighted mean chloride and specific conductance in Crystal Lake, 1986-1994.....	1-184

Figure I-111. Time-series of volume-weighted mean sum of base cations and silicate in Crystal Lake, 1986-1994.....	1-185
Figure I-112. Time-series of volume-weighted mean pH and ANC in Emerald Lake, 1982 - 1994.....	1-186
Figure I-113. Time-series of volume-weighted mean nitrate and sulfate in Emerald Lake, 1982-1994.....	1-187
Figure I-114. Time-series of volume-weighted mean chloride and specific conductance in Emerald Lake, 1982-1994.....	1-188
Figure I-115. Time-series of volume-weighted mean sum of base cations and silicate in Emerald Lake, 1982-1994.....	1-189
Figure I-116. Time-series of volume-weighted mean pH and ANC in Lost Lake, 1989 - 1993.....	1-190
Figure I-117. Time-series of volume-weighted mean nitrate and sulfate in Lost Lake, 1989-1993.....	1-191
Figure I-118. Time-series of volume-weighted mean chloride and specific conductance in Lost Lake, 1989-1993.....	1-192
Figure I-119. Time-series of volume-weighted mean sum of base cations and silicate in Lost Lake, 1989-1993.....	1-193
Figure I-120. Time-series of volume-weighted mean pH and ANC in Pear Lake, 1986 - 1993.....	1-194
Figure I-121. Time-series of volume-weighted mean nitrate and sulfate in Pear Lake, 1986-1993.....	1-195
Figure I-122. Time-series of volume-weighted mean chloride and specific conductance in Pear Lake, 1986-1993.....	1-196
Figure I-123. Time-series of volume-weighted mean sum of base cations and silicate in Pear Lake, 1986-1993.....	1-197
Figure I-124. Time-series of volume-weighted mean pH and ANC in Ruby Lake, 1986 - 1994.....	1-198
Figure I-125. Time-series of volume-weighted mean nitrate and sulfate in Ruby Lake, 1986-1994.....	1-199
Figure I-126. Time-series of volume-weighted mean chloride and specific conductance in Ruby Lake, 1986-1994.....	1-200
Figure I-127. Time-series of volume-weighted mean sum of base cations and silicate in Ruby Lake, 1986-1994.....	1-201
Figure I-128. Time-series of volume-weighted mean pH and ANC in Spuller Lake, 1989 - 1993.....	1-202
Figure I-129. Time-series of volume-weighted mean nitrate and sulfate in Spuller Lake, 1989-1993.....	1-203
Figure I-130. Time-series of volume-weighted mean chloride and specific conductance in Spuller Lake, 1989-1993.....	1-204

Figure I-131. Time-series of volume-weighted mean sum of base cations and silicate in Spuller Lake, 1989-1993.....	1-205
Figure I-132. Time-series of volume-weighted mean pH and ANC in Topaz Lake, 1986 - 1994.....	1-206
Figure I-133. Time-series of volume-weighted mean nitrate and sulfate in Topaz Lake, 1986-1994.....	1-207
Figure I-134. Time-series of volume-weighted mean chloride and specific conductance in Topaz Lake, 1986-1994.....	1-208
Figure I-135. Time-series of volume-weighted mean sum of base cations and silicate in Topaz Lake, 1986-1994.....	1-209
Figure I-136. ANC time-series from Treasure, Gem, Upper Gaylor and Granite lakes (Eastern Sierra Nevada), 1981-1995. Lakes were sampled in the autumn after lake mixing.	1-210
Figure I-137. ANC time-series from Heather, Upper Mosquito, Crystal (Mineral King) and Emerald lakes (Western Sierra Nevada), 1981-1995. Lakes were sampled in the autumn after lake mixing.	1-211
Figure I-138. pH time-series from Treasure, Gem, Upper Gaylor and Granite lakes (Eastern Sierra Nevada), 1981-1995. Lakes were sampled in the autumn after lake mixing.	1-212
Figure I-139. pH time-series from Heather, Upper Mosquito, Crystal (Mineral King) and Emerald lakes (Western Sierra Nevada), 1981-1995. Lakes were sampled in the autumn after lake mixing.	1-213
Figure I-140. Variation of nitrate, sulfate and ANC with time in the outflows of Emerald Lake and Spuller Lake: 1990 through 1994.	1-214
Figure I-141. Superposition analyses for Emerald and Spuller lakes.....	1-215
Figure I-142. Comparison of ANC depression predicted from superposition analysis and percent-difference method.....	1-216
Figure I-143. Episode ANC vs fall-overtum ANC.	1-217
Figure I-144. Episode ANC vs pre-melt ANC.....	1-218
Figure I-145. The Eshleman model applied to the study lakes.....	1-219
Figure I-146. The Eshleman model revised as an acidification model and applied to the study lakes.....	1-220
Figure I-147. Histogram of the number of lakes in the Sierra Nevada in various ANC classes under present and future acidification scenarios.	1-221

1. Chapter One

1.1. Introduction

High elevation lakes and streams in the Sierra Nevada mountains are some of the most dilute, weakly buffered waters in the United States (Landers et al. 1987, Melack and Stoddard 1991). The catchments that supply runoff to these waters are underlain, predominantly, by granitic rocks, have poorly developed, thin soils and sparse vegetation. The hydrologic cycle of these watersheds is dominated by the annual accumulation and melting of a dilute, mildly acidic (pH ca. 5.5) snowpack (Melack et al. 1997). These conditions indicate that aquatic ecosystems in the Sierra Nevada may be susceptible to affects of anthropogenic acid-deposition.

Since the early 1980s, aquatic ecosystems in the Sierra Nevada have been studied to determine if, and to what extent, they have been affected by atmospheric acid deposition. Evaluating the harm posed by acid deposition in California required an assessment of the current status of aquatic resources and their possible responses to acidification. In the early years of this effort, surveys of lake and stream chemistry were conducted to determine the geographic extent of sensitive habitats (Melack et al. 1985, Melack and Setaro 1986, Landers et al. 1987). Upon completion of these initial surveys, the California Air Resources Board initiated an Integrated Watershed Study (IWS) of the Emerald Lake watershed to detect acid-induced damage and determine the possible consequences of acidification on Sierran lakes and streams. The IWS included investigations of atmospheric deposition (wet and dry), terrestrial systems (soils, vegetation and geology) and aquatic systems (lake and stream chemistry and biology). These studies were completed by the end of the 1980s (Amundsen et al. 1988, Brown et al. 1990, Bytnerowicz and Olszyk 1988 and 1991, Cooper et al. 1988a, Cooper et al. 1988b, Dozier et al. 1987, Dozier et al. 1989, Huntington and Akeson 1987, Lund et al. 1989, Melack et al. 1987, Melack et al. 1989, Rundel et al. 1988).

Focus then shifted to a larger set of Sierran lakes and catchments to assess the generality of the Emerald Lake IWS and characterize the year-round sensitivity of a larger set of Sierran catchments. In addition to continuing work at Emerald Lake, research on the Pear Lake, Topaz Lake, Crystal Lake and Ruby Lake watersheds was begun in 1986 (Sickman and Melack 1989). In 1990, two additional lake basins were added to the monitoring program: Spuller Lake and Lost Lake (Melack et al. 1993). Extensive monitoring of wet deposition to high elevations in the Sierra Nevada was begun in 1990 at nine additional sites (Melack et al. 1997). The upper Marble Fork drainage of the Kaweah River was added to the monitoring program in 1992. These studies were designed to measure solute inputs and losses to Sierran watersheds and quantify the link between acid deposition and changes in surface water chemistry. Results from these investigations are presented in this report.

In 1997, an overall assessment of ARB-funded research in high altitude aquatic ecosystems in the Sierra Nevada was completed (Engle and Melack 1997). This assessment integrates results from the research described above with data from the Alpine Wet Deposition Project (Melack et al. 1997) and the findings presented in this report. The assessment describes the current status of high-elevation aquatic ecosystems in the Sierra Nevada with respect to acid deposition and provides recommendations for future

monitoring. The reader is referred to this report for a complete summary of ARB-funded investigations in the Sierra Nevada.

In this report we present results from regional studies of Sierra Nevada watersheds. The period of record runs from water year 1990 (October 1989 through September 1990) through water year 1994 at Emerald, Ruby and Spuller lakes and through 1993 at Topaz, Pear, Crystal and Lost lakes. Data from water years 1993 and 1994 are included from the Marble Fork drainage of the Kaweah river. We have also included previously unpublished solute balances for the Emerald Lake watershed from 1985, 1986 and 1987. The major objectives of these studies are:

1. Measure the major inputs and losses of water and solutes to high elevation catchments of the Sierra Nevada.
 2. Quantify the link between acid deposition and chemical changes in surface water chemistry.
 3. Determine if there are trends and patterns in surface water chemistry and wet deposition (rain and snow) in the watersheds.
 4. Provide data for hydrologic and hydrochemical models of Sierran watersheds.
- These data include meteorologic measurements, surface water chemistry, discharge and surveys of snow deposition, soils and vegetation.

Fulfilling these objectives allowed us to assess the year-round and long-term susceptibility of a diverse subset of Sierran Lakes to acid deposition. Overall, the investigations in this report were designed to provide information on the current and future status of high-altitude catchments in the Sierra Nevada which will be used by the California Air Resources Board in evaluating the need for acid deposition standards in this region.

This report is divided into four chapters and an appendix. Chapter One contains background information such as site descriptions, methodologies, soils and vegetation maps, lake bathymetry and results from our Quality Control program for analytical chemistry. We also present hydrochemical time-series data from the seven lakes' basins and the Marble Fork drainage and discuss the annual and long-term variability of surface water chemistry (Objectives 2 and 3). Trends are identified and generalizations are drawn and statistically tested about annual hydrochemical patterns (Objective 3). We include an analysis of episodic ANC depression in Sierran Lakes and quantify the relative influence of snowmelt dilution and acidification in the spring ANC depression (Objective 2). Using quantitative relationships between acid deposition and surface water ANC (Objective 2), we assess the impact of current and increased acid loading on Sierran lakes.

In Chapter Two we present results from water balances from the catchments and discuss the major sources of error in quantifying inputs and losses of water from these basins (Objective 1). Chapter Three builds on the water balances by combining surface water and precipitation chemistry with water fluxes, to calculate solute balances for the basins (Objective 1). In Chapter Three we describe the major biogeochemical reactions that occur in the basins and assess their relationship to atmospheric deposition. We also examine the annual variability of solute loading to and yield from the catchments and statistically test for differences among catchments and through time (Objectives 1, 2 and 3). We use these comparisons to evaluate the relative susceptibility of the individual catchments to acid deposition.

A detailed study of evaporative loss of water from the catchments is presented in Chapter Four (Objective 1). While the major motivation was to improve the water balances and evaluate the accuracy of the discharge and precipitation volumes, the study of evaporation in montane regions is worthwhile in its own right given the contradictory conclusions of past research.

In the appendix we present data from the soil surveys conducted in the study catchments. The major soil types are described and their distribution within the individual catchments discussed (Objective 4). There were two reasons for the soil and vegetation investigations: (1) these data were needed as input parameters to ARB funded hydrologic (Elder 1995) and hydrochemical models (Wolford et al. 1996, Wolford and Bales 1996) (Objective 4) and (2) the surveys will be used for more in-depth analyses of Sierran biogeochemistry that are in progress with funding from NASA. Soil profiles and chemical characteristics will be used for quantitative analyses and models of soil biogeochemical properties at small watershed scales. This work, conducted with the cooperation of other UCSB scientists, will require more time and is outside the scope of this report. As publications of these efforts are produced for peer-reviewed journals, copies will be forwarded to ARB. Results from a soil survey performed for the ARB-funded Miniwatershed project was also included in the appendix, but as this work was performed under a different ARB contract (A032-116), no discussion of these results (including the soil and vegetation maps) are presented in this report.

While one of the objectives of the present study was to provide data for hydrologic and hydrochemical modeling, no modeling results are included in this report. This work was carried out by other ARB contractors, e.g., Ross Wolford and Roger Bales of the University of Arizona, Rick Hooper of the USGS and Kelly Elder now at the Colorado State University. The reader is referred to Engle and Melack (1997) for a summary of the models and modeling results.

Plankton sampling was part of the original design for the Lake Comparison project begun in 1990. Results from the first three years of plankton sampling were reported to the ARB (Melack et al. 1993) and results from the zooplankton monitoring published in the scientific literature (Engle and Melack 1995). From these studies we concluded that zooplankton sampling in the study lakes was not of sufficient frequency or intensity (i.e., ~six times per year) to detect trends in abundance or community structure. Similarly, trends in phytoplankton populations, as measured by chlorophyll concentrations, are not detectable at the coarse sample frequency we employed. We therefore decided that there would be little gain from continued monitoring of zooplankton and phytoplankton and sampling was halted. All available data have been published in the above references, thus no additional data are presented in this report.

1.2. Watershed Descriptions

The eight study sites are located in the alpine and subalpine zones of the Sierra Nevada of California (Figure I-1). Their geographic locations span a majority of the north-south extent of the Sierran range. Four of the watersheds are located along the eastern slope of the range (Ruby Lake, Crystal Lake, Spuller Lake, Lost Lake) and the remainder are situated along the western slope (Emerald Lake, Pear Lake, Topaz Lake and the Marble Fork of Kaweah River). Seven of the catchments are glacial cirques (less

than 500 ha) containing lakes. The upper Marble Fork drains the Tokopah Valley of Sequoia National Park, a glacially carved basin of about 2000 ha which included, within its boundaries, the watersheds for Emerald, Pear, and Topaz lakes along with several other small lakes and ponds (Figure I-2).

1.2.1. Crystal Lake Watershed

The Crystal Lake basin (37°35'36"N, 119°01'05"W), situated in the eastern Sierra Nevada, is located about 10 km southwest of the town of Mammoth Lakes. Acid deposition studies were initiated in 1986. The lake has an area of 5.0 ha and volume of 324,000 m³ (Figure I-3). Typically, one to two meters of ice cover the lake for about 6 months of the year, displacing about 15-30% of the lake's volume (Figure I-3). During the years of record, Crystal Lake was usually ice-free by the end of June.

Crystal Lake has a maximum depth of 14 meters and mean depth 6.5 meters. The lake is dimictic, meaning its waters thoroughly mix twice a year. These mixing events occur in the spring during the breakdown of ice cover and during the autumn (Figure I-4). Maximum summertime surface temperatures in the lake ranged from 12 to 15 °C. Surface waters of the lake were well oxygenated (dissolved oxygen > 7 mg L⁻¹), however, dissolved oxygen concentrations of less than 5 mg L⁻¹ in the hypolimnion (i.e., waters below thermocline) were common during the winter months (Figure I-4).

The gauged Crystal Lake watershed is 135 ha and has a vertical relief of 293 meters (Figure I-5). The elevation of the outlet to the gauged catchment is 2,951 meters. The basin has a north-facing aspect and is sparsely forested for about half its area with a mixture of Whitebark and Lodgepole pine (Figure I-6). Much of the runoff from the catchment flows through an extensive meadow complex (heather, grasses, sedges and other shrubs) located along the south shore of the lake.

The eastern and southern portions of the Crystal Lake basin are dominated by a granitic dome and extensive talus. These rocks range in composition from granodiorite to alaskite with an average composition of mafic quartz monzonite. The rocks are generally coarse-grained and commonly porphyritic with phenocrysts of potassium feldspar. The remaining basin is dominated by bedrock and soils of volcanic origin. The rocks are a series of interbedded andesitic flows, cinders and rubble. The flow rock is commonly vesicular and essentially, nonporphyritic (Huber and Rinehart 1965). The soils are classified as Volcanic Brown Soils (appendix) and occur in various assemblages of rock, scree and talus (Figure I-7). Soils in the inlet meadow are classified as Volcanic Wet Meadow. The typical Alpine Brown Soils found at most of the other catchments were not found in the Crystal Lake watershed. Compared to other study catchments, the Crystal Lake watershed has a high percentage of soil cover and vegetation.

During snowmelt three major runoff channels were identified. Inflow #1 and the Main Inflow drain the eastern and southern portions of the basin. A smaller channel, Inflow #2, drains the western region of the watershed. These inflow and outflow streams are ephemeral and flow only during snowmelt or shortly after autumn precipitation; during the winter outflow is usually absent. Groundwater discharge comprises a substantial fraction of the annual loss of water from the catchment (see Chapter Two). Crystal Lake contains brook and rainbow trout.

1.2.2. Emerald Lake Watershed

The Emerald Lake basin (36°35'49"N, 118°40'29"W) is located in Sequoia National Park along the western slope of the Sierra Nevada. Monitoring at the Emerald Lake basin was begun in 1982. The outlet to the basin lies at an elevation of 2800 m (Table 1). The 120 ha watershed is granitic with steep slopes (mean slope 31°) and 616 meters of vertical relief. Bedrock is mainly granodiorite with mafic inclusions, aplite dikes and pegamite veins (Sisson and Moore 1987, Clow 1987). Poorly developed soils cover about 20% of the watershed and these are acidic and weakly buffered (Huntington and Akeson 1987, Lund et al. 1987). The soils are of the Alpine Brown variety (see appendix). The primary clay minerals are vermiculite, kaolinite and gibbsite (Lund et al. 1987). Vegetation in the Emerald Lake basin is sparse (Rundel et al. 1988), consisting of scattered conifers (Lodgepole and Western White Pine), low woody shrubs, grasses and sedges.

Precipitation in the Emerald Lake basin is strongly seasonal, with snowfall accounting for most of the deposition (Chapter Two, Melack et al. 1997). Ice covers the lake during the winter and spring and typically persists for 6 to 9 months (Figure I-8). Ice thickness and persistence depend on the quantity of snowfall during the winter as well as the frequency and severity of avalanches onto the lake. The thickest ice-cover measured on Emerald Lake occurred during water year 1986 when, due to abundant snowfall and a large avalanche, the lake was covered by 6 meters of slush and ice. Over 75% of the lake's volume was displaced by ice during the winter of 1986. In other years ice thicknesses ranged from about 1 to 3 meters which represents about 20-40% of the volume of the unfrozen lake. Typically ice-cover disappeared by mid June but in 1983, 1986 and 1993 some ice persisted until mid July or early August.

Emerald Lake is fed by 4 channelized inflows during the snowmelt season; a single outflow channel drains the basin. No significant outflow is lost via groundwater or seeps (Kattelmann and Elder 1991). A reproducing population of brook trout are found in the lake and its outflow stream.

Emerald Lake covers an area of 2.7 ha or 2.3% of its watershed (Table 1). The maximum depth of the lake is 10 meters and the mean depth 6.0 meters (Figure I-8). Emerald Lake has a volume of approximately 162,000 m³. The lake is of modest size compared to its catchment based on comparisons among the lake volume to watershed area indices (V/A index) for other catchments (Table 1). This index is a rough approximation of the affect of lakes on outflow discharge and chemistry. The larger the index the more lake influence on outflow discharge (via lake storage and release of water) and chemistry (via biogeochemical processes in the lake). The units for this ratio express the amount of runoff (i.e., discharge expressed as the average depth of water covering the basin) required to completely flush the lake. At Emerald Lake, 0.14 meters of runoff are required to displace the lake's volume. Hence, in 1993 when 1.6 meters of runoff was measured, Emerald Lake was flushed more than eleven times.

The lake is dimictic, with spring turnover typically in late May or early June (Figure I-9). Fall turnover occurs during September or early October. Thermal stratification is weak during the summer; inverse stratification occurs during winter and spring. During the 12 years of record, peak summer temperatures in the lake ranged from a low of 11°C in 1983 to 20°C in 1990 and were related to the quantity of snowmelt

runoff: higher runoff resulted in lower maximum temperatures. Surface waters in Emerald Lake are well oxygenated year-round. Periods of low oxygen were observed during both winter and summer stratification during the early years of the monitoring program (i.e., 1983 through 1986). The lake was sampled less frequently during water years 1988 through 1994 and it is likely that low-oxygen periods were missed.

1.2.3. Lost Lake Watershed

The Lost Lake watershed (38°51'37"N, 120°5'48"W) is located in the northern Sierra Nevada near Lake Tahoe in the Desolation Wilderness of Eldorado National Forest. Research at Lost Lake began in 1989. The lake is shallow (mean depth 1.9 m) and small in comparison to the other lakes (V/A index, 0.05 m; Table 1). During winter, the lake freezes to a depth of 1 to 2.5 m which represent 35-72% of the lake's volume (Figure I-10). Ice typically formed in November and persisted until June.

Lost Lake has the smallest volume (12,500 m³) and surface area (0.7 ha) of the seven study lakes (Table 1, Figure I-10). Complete mixing of the lake took place in late spring and in the autumn (Figure I-11). Thermal stratification occurs during the summer but is weaker than winter (inverse) stratification. Winter stratification is associated with near anoxia (dissolved oxygen ~ 0) in the hypolimnion during most winters; surface waters had O₂ levels above 5 mg L⁻¹ during other periods. Maximum lake temperature ranged from 13°C (1993) to 21°C (1991). A healthy population of brook trout is present.

The Lost Lake watershed has the lowest elevation (2,475 m) and has the least vertical relief of the study catchments: 160 m (Table 1, Figure I-11). The watershed has a north-facing aspect. Two channelized inflows have been identified during snowmelt: Inflows #1 and #2. Hemlock, Lodgepole Pine and Western White Pine line the shore of the lake and are scattered, along with patches of shrubs, throughout the watershed. Several areas of wet meadows are found around the lake. Most of the remaining catchment is composed of bedrock or bedrock with small inclusions of grass-covered, Alpine Brown Soils.

1.2.4. Pear Lake Watershed

The Pear Lake basin (36°36'02"N, 118°40'00"W) is located in Sequoia National Park about 1 km northeast from Emerald Lake (Figure I-2). Monitoring began in 1986. Pear Lake is relatively large and deep compared to most of the other lakes. The lake has a maximum depth of 27 m, a mean depth of 7.4 m and volume of 591,000 m³ (Table 1, Figure I-15). Because of its depth, thermal stratification is strong during much of the year and low dissolved oxygen concentrations occur in the hypolimnion (Figure I-16). Mixing of the lake occurred during the spring and autumn but appeared to be incomplete; water temperatures at a depth of 25 meters rarely exceeded 5°C. As a consequence, redox potentials are low in the hypolimnion as evidenced by the accumulation of hydrogen sulfide, ammonium, and iron and the low pH in these waters (Sickman and Melack 1989).

The outlet to Pear Lake lies at an elevation 2,904 m and the vertical relief of the drainage basin is 471 m (Table 1, Figure I-17). Owing to the large volume of the lake, the V/A index is high (0.45 m) relative to the other study sites indicating that Pear Lake has a greater influence on outflow discharge and chemistry. The lake is fed by one major inlet stream during most of the year, but probably receives a significant portion of snowmelt

from sheet flow off of extensive areas of exposed bedrock surrounding the lake (see Figure I-18). The outlet typically flows year round, but can dry up when snowfall is low and non-winter precipitation light (e.g., water year 1990).

Most of the Pear Lake watershed is composed of coarse-grained granites containing sparse mafic inclusions of widely variable size and texture. The remainder of the basin is underlain by medium-grained, porphyritic granodiorite (Sisson and Moore 1987). Greater than 90% of the catchment is composed of bedrock, talus and boulders (Figure I-18). What little vegetation is found in the basin consists of a few stands of coniferous trees (Lodgepole Pine, Western White Pine, Red Fir), shrubs, grasses and sedges. Soils, where present, are classified as Alpine Brown.

1.2.5. Ruby Lake Watershed

The Ruby Lake watershed (37°24'50"N, 118°46'15"W) is situated on the eastern slope of the Sierra Nevada in the John Muir Wilderness of Inyo National Forest. Research in this basin began in 1986. The lake is the largest (12.6 ha) and deepest (maximum depth 35 m) in the study, has the greatest volume ($2 \times 10^6 \text{ m}^3$) and lies at the highest altitude (3,390 m) (Table 1, Figure I-20). Ice typically covers the lake from November through May and continues into June and July during years with abundant snowfall. Ice thickness varied from 1 to 2 meters during the 8 years of record which corresponds to a displacement of 12-17% of the lake's volume. Ruby Lake is dimictic, turning over in the late spring and in the autumn. Strong to moderate thermal stratification occurred during both winter and summer (Figure I-21). Maximum summer lake temperature ranged from 11 to 16°C. Similar to Pear Lake, waters near the bottom of the lake rarely warmed above 5°C which may indicate that Ruby Lake does not mix completely during overturn. Associated with stratification were intervals of low hypolimnetic oxygen, however, unlike Pear Lake, no accumulation of hydrogen-ion, hydrogen sulfide, ammonium or iron was observed in Ruby Lake.

Ruby Lake has the highest V/A index of the study catchments (0.47 m) indicating substantial lake influence on the quantity and quality of basin discharge. This influence was greatest in years such as 1992 when the quantity of runoff (0.44 meters) was insufficient to completely flush the lake. The outflow runs year-round, suggesting there is substantial groundwater and lake storage and release. Of the seven lake basins, Ruby Lake has the largest catchment (gauged area 441 ha) and most watershed relief (812 m) (Table 1). The highest elevation in the catchment is 4,202 m asl (Figure I-22) and the basin has a northwestern exposure.

The bedrock in the Ruby Lake watershed is composed predominantly of quartz monzonite of Mono recesses. This rock is typically coarse-grained and strongly porphyritic and contains minor amounts of hornblende and sphene (Lockwood and Lydon 1975). Bedrock outcrops, talus and boulders cover most of the catchment (Figure I-23). Soil cover is sparse (Figure I-24) and most are classified as Alpine Brown (see appendix). The higher cirques of the basin contain talus fields and rock-covered glaciers. These glaciers are actively eroding the watershed, as evidenced by glacial flour in the major inflow to the lake. Two other significant runoff channels have been identified (1) the Cirque Inflow which drains a portion of the watershed southwest of the lake that is covered with bedrock, boulders and talus and (2) the Mono Pass Inflow which originates

from the northern portion of the watershed containing a large areas Alpine Brown Soils-complexes and talus. Sparse stands of Whitebark and Lodgepole Pine are confined to areas along the north and northeast edge of the lake (Figure I-23), however, the in the majority of the grasses, sedges and low shrubs are the dominant vegetation classes.

1.2.6. Spuller Lake Watershed

The Spuller Lake basin (37°56'55"N, 119°17'2"W) is located in the Hall Research Natural Area near Tioga Pass. Research began in 1989. Spuller Lake is shallow (mean depth 1.6 m), has small volume (34,700) but in area (2.2 ha) is similar to Emerald Lake (Table 1, Figure I-25). From November thorough June the lake was covered by 1 to 3 meters of ice, and these thicknesses correspond to 50 to 85% of the lake's volume. Little or no thermal stratification occurred in Spuller Lake during the summer because of its shallow depth (Figure I-26). In the winter the lake was inversely stratified and oxygen depletion occurred in the hypolimnion. At other times of the year, lake waters were well oxygenated.

The watershed has a predominantly northeast aspect and large vertical relief (537 m) (Figure I-27). The V/A index is small (0.04 m) and the lake probably exerts little influence on outflow discharge or chemistry. The lake is supplied by one major inflow. The lower portions of the watershed are composed of ancient tuffaceous lake beds. These beds are fine-grained and thin and composed chiefly of volcanogenic sediment. Common minerals include plagioclase, quartz, biotite, hornblende and opaque minerals; calcareous layers contain calcite, diopside, hornblende, epidote and trace amounts of sheelite (Bateman et al. 1983). Most of the watershed, however, is composed of talus and bedrock outcrops with associated Alpine Brown Soils (Figures I-28, 29). These rocks are dark-colored, medium-grained hornblende-biotite granodiorite (Bateman et al. 1983). The watershed is nearly devoid of trees and most vegetation is confined to areas near the lake. The dominant vegetation classes are meadows of grass and sedges and small stands of dwarfed and stunted White Bark Pine (Figure I-28). A small population of reproducing Brown Trout is present.

1.2.7. Topaz Lake Watershed

Topaz Lake (36°37'30"N, 118°38'11"W) is located at the head of the Tokopah Valley in Sequoia National Park, about 6 km north-northwest of Emerald Lake (Figure I-2). Research at this catchment began in 1986. The lake is shallow (mean depth 1.5 m) covering an area of 5.2 ha and with a volume of 76,900 m³. The lake is connected by a narrow channel to a small, shallow pond during high-water periods. This pond is similar in chemical composition to Topaz Lake. During the seven years of record, the lake froze to depths of 1 to 2.9 meters which corresponds to 50-94% of the lake's volume. In extreme winters, such as 1983, it is likely that the entire lake is composed of ice and slush. Thermal stratification of the lake is confined to winter months (Figure I-31). Low dissolved oxygen concentrations were measured during most winters; surface waters were always well oxygenated. Maximum summertime lake temperatures ranged from 14 to 19°C.

No fish were observed in Topaz Lake despite the fact that trout were stocked several times this century; the lake is probably too shallow and the outlet stream too

rugged and steep to support fish. Trout exert a substantial influence on the zooplankton and zoobenthos of Sierran lakes (Stoddard 1986 and 1987, Melack et al. 1989). In contrast to lakes with fish, large zooplankters (Diaptomus eiseni, Daphnia middendorfianna) are plentiful in Topaz Lake (Melack et al. 1993). Callisbaetis, hemipterans and dytiscid beetles (Hydroporus) were also abundant relative to populations in other lakes and ponds within the Tokopah Valley (Melack et al. 1989).

Vertical relief in the basin is 275 meters and the watershed has a southern exposure (Figure I-32). Parts of the upper basin have extensive meadows (grasses and sedges) and short-lived ponds during snowmelt (Figure I-33). There is a small stand of Foxtail Pines in the upper eastern portion of the watershed (~25 trees). Alpine Brown Soils are found throughout the watershed, often forming complexes with rocks and bedrock outcrops (Figure I-34). Extensive wet meadows are found along the north shore of Topaz Lake and around the other ponds in the basin. The geology of the basin is dominated by fine-grained, porphyritic granodiorite containing abundant mafic inclusions. The phenocrysts include potassium feldspar, hornblende, biotite and plagioclase (Moore and Sisson 1987). Because of the gentle relief surrounding it, the lake expands during snowmelt, flooding a small meadow along the northern shore and forming a large bay (see Figures I-32 and 33). This bay comprises a substantial portion of the lake's area, although not its volume. As summer progresses the lake level declines and the water retreats from the bay. Besides the lake and the shallow pond, other surface waters in the catchment are short-lived. During drought years, the water level in the lake dropped by as much as a meter below the outlet elevation.

1.2.8. Marble Fork of the Kaweah River

The headwaters of the Marble Fork of the Kaweah River (Figure I-2) (36°36'22"N, 118°40'59"W) are located in the Tokopah Valley of Sequoia National Park. The Tokopah Valley includes the Emerald, Pear and Topaz lakes which, along with several other small ponds and lakes, comprise 30 ha of the basin's 1,908 ha drainage area. The river is a second order stream where it is gauged near the mouth of the valley (elevation 2,621 m). The highest point in the watershed lies at an altitude of 3,493 meters. The V/A index for the Marble Fork watershed is small, suggesting that lakes and ponds in the basin have little influence on river discharge or chemistry. The river never went dry during the two years of study, but during the 1987-1992 drought, periods of zero or near zero flow were observed early in the autumn.

The geology of the Tokopah Valley is dominated by fine and medium-grained, porphyritic granodiorite and coarse-grained granite. Most of the basin is composed of bedrock and talus but there are significant areas of Wet Meadow Soils in upper portions of the basin (i.e., Table Meadows) and along the margins of the river-course. Trees, mainly Lodgepole Pine and Western White Pine and willows, are found along side the river as it meanders through the valley. The higher elevations of the catchment, including the upper portions of the Pear and Emerald lake watersheds, have sparse vegetation composed primarily of sedges and grasses.

Brook trout have been observed in the Marble Fork River but appear to be restricted to reaches below the confluence of the Pear Lake outlet. Just above this confluence the bed of the river is composed of steep, smooth bedrock. Rapid and

turbulent flows occur during snowmelt and under low-flow conditions the river fans out over the rock surface, reducing water depths to just a few centimeters. These conditions preclude the migration of trout upstream and may partially explain the lack of fish in the upper reaches of the river and at Topaz and Frog lakes.

1.3. Methods

1.3.1. Lake and Stream Monitoring

Lakes were sampled approximately bimonthly (i.e., 6 -7 times per year) during the period from October 1986 through June 1994. From 1983 through 1987, Emerald Lake was sampled biweekly (i.e., every two weeks) during the ice-free seasons and monthly during the winter. Samples for chemical analyses were collected from three or four depths in the lakes. A single sampling station, overlying the deepest portion of each lake was used during most years. Multiple (2 to 4) stations were periodically sampled in Emerald lake during water years 1983 through 1986. Lake samples were obtained from a small inflatable boat (ice-free seasons) using a Kemmerer bottle (1983-1986) or an all-plastic peristaltic pump connected to Tygon tubing (1987-1994). The tubing was weighted with a rubber stopper and lowered to the proper depth. At least two tubing volumes were flushed before sample collection. During periods of ice cover, an ice auger was used to reach the water. Water from each sampling depth was split into filtered and unfiltered subsamples for transport. Vertical profiles of dissolved oxygen and temperature (1 meter intervals) were measured using a portable meter (YSI model 58) equipped with polarographic oxygen electrode and thermistor.

Outflows and inflows were sampled concurrently with the lakes. Outflow chemistry was monitored more intensively during snowmelt (ca. April through June) beginning in water year 1990 (see Chapter Three). Inflows were sampled during snowmelt when they were free of snow (data not reported here). Prior to water year 1993, samples were collected by hand (grab sample) in polyethylene bottles. Beginning in water year 1993, automated samplers (ISCO) were used to collect outflow samples at some catchments (Chapter Three).

All apparatus and bottles used in surface water sampling were soaked in deionized water (DIW) for several days and then rinsed 5 times with DIW. During the early years of the project (1983 through 1989) bottles were routinely soaked with 10% HCl then rinsed with DIW. Our experience has shown, however, that acid washing does little to clean the bottles and increases the risk of sample contamination, hence this practice was discontinued. Major solute and nutrient samples were filtered with either Gelman A/E filters (prior to 1990) which were rinsed with at least 1 liter of deionized water or Nuclepore polycarbonate filters (1.0 micron pore size; 1990 to 1994). Our studies have shown that Gelman A/E filters can contribute sodium to samples unless they are thoroughly rinsed. All samples were kept cool and in the dark during transport. For long-term storage, major solute and nutrient samples were held in a coldroom or refrigerator at 5 °C.

Gran titration (Talling 1973) and pH measurements were done on unfiltered subsamples (grab samples) within 72 hours of collection using a digital pH meter and Ross (Orion) combination electrode. For samples collected in automated samplers, processing

was delayed up to two weeks. Specific conductance of unfiltered water was measured with a conductivity bridge (cell constant = 0.1) and readings corrected to 25 °C. Ammonium was determined on filtered samples generally within 72 hours by the indophenol blue method (Strickland and Parsons 1972). In general, samples collected during water years 1983 through 1988, had shorter delays before processing compared to later years.

For water years 1986 through 1994, chloride, nitrate and sulfate were measured by ion chromatography on a DIONEX model 2010i ion chromatograph, employing an AS4A separation column, conductivity detection and a micro-membrane suppressor. During water years 1983 through 1985, nitrate was determined colorimetrically within one week of collection using cadmium reduction (Strickland and Parsons 1972), and chloride and sulfate measured with ion chromatography. Delays for nitrate determination were on the order of weeks during water years 1986 and 1987 and on the order of months from 1990 onward. Calcium, magnesium, sodium and potassium were measured by flame atomic-absorption spectroscopy within a few months of collection. A Varian model AA6 spectrophotometer was used prior to 1992 and a Varian SpectrAA model 400 equipped with an autosampler was used from 1992 through 1994 for base cation analyses. Samples for calcium and magnesium had lanthanum or potassium added to reduce chemical interferences.

1.3.2. Precipitation Sampling

Detailed methods for precipitation sampling are found in Chapter Two of this report and in Melack et al. (1997). Samples of the snowpack were obtained by digging pits to the ground and collecting duplicate, contiguous, vertical sections every 40 cm using a transparent, PVC tube (5 cm diameter, 50 cm long, with a sharp, beveled cutting edge). Sampling was timed to coincide with the period of maximum snow accumulation which usually occurred during late March or early April. Two to four snowpits were dug in each catchment to sample snow with different exposure and altitude.

Each 40 cm snow section was placed into a separate polyethylene bag. Bags and sampling apparatus were soaked in deionized water for several days before use and kept scrupulously clean. Prior to 1989, bags were soaked with 10% HCl and then rinsed thoroughly with deionized water. This practice was abandoned because of the risk of HCl contamination (see Chapter Three and Melack et al. 1997). All snow samples were kept frozen at -20 °C until they were placed into polyethylene buckets and thawed at 5 °C. After melting, pH, ANC and specific conductance were determined using unfiltered samples employing the same equipment and techniques as used for the lake and stream samples. All samples for major solutes and nutrients were filtered through either Nuclepore polycarbonate filters (1.0 micron pore size, water years 1986-1994) or Gelman A/Es. A separate filtered subsample for organic anion analysis (formate and acetate) was preserved with chloroform. Tests showed no chloroform contamination of the organic anion samples. Anion concentrations (Cl^- , NO_3^- , SO_4^{2-} , HCO_2^- and CH_3CO_2^-) were determined by ion chromatography. Beginning in 1993, determinations of organic anions were completed within 24 hours of melting. Cations (Ca^{2+} , Mg^{2+} , Na^+ , K^+) were determined by the flame atomic absorption technique within a few weeks of melting.

Ammonium ion was determined within 48 hours of melting in filtered samples by the indophenol blue method (Strickland and Parsons 1972).

In order to estimate snow water equivalence (i.e., snowpack water content), snow density and snow-covered area were estimated for each basin (See Chapter Two for details). Snow density was determined in vertical 10 cm intervals along a continuous vertical profile in each sampling pit using a wedge-shaped, stainless steel cutter (Melack et al. 1997). Sections were weighed with a portable electronic balance. All cutters were calibrated and found to have less than 1% error in volume. Snow depth was measured with graduated, aluminum probes along transects from the lake shore to watershed boundary. Two to four transects representing approximately 200-300 depth measurements were made at each basin. Snow-covered area was estimated from aerial photographs taken near the time of the survey (± 10 days).

During snow-free seasons, precipitation was measured at each lake using a tipping-bucket rain-gauge (Qualimetrics model 6011-B) connected to a solid-state data logger. Precipitation samples were collected in polyethylene buckets using an Aerochemetrics rain collector during the months of ca. June through October. Snowboards and shallow snowpits were used to measure snow that fell after the maximum accumulation surveys. At some watersheds during some years, precipitation quantities were estimated from records collected at nearby catchments or weather stations. Non-winter precipitation monitoring is discussed in detail in Chapter Two.

1.3.3. Outflow Gauging

An automatic, stream gauging station, consisting of an Easylogger field computer (Omnidata International) and powered by a durable, weather-proof battery pack or solar panel, was installed in the outlet stream of each catchment. The field computers were mounted in trees or metal towers adjacent to the outflow streams. Stage (i.e., water depth) was continuously monitored with pressure transducers, installed in the stream bed and connected to the loggers. Staff gauges were installed near each transducer as a benchmark to check for transducer movement or electronic drift. Stream temperature was recorded on the dataloggers beginning in 1990. Stream gauging methods are covered more completely in Chapter Two. For details regarding stream gauging at Emerald Lake during water years 1985-87 see Dozier et al. (1989).

To develop relationships between the pressure transducers (i.e., stage) and outflow discharge, a lengthy calibration, using salt dilution estimates of discharge, was required. The salt dilution technique is described in Chapter Two. Discharge measurements were made during each sampling trip and intensively during the snowmelt periods. At all catchments, the range of the calibration discharges spanned the range of observed discharges. Weirs were installed in the outlets to Emerald and Spuller lakes during 1990 to improved discharge measurements.

1.3.4. Water Balance

The water balances involved estimating all hydrologic inputs and losses to the basins. The inputs to the watersheds were rain and snow; the losses were lake outflow and evaporation. The evaporation term includes sublimation of snow, lake evaporation and evapotranspiration.

Outflow discharge was calculated by converting transducer voltage (time-steps: 15 minutes from 1985 through September 1990; 1 hour from October 1990 through 1994) to discharge and then summing the flow from October 1 through September 30 (i.e., the water year). The major input to the water balance was snow. Winter snowfall was assumed to equal the amount of water present in the snowpack at or near peak accumulation (late March or early April), as calculated from basin snow-water equivalence and area. Non-winter precipitation was added to SWE to yield annual precipitation. See Chapter Two for details of the water balance calculations.

1.3.5. Watershed Solute Balance

Details on methods and results from the solute balances are presented in Chapter Three. The mass balance of solutes consisted of two components: loading of solutes by atmospheric deposition and outflow solute losses. Loading was subdivided into snow and non-winter precipitation. Solute loading by snow was calculated from the volume-weighted mean (VWM) concentration of each solute multiplied by the total volume of snow at maximum accumulation divided by catchment area. The solute flux for non-winter precipitation was calculated by multiplying the volume-weighted mean concentration for this precipitation by its total volume and dividing by catchment area. Total solute loading is the sum of snow and non-winter precipitation loading. Solute export in the outflow of each lake was calculated from annual VWM outflow chemistry and annual discharge normalized to catchment area.

Solute yield from watersheds was computed as the difference between loading and export and expressed as equivalents per hectare per year. A positive yield indicates that the loss of the ion from the watershed was greater than the supply; a negative yield indicates that the loss of the ion was less than the supply.

1.3.6. Meteorological Measurements

Evaporation can be calculated as the missing water balance term or it can be independently estimated. Independent evaporation estimates can be used as a check on the accuracy of precipitation and outflow measurements, i.e., if all of the water balance terms are separately derived, the overall error can be determined. Meteorological data are required for estimating evaporation. These data are available from existing stations near some of the watersheds (i.e., Mammoth Mountain near Crystal Lake, Eastern Brook Lake near Ruby Lake) and two meteorological stations were constructed; one at Emerald Lake (to provide data for Tokopah Valley catchments) and another at Spuller Lake. Variables measured included air temperature, relative humidity, wind speed and direction and incident radiation. Two radiation sensors were used: a pyrgeometer to measure long-wave radiation (4-50 μm) and a pyranometer to measure solar radiation (285-2800 nm). Easylogger units were used to record data at hourly intervals. For details of the evaporation studies and models used in this report see Chapter Four.

1.3.7. Soil Surveys

Soils were mapped in all lake basins with the exception of Emerald Lake which had previously been mapped by Huntington and Akeson (1987). The only portions of the Marble Fork watershed mapped were the Pear Lake, Topaz Lake and Emerald Lake

watersheds which together make up 23% of the Marble Fork drainage. In contrast to more traditional classification schemes, an alternative approach, specifically designed to aid biogeochemical and hydrological investigations, was used to map the soils. The approach was a synthesis of old and new ideas in pedology, utilizing genetic soil groups, with no operational linkage to soil taxonomy per se. The genetic soil groups were locally defined based on their morphology, landscape setting and accepted theories in pedology, soil biogeochemistry and ecology. The appendix describes the soil classification approach fully and contains a more detailed account of the soil characteristics of each watershed than was presented in the site descriptions.

1.3.8. Geographic Information Systems (GIS) and Vegetation Mapping

Hand drawn maps produced from the soil inventories described above were converted to digital form using Arc/Info, a Geographic Information System. In building the database of coverages, tics (geographic control points) were chosen that could be easily located on areal photos and topographic maps. These reference points were permanent landscape features that were marked on the mylar sheets of the preliminary soil and vegetation maps.

Coverages were digitized using Arc/Info Version 7.0.3 on a Sun Sparc Station and labeled according to the mylar classifications. Cleaned and labeled coverages were imported into ArcView Version 2.0 (Windows) and maps were created for each soil and vegetation coverage. Digital Elevation Models (DEMs) for each basin were cropped out of standard USGS DEMs of each area.

Vegetation classification was done using a combination of color infrared and true-color photographs of each basin. The aerial photographs were shot at a scale of 1:4000 except at Lost Lake where the scale was 1:2000. Vegetation mapping of the Emerald Lake basin was done by Rundel et al. (1988). Because vegetation correlated highly with soil distribution, soil polygons were used as a base for the vegetation maps. Polygons were altered and created, where necessary, to accurately map vegetation types and coverages. Color infrared photographs were not available for the Lost Lake watershed. As for soils, the only portions of the Marble Fork watershed mapped for vegetation were the Pear, Topaz and Emerald lake drainages.

Vegetation was classified based on both form and percent cover. Vegetation types include T (trees), S (shrubs, i.e., dry soils with shrubs and grasses), M (meadow, i.e., wet soils with shrubs and grasses), and G (grass and sedges). Bare rock and water are also included as categories. Vegetation types were assigned a percent cover class of 1 (5-20% coverage), 2 (21-40% coverage), 3 (41-65% coverage), and 4 (66-100% coverage). It is assumed that the remaining percentage of each polygon is devoid of vegetation.

Each polygon was assigned only one vegetation type which is problematic since actual vegetation is often a mixture of several types. For example, in the tree category many of the polygons are a mix of trees and some form of understory vegetation, mainly grass and/or shrub. Vegetation types are not identical at all basins. For example, trees species, shrubs and grasses types may vary from basin to basin. Trees tend to grow near each other but with no overlapping of crowns. Shrubs tend to have similar patterning and distribution as trees. Grasses and meadow tend to be evenly distributed over a given polygon. The G1 and G2 classes were colored in gray tones to reflect the large

percentage of bare rock in these polygons. Vegetation classification was done entirely from the aerial photographs with no field checking.

Some minor error resulted from the delineation of the drainage areas of some basins. Boundaries used were transferred from USGS 7.5 minute topographic maps and overlaid on areal photos. Because of this, features of adjoining basins sometimes overlap into the drainage basin being mapped. Using watershed boundaries derived from the aerial photographs avoids this error but introduces incongruities with DEM data. An additional source of error was caused by incomplete coverage of some basins by the aerial photographs. Vegetation in missing areas was extrapolated from nearby polygons.

1.3.9. Quality Assurance and Control Procedures

A long-term investigation of regional differences in precipitation or surface water chemistry requires a strong quality assurance (QA) plan for sampling and analysis. Our QA plan was comprised of rigorous field and laboratory quality control (QC) procedures. We also implemented a QA program to ensure the integrity of precipitation and surface water samples collected in the field and to produce reliable analytical data for samples analyzed in the laboratory.

Our QA procedures included the following components: identical instruments are used and adherence to standardized data collection procedures and field protocols are emphasized with the field staff at all sites. Procedural variability in the field was assessed by duplicate cores and replicate samples at 5% frequency for snow and lake water, respectively, and by means of field blanks obtained on some sampling trips. In the laboratory, blanks include deionized water processed through plastic bottles, filters and buckets which assess contamination from buckets employed to melt snow and collect rain, from the membranes used to filter melted snow, and from bottles used to contain lake water.

Our analytical procedures incorporated the following internal and external checks of precision and accuracy:

pH: After a two point calibration with NBS-traceable buffers, the accuracy of the electrode was checked using dilute solutions of HCl (10^{-4} and 10^{-5} N).

ANC: After electrode calibration and accuracy checks as with pH, a titration was performed with NaOH (ANC, $30 \mu\text{Eq L}^{-1}$) or a synthetic water sample (ANC, $25\text{-}30 \mu\text{Eq L}^{-1}$).

Specific Conductance: A 10^{-4} M KCl conductivity standard, which had a theoretical specific conductance of $14.7 \mu\text{S}\cdot\text{cm}^{-1}$ at 25°C was measured frequently.

Cations and Anions: Duplicate samples were analyzed at a 5% frequency in each assay session to estimate within-run precision. Known additions were made to samples and standards in duplicate at a 5% frequency during each run to estimate within-run accuracy.

We also employed independent (external) checks on the accuracy of our chemical analyses. Routine analyses of standard reference materials (SRM) from the National Bureau of Standards (NBS) and the U.S. Environmental Protection Agency (EPA) were performed. The SRM was synthetic rain-water with certified concentrations for major cations and anions. Another independent check on our chemical data involved participation in the U.S. Geological Survey's Analytical Evaluation Program and Environment Canada's LTRAP Audit. These are regular audits that test the quality and

accuracy of the analytical procedures used in laboratories throughout the U.S. and Canada. These agencies distribute water samples to participating laboratories and participants submit their results to these agencies and are assigned a score based on how close their results come to the mean value obtained from all participants. Our laboratories have always scored well (good to excellent ratings) in these audits (see Sickman and Melack 1989, Melack et al. 1993, Melack et al. 1997 for results from these audits).

In addition to the above procedures, the internal consistency of the chemical data was validated by adherence to the criteria proposed by Drouse et al. (1985). Tests for consistency included departure from electroneutrality (i.e., charge balance) and comparison of calculated and measured specific conductance. Charge balance was evaluated as an ion balance ratio and as the absolute value of the sum of positive ions minus the sum of negative ions. The ratio was calculated as the percent difference (%IOD) between cations or anions: $[(\Sigma\text{cation} - \Sigma\text{anion}) \div (\Sigma\text{cation} + \Sigma\text{anion})] \times 100$. Theoretical specific conductance was calculated from the equivalent conductances (i.e., $\mu\text{S cm}^{-1}$ per $\mu\text{Eq L}^{-1}$) of measured ions and then compared with measured specific conductance. If ion concentrations are measured accurately then all major constituents are accounted for and the sum of cations should equal the sum of anions. If measured conductance is the same as theoretical conductance, all of the important ionic species have been determined and the measurements are unbiased.

1.3.9.1. QA/QC Results

The findings described below deal mainly with QA/QC results for lake and stream samples. Since these samples tend to have higher solute concentrations than snow samples and lower concentrations than summer rains, the QA/QC results were tabulated separately. Results from the QA/QC program for precipitation samples are contained in our companion report, Melack et al. (1997).

1.3.9.1.1. Specific Conductance

The YSI 3402 cell ($K = 0.1 \text{ cm}^{-1}$) was calibrated with 10^{-4}N KCl throughout the measurement period of 1990-1994. The specific conductance of the KCl standard was always within 12% of the theoretical value of $14.9 \mu\text{S}\cdot\text{cm}^{-1}$ at 25°C . Overall, precisions were better than ± 5 percent relative standard deviation for specific conductance.

1.3.9.1.2. pH

The Orion EA 920 meter equipped with a Ross 8104 electrode was first calibrated with NBS traceable pH 7.00 and pH 4.00 buffers. A further calibration with various concentrations of HCl prepared from certified 10^{-2}N HCl (Fisher-SA62-1) solution was then performed. Overall precision computed from pH 4.0 and pH 4.7 HCl standards were better than $\pm 2\%$ during the course of the study. Precisions of 0.5 and 0.6 percent relative standard deviation for pH measurements on a single day were computed using replicate measurements of snowmelt samples and of a USGS simulated snowmelt sample, respectively. Overall precisions for 1990 through 1994 were less than 2 %RSD for the 10^{-4}N and 10^{-5}N HCl solutions

1.3.9.1.3. Anion Accuracy

Accuracy was assessed by comparing measured values with certified values of NBS and EPA standard reference materials (SRM) and by spike recovery after known additions to duplicates of natural samples. The anion values measured for the NBS and EPA SRM's (which were included in each analytical run) were within the stated confidence limits for all situations except for sulfate in NBS-I and chloride in NBS-II (Table 2). However, the chloride concentration in this SRM was below the detection limit for the ion chromatograph (IC) and the sulfate level in NBS-I was outside the range of our usual IC calibration. It should be noted that few of our samples contain this much sulfate (i.e., $15 \mu\text{Eq L}^{-1}$) and when they did the IC was calibrated with higher standards. Overall accuracies, based on spike recoveries, were 95%, 98%, and 103% for chloride, nitrate and sulfate, respectively and include all sample runs from 1990 through 1994. Comparison of measured values with the SRM control values yielded accuracies of 98%, 103%, and 100% for chloride, nitrate and sulfate, respectively, excluding situations where the certified concentrations were below detection or outside the range of our typical calibration.

1.3.9.1.4. Anion Precision

Within run precision was computed as the percent relative standard deviation of the means of three kinds of samples. Randomly selected samples were analyzed in duplicate as natural and as augmented (known addition) samples. A synthetic laboratory control (LC) consisting of a known addition to a calibration standard was analyzed in duplicate in each run. For lake and stream water, overall precisions for chloride, nitrate and sulfate were 3.8%, 2.5% and 2.0% relative standard deviation, respectively (Table 2).

1.3.9.1.5. Cation Accuracy

Accuracy was assessed by comparing measured values with certified values of NBS and EPA standard reference materials and by spike recovery after known addition to duplicates of natural samples. For lake and stream water, the values measured for the NBS and EPA SRM's were within the stated limits for all situations except for calcium in the NBS-I control which indicated a slight bias for calcium (Table 2). However, the certified concentration was below the range of calcium values that we typically calibrate for. In addition, lake and streams samples have calcium levels greater than $0.6 \mu\text{Eq L}^{-1}$, i.e., 10 to $100 \mu\text{Eq L}^{-1}$. Using spike recoveries, overall accuracies were 96%, 103%, 106% and 103% for calcium, magnesium, sodium and potassium, respectively during the period of 1990 through 1994. Accuracies based on measured values of SRM's were (excluding calcium in NBS-I): 103%, 111%, 99% and 112%, respectively for calcium, magnesium, sodium and potassium.

1.3.9.1.6. Cation Precision

Within run precision was computed as the percent relative standard deviation of randomly selected natural and augmented samples analyzed in duplicate. For lake and stream water, overall precision for calcium, magnesium, sodium and potassium was 1.0%, 1.5%, 1.0%, and 2.0% standard deviation, respectively, and included all analytical runs from 1990 through 1994 (Table 2).

1.3.9.1.7. Field Blanks

Each year, prior to snow surveys, the polycarbonate snow corers were rinsed three times with deionized water and a final, fourth rinse was collected for chemical analysis. Contamination with major ions was undetectable ($< 0.1 \mu\text{Eq}\cdot\text{L}^{-1}$). Prior to installation, Aerochemetrics collection buckets were rinsed three times with deionized water. A final, fourth rinse with ca. 150 ml was collected for a chemical analysis. Contamination with major ions was usually negligible ($0.1\text{-}0.3 \mu\text{Eq}\cdot\text{L}^{-1}$). Detailed results from these rinses and other quality control indices can be found in Melack et al. (1997).

1.3.9.1.8. Laboratory blanks

Plasticware blanks included samples from ziplock bags, 125 ml and 30 ml high density polyethylene bottles, and filters at ca. 10% frequency. Plasticware was soaked in deionized water for several days and then rinsed 5 times with deionized water. Filter blanks were obtained from the buckets used to melt snow by filtering (1.0 micron polycarbonate membrane) a ca. 100 ml portion of the 250 ml of deionized water kept in contact at 4°C with the bucket for 24 hours. No significant contamination was detected in any of these blanks.

1.3.9.1.9. Charge and Conductance Balances

Electroneutrality indexed as the absolute value of the sum of positive ions minus the sum of negative ions affirms that measured ionic concentrations were accurate and that all major constituents were measured. Figures I-35 and 36 depict the frequency distribution of cations minus anions (both in absolute terms and as a percentage of total charges i.e., %IOD) for lake and stream samples for the period of 1982 through 1994. For lake and stream samples a mean %IOD of 0.003 was calculated and the frequency distribution indicates a slight bias toward excess negative charge (Figure I-35). The mean difference between cations and anions was -0.4 and indicating a small bias toward excess anion. The average total charges for a lake and stream sample was $126 \mu\text{Eq}\cdot\text{L}^{-1}$.

Another criterion applied to the data set was the computation of a conductance balance (theoretical divided by measured conductance). The mean conductance balance for lake and stream samples was 0.99 for the period of 1982 through 1994 (Figure I-35). The frequency distribution is slightly skewed towards balances greater than one, however the vast majority of samples have balances between 0.9 and 1.1. The conductance balance is especially useful when combined with %IOD (Figure I-36). Plotted together, they show the likely cause of observed charge imbalance. For example, %IOD greater than zero can be caused by either an over-estimation of cation or an under estimation of anion; the conductance balance can determine which of these errors is most likely. If the conductance balance was less than 1 (theoretical $<$ measured) then the charge imbalance was probably due to an underestimation of cation(s). In Figure I-36, four quadrants are delineated based on the type of error associated with the charge imbalance: left upper quadrant, overestimated anion; left lower quadrant, underestimated cation; right upper quadrant, overestimated cation; lower right quadrant, underestimated anion. The distribution of points in Figure I-36 shows a cloud of points centered around zero %IOD and conductance balance of one. No systematic over or under estimate is discernible from the plot which indicates that our analytical measurements are accurate and unbiased.

1.4. Results and Discussion

1.4.1. Annual Variability of Outflow Chemistry

Time-series plots of solute chemistry (pH, ANC, nitrate, sulfate, sum of base cations (i.e., calcium, magnesium, sodium, potassium), and dissolved silica) are presented for the outflow to each catchments for the snowmelt seasons of 1990 through 1993 for Pear, Topaz, Crystal and Lost lakes, for the snowmelt seasons of 1990 through 1994 for Emerald, Ruby and Spuller lakes and for 1993 and 1994 for the Marble Fork of the Kaweah (Figures I-37 through 84). Chemistry samples are denoted by open circles. The figures show daily discharge such that changes in stream chemistry can be related to the timing and magnitude of snowmelt runoff. Special attention is given to the period of snowmelt (i.e., April through September) because the majority of the efflux of solutes and water from the catchments occurs during these months, and solute concentrations rapidly change during the course of snowmelt runoff. Outflow from most catchments during the autumn and winter is either low or nonexistent.

Our goal in this section is to characterize the seasonal patterns in hydrochemical conditions and discuss similarities and differences in solute chemistry among the catchments. We will not describe each chemical time series ($n=178$) but will instead summarize the typical patterns of solute chemistry observed in these catchments (Figure I-85). Exceptions to these generalized patterns will be discussed.

Patterns were verified by statistical analysis of temporal changes in solute chemistry during the snowmelt periods of 1990 through 1994. The snowmelt period was divided into 4 stages based on cumulative discharge: stage one was the period from the onset of snowmelt through the first 25% of snowmelt runoff, stage two was the period between the end of stage one through 50% of cumulative runoff, stage three was the period between the end of stage two through 75% of cumulative runoff and stage four ran from the end of stage three until the end of snowmelt runoff. The volume-weighted mean concentrations for each solute were calculated for each stage for each year of data at all catchments. The Friedman analysis of variance on ranks was used to test for significant differences in solute chemistry among the snowmelt stages (Sokal and Rolf 1981). The test compared the effects of a series of different treatments, in this case snowmelt stages, on VWM snowmelt chemistry. For each year, the VWM concentrations for each catchments were ranked from smallest to largest without regard to other catchments or other years, then the rank sums for the stages were compared for the combined data set (33 catchment-years). When significant differences ($p<0.05$) were detected, the Student-Newman-Keuls multiple comparison test was used to isolate snowmelt stages with significant differences in chemistry ($p<0.05$). The Friedman repeated measures ANOVA on ranks is a nonparametric test that does not require normally distributed differences nor equal variance.

The four stages of snowmelt were chosen because they represent identifiably different parts of the snowmelt season and allowed us to verify the generalized patterns of solute chemistry we observed. Using fewer stages precluded us from identifying certain features such as the ionic-pulse of nitrate and the recovery of base cations, ANC and silicate in the later stages of snowmelt. Greater division was not possible because sampling frequency was usually too low.

Stage one of snowmelt was characterized by a mostly snow-covered watershed, an inversely stratified, ice-covered lake and low but increasing daily discharge. Stage two had significantly higher daily discharge, complete ice-cover and a high percentage of snow-covered area (SCA) in the watershed. Moderate SCA, incomplete ice-cover, a breakdown in lake stratification and high daily discharge characterized the third stage of snowmelt. By the fourth stage, the lakes were usually ice-free and weakly stratified, snow cover was sparse and discharge was low and declining.

1.4.1.1. Patterns of pH During Snowmelt

In contrast to other solutes, it is difficult to describe a consistent pattern of pH variation among the catchments or among water years (Figures I-37 through 44). The most common pattern was one of declining pH as discharge increased, with lowest pH's occurring sometime near the peak of runoff (Figure I-85). This pattern was often punctuated with transient pH increases or decreases that appear unrelated to discharge. The best examples of this pattern are from Emerald Lake 1993 and 1994 (Figure I-38) and Spuller 1993 (Figure I-43). Several other patterns of outflow pH were observed: (1) pH increased as discharge increased (e.g., Pear and Topaz lakes, 1991; Figures I-41 and 44), (2) pH reaches maximum at the peak of snowmelt runoff (e.g., Crystal and Ruby lakes, 1993; Figure I-37 and 42), (3) pH exhibits a pattern seemingly independent of discharge (e.g., Lost Lake, 1993; Figure I-39), (4) pH remains fairly constant despite large changes in runoff (e.g., Ruby Lake, 1990; Figure I-43). Based on the Friedman ANOVA, there was no significant difference in pH among the first 3 stages of snowmelt, but stage four had significantly higher pH than all other stages (Table I-1).

The change in outflow pH from premelt to peak runoff varied among lakes and among water years. When samples were available prior to the onset of snowmelt, the typical pH change was about ± 0.5 pH units. The range of observed changes varied from ± 0.2 to 1.0 pH units. Minimum pH values ranged from 5.5 to 6.1 but were usually near 5.8 and fairly consistent from year to year and among catchments with the exception of situations where ISCO samplers were used. Samples collected in this manner were equilibrated with ambient air prior to being sealed. In contrast, grab samples were sealed in polyethylene bottles immediately after collection so they had minimum contact with air. During snowmelt, equilibration with air had the effect of raising the pH between 0.2 and 0.4 units (see Emerald Lake 1993 and 1994; Figure I-38). This effect appears diminished during the summer and autumn; there was little or no difference in pH between ISCO and grab samples for this period. The ISCO effect is probably the result of out-gassing of dissolved CO_2 from the samples; stream waters in the Sierra are known to be supersaturated with CO_2 during snowmelt (Dr. John Stoddard, personal communication). Supersaturation has not been seen in surface waters during low flows which may explain the lack of an ISCO-effect on autumn stream samples. Automated samplers had no effect on ANC or other dissolved constituents.

1.4.1.2. Patterns of ANC During Snowmelt

The dominant pattern of ANC during snowmelt runoff is ANC decline as discharge increases with minimum ANC occurring at or near peak runoff (Figures I-45 through 52 and see Figure I-85). Near the end of snowmelt, ANC recovered but did not usually

match pre-melt levels. This generalized pattern is supported by the statistical analysis (Figure I-4) which shows significantly lower ANC during stages two and three; ANC in stage one was significantly higher ($p < 0.1$) than in stage four. The best examples of this pattern are from Emerald Lake in 1993 and 1994 (Figure I-46), and Crystal, Ruby and Spuller lakes in 1993 (Figures I-45, 50 and 51). At Topaz Lake, ANC minima tended to occur a few weeks after the peak discharge (e.g., 1991-93, Figure I-52). A pattern of increasing ANC with increasing runoff was also observed in few a cases (e.g., Crystal and Ruby lakes 1992, Figures I-45 and 50; Pear Lake 1990 and 1991, Figure I-49), but these examples were most likely the result of infrequent sampling and poor resolution of the ANC time-series.

Depression of ANC caused by runoff often began in the early stages of snowmelt (see Spuller Lake, Figure I-51). Outflow ANC declined by 25% to 80% as a result of snowmelt; the most frequently observed change was a decline of about 50% from premelt conditions. Minimum outflow ANCs observed during the study were typically in the range of 15 to 30 $\mu\text{Eq L}^{-1}$. The lowest values were usually observed in the Lost Lake and Pear Lake watersheds (i.e., 10 to 15 $\mu\text{Eq L}^{-1}$) and highest values were measured at Crystal Lake (i.e., 50 to 65 $\mu\text{Eq L}^{-1}$). The greatest absolute ANC change was observed in the Spuller and Ruby lake watersheds (declines of 70 to 90 $\mu\text{Eq L}^{-1}$ and 40 to 60 $\mu\text{Eq L}^{-1}$, respectively). At Crystal Lake, snowmelt induced changes were on the order of 20 $\mu\text{Eq L}^{-1}$ or a depression of about 25% from premelt conditions. At all catchments ANC depression tended to be greater during years with high runoff compared to drought years, with the best example of this being Emerald Lake in 1993 and 1994 (ANC minima of 10 and 15 $\mu\text{Eq L}^{-1}$, respectively; Figure I-46). The pattern of ANC in high-elevation catchments of the Sierra Nevada indicates that dilution of streamwaters with snowmelt is a major cause of ANC depression during the runoff season (Figure I-85).

1.4.1.3. Patterns of Nitrate During Snowmelt.

Nitrate had several patterns during snowmelt runoff (Figures I-53 through 60 and 85). In some catchments nitrate concentrations declined throughout the snowmelt period. The best examples of this pattern are Topaz Lake 1990-92, Marble Fork 1993, Pear Lake 1990 and 1992 and Spuller Lake 1991 and 1993. Results from the Friedman ANOVA on ranks support this pattern for the data set as a whole (Table I-4). A second pattern where a nitrate pulse occurred during stage 2 was seen during some years at nearly all catchments (Topaz Lake was the exception), most notably at Emerald and Ruby lakes (see Nitrate-2 in Table I-4). The ANOVA on ranks for Emerald and Ruby lakes showed significantly higher nitrate concentrations during stage two than in stages one or three. Good examples of the pulse pattern at other catchments include Crystal 1993, Lost Lake 1990, Marble Fork 1994, Pear Lake 1991 and Spuller 1990 and 1992. Mechanistically, the pattern appears to be the result of a pulse of nitrate during the early stages of melt followed by depletion of nitrate caused by biological uptake in later stages, hence the label: Pulse/Depletion in Figure I-85. Because of high sample frequency during the onset of snowmelt, the best examples of this nitrate pattern are from Emerald Lake during 1993 and 1994. The pulse-dilution pattern may have been missed at other lakes because stream samples in the very earliest portions of snowmelt were often lacking (e.g., Lost Lake

1991-93, Marble Fork 1993, Pear Lake 1990, 1992 and 1993 and Spuller Lake 1991 and 1993).

At Topaz Lake during water years 1988, 1991 and 1993, unusually high nitrate concentrations were measured during the winter and in the spring prior to snowmelt. Levels were on the order of 40 to 175 $\mu\text{Eq L}^{-1}$, much higher than peak nitrate values of less than 20 $\mu\text{Eq L}^{-1}$ observed at other catchments. At Topaz Lake, nitrate declined rapidly during snowmelt (Figure I-60) suggesting that dilution is the major process controlling nitrate levels during snowmelt. However, as snowmelt declined in the summer and autumn, nitrate concentrations in the outflow to Topaz Lake often increased rapidly, reaching levels of tens of microequivalents per liter (i.e., 1991 and 1993; Figure I-60 and 106).

High nitrate concentrations at Topaz Lake were not associated with nitrate-rich precipitation events. Preferential elution of nitrate from the seasonal snowpack is also unlikely since no snowmelt was generated prior to March (see Chapter Two). During low-flow periods, the outflow stream is supplied by groundwater and, in winter, lakewater that is displaced by snowfall. The groundwaters in this basin have never been sampled, but high nitrate ($>20 \mu\text{Eq L}^{-1}$) and ammonium ($>10 \mu\text{M}$) levels have been measured in the lake on several occasions. These data suggest that biological processes exert a large degree of control on the accumulation and release of nitrate in the Topaz Lake catchment. The influence of biogeochemical processes on nitrogen dynamics in Sierran watersheds are discussed in detail in Chapter Three of this report.

Peak nitrate concentrations in catchment outflow during snowmelt varied by as much as ten-fold among the study catchments. Significantly lower ($p < 0.01$) concentrations were observed at Lost and Crystal lakes (Figures I-53 and 55) where peak values ranged from about 0.5 to 2.0 $\mu\text{Eq L}^{-1}$, despite inflowing waters commonly having nitrate levels greater than 5 $\mu\text{Eq L}^{-1}$ (see Sickman and Melack 1989). The Emerald Lake and Marble Fork drainages had nitrate maximums of between 6 and 8 $\mu\text{Eq L}^{-1}$ during most years (Figures I-54 and 56). Despite different snowmelt seasons (e.g., timing and total quantity) the peak nitrate concentration was nearly the same at Emerald Lake during 1993 and 1994. At Pear and Ruby lakes peak nitrate levels ranged from 7 to 12 $\mu\text{Eq L}^{-1}$ during snowmelt. Highest snowmelt nitrate levels were observed in the outflow from Spuller Lake. Peak concentrations were consistent from year to year, i.e., $13 \pm 3 \mu\text{Eq L}^{-1}$.

1.4.1.4. Patterns of Sulfate During Snowmelt.

Patterns in sulfate concentration were qualitatively similar to nitrate patterns but the magnitude of the changes were smaller (Figures I-61 through 68). Sulfate, on some occasions, exhibited a Pulse/Dilution pattern similar to nitrate, however, changes in sulfate concentration during the course of snowmelt were smaller. The best examples of this pattern are Marble Fork 1994, Ruby Lake 1990, 1991 and 1993, and Emerald Lake 1991 and 1994. In other cases dilution throughout snowmelt was the observed pattern and this was the overall pattern identified from the statistical analysis (Figure I-4). This pattern was particularly striking at Spuller Lake where sulfate declined from levels of 15 to 25 $\mu\text{Eq L}^{-1}$ before melt to ca. 5 $\mu\text{Eq L}^{-1}$ at peak runoff (Figure I-67). However, the magnitude of sulfate decline varied considerably among the watersheds and reductions of less than 1 to 2 $\mu\text{Eq L}^{-1}$ were observed in many cases (e.g., Crystal Lake 1990, 1992,

1993, Emerald Lake 1990, 1992, 1993 and Pear Lake 1990, 1992). In these situations, sulfate declined by less than 30% from concentrations prior to snowmelt. Sulfate dilution was less, in both absolute and relative terms, than dilution of ANC, base cation or silicate in most cases. These findings suggest there is some biogeochemical process(es) in the catchments regulating sulfate concentrations. This process(es) initially sequesters sulfate released from the snowpack during the ionic pulse and then releases sulfate back into surface water during periods of high runoff, mitigating the dilution effect which was observed for ANC, base cations and silicate (see below).

Possible mechanisms of sulfate regulation include pH- or discharge-dependent sulfate adsorption in soils. Williams and Melack (1997) found evidence that sulfate loading from precipitation and snowmelt was temporarily stored by catchment soils in two mixed conifer watersheds in Sequoia National Park and its release controlled by the extent of soil flushing. Clow et al. (1996) in a study of surface water chemistry in the Upper Merced River Basin (Yosemite National Park) found that sulfate concentrations varied much less than other solutes and suggested sulfate levels are regulated, to some extent, by within-watershed processes such as sulfate-adsorption onto the surfaces of Al and Fe sesquioxides. However, studies of geochemical controls on surface water chemistry from the Miniwatersheds (Tokopah Valley) show that soil pH remained fairly constant or decreased slightly over the course of snowmelt (Williams 1997). Since sulfate absorption is enhanced when soil pH is low and decreases as pH increases, the authors concluded that desorption of sulfate was not occurring in these small catchments.

1.4.1.5. Patterns of Base Cations and Silicate During Snowmelt

The dominant pattern of base cations (i.e., sum of calcium, magnesium, sodium and potassium) and dissolved silica in outflow was dilution caused by snowmelt (Figures I-63 through 84 and 85). All of these solutes declined substantially during snowmelt, reaching minima at or near the time of peak runoff (see Emerald 1993-94, Figures I-70 and 78); a pattern confirmed by results from the statistical analysis of snowmelt chemistry (Table I-4). Base cations were significantly lower ($p < 0.05$) during stage three (highest daily discharge) than stages one and two; SBC in stage four was significantly higher ($p < 0.1$) than in stage 3 but less than in stage one, indicating an incomplete recovery of base cation at the end of snowmelt. Silicate showed a similar pattern but there was no statistical difference between stages two and three.

Similar to ANC, snowmelt dilution of base cations and silicate in outflow streams tended to be greater in years with high runoff (i.e., 1993) compared to drier years (i.e., 1994). Silicate and base cations were sensitive to fluctuations in runoff during snowmelt. Fluctuations in streamflow caused by passing weather systems (cold fronts) are common during the months of April through June and a good example of this occurred during the snowmelt period of 1993. In late May and early June a series of cold fronts brought light snow and colder temperatures to California. Snowmelt runoff declined during these intervals causing an increase or leveling off of base cations and silicate concentrations in the outflow from nearly all catchments (Figures I-69 through 84). The exceptions were Lost Lake, where sampling frequency was too low to discern an affect, and the Marble Fork where increased concentrations lagged behind the decline in discharge (Figures I-72 and 80).

Two additional observations are worth noting. Silicate concentrations at Crystal Lake changed little during snowmelt in comparison with the other catchments (see 1993, Figure I-77). This finding is similar to the pattern found for sulfate at this watershed and suggests some regulatory mechanism for moderating silicate concentrations. We also observed a sharp decline in silicate levels in surface waters during May 1992. During this period silicate concentrations ranged from below detection to about 15 μM in the inflows and outflows of all catchments. For example, at Lost Lake, silicate concentrations were 5 μM on May 3, 9 μM on May 9 and 0 μM on May 21. Similar values were measured at other catchments. By the beginning of June levels had returned to normal at nearly all sites. No cause has been identified for these low silicate concentrations. Precipitation can be ruled out as there was only a trace of snow during this period and no large fluctuations in runoff were associated with the silicate decline. Since the decline occurred in the inflows to the lakes as well as the outflows it is unlikely that in-lake processes (i.e., diatom bloom) were responsible. Given the universal extent of the phenomenon and the lack of a reasonable cause, analytical error must be considered. One possibility is that the sub-samples for silicate analyses were mistakenly frozen prior to processing. We have run tests that demonstrate a near total loss of silicate in samples due to freezing and we believe this is the most probable explanation. No unfrozen samples from these dates exist so we are unable to determine the true silicate concentrations for these dates.

1.4.2. Long-term Trends in Lake and Outflow Chemistry

One objective of our monitoring program was the characterization of long-term variability and trends of surface water chemistry in the Sierra Nevada. The time required to detect a significant trend in water quality data is a function of several factors: (1) the frequency of sampling (more frequent sampling gives greater detection power), (2) the natural variability of the water quality parameter (the more variability the lower the detection power) and (3) the magnitude of the change to be detected (smaller changes require longer data records). Moreover, if a trend is detected it may be difficult, especially in the case of the Sierra Nevada, to separate natural causes (e.g., droughts, unusually wet winters) from anthropogenic forcings (e.g., acid/nutrient deposition). Based on the literature, time periods of 10 to 25 years are usually required to detect small to moderate changes in water quality (Rajaram and McLaughlin 1990, Hirsch et al. 1982).

Because of large annual and inter-annual variability in surface water chemistry of the study catchments and the relatively short data records, our ability to detect small, significant trends is low. Our best data sets for detecting changes are the outflow and lake chemical time-series from Emerald Lake. These data sets cover an uninterrupted period beginning in 1982. Lake and outflow time-series from 1987 through 1993 or 1994 are available from Pear Lake, Topaz Lake, Crystal Lake and Ruby Lake. The data records for Spuller and Lost lakes are only four years in length; too short to detect anything but a major change in surface water chemistry. The records for the Marble Fork of the Kaweah River cover only two years. There are also data from seven High Sierran lakes sampled after fall overturn from 1981 through 1995. These lakes include four from the east side of the Sierra (Treasure and Gem lakes in Rock Creek Canyon, Upper Gaylor and Upper Granite Lake near Tioga Pass) and three located in Sequoia National Park (Heather Lake

in the Tokopah Valley, Upper Mosquito and Upper Crystal lake in the Mineral King Valley).

To investigate trends in water quality, plots of outflow chemistry and VWM lake chemistry were made for each catchment (but not Marble Fork) and the set of seven Sierran lakes that have been sampled during the autumn since 1981. The logic for the autumn lake-survey is based on the assumption that snowmelt-effects on lake chemistry (primarily dilution which varies considerably from year to year depending on the amount of runoff) will be smaller in autumn. An autumn sampling also has the advantage that a single surface sample of the lake will be representative of the lake as whole since there is no thermal stratification. If, as assumed, the autumn samples reflect baseflow chemical conditions, then intra-annual trends in lake chemistry can be detected with a time-series of yearly samples.

Outflow data are displayed in Figures I-86 through 107, lake data in Figures I-108 through 135 and autumn survey data (pH and ANC only) in Figures I-136 through 139. Visual inspection was used to detect trends due to the problematic nature of statistical trend analysis on data with large seasonal variation and variable sampling intensity (e.g., biweekly lake samples in some years, bimonthly samples in other years). Given these problems, we believe that if trends were not evident from visual assessment there was little to be gained from statistical trend detection. We examined the figures to find trends occurring over time scales of several years; short-term trends introduced by the annual snowmelt cycle were ignored. Since annual variability of outflow chemistry has been discussed in the previous section, and VWM lake chemistry is very similar to outflow chemistry within a basin, we will not present narratives of the annual cycles of chemistry presented in these figures.

1.4.2.1. Long-term Trends in pH and ANC

No trend in pH or ANC was found at Emerald Lake or its outflow during the period of 1983 through 1994. Annual maximum and minimum values of pH and ANC were variable over this period but do not trend either up or down (Figures I-89 and 112). Because of lower sampling frequency in water years 1988 through 1994, solute chemistry in Emerald Lake exhibits less variability than in earlier years (1983-1987). Annual minimum and maximum values in Emerald Lake are less extreme than in the outflow owing to lower sampling frequency for the lake.

In the other catchments there was no identifiable trend in ANC or pH in the outflows from 1987 through 1994 (Figures I-86, 93, 96, 99, 102 and 105) nor any trend in VWM lake chemistry (Figures I-108, 116, 120, 124, 128 and 132). In general, the annual ANC minimum at each lake was higher than that found in the outflow (the major exception is Topaz Lake where the minima are nearly identical). Examination of the autumn-survey data shows there is considerable inter-annual variability in ANC at most lakes with differences of 25 to 100% common. Fall overturn pH was also variable with differences of ± 0.5 pH typical. This variability casts some doubt on the utility of autumn lake-surveys as a tool for detecting long-term trends in chemistry and suggests many decades of data will be required. No long-term trends in pH or ANC are identifiable for the period of 1981 to 1995 for any of these lakes, or for autumn samples of Emerald Lake which are included for purposes of comparison. Based on these observations, we

conclude that surface waters in high elevation regions of the Sierra Nevada have not undergone measurable acidification since 1981. In addition, based on a pH history estimated from diatom assemblages in Emerald Lake sediment, there has been no increase in acidity or decrease of ANC in Emerald Lake from 1825 to 1982 (Melack et al. 1989, Holmes et al. 1989). Thus, we conclude that the acid-neutralizing ability of the Emerald Lake watershed has not measurably changed during the last 180 years.

1.4.2.2. Long-term Trends in Other Solutes

From the time-series plots of lake and outflow chemistry only two catchments had long-term trends in surface water chemistry. At Ruby Lake, there was an increase in sulfate and base cations (lake only) in surface waters of the catchment from 1987 to 1994 (Figures I-100 125 and 127). There was also a lowering of annual maxima and minima of nitrate in the Emerald Lake basin during the period of 1983 through 1994 (Figures I-90 and 113). We will discuss the Ruby Lake trends first.

From October 1987 through April 1994, sulfate concentrations increased from about 6 $\mu\text{Eq L}^{-1}$ to ca. 12 $\mu\text{Eq L}^{-1}$ in Ruby Lake and its outflow. Similar trends were measured in only one of the three routinely sampled inflows to the lake i.e., the main inflow which drains >75% of the catchment and includes areas of rock glaciers (see Site Descriptions and Figure I-24). The upward trend in sulfate ended early in 1994 when levels began to decline (see Figure I-125). Subsequent samples of the Ruby Lake outflow from 1995 and 1996 showed a continued decline in sulfate concentration (data not presented in this report). A brief decrease in sulfate was also observed during the period of April 1987 to October 1987, just prior to the start of the long-term increase in sulfate. The sulfate increase of 6 $\mu\text{Eq L}^{-1}$ was balanced by a similar increase in base cations (Figures I-101 and 126), however, because of higher concentrations and greater annual variability, the base cation trend was not as clear; it is most easily identified in the lake time-series (Figure I-126).

The cause of increased sulfate in surface waters in the Ruby Lake basin is open to conjecture but some causes can be ruled out. Changes in precipitation chemistry can be eliminated since there was no increase in sulfate deposition in the Ruby Lake basin (or at any study site) during this period (see Chapter Three). Analytical error can be ruled out for several reasons: (1) no increasing trend was observed for sulfate in other catchments or in two of the major inflows to Ruby Lake (i.e., Cirque and Mono Pass), (2) no changes in analytical or field methods occurred during the period of October 1987 through April 1994, and (3) the QA/QC program gave no indication of analytical problems.

Perhaps not coincidentally, the upward sulfate trend at Ruby Lake occurred during one of the worst droughts in the recent history of California. Sub-normal precipitation was recorded during water years 1987 through 1992 throughout the Sierra Nevada. The drought ended in water year 1993. The only periods when sulfate exhibited a downward trend occurred in the year following high snowmelt runoff. For example, sulfate decline from 9 $\mu\text{Eq L}^{-1}$ to 5 $\mu\text{Eq L}^{-1}$ during 1987, a year with above normal precipitation in the preceding water year: 1986. Likewise the downward trend in sulfate that began in early 1994 was preceded by the wet year of 1993.

These findings suggest that low precipitation caused an increase in sulfate concentration in surface waters of the Ruby Lake basin. That changes in sulfate were not

measured until the following water year suggests a time-lag in the hydrologic system of the basin. The mechanism through which precipitation quantity affects sulfate chemistry in the Ruby Lake basin is unknown but is unique among the study sites as evidenced by the absence of sulfate trends elsewhere. Several, morphological characteristics set the Ruby Lake basin apart from the other study sites including its large size and high elevation, substantial storage and release of groundwater within the basin (see Chapter Two) and the presence of rock glaciers. In addition, much of the Ruby Lake basin is underlain by granites that are high in sulfide minerals (e.g., FeS₂).

Low precipitation may increase the melt rate of the glaciers due to the shorter duration of snow-cover during the winter. Streams supplied by glacial meltwater in other mountain ranges are known to be enriched with sulfate compared to streams in basins without glaciers (Hodgkins et al. 1995). Alternatively, the influence of ground water on surface water chemistry might increase as precipitation quantity and thus snowmelt runoff decline, resulting in higher solute concentrations in streams and the lake. A gradual reduction of outflow discharge during the drought years (Figure I-II-29, Chapter Two). In either case, as precipitation and snowmelt decrease, the relative influence of alternate sources of water to streams increases, which could result in changes in stream chemistry. In addition, weathering of sulfide minerals may have increased due to the shorter duration of snowcover and/or increased air temperature during the drought.

The other observable trend in surface water chemistry during the last 12 years was the decline of nitrate in the Emerald Lake watershed. From 1983 through 1987, peak concentrations in the lake and outflow were above 10 $\mu\text{Eq L}^{-1}$ in nearly all years (Figures I-90 and 113). Peak concentrations during water years 1990 through 1994 were less than 5 $\mu\text{Eq L}^{-1}$ in the lake and 8-9 $\mu\text{Eq L}^{-1}$ in the outflow. Prior to 1986, nitrate levels never fell below 1 $\mu\text{Eq L}^{-1}$ in the outflow or less than 0.5 $\mu\text{Eq L}^{-1}$ in the lake; during later years nitrate regularly declined to below the detection limit in both the lake and outflow stream. Overall, the reduction of nitrate in the Emerald Lake basin was more noticeable in the lake than in the outflow and appears to occur abruptly during 1988. However, this conclusion may be erroneous since the 1988 and 1989 sampling frequency was very low and the chemical time-series poorly defined. Thus, a gradual downward trend of nitrate can not be ruled out.

There are several possible explanations for the decline in nitrate. One possibility is a change in sampling procedures or analytical techniques. Samples were collected by hand during most of the project; we used ISCO samplers during only 1993 and 1994 so this change can be eliminated. Nitrate was determined by ion chromatography during most years, but a colorimetric technique (cadmium reduction; Valderrama 1981) was employed during 1983, 1984 and 1985. The switch to ion chromatography (IC) was made prior to the snowmelt season of 1986 thus it is unlikely that a change in analytical technique explains the reduction of nitrate peaks since maximum values for 1986-87 were relatively high (Figure I-90). Moreover analytical changes cannot explain the decrease in nitrate minima since both methods have similar detection limits i.e., 0.05 $\mu\text{Eq L}^{-1}$ for cadmium reduction and 0.20 $\mu\text{Eq L}^{-1}$ for IC.

Of more concern are changes in the sample holding times during the 12 years of study. From 1983 through 1987, nitrate was routinely determined within a few days to weeks of collection. In later years delays of weeks to months were the norm. Given the

potentially labile nature of nitrate, it is possible that nitrate was lost from these samples prior to analysis. This possibility was tested in 1995 and 1996 by analyzing outflow samples within one week of collection. Since ISCO's samples were collected on a weekly basis during 1996, the maximum delay before analysis was 2 weeks and the average delay was less than 10 days. The nitrate maximum during 1996 was $8 \mu\text{Eq L}^{-1}$ and nitrate declined below the detection limit in the autumn i.e., similar to measurements in 1990 through 1994 using samples with longer holding times. Thus, we believe that the decrease in the magnitude of nitrate maxima and minima at Emerald Lake was not an artifact of sampling procedures and analysis.

Nitrogen deposition at Emerald Lake was not measured during 1983 and 1984 so we are unable to tell if loading was unusually high during these years. However, no decreasing trend in nitrogen deposition was seen from 1985 through 1994. Nitrogen deposition was monitored from 1984 through 1993 at two mixed-conifer catchments (Log and Tharp's creeks) within the Kaweah River drainage by Williams and Melack (1997). In this study no decrease in nitrogen loading was observed during the monitoring period.

Increased biological demand for nitrate is a possible explanation for the decline of nitrate in Emerald Lake. From 1983 through 1985, bioassays were conducted to determine the nutrients limiting phytoplankton primary productivity and biomass in the lake (Sickman 1991). In 5 out of a total of 7 experiments, phosphorus was the sole limiting nutrient; in the other experiments either no limitation was found or both nitrogen and phosphorus were limiting. During these experiments, which were conducted in the summer and early autumn, nitrate concentrations in the lake were above $2 \mu\text{Eq L}^{-1}$. Another bioassay experiment was conducted in Emerald Lake during the autumn of 1992. Nitrogen was found to be the sole limiting nutrient in this experiment, and nitrate concentrations were below detection in the lake. While circumstantial, this finding suggests that phytoplankton in Emerald Lake had shifted from year-round phosphorus limitation in 1983-85 to periods with nitrogen limitation in 1992. A shift to nitrogen limitation could be the result of increased phosphorus loading or declining nitrogen supply to the lake. Since there was no identifiable trend in atmospheric phosphorus or nitrogen loading to the Emerald Lake or the nearby Log and Tharp's creek basins during the study period, we conclude that biogeochemical processes within Emerald Lake or its catchment are probably the cause of the change in trophic status observed. Furthermore, comparisons of inflow and outflow chemistry at Emerald Lake show that the lake exerts little influence on nitrate concentrations during the spring and summer, suggesting that lower nitrate levels are a result of greater N retention in the terrestrial portions of the catchment.

While we have no definitive explanation for increased N retention, recent studies in forested watersheds in the northeastern U.S. (Mitchell et al. 1996) and high elevation catchments of the Alps (Sommaruga-Wögrath et al. 1997) suggest that climate change may effect N cycling within catchments. These studies found that increases in air temperature stimulated biological activity and demand for N, thereby decreasing nitrate levels in surface waters and lowering N losses from catchments. Another possible explanation is that the 1987-1992 drought may have increased N-uptake in the Emerald Lake catchment by lengthening the growing season since snowpacks were shallower and melted faster than in the relatively wet years of 1983 through 1986. The shallower snowpacks during the

drought tended to form later in the year which may have affected rates of N mineralization and nitrification based on findings from microbial studies in soils underlying Rocky Mountain snowpacks conducted by Brooks et al. (1995 and 1996). Assuming that some nitrate exported from the Emerald Lake watershed is derived from catchment sources (see Chapter 3), less nitrate was produced within the catchment, hence less was available for export during snowmelt.

Interestingly, Williams and Melack (1997) also measured a decline in nitrate concentration in Log Creek which was contemporaneous with changes seen in Emerald Lake. This stream drains a small (50 ha), mixed conifer catchment (elevation 2067 m) located within 15 km of the Emerald Lake basin. Prior to 1990, nitrate concentrations ranged from the detection limit to 1.0 μM ; after 1990 levels were nearly always below the detection limit. The correspondence of temporal changes in nitrate concentrations between Emerald Lake and Log Creek supports the hypothesis that N dynamics in the Sierra Nevada are susceptible to climatic forcings.

1.4.3. Mechanisms for ANC Depression During Snowmelt

Two mechanisms have been identified as causing the annual depletion of ANC during snowmelt in high altitude catchments of the Sierra Nevada: acidification by strong acids and dilution by low ANC snowmelt (Williams et al. 1993). Acidification of surface waters by strong acids, primarily HNO_3 and H_2SO_4 , from the melting snowpack was identified as a major cause of ANC depletion during the snowmelt seasons of 1986 and 1987 at Emerald Lake (Williams et al. 1993). In the previous sections of the report, examination of solute patterns during snowmelt clearly demonstrated that dilution plays an important role in controlling surface water chemistry. However, it is not possible to judge the relative contribution of each process from time-series plots of solute chemistry and a quantitative approach is called for.

In this section we present an analysis of episodic ANC depression using a method introduced by Molot et al. (1989), comparing strong acid and base cation concentrations at the point of minimum ANC with concentrations prior or subsequent to snowmelt, and a newer technique we call "superposition." We also modify a model proposed by Eshleman et al. (1995) and use it to estimate percent acidification (defined as an episodic increase in acid anions) and dilution (defined as an episodic decrease in base cations). The modified Eshleman et al. model is then used in a predictive mode to estimate the effect of future increases in acid loading on the study catchments, and on all Sierra Nevada lakes by applying it to the Western Lakes Survey (WLS) statistical data set (Baker et al. 1990).

1.4.3.1. The d-value Analysis

The traditional tool used in analyzing episodic acidification compares ion concentrations at an episodic ANC minimum with concentrations during some pre- or post-episode index period (Molot et al. 1989; see also Schaefer et al. 1990; DeWalle and Swistock 1994; Evans et al. 1995). We call this method "d-value" analysis. The analysis is derived from the basic ion difference equation of ANC:

$$\text{ANC} = \text{SBC} - \text{SO}_4^{2-} - \text{NO}_3^- - \text{Cl}^- \quad (1)$$

where SBC is the sum of the base cations and each term represents concentration in $\mu\text{Eq}\cdot\text{L}^{-1}$. In this study other proton acceptors and donors, e.g., organic acids and monomeric aluminum, were undetected in outflow and lake samples (minimum outflow pH ~ 5.8) and are omitted in equation (1). The change in ANC between an index value (subscript i) and the ANC minimum during an acidification episode (subscript e) is:

$$\Delta\text{ANC} = \Delta\text{SBC} + \Delta\text{SO}_4^{2-} + \Delta\text{NO}_3^- + \Delta\text{Cl}^- \quad (2)$$

where:

$$\begin{aligned} \Delta\text{ANC} &= [\text{ANC}]_i - [\text{ANC}]_e, \\ \Delta\text{SBC} &= [\text{SBC}]_i - [\text{SBC}]_e, \\ \Delta\text{SO}_4^{2-} &= [\text{SO}_4^{2-}]_e - [\text{SO}_4^{2-}]_i, \\ \Delta\text{NO}_3^- &= [\text{NO}_3^-]_e - [\text{NO}_3^-]_i, \text{ and} \\ \Delta\text{Cl}^- &= [\text{Cl}^-]_e - [\text{Cl}^-]_i. \end{aligned}$$

Episodic decreases in base cations (dilution) and increases in anion concentrations (acidification) are both positive, i.e., both decrease ANC. If both sides of equation (2) are divided by ΔANC , and $\Delta(\text{species})/(\Delta\text{ANC})$ is defined as “d(species),” then the relative influences of dilution and acidification (expressed as fractions of the total change in ANC) are:

$$d\text{SBC} + d\text{SO}_4^{2-} + d\text{NO}_3^- + d\text{Cl}^- = 1 \quad (3)$$

The actual “sum of the ds” (equation 3) rarely equals 1.0 (actual values varied from -3.50 to +7.08 in Molot et al. 1989; 0.79 to 1.81 in DeWalle and Swistock 1994; -0.23 to +1.41 in Schaefer et al. 1990); deviations from 1.0 are usually attributed to analytical error and/or unevaluated ions.

Using fall-overturn as the index period in the d-value analysis produced erratic results (Table I-5). Fall-overturn is not an appropriate index for the Sierra Nevada, nor, we expect, for any region having a deep snowpack and long snowmelt season. (e.g., the Rocky Mountains). In the east, where the method was developed and has been extensively applied, the shallow snowpack melts rapidly and fall-overturn lake samples provide a good approximation of pre-melt (pre-episode) values. In the Sierra Nevada, lake ANC and SBC have only recovered a third to half of their pre-melt concentrations by fall-overturn. Only with winter groundwater flows do the lakes fully recover. Using a fall-overturn index period minimizes ANC depression and the contribution of base cation dilution as a cause of depression; and since nitrate concentrations are typically at a minimum during overturn, the contribution of this ion to acidification is exaggerated.

Using pre-melt concentrations as index values (from outflow and upper level lake samples collected prior to the start of snowmelt) gave a more consistent picture of the roles of dilution and acidification in ANC depression (Table I-6). However, the relative effects of nitrate and sulfate were still distorted. As long as a chemical species behaves similarly to ANC, proportionally increasing or decreasing between its pre-melt and episodic concentrations, the d-value comparison is realistic. Since both SBC and Cl^- behave in this fashion, their relative roles are reasonably portrayed. Nitrate concentrations, due to preferential elution from the snowpack and the flushing of nitrate from soils, peak early in snowmelt and decline to relatively low values by the ANC minimum. Thus, the d-value analysis minimizes the role of nitrate in early acidification i.e., prior to the maximum ANC depression.

The role of sulfate in ANC depression is also underestimated. Sulfate, decreasing in concentration between the index and minimum ANC reference points, appears to increase ANC (i.e., has a negative d-value). In actuality, sulfate is (1) typically the dominant anion at minimum ANC, (2) an equal contributor with nitrate to acidification during the first part of snowmelt (Figure I-140a), and (3) often the only significant anion (especially in basins where it is a product of weathering; Figure I-140b). High sulfate concentrations are maintained throughout snowmelt as a result of soil desorption, accounting for sulfate's dominance in acidification—a process that d-value analysis fails to capture.

An additional problem in applying d-value analysis to the study lakes is that the small differences between acid anion index and episodic concentrations exaggerate the effect of analytical and sampling error. As an example, Eshleman et al. (1995) report the following changes in concentrations (index to episode) for the Adirondacks (corresponding concentrations for this study are shown in parentheses): nitrate, 0 to 30 $\mu\text{Eq}\cdot\text{L}^{-1}$ (0.5 to 2.8); and sulfate, 119 to 95 $\mu\text{Eq}\cdot\text{L}^{-1}$ (7.6 to 6.4). Another difficulty is that our pre-melt sampling may be capturing elevated nitrate concentrations from early snowmelt-pulses, minimizing the impact of nitrate on acidification.

In spite of problems, the d-value results consistently show cation dilution as the primary cause of ANC depression (Table I-7). In contrast, most eastern north-American studies (Schaefer et al. 1990; DeWalle and Swistock 1994; Evans et al. 1995) conclude that while cation dilution is predominant in high ANC lakes, increased nitrate is the major factor in lakes with low index ANC.

Evans et al. (1995) used d-value analysis to examine the role of individual cations and concluded that, in the Catskills, K^+ tended to increase rather than decrease during episodes; behavior they attributed to biological influences. Our study showed no such tendency (Table I-6); the biota play a much reduced role in the Sierra Nevada. In the Adirondacks, they noticed significant differences between Na^+ and Ca^{2+} ; Na^+ dilution was more important in ANC depression despite calcium concentrations 3 \times higher, a difference attributed to Ca buffering via ion-exchange in catchment soils. Although a similar hypothesis was proposed at Emerald (Williams et al. 1993) our data (Table I-6) show no evidence of a major role for ion exchange. When ratios of $d\text{Na}^+/d\text{Ca}^{2+}$ were compared with those for $\text{Na}^+/\text{Ca}^{2+}$ (calculated from fall-overtake lake samples or VWM outflow chemistry), the intercept of the regression line was not significantly different than zero nor the slope different from 1.0, indicating that the respective roles of these cations in ANC depression was in proportion to their relative concentrations.

1.4.3.2. The Superposition Analysis

Given the shortcomings of the d-value analysis, a different approach was needed to assess episodic acidification in the study catchments. Snowmelt acidification and dilution can be continually quantified using a technique we call superposition. The analysis requires three steps: (1) determining the ratio (R) of SBC/ANC in catchment base-flow; (2) multiplying outflow ANC by this ratio ($R\cdot\text{ANC}$); and (3) superimposing the temporal variation in $R\cdot\text{ANC}$ upon that of the outflow base cations. If the $R\cdot\text{ANC}$ curve falls below that for base cations, acidification has taken place, i.e., superposition scales the SBC and ANC vs. time relationships and, since the SBC depression measures dilution, any

proportionally greater decrease in ANC is a measure of acidification. If discharge is known, dilution and acidification can be quantified. Dilution is calculated as the SBC depression \times areal discharge \times time interval ($\text{Eq}\cdot\text{ha}^{-1}\cdot\text{day}^{-1}$) and acidification is similarly calculated using the difference between the SBC and R*ANC depressions.

Superposition is based on the Henriksen (1979; 1980) model of chronic acidification, where un-acidified ANC, i.e., the ANC prior to acid deposition, is equated with Ca^{2+} and Mg^{2+} concentrations found in lake samples. Stoddard (1987) and Williams et al. (1993) substituted SBC for calcium and magnesium, using SBC/ANC ratios >1.0 as indicators of episodic acidification: based on the assumption that “the stoichiometric weathering of granitic materials yield HCO_3^- in equal proportion to the sum of base cations liberated.” However, if the contributions of wet and dry deposition, the formation of cation rich clays, the weathering of other minerals (e.g., pyrite) and catchment and lake biological processes are taken into account, the unacidified SBC/ANC ratio can vary considerably from 1.0.

We used base-flow (late fall to the beginning-of-snowmelt) stream and lake samples to determine the pre-acidification SBC/ANC ratios (Table I-8). We made no attempt to correct either the base-flow SBC/ANC ratios or snowmelt SBC concentrations for atmospheric deposition because of the impossibility of correctly apportioning depositional cations to periodic samples; this omission may minimize the acidification estimates ($<10\%$). Figure I-141 illustrates superposition analysis for both Spuller and Emerald lakes, which exemplify the range in variation found in the study—Spuller, with an abnormally large depression caused almost solely by dilution, and Emerald, where a third of the ANC depression is caused by acidification.

Superposition also identified dilution as the predominant factor in ANC depression (Table I-9). The study lakes can be divided into two classes (Figure I-142): shallow, short residence-time (i.e., rapidly flushed) lakes where acidification accounts for $<10\%$ of the ANC decrease (Lost, Spuller and Topaz); and lakes where acidification causes 25 to 35% of the depression—where the effects of dilution are reduced due to larger lake volumes or slower catchment melting rates (Crystal, Emerald, Pear and Ruby).

Successful superposition analysis requires sufficient samples to establish the base flow ratio and to adequately describe changes in SBC and ANC throughout snowmelt. Much of our data consist of biweekly outflow samples during snowmelt, which only allow a coarse evaluation. With daily, or every other day, sampling in 1993 and 1994 more accurate results were obtained. We have confidence in the overall analysis since the results for lakes and years with limited sampling are in good agreement with those more intensively sampled in terms of both average values and specific trends, e.g., the increased importance of dilution in heavy snow years.

The percent decrease in SBC and ANC between the pre-melt index period and the maximum depression ($\Delta\text{SBC}/\text{SBC}_{\text{index}}$ and $\Delta\text{ANC}/\text{ANC}_{\text{index}}$) can also be used to estimate percent acidification in the absence of sufficient samples for superposition analysis. For example, if the ANC depression is 48% and the SBC depression is 36%, then the percent acidification is $(48 - 36)/48$ or 25%, i.e., if dilution resulted in a base cation decrease of 36%, then any further percentage decrease in ANC can be attributed to acidification. The use of percentages scales both depressions and allows them to be directly compared.

Results using this calculation were in good agreement with those from superposition (Figure I-142 and Table I-9).

1.4.3.3. The Minimum ANC vs. Index ANC Relationship

A linear equation relating minimum episodic ANC to index ANC for a region's lakes or streams forms the basis of a simplified two compartment chemical mixing model proposed by Eshleman et al. (1995; see also Eshleman 1988):

$$\text{minimum ANC} = m \{\text{index ANC}\} - b \quad (4)$$

The first compartment in the model represents the chemistry of baseflow, presumably ground water and deeper sub-surface flows. The second compartment includes atmospheric deposition and its modification by more ephemeral catchment flow paths—primarily those of overland and shallow sub-surface flow. In fact, neither of the two compartments is physically defined. Instead, operational definitions are used: compartment 1 represents the chemistry of index period water, and compartment 2 represents the chemistry of another water that when added to index period water produces the known outflow chemistry at minimum ANC.

In the model, the slope (m) of equation (4) represents the fraction of compartment 1 water ($m = Q_1/Q_{\text{total}}$) contributing to episodic ANC. For simplicity, the two compartments will be called old- and new-water respectively. While Eshleman (1988), in a literature review, found that an old/new ratio of 0.5/0.5 was typical for most hydrograph separation studies, Eshleman et al. (1995) used a ratio of 0.74/0.25 for Catskill streams. The intercept (b) of equation (4) is:

$$b = \text{ANC}_2 \times Q_2/Q_{\text{total}} \quad (5)$$

where ANC_2 is the new-water ANC (compartment 2) and Q_2/Q_{total} is the fraction of new-water contributing to discharge at minimum ANC.

We tabulated pre-melt and fall-overturn index ANC and episodic ANC values for each catchment and year using both outflow and lake chemistry samples. A surprising observation was that the bimonthly (every other month) lake samples captured the annual ANC depression almost as well as the more intensive outflow sampling. The interval of minimal lake ANC was so extended, that typically, any sample taken during the latter part of May through the first week in August captured most of the depression, e.g., in 1993 at Emerald the ANC was below $20 \mu\text{Eq}\cdot\text{L}^{-1}$ from the 19th of May until the end of September. This finding enabled us to assemble additional minimum and index ANC data from older surveys. In many ways lake samples proved more valuable for determining index values: (1) ANC could be compared at different depths to establish that overturn had occurred; (2) multiple lake samples with similar ANC gave increased assurance of precision (vs. a single streamflow sample taken at the same time); (3) when snowmelt began prior to collecting the first outflow sample, lower lake levels retained pre-melt ANC concentrations; and (4) lake samples avoided anomalous outflow ANC values during low flow and stagnant periods.

Using study data, the equation for minimum ANC vs. pre-melt index ANC was

$$\text{minimum ANC} = (0.73 \pm 0.12) \{\text{pre-melt ANC}\} - (11.6 \pm 8.0) \quad (6)$$

The square of the regression coefficient (r^2) was 0.74 and the standard error of the estimate (SE) was $8.8 \mu\text{Eq}\cdot\text{L}^{-1}$; the 95% confidence intervals for the slope and intercept are given in the equation. Data from Spuller were omitted from the regression. Spuller, and other small lakes with shallow depths and appreciable year-round groundwater flows, have abnormally large snowmelt ANC depressions. These lakes have high pre-melt ANC and dilution is the primary depression mechanism; they are not considered to be in danger of becoming acidified and ignoring them in the analysis has little impact on accessing current and future acidification in the Sierra Nevada.

The old-water/new-water ratio in equation (6) is 0.73/0.27, close to the 0.62/0.38 hydrograph separation ratio calculated by Williams and Melack (1991) for an Emerald Lake inlet using silica concentrations. The new-water ANC of $-43 \mu\text{Eq}\cdot\text{L}^{-1}$ seems low [derived from equation (5)], e.g., snowpack ANC $\approx -5 \mu\text{Eq}\cdot\text{L}^{-1}$; however assimilation of NH_4^+ , anion elution, soil-flushing and other compartment 2 processes could appreciably decrease ANC_2 below that of the snowpack.

The equation for minimum ANC vs. fall-overturn index ANC was

$$\text{minimum ANC} = (0.87 \pm 0.12) \{\text{overturn ANC}\} - (8.1 \pm 5.4) \quad (7)$$

The regression r^2 and SE are 0.84 and $6.7 \mu\text{Eq}\cdot\text{L}^{-1}$, respectively (Spuller data were again excluded). A review of previous lake surveys (Melack et al. 1982; Melack et al. 1985; and Melack and Setaro 1986) provided fall-overturn and minimum ANC data for 15 additional lakes. The equation derived solely from this data was statistically indistinguishable from equation (7) (see Figure I-143). Combining both data sets produced the following equation ($r^2 = 0.98$, $\text{SE} = 8.0 \mu\text{Eq}\cdot\text{L}^{-1}$):

$$\text{minimum ANC} = (0.88 \pm 0.03) \{\text{overturn ANC}\} - (8.6 \pm 2.8) \quad (8)$$

Since almost all previous Sierra Nevada surveys collected lake samples during fall-overturn, equations (7) or (8) can be used to estimate minimum ANC.

1.4.3.3.1. Drought vs. Wet-year Differences

Separate minimum ANC vs. pre-melt ANC relationships were derived for the wet year of 1993 and the drought years of 1991 1992 and 1994 (Figure I-144):

$$1993: \quad \text{minimum ANC} = (0.54 \pm 0.35) \{\text{pre-melt ANC}\} - (4.8 \pm 18.5) \quad (9)$$

$$\text{drought years: minimum ANC} = (0.80 \pm 0.22) \{\text{pre-melt ANC}\} - (11.8 \pm 12.5) \quad (10)$$

High and Treasure lakes (Stoddard 1995) were included in the 1993 regression. The r^2 and SE were 0.66 and $10.2 \mu\text{Eq}\cdot\text{L}^{-1}$ for equation (9) and 0.83 and $7.2 \mu\text{Eq}\cdot\text{L}^{-1}$ for equation (10). Although the equations are not statistically different at $p < 0.05$ ($m_9 < m_{10}$ at $p = 0.10$) because of limited 1993 data, the decreased slope and higher intercept of equation (9) indicates a larger, less acidic, new-water contribution. While greater amounts of new-water are an obvious expectation for wet year, decreased acidity suggests finite catchment sources (in various soil, tallus and rock compartments) and the flushing-out of stored anions rather than preferential snowpack elution. Solute balances for the Emerald Lake watershed support the hypothesis that the annual pulse of nitrate seen in the outflow during snowmelt is derived, to some extent, from catchment N-sources (see Chapter 3).

Equation (9) also suggests reduced depressions for very low ANC lakes, and greater ANC depression due to increased dilution for lakes of high ANC. The primary impact of 1993 was a slow and incomplete recovery of ANC in the study lakes, rather than greater ANC depression.

1.4.3.4. The Eshleman, Acidification and Predictive Models

1.4.3.4.1. The Eshleman Model

Besides the minimum episodic vs. index ANC equation used to establish the relative contributions of old- and new-water and the ANC of compartment 2 water, the Eshleman et al. (1995) model has 7 additional equations: 2 for the computation of ANC in each of the two compartments and 1 for the ANC of outflow during a minimum ANC episode — all based on the definition of ANC expressed in equation (1); and 4 equations for the two compartment mixing of SBC, nitrate, sulfate and organic acids. Regional estimates of both index and episodic acid anion concentrations are used for the remaining unknowns needed to solve the model.

We found that the concentrations of index and episodic acid anions (substituting chloride for organic acids) were reasonably consistent among the lakes and years in this study, and that using regional values was appropriate (Table I-10). While the year-by-year results were erratic, the model worked reasonably well for average catchment values (Figure I-145) and was relatively insensitive to changes in assumptions and input within a range of values appropriate for the study lakes. The model worked better with pre-melt index concentrations than with fall-overturn values, principally because the measured anion changes were larger and more consistent. The results again demonstrate the importance of dilution as the principle mechanism of ANC depression in the Sierra Nevada; results from Eshleman's Adirondack model (Eshleman et al. 1995) are also shown on Figure I-145 to emphasize the regional differences.

1.4.3.4.2. The Acidification Model

The Eshleman et al. model, however, suffers from the same deficiencies as d-value analysis in that it only considers changes between the index period and the minimum ANC episode. Thus the model, like d-value analysis, does not accurately portray the effect of nitrate and sulfate concentrations on ANC depression.

To correct for this problem we revised the model by using estimates of the "effective" acid-anion concentrations in place of actual values. The revised "acidification model" computes % acidification and % dilution for both present and future acid deposition scenarios.

Typically, snowmelt dilutes outflow solute concentrations by 30 to 40% (measured by decreases in Na^+ , Cl^- or silica), however sulfate concentrations, are reduced by only ~10%. Relative to dilution, episodic SO_4^{2-} concentrations show an increase of 128 to 150%. In the acidification model, sulfate increases from $7.55 \mu\text{Eq}\cdot\text{L}^{-1}$ at pre-melt to an effective concentration of $8.93 \mu\text{Eq}\cdot\text{L}^{-1}$ at minimum ANC (the average episodic concentration of $6.38 \mu\text{Eq}\cdot\text{L}^{-1} \times 140\%$). Data from Spuller Lake were not used to determine the average pre-melt sulfate value. Spuller Lake exhibits high pre-melt sulfate concentrations due to appreciable groundwater inflows influenced by sulfide-mineral

weathering. Although excluding Spuller was statistically significant, the change in concentration was minor, $< 2 \mu\text{Eq}\cdot\text{L}^{-1}$, and did not effect results.

In the model, nitrate concentrations increase from 0.54 to $7.06 \mu\text{Eq}\cdot\text{L}^{-1}$. The average fall-overturn nitrate value was used for the pre-melt index because early snowmelt-pulses may have exaggerated measured concentrations. The effective value of episodic nitrate lies somewhere between its actual ($2.84 \mu\text{Eq}\cdot\text{L}^{-1}$) and peak ($7.25 \mu\text{Eq}\cdot\text{L}^{-1}$) concentrations and, as with sulfate, it will be relatively increased by the snowmelt dilution of other ions. We arbitrarily used a concentration midway between the peak and episodic mean and increased it by 140% for dilution to compute the effective value of $7.06 \mu\text{Eq}\cdot\text{L}^{-1}$. Percent acidification and dilution estimates from the acidification model compared favorably with calculated values from superposition analysis (Figure I-146).

1.4.3.4.3. The Predictive Model

The predictive model (Eshleman et al. 1995) is based on (1) a consistent hydrologic response, i.e., the old-water/new-water ratio is constant over time; (2) equation (6), the present-day minimum vs. pre-melt ANC relationship; and (3) Henriksen's "F" factor concept (Wright and Henriksen 1983). Henriksen's F is a measure of catchment base cation response to changes in acidic deposition, i.e., how many base cation equivalents will be produced for each additional equivalent of depositional acidity:

$$F = \Delta[\text{SBC}]^* / \{ \Delta[\text{SO}_4^{2-}]^* + \Delta[\text{NO}_3^-]^* \} \quad (11)$$

where the asterisk symbolizes long-term changes in concentration over time. In each compartment, an increase in acid loading will produce a change in ANC:

$$\Delta\text{ANC}^* = (F - 1) \{ \Delta[\text{SO}_4^{2-}]^* + \Delta[\text{NO}_3^-]^* \} \quad (12)$$

Equation (6) can be modified to reflect future changes in ANC:

$$\text{minimum ANC}_f = (Q_1/Q_{\text{total}}) \{ \text{ANC}_{c,1} + \Delta\text{ANC}^*_1 \} + (Q_2/Q_{\text{total}}) \{ \text{ANC}_{c,2} + \Delta\text{ANC}^*_2 \} \quad (13)$$

where $\text{ANC}_{c,1}$ is pre-melt index ANC and the subscripts f and c indicate future and current values, respectively. Combining equations (12) and (13)

$$\text{minimum ANC}_f = (Q_1/Q_{\text{total}}) \{ \text{ANC}_{c,1} + (F_1 - 1)(\Delta[\text{SO}_4^{2-}]^* + \Delta[\text{NO}_3^-]^*)_1 \} + (Q_2/Q_{\text{total}}) \{ \text{ANC}_{c,2} + (F_2 - 1)(\Delta[\text{SO}_4^{2-}]^* + \Delta[\text{NO}_3^-]^*)_2 \} \quad (14)$$

Equation (14) estimates future minimum ANC from present pre-melt ANC for assumed values of F and the predicted changes in anion concentrations; it will have the same slope as equation (6) because the Q_1/Q_{total} ratio remains constant, but an intercept that decreases with increasing acid deposition.

Brakke et al. (1990) theorized an F factor of 0.2-0.4, for a mountain range of low buffering capacity, e.g., the Sierra Nevada, based on paleo-limnological studies and base cation/sulfate comparisons between acidified and unacidified lakes in Norway. For the Adirondacks, Brakke et al. suggested a range of 0.4-0.7 and Sullivan et al. (1990) values of > 0.6 . Both papers proposed intra-regional variations: a decrease in catchment F with decreasing index ANC. F may also vary with time, e.g., as cation buffering capacity in soils becomes exhausted or as flora and fauna change. The F factors are typically based on long-term basin response, but individual hydrological compartments or episodic events

may have unique values. For example, different F factors may apply to the two Eshleman model compartments: a higher F for the index compartment, dominated by slower and more consistent base flow weathering patterns; a lower value for the quick-flow response and shallower pathways of compartment 2.

We used an F of 0.4 and assumed that $F = F_1 = F_2$ (Eshleman et al. 1995). We suspect that an appropriate Sierra Nevada F factor may be higher. Base-saturation of catchment soils remains high (~30 %; Williams et al. 1993) and catchment response to widely varying depositional inputs is surprisingly consistent, e.g., acidic deposition at Emerald was 4× greater in 1987 than in 1994, yet the lake ANC depressions were about the same. For whatever combination of reasons (faster than anticipated weathering, a build-up of under-snow alkalinity, sizable buffering capacity of talus fines, secondary weathering, ion exchange, etc.) the catchments seem to generate unexpected reserves of ANC.

The pre-melt and effective episodic nitrate and sulfate concentrations used in the acidification model defined the present day conditions for equation (14). In the predictive model, the catchments were subjected to increases in both nitrate and sulfate of 50, 100 and 150% (respectively 150, 200 and 250 % of present day acid loading). For sulfate, increased deposition was assumed to produce proportional pre-melt and episodic increases. For nitrate, however, the proportional increases were applied only to the episodic value. In Stoddard's (1994) classification scheme, the study catchments are currently at "stage 0" or "stage 1" nitrogen saturation: where increased nitrogen deposition causes a larger nitrate pulse with little change in base-flow concentrations. Nitrate increases above 150% would probably be needed to inaugurate "stage 2" conditions, where base-flow concentrations appreciably increase.

The anticipated changes in index and episodic nitrate and sulfate concentrations, along with new-water values calculated with the mixing fractions defined by equation (6) (e.g., $0.73[\text{SO}_4^{2-}]_1 + 0.27[\text{SO}_4^{2-}]_2 = [\text{SO}_4^{2-}]_{\text{episodic}}$), were used to derive different versions of equation (14) for each of the proposed scenarios. These in turn were used to predict episodic ANC and fall-overturn ANC for the study catchments (Table I-11). The various versions of equation (14) were also used with the acidification model to estimate percent acidification and dilution (see Figure I-145).

The results, while speculative, provide a basis to assess the sensitivity of the study lakes to increased acid deposition. The 150% (150/150 scenario) increase in deposition decreased minimum ANC at Emerald to $5 \mu\text{Eq}\cdot\text{L}^{-1}$ (from an average present-day value of $16 \mu\text{Eq}\cdot\text{L}^{-1}$) with 65% of the depression being caused by acidification. For the 150% depositional increase, only High and Pear lakes have acidic episodes ($\text{ANC} < 0$); no lakes become chronically acidic. Less conservative assumptions, such as higher F values or using actual anion concentrations in-place of the effective values, produced smaller fall-overturn and episodic ANC decreases.

1.4.3.5. Future Acidification in the Sierra Nevada

Forms of equation (14), developed for various study catchment depositional scenarios, can be used with the Western Lakes Survey (WLS) data set to provide a regional assessment of future episodic and chronic acidification in the Sierra Nevada. The WLS divided California into three strata or classes based on expected fall-overturn ANC:

less than 100 $\mu\text{Eq}\cdot\text{L}^{-1}$ (class 4A1, $n = 54$); between 100 and 199 (4A2, $n = 53$); and between 200 and 400 (4A3, $n = 42$). It also divided the state into three geographical areas, the Sierra Nevada, the Cascades and the Klamath Mountains. For the Sierra Nevada, the three ANC classes are represented by 52 (4A1), 40 (4A2) and 22 (4A3) lakes that were actually sampled. Since each class had a different sampling density, any analysis of the entire range must first be done by class and then combined using the appropriate “weights.” The respective weights are 31.978, 8.422 and 5.416, e.g., each lake in 4A1 represents approximately 32 lakes, etc. The estimated total number of lakes in the Sierra Nevada is the summation of the products of weight and n for each class, i.e., $(52 \times 31.987) + (40 \times 8.422) + (22 \times 5.416) = 2119$.

The WLS lakes were analyzed for present episodic acidification using equation (7) with measured fall-overturn ANC; for future episodic acidification by using the version of equation (14) developed for a 150 % increase in both sulfate and nitrate deposition; and for future fall overturn ANC by using the correction to the first term of equation (14) from the same model. The following equation, developed from the study lakes, was used to convert fall-overturn ANC in the WLS data to the pre-melt ANC values used in the predictive model ($r^2 = 0.76$, $\text{SE} = 11.7 \mu\text{Eq}\cdot\text{L}^{-1}$):

$$\text{pre-melt ANC} = (1.32 \pm 0.07) \{\text{overturn ANC}\} \quad (15)$$

Data from all lakes, including Spuller, were used in the regression; the intercept of equation (15) was not significantly different than zero.

Results are shown in Figure I-147. No WLS lakes were found to be chronically acidic in 1985 and our analysis indicates that none were episodically acidified by snowmelt. In the 150/150 scenario approximately 14% (~290) of Sierra Nevada lakes become episodically acidified; however, no lakes become chronically acidic. A lower depositional scenario, the 50/50 model, indicates that 6% (~140) of the lakes become episodically acidified. One difference between the two scenarios is that minimum ANC's are driven only slightly below zero for the latter, while they decrease to values of ca. $-10 \mu\text{Eq}\cdot\text{L}^{-1}$ for the former. The actual WLS lakes that become acidified with both scenarios (12 and 5 lakes, respectively) are geographically well dispersed.

In the WLS, the least buffered lakes have fall-overturn ANC of ca. $15 \mu\text{Eq}\cdot\text{L}^{-1}$. For this value, equation (7) estimates a minimum ANC and 95% confidence interval of $5 \pm 4 \mu\text{Eq}\cdot\text{L}^{-1}$ for the average minimum ANC, and $5 \pm 14 \mu\text{Eq}\cdot\text{L}^{-1}$ for a predicted minimum ANC at a single lake. Thus, statistically, about 24% of Sierra Nevada lakes with an overturn ANC of $\sim 15 \mu\text{Eq}\cdot\text{L}^{-1}$ may have a minimum ANC below zero ($p = 0.05$). There are 3 WLS lakes in this category; they represent 72 Sierra Nevada lakes, 17 of which could be episodically acidic. If a similar analysis is performed on every WLS lake with a minimum ANC confidence limit $< 0 \mu\text{Eq}\cdot\text{L}^{-1}$, a total of 38 Sierra Nevada lakes (1.8 %) could currently have acidic snowmelt depressions, e.g., High Lake, the only episodically acidified lake documented in the Sierra Nevada (Stoddard 1995).

However, this estimate may be too conservative. The standard error for an single minimum ANC prediction for a low ANC lake may not be as large as indicated since dilution, the major mechanism of ANC depression, can never drive ANC below zero by itself. This may limit the possibility of ANC values much below zero, i.e., the error distribution in this range may not be normal. Until more of these low ANC lakes are

sampled, the most accurate statement we can make is that while episodic acidification is not yet a problem, the analysis allows for the possibility that presently up to 1.8 % of Sierra Nevada lakes may undergo snowmelt ANC depressions slightly below zero.

1.5. Conclusions

The quantity and timing of snowmelt greatly affects annual and interannual variability of surface-water chemistry in seasonally snow-covered catchments in the Sierra Nevada. General patterns of surface-water chemistry were identified using statistical analysis, however, there was considerable variation in these patterns among the watersheds. For example, it was difficult to describe a consistent pattern of pH change during snowmelt. In most cases, pH decreased as runoff increased, reaching a minimum near the peak of snowmelt runoff. Several other pH patterns were observed: (1) pH increased as discharge increased, (2) pH reached a maximum at peak runoff, (3) pH was seemingly unaffected by changes in discharge and (4) pH remained fairly constant despite large changes in discharge.

Temporal changes for most other solutes demonstrated one of three different patterns: dilution, pulse/dilution or pulse/depletion. Acid anions such as nitrate and sulfate often increased in concentration in early snowmelt, with nitrate becoming depleted (i.e., analytically undetectable) and sulfate declining at peak runoff. At most catchments, nitrate peaks of between 5 and 15 $\mu\text{Eq L}^{-1}$ were common; in nitrogen limited lakes, e.g., Crystal and Lost, nitrate peaks during snowmelt were usually less than 2 $\mu\text{Eq L}^{-1}$. However, nitrate concentrations at some catchments e.g., Topaz Lake, were highest in the winter, prior to snowmelt, and declined as runoff increased in the spring. Sulfate patterns were qualitatively similar to nitrate, but the magnitude of the changes were smaller. Differences in sulfate maxima and minima were less than 1 to 2 $\mu\text{Eq L}^{-1}$ in most cases. In catchments with considerable groundwater and sulfur bearing bedrock, i.e., Spuller and Ruby lakes declined by 10 to 20 $\mu\text{Eq L}^{-1}$ over the course of snowmelt. Biogeochemical regulation of sulfate concentrations in surface waters was noted in most catchments. While the exact nature of sulfate regulation is unknown, discharge or pH dependent sulfate adsorption-desorption in catchment soils are possible mechanisms.

Base cations and ANC most commonly exhibited a dilution pattern: concentrations declined as snowmelt runoff increased, with minima occurring near peak runoff. In the dilution pattern, solute concentrations often recovered to near pre-melt levels at the end of snowmelt. Depressions of ANC usually began in the early stages of melt. Outflow ANC, declined by 25% - 80% over the course of the spring; the average decline was about 50%. ANC minima ranged from ca. 15 to 30 $\mu\text{Eq L}^{-1}$; Lost and Pear lakes had the lowest minima while ANC minima at Ruby and Crystal lakes were highest. At all catchments, ANC depression was greatest during years with deep snowpacks and high snowmelt runoff.

Dilution was the primary factor in ANC depression in surface waters during our study. The study lakes could be divided into two classes based on their response to snowmelt: shallow, short residence-time (i.e., rapidly flushed) lakes where acidification accounted for <10% of the ANC decrease; and lakes where acidification caused 25 to 35% of the depression due to larger lake volumes or lower snowmelt rates. In lakes where acidification was important, nitrate and sulfate contributed equally during the first

half of snowmelt, while sulfate dominated in the latter half. Traditional analysis, examining the change in ANC, base cation and anion concentrations between minimum ANC and an index period, failed to capture the importance of nitrate and sulfate because their variation over the snowmelt pulse was fundamentally different from that of ANC and base cations; an analysis examining changes in concentrations over time was required to fully evaluate acidification.

The relationship between minimum and fall-overturn ANC for the lakes in this study was linear ($r^2 = 0.84$) and the equation remained unchanged as additional data from earlier synoptic surveys were added. This linear model, applied to Western Lakes Survey data for the Sierra Nevada, estimated that no lakes are currently acidified by snowmelt. However, the model's confidence limits allow for the possibility that up to 1.8% (~38) of Sierra Nevada lakes undergo snowmelt ANC depressions slightly below $0 \mu\text{Eq L}^{-1}$.

We used a simple prediction model to estimate the impact of increases in acid deposition of 50, 100 and 150 %: approximately 6, 9 and 14 %, respectively, of Sierra Nevada lakes (approximately 135, 185 and 290 lakes) became episodically acidified in these scenarios, i.e., $\text{ANC} < 0 \mu\text{Eq}\cdot\text{L}^{-1}$, but no lakes experienced chronic acidification ($\text{ANC} < 0$ at fall-overturn).

No long-term trends in pH or ANC were identified in surface waters of the Sierra Nevada during the period of 1983 through 1994. Annual ANC and pH maxima and minima were variable over this period, but did not appear to be increasing or decreasing. Trends were detected in other solutes that suggest that Sierran ecosystems are potentially sensitive to increased nutrient loading and climatic perturbations. Drought conditions in the Sierra Nevada probably were responsible for increasing the proportion of runoff derived from shallow groundwater in the Ruby Lake basin as evidenced by an increase in sulfate concentrations from ca. 6 to $12 \mu\text{Eq L}^{-1}$ during the period of 1987 through 1994. Drought may also be partially responsible for increased retention of N in the Emerald Lake catchment. In the Emerald Lake basin, long-term monitoring has revealed a 25 to 50% reduction in annual nitrate maxima and nitrate minima during the autumn and winter have declined below the detection limit. These changes resulted in a concomitant shift of the lake's phytoplankton community from phosphorus limitation towards nitrogen limitation. These findings supports recent evidence that N uptake in alpine catchments may increase due to climate warming and runs counter to the recent shift of Lake Tahoe to P limitation of phytoplankton (Jassby et al. 1994).

1.6. References

- Amundson, R.G., J. Harte, H. Michaels and E. Pendall. 1988. The role of sediments in controlling the chemistry of subalpine lakes in the Sierra Nevada, California. Final Report, Contract A4-042-32. California Air Resources Board. 182 p.
- Baker, L., P. Kaufman, A. Herlihy, J. Eilers, D. Brakke and M. Mitchell. 1990. Current status of surface water acid-base chemistry. U. S. National Acid Precipitation Assessment Program, Report 9, Washington, D.C., 367 pp..
- Bateman, P.C. 1961. Granitic formations in the east-central Sierra Nevada near Bishop, California. Geol. Soc. Amer. Bull. 72: 1521-1538.
- Brakke, D. F., A. Henriksen and S. A. Norton. 1990. A variable F-factor to explain changes in base cation concentrations as a function of strong acid deposition. Verh. Internat. Verein. Limnol. 24: 146-149.
- Brooks, P.D., M.W. Williams and S.K. Schmidt. 1995. Snowpack controls on soil nitrogen dynamics in the Colorado alpine, pp. 283-292. In: K.A. Tonnessen, M.W. Williams and M. Tranter (eds.), *Biogeochemistry of Seasonally Snow-Covered Catchments*. IAHS Publication no. 228.
- Brooks, P.D., M.W. Williams and S.K. Schmidt. 1996. Microbial activity under alpine snowpacks, Niwot Ridge, Colorado. *Biogeochemistry* 32: 93-113.
- Brown, A. D., L.J. Lund and M.A. Luecking. 1990. Integrated soil processes at the Emerald Lake Watershed. Final report, Contract A5-204-32. California Air Resources Board.
- Bytnerowicz, A. and D.M. Olszyk. 1988. Measurement of atmospheric dry deposition at Emerald Lake in Sequoia National Park. Final Report, Contract A7-32-039. California Air Resources Board. 48 p.
- Bytnerowicz, A., P.J. Dawson, C.L. Morrison and M.P. Poe. 1991. Deposition of atmospheric ions to pine branches and surrogate surfaces in the vicinity of Emerald Lake, Sequoia National Park. *Atmospheric Environment* 25A: 2203-2210.
- Clow, D. 1987. Geologic controls on the neutralization of acid deposition and on the chemical evolution of surface and ground waters in the Emerald Lake watershed, Sequoia National Park, California. M.S. thesis, California State University, Fresno, 216 p.
- Clow, D.W., M.A. Mast and D.H. Campbell. 1996. Controls on surface water chemistry in the Upper Merced River Basin, Yosemite National Park. California. *Hydrol. Proc.* 10: 727-746.
- Cooper, S.D., K. Kratz, R.W. Holmes and J.M. Melack. 1988a. An integrated watershed study: An investigation of the biota in the Emerald Lake system and stream channel experiments. Final Report, Contract A5-139-32. California Air Resources Board. 75 p.

- Cooper, S.D., T.M. Jenkins and C. Soiseth. 1988b. Integrated watershed study: An investigation of fish and amphibian populations in the vicinity of the Emerald Lake basin, Sequoia National Park. Final Report, Contract A4-122-32. California Air Resources Board. 91 p.
- DeWalle, D. R., and B. R. Swistock. 1994. Causes of episodic acidification in five Pennsylvania streams on the northern Appalachian Plateau. *Water Resources Research* 30: 1955 -1963.
- Dozier, J., J. M. Melack, D. Marks, K. Elder, R. Kattelman, and M. Williams. 1988. Snow deposition, melt, runoff, and chemistry in a small alpine watershed, Emerald Lake basin, Sequoia National Park. Final report submitted to the California Air Resources Board, Contract A3-106-32. 156 pages.
- Dozier, J., J. M. Melack, K. Elder, R. Kattelman, D. Marks, S. Peterson, and M. Williams. 1989. Snow, snowmelt, rain, runoff, and chemistry in a Sierra Nevada Watershed. Final report submitted to the California Air Resources Board, Contract A6-147-32.
- Drouse, S.K., D.C. Hillman, L.W. Creelman and S.J. Simon. 1986. The National Surface Water Survey, Eastern Lakes Survey, Phase I, Quality Assurance Plan. EPA/600/4-86/008. U.S. EPA. Las Vegas, NV.
- Eilers, J., P. Kanciruk, R.A. McCord, W.S. Overton, L. Hook, D.J. Blick, D.F. Brakke, P.E. Kellar, M.S. DeHaan, M.E. Silverstein and D.H. Landers. 1987. Characteristics of Lakes in the Western United States. Volume II. Data Compendium for Selected Physical and Chemical Variables. EPA-600/3-86/054b, U.S. Environmental Protection Agency, Washington, D.C.
- Elder, K.J. 1995. *Snow Distribution in Alpine Watersheds*. Doctoral dissertation, University of California, Santa Barbara. 309 pp.
- Eshleman, K. N. 1988. Predicting regional episodic acidification of surface waters using empirical models. *Water Resources Research* 24: 1018-1026.
- Eshleman, K. N., T. D. Davies, M. Tranter and P. J. Wigington Jr. 1995. A two component mixing model for predicting regional episodic acidification of surface waters during spring snowmelt periods. *Water Resources Research* 31: 1011-1021.
- Evans, C. D., T. D. Davies and P. J. Wigington Jr. 1995. Assessing the contribution of individual dissolved ions to depressions in acid neutralizing capacity of streams in the Adirondack and Catskill Mountains, New York. *Water, Air and Soil Pollution* 85: 425 - 432.
- Henriksen, A. 1979. A simple approach for identifying and measuring acidification of freshwater. *Nature* 278: 5442-545.
- Henriksen, A., Acidification of freshwaters—a large-scale titration. 1980. In: *Ecological Impact of Acid Precipitation*. Symp. Proc. SNSF Proj., Oslo, pp 68-74.
- Hodgkins, R., M. Tranter and J.A. Dowdeswell. 1995. Interpretation of hydrochemical evidence for meltwater routing at a high-arctic glacier, pp. 387-394. In: K.A. Tonnessen, M.W. Williams and M. Tranter (eds.), *Biogeochemistry of Seasonally Snow-Covered Catchments*. IAHS Publication no. 228.

- Holmes, R.W., M.C. Whiting and J.L. Stoddard. 1989. Diatom-inferred pH and acid neutralizing capacity changes since 1825 A.D. in a dilute, high elevation, Sierra Nevada lake. *Freshwat. Biol.*
- Huber, N.K., and C.D. Rinehart. 1965. Geologic map of the Devil's Postpile quadrangle, Sierra Nevada, California. USGS quadrangle map: GQ-437.
- Huntington, G.L., and M.A. Akeson. 1987. Soil resource inventory of Sequoia National Park, central part. University of California, Davis and National Park Service, U.S. Department of Interior.
- Hyer, K. E., J. R. Webb and K. N. Eshleman. 1995. Episodic acidification of three streams in Shenandoah National Park, Virginia, USA. *Water, Air and Soil Pollution* 85: 523 - 528.
- Jassby, A.D., J.E. Reuter, R.P. Axler, C.R. Goldman and S.H. Hackley. 1994. Atmospheric deposition of nitrogen and phosphorus in the annual nutrient load of Lake Tahoe (California-Nevada). *Wat. Resour. Res.* 30: 2207-2216.
- Kattelmann, R. and K. Elder. 1991. Hydrologic characteristics and water balance of an alpine basin in the Sierra Nevada. *Water Resour. Res.* 27: 1553-1562.
- Kendall, C., D.H. Campbell, D.A. Burns, J.B. Shanely, S.R. Silva and C.C.Y. Chang. 1995. Tracing sources of nitrate in snowmelt runoff using the oxygen and nitrogen isotopic compositions of nitrate, pp. 339-347. In: K.A. Tonnessen, M.W. Williams and M. Tranter (eds.), *Biogeochemistry of Seasonally Snow-Covered Catchments*. IAHS Publication no. 228.
- Landers, D.H., J.M. Eilers, D.F. Brakke, W.S. Overton, P.E. Kellar, M.E. Silverstein, R.D. Schonbrod, R.E. Crowe, R.A. Linthurst, J.M. Omernik, S.A. Teague, and E.P. Meier. 1987. Characteristics of Lakes in the Western United States. Volume I. Population Descriptions and Physico-Chemical Relationships. EPA/600/3-86/054a. U.S. Environmental Protection Agency, Washington, D.C.
- Lockwood, J.P. and P.A. Lydon. 1975. Geologic map of the Mount Abbot quadrangle, central Sierra Nevada, California. USGS quadrangle map: GQ-1155.
- Lund, L.J. and A.D. Brown. 1989. Integrated soil processes studies at Emerald Lake Watershed. Final Report. Contract A5-204-32. California Air Resources Board.
- Melack, J. M., J.L. Stoddard and D.R. Dawson. 1982. Acid precipitation and buffer capacity of lakes in the Sierra Nevada, California. pp. 465-471, In: A.J. Johnson and R.A. Clark (eds.), *Proc. Internat. Symp. on Hydrometeorology*. Amer. Water Res. Assoc., Bethesda, MD.
- Melack, J.M., J.L. Stoddard and C.A. Ochs. 1985. Major ion chemistry and sensitivity to acid precipitation of Sierra Nevada lakes. *Water Resour. Res.* 21: 27-32.
- Melack, J. and F. Setaro. 1986. Survey of sensitivity of southern Californian lakes to acid deposition. Final report to California Air Resources Board, Contract A3-107-32B.

- Melack, J.M., S.D. Cooper, R.W. Holmes, J.O. Sickman, K. Kratz, P. Hopkins, H. Hardenbergh, M. Thieme, and L. Meeker. 1987. Chemical and biological survey of lakes and streams located in the Emerald Lake Watershed, Sequoia National Park. Final Report, Contract A3-096-32. California Air Resources Board. 345 pp.
- Melack, J.M., S.D. Cooper, T. M. Jenkins, L. Barmuta, S. Hamilton, K. Kratz, J. Sickman and C. Soiseth. 1989. Biological and chemical characteristics of Emerald Lake and the streams in its watershed, and the response of the lake and streams to acidic deposition. Final Report, Contract A6-184-32. California Air Resources Board. 480 pp.
- Melack, J.M., J.O. Sickman, F.V. Setaro and D. Engle. 1993. Long-term studies of lakes and watersheds in the Sierra Nevada, patterns and processes of surface-water acidification. Final Report, Contract A9-320-60. California Air Resources Board. 345 pp.
- Melack, J.M., J.O. Sickman, F. Setaro and D. Dawson. 1997. Monitoring of wet deposition in alpine areas in the Sierra Nevada. Final Report, Contract A932-081. California Air Resources Board. 198 pp.
- Mitchell, M.J., C.T. Driscoll, J.S. Kahl, G.E. Likens, P.S. Murdoch and L.H. Pardo. 1996. Climatic control of nitrate loss from forested watersheds in the northeast United States. *Environ. Sci. Technol.* 30: 2609-2612.
- Molot, L. A., P. J. Dillon and B. D. LaZerte. 1989. Factors affecting alkalinity concentrations of streamwater during snowmelt in central Ontario. *Can. J. Fish Aquat. Sci.* 46: 1658 - 1666.
- Rundel, P.W., T.V. St. John, and W.L. Berry. 1988. Vegetation process studies. Final Report, Contract A4-121-32. California Air Resources Board.
- Schaefer, D. A., C. T. Driscoll Jr., R. Van Dreason and C. P. Yatsko. 1990. The episodic acidification of Adirondack lakes during snowmelt. *Water Resources Research* 26: 1639 -1647.
- Sickman, J. O., and J. M. Melack. 1989. Characterization of year-round sensitivity of California's montane lakes to acidic deposition. Final Report, Contract A5-203-32. California Air Resources Board. 102 pp.
- Sickman, J.O. 1991. Planktonic primary productivity and responses of phytoplankton to acid and nutrient additions in Emerald Lake, Sierra Nevada, California. M.A. Thesis. University of California, Santa Barbara.
- Sisson, T.W., and J.G. Moore. 1984. Geology of the Giant Forest-Lodgepole area, Sequoia National Park, CA. USGS Open File Rep. No. 84-254.
- Sommaruga-Wögrath, S., K.A. Koinig, R. Schmidt, R. Sommaruga, R. Tessadri and R. Psenner. 1997. Temperature effects on the acidity of remote alpine lakes. *Nature* 387: 64-67.
- Stoddard, J.L. 1986. Nutritional status, microcrustacean communities and susceptibility to acid precipitation of high elevation lakes in the Sierra Nevada, California. Ph.D. Thesis. University of California, Santa Barbara. 188 pp.

- Stoddard, J. L. 1987. Alkalinity dynamics in an unacidified alpine lake, Sierra Nevada, California. *Limnol. Oceanogr.* 32: 825-839.
- Stoddard, J.L. 1987. Micronutrient and phosphorus limitation of phytoplankton abundance in Gem Lake, Sierra Nevada, California. *Hydrobiol.* 154: 103-111.
- Stoddard, J. L. 1994. Long-term changes in watershed retention of nitrogen: Its causes and aquatic consequences. In: *Environmental Chemistry of Lakes and Reservoirs*, Baker, L.A., Ed., Advances in Chemistry Series 237, American Chemical Society, Washington D.C., pp 223-284.
- Stoddard, J. L. 1995. Episodic acidification during snowmelt of high elevation lakes in the Sierra Nevada mountains of California. *Water, Air and Soil Pollution* 85: 353-358.
- Strickland, J.D. and T.R. Parsons. 1972. A practical handbook of seawater analysis. *Bull. Fish. Res. Bd. Can.* 167 p.
- Valderrama, J.C. 1981. The simultaneous analysis of total nitrogen and total phosphorus in natural waters. *Mar. Chem.* 10: 109-122.
- Weintraub, J. 1986. An assessment of the susceptibility of two alpine watersheds to surface water acidification: Sierra Nevada, California. M.S. Thesis, Indiana University.
- Williams, M.R. 1997. Sources of solutes in precipitation and surface runoff of mixed-conifer and alpine catchments in the Sierra Nevada, California. Ph.D. Thesis. University of California, Santa Barbara. 183 pp.
- Williams, M.R. and J.M. Melack. 1997. Atmospheric deposition, mass balances, and processes regulating streamwater solute concentrations in mixed-conifer catchments of the Sierra Nevada, California. *Biogeochemistry* 37: 111-144.
- Williams, M.W., A.D. Brown and J.M. Melack. 1993. Geochemical and hydrologic controls on the composition of surface water in a high elevation basin, Sierra Nevada, California. *Limnol. Oceanogr.* 38: 775-797.
- Wolford, R., R. Bales and S. Sorooshian. 1996. Development of a hydrochemical model for seasonally snow-covered alpine watersheds: application to Emerald Lake watershed, Sierra Nevada, California. *Water Resour. Res.* 32: 1061-1074.
- Wolford, R. and R. Bales. 1996. Hydrochemical modeling of Emerald Lake Watershed, Sierra Nevada, California: sensitivity of stream chemistry to fluxes and model parameters. *Limnol. Oceanogr.* 41: 947-954.

Table I-1. Summary of basin and lake characteristics. Basin area is the amount of drainage area above the outflow gauging station. The lake volume to watershed index is the volume of a lake (cubic meters) divided by the area of the lake's drainage basin (square meters). For the Marble Fork, lake volume is the sum of volumes from Emerald, Pear and Topaz Lakes plus an additional 230,000 m³ estimated lake volume from Aster Lake and other small ponds in the catchment.

Lake/Basin	Basin Area (ha)	Basin Relief (m)	Lake Area (ha)	Outlet Elev. (m)	Lake Max. Depth (m)	Lake Mean Depth (m)	Lake Volume (m ³)	Lake Volume to Watershed Area Index (m ³ /m ²)
Crystal	135	293	5.0	2,951	14	6.5	324,000	0.24
Emerald	120	616	2.7	2,800	10	6.0	162,000	0.14
Lost	25	160	0.7	2,475	5.5	1.9	12,500	0.05
Pear	136	471	8.0	2,904	27	7.4	591,000	0.43
Ruby	441	812	12.6	3,390	35	16.4	2,080,000	0.47
Spuller	97	537	2.2	3,131	5.5	1.6	34,700	0.04
Topaz	178	275	5.2	3,218	5.0	1.5	76,900	0.04
Marble Fork of Kaweah River	1,908	872	30	2,621	NA	NA	1,059,000	0.06

Table I-2. Summary of the water and solute balances in this report. At each catchment, water balances include measurements of annual non-winter and winter precipitation along with evaporation and outflow discharge measurements. Solute balances were computed from the water balances and measurements of rain, snow and outflow chemistry. At Crystal, Lost, Pear and Topaz lake watersheds outflow records for water year 1994 were collected and are included in Chapter Two, however, since no precipitation was sampled and no outflow chemistry measured it was impossible to compute water or solute balances for these catchment-years. In the present report we have also included solute balances from the Emerald Lake catchment for water years 1985, 1986, 1987. The water balances for these years has been previously published (Kattelman and Elder 1991) and were not reproduced in this report.

Catchment	Water Balance Records	Solute Balance Records
Crystal Lake	1990 - 1993	1990 - 1993
Emerald Lake	1990 - 1994	1985 - 1987, 1990 - 1994
Lost Lake	1990 - 1993	1990 - 1993
Marble Fork of Kaweah	1993 - 1994	1993 - 1994
Pear Lake	1990 - 1993	1990 - 1993
Ruby Lake	1990 - 1994	1990 - 1994
Spuller Lake	1990 - 1994	1990 - 1994
Topaz Lake	1990 - 1993	1990 - 1993
Total	33	36

Table I-3. Summary of quality assurance data for chemical analysis of lake and stream samples for the period of 1990 through 1995. Precision was computed as percent relative standard deviation of samples (lake or stream) run in duplicate at a 5% frequency within each analytical run. Accuracy was assessed by computing recovery after known additions to duplicates of natural samples at a 10% frequency within each run. Overall precision and accuracy data are computed as the mean percent relative deviation (%RSD) and the mean percent spike recovery (%SR), respectively. N is the number of determinations. Measured values (mean \pm standard deviation) and certified values (mean \pm standard deviation) for standard reference materials (SRM) are tabulated in $\mu\text{Eq L}^{-1}$. Three reference materials were used: National Bureau of Standards (NBS) I and II and one from the United States Environmental Protection Agency (EPA). Values for chloride were not certified by NBS or EPA. No SRM was available for silicate.

Solute	Overall Precision %RSD	Overall Accuracy %SR	Measured SRM Concentration	Certified SRM Concentration
Calcium	1.0 (N=82)	96 (N=41)	NBS-I 1.3 \pm 1.0 (N=11) NBS-II 2.6 \pm 0.8 (N=13) EPA 4.7 \pm 0.5 (N=10)	0.6 \pm 0.1 2.5 \pm 0.6 4.6 \pm 0.6
Magnesium	1.5 (N=82)	103 (N=41)	NBS-I 2.3 \pm 0.3 (N=11) NBS-II 4.6 \pm 0.4 (N=13)	2.0 \pm 0.1 4.2 \pm 0.3
Sodium	1.0 (N=82)	106 (N=41)	NBS-I 8.6 \pm 0.4 (N=11) NBS-II 18.2 \pm 0.7 (N=13)	9.0 \pm 0.2 18.2 \pm 0.7
Potassium	2.0 (N=82)	103 (N=41)	NBS-I 1.6 \pm 0.1 (N=11) NBS-II 3.0 \pm 0.3 (N=13)	1.4 \pm 0.4 2.7 \pm 0.2
Chloride	3.8 (N=96)	95 (N=48)	NBS-I 2.0 \pm 0.5 (N=33) NBS-II 0.9 \pm 0.5 (N=20) EPA 7.0 \pm 0.5 (N=17)	1.9 1.7 7.3
Nitrate	2.5 (N=96)	98 (N=48)	NBS-I 7.6 \pm 0.3 (N=33) NBS-II 3.0 \pm 0.4 (N=20)	7.6 \pm 0.2 2.7 \pm 0.3
Sulfate	2.0 (N=96)	103 (N=48)	NBS-I 16.8 \pm 0.8 (N=33) NBS-II 6.6 \pm 1.0 (N=20) EPA 2.2 \pm 0.2 (N=17)	15.1 \pm 0.3 6.7 \pm 0.3 2.1 \pm 0.3
Silicate	1.7 (N=46)	102 (n=23)	---	---

Table I-4. Statistical analysis of temporal changes in solute chemistry during snowmelt for water years 1990-1994. For the analysis the snowmelt period was divided into 4 stages based on cumulative discharge i.e., first, second, third and fourth stages. Stage one was the period from the onset of snowmelt through the first 25% of runoff, stage two was the period between the end of stage one through 50% of runoff, stage three was the period between the end of stage two through 75% of runoff and stage four ran from the end of stage three through the end of snowmelt runoff. For each stage, the volume-weighted mean concentration for each solute was calculated then ranked from 1 through 4 in order of decreasing concentration. The ranked data from all lakes was then combined into a single data set. The Friedman analysis of variance on ranks was used to test for significant differences in solute chemistry among the snowmelt stages. Stages with different letter designations are significantly different at the 95% confidence limit or at the 90% limit when given in parenthesis. The differences are ranked by their letter designations i.e., the letter b indicates higher concentration, pH or discharge than the letter a. SBC is the sum of calcium, magnesium, sodium and potassium. AVG Q represents the average daily discharge for the individual stages. Data for Nitrate-2 are from Emerald, Pear and Ruby lakes only.

Solute	Stage 1	Stage 2	Stage 3	Stage 4
pH	a	a	a	b
ANC	c	a	a	a(b)
Chloride	d	c	b	a
Nitrate	d	c	b	a
Nitrate-2	b	c	b	a
Sulfate	d	c	b	a
SBC	d	c	a	a(b)
Silicate	c	a	a	b
AVG Q	a	b	b	a

Table I-5. Fall-overturn d -values for the 7 study lakes; the d-values represent the change in concentration of a chemical species between the fall-overturn index period and the time of minimum episodic ANC divided by the ANC depression $\{\Delta(\text{species})/(\Delta\text{ANC})\}$. Decreases in the sum of the base cations (SBC) and anion increases are positive, i.e., contribute to ANC depression, negative values increase ANC. The theoretical sum of the d-values equals 1.0.

Lake	Water year	dSBC	dNO ₃ ⁻	dSO ₄ ²⁻	dCl ⁻	Sum
Crystal	87	1.33	0.02	-0.13	-0.05	1.17
	88	0.50	0.04	0.03	0.05	0.62
	89	0.75	-0.01	-0.07	-0.09	0.58
	90	0.74	-0.06	-0.12	-0.17	0.39
	91	0.47	0.02	0.00	-0.01	0.48
	92	0.92	0.10	0.06	0.00	1.08
	93	0.73	0.03	-0.09	-0.16	0.51
	avg.	0.71	0.01	-0.04	-0.06	0.62
Emerald	83	0.91	-0.09	-0.11	0.10	0.81
	84	0.20	0.17	0.04	-0.04	0.37
	85	1.50	0.20	-0.05	-0.01	1.64
	86	0.27	0.24	-0.05	-0.07	0.39
	87	-0.08	0.70	0.12	0.05	0.78
	88	0.40	0.42	-0.07	-0.03	0.72
	90	1.00	0.29	-0.12	-0.24	0.92
	91	0.65	0.25	-0.05	-0.03	0.82
	92	0.63	0.58	-0.03	-0.06	1.11
	93	0.90	0.17	-0.03	-0.03	1.01
	94	-0.18	0.47	-0.03	-0.08	0.18
	avg.	0.58	0.27	-0.04	-0.03	0.78
Lost	90	1.39	0.01	-0.07	-0.26	1.07
	91	0.71	0.02	0.03	0.01	0.78
	92	1.86	-0.09	-0.25	-0.60	0.91
	93	1.56	0.02	-0.11	-0.14	1.34
	avg.	1.29	-0.00	-0.08	-0.21	1.00
Pear	87	-0.08	0.38	0.09	0.01	0.40
	88	-0.09	0.00	0.17	-0.06	0.02
	89	1.06	-0.01	0.02	-0.14	0.92
	90	0.33	0.71	0.02	0.06	1.13
	91	0.24	0.12	-0.02	-0.06	0.28
	92	1.67	0.40	0.00	-0.17	1.90
	93	0.60	0.10	0.00	-0.18	0.53
	avg.	0.44	0.20	0.04	-0.08	0.60
Ruby	88	0.12	0.31	0.11	0.02	0.55
	89	0.10	0.18	0.07	-0.01	0.33
	90	0.47	0.11	0.16	-0.02	0.72
	91	0.38	0.35	-0.01	-0.01	0.71
	92	0.43	-0.01	0.12	-0.04	0.50
	93	0.28	0.30	-0.02	-0.04	0.52
	94	0.55	0.09	-0.06	0.04	0.61
	avg.	0.30	0.22	0.05	-0.01	0.56
Spuller	90	1.09	0.03	-0.13	-0.04	0.95
	91	0.90	0.09	-0.07	-0.01	0.91
	92	0.90	0.02	-0.15	-0.03	0.74
	93	0.94	0.00	-0.17	-0.03	0.75
	94	1.08	0.08	0.01	0.07	1.24
	avg.	0.96	0.04	-0.11	-0.01	0.88
Topaz	87	-0.25	0.00	0.02	0.35	0.12
	88	1.05	-0.04	-0.19	-0.07	0.76
	91	3.67	-0.37	-0.70	0.00	2.60
	93	1.60	0.21	-0.65	-0.12	1.04
	avg.	1.27	0.01	-0.33	-0.03	0.91

Table I-6. Pre-melt d-values for the 7 study lakes; the d-values represent the change in concentration of a species between the pre-melt index period and the time of minimum episodic ANC divided by the ANC depression $\{\Delta(\text{species})/(\Delta\text{ANC})\}$. The theoretical sum of the d-values equals 1.0. The individual cation contributions to total dSBC are also shown.

Lake	year	dSBC	dNO ₃ ⁻	dSO ₄ ²⁻	dCl ⁻	sum	dCa ²⁺	dNa ⁺	dMg ²⁺	dK ⁺
Crystal	87	1.35	0.00	-0.10	-0.09	1.16	0.70	0.45	0.18	-0.01
	88	0.49	0.03	0.00	0.02	0.54	0.25	0.06	0.11	0.07
	90	0.72	0.00	-0.03	-0.01	0.68	0.26	0.16	0.15	0.11
	91	0.81	0.01	-0.07	-0.05	0.70	0.35	0.27	0.17	0.02
	92	0.70	0.07	0.02	0.01	0.80	0.22	0.19	0.18	0.09
	93	0.78	0.01	-0.08	-0.15	0.56	0.21	0.25	0.19	0.13
	avg.	0.75	0.02	-0.04	-0.04	0.70	0.30	0.21	0.16	0.07
Emerald	84	0.68	-0.25	-0.02	-0.15	0.26	0.55	0.14	-0.00	-0.01
	85	1.02	-0.05	-0.02	-0.03	0.91	0.70	0.17	0.11	0.04
	86	0.84	-0.01	-0.03	-0.17	0.63	0.48	0.30	0.00	0.05
	87	0.41	0.30	0.15	-0.02	0.84	0.36	0.04	0.00	0.01
	88	1.10	0.11	-0.07	-0.19	0.95	0.59	0.37	0.08	0.06
	90	0.73	0.16	-0.03	-0.11	0.75	0.48	0.17	0.05	0.03
	91	1.03	0.12	-0.07	-0.08	0.99	0.62	0.28	0.08	0.05
	92	0.82	0.19	-0.04	-0.09	0.88	0.47	0.23	0.06	0.05
	93	1.02	-0.07	-0.06	-0.04	0.85	0.55	0.27	0.08	0.12
	94	0.81	0.17	-0.05	-0.10	0.83	0.53	0.16	0.07	0.05
		avg.	0.84	0.07	-0.02	-0.09	0.80	0.53	0.21	0.05
Lost	90	1.07	0.00	-0.05	-0.14	0.89	0.58	0.27	0.11	0.10
	91	1.00	-0.00	-0.05	-0.03	0.92	0.58	0.19	0.10	0.11
	92	1.42	0.00	-0.15	-0.22	1.05	0.78	0.26	0.15	0.18
	93	1.21	0.00	-0.10	-0.10	1.01	0.68	0.26	0.12	0.12
	avg.	1.16	0.00	-0.09	-0.11	0.96	0.65	0.24	0.12	0.13
Pear	87	0.60	0.26	0.03	-0.11	0.78	0.43	0.20	-0.00	-0.03
	88	0.61	0.01	-0.01	-0.04	0.56	0.12	0.32	0.04	0.04
	89	0.98	-0.06	-0.03	-0.10	0.80	0.56	0.12	0.13	0.08
	90	0.35	0.57	-0.01	0.03	0.93	0.17	0.10	0.02	0.06
	91	1.05	-0.25	-0.13	-0.12	0.55	0.53	0.25	0.10	0.10
	92	1.11	0.10	-0.08	-0.22	0.91	0.48	0.26	0.10	0.15
	93	1.27	-0.25	-0.08	-0.09	0.86	0.75	0.33	0.13	0.10
		avg.	0.83	0.04	-0.04	-0.08	0.74	0.42	0.23	0.07
Ruby	87	1.28	-0.16	-0.06	-0.18	0.88	0.68	0.26	0.09	0.24
	88	0.53	0.23	0.01	0.01	0.78	0.30	0.10	0.02	0.07
	89	1.47	-0.09	-0.20	-0.02	1.16	1.13	0.15	0.09	0.05
	90	0.72	0.04	0.06	-0.02	0.80	0.52	0.12	0.02	0.04
	91	0.56	0.17	-0.03	0.00	0.70	0.37	0.13	0.02	0.02
	92	0.63	-0.10	0.00	0.07	0.60	0.47	0.13	0.03	0.01
	93	0.89	0.10	0.04	-0.04	0.99	0.71	0.11	0.03	0.05
	94	0.95	-0.08	-0.06	-0.04	0.77	0.70	0.18	0.08	0.03
	avg.	0.84	0.04	-0.02	-0.02	0.84	0.60	0.14	0.04	0.05
Spuller	90	1.10	0.04	-0.24	-0.02	0.88	0.85	0.15	0.09	0.02
	91	1.00	0.05	-0.18	-0.01	0.86	0.66	0.22	0.08	0.04
	92	1.05	-0.00	-0.20	-0.02	0.82	0.71	0.19	0.10	0.03
	93	1.31	-0.02	-0.22	-0.03	1.04	1.01	0.12	0.13	0.05
	94	1.09	-0.11	0.03	-0.01	1.00	0.78	0.17	0.09	0.05
	avg.	1.12	-0.01	-0.17	-0.02	0.92	0.81	0.17	0.10	0.04
Topaz	87	1.13	0.02	-0.02	-0.06	1.07	0.68	0.24	0.07	0.13
	88	1.00	-0.04	-0.07	-0.09	0.80	0.62	0.21	0.08	0.10
	90	1.12	0.05	-0.17	-0.10	0.90	0.61	0.33	0.06	0.12
	91	1.37	-0.04	-0.12	-0.06	1.15	0.59	0.38	0.11	0.19
	92	1.33	-0.15	-0.11	-0.10	0.97	0.75	0.17	0.11	0.10
	93	1.12	0.03	-0.14	-0.09	0.92	0.64	0.26	0.11	0.10
	avg.	1.16	-0.02	-0.10	-0.08	0.96	0.64	0.26	0.09	0.12

Table I-7. Comparison of the d-values for the 7 study lakes based on: (1) fall overturn as the index period; and (2) a pre-melt index period, typically the first of April. Average catchment values \pm the 95% confidence interval are shown. Decreases in the sum of the base cations (SBC) and anion increases are positive, i.e., contribute to ANC depression, negative values increase ANC.

Catchment	Index Period	dSBC	dNO ₃ ⁻	dSO ₄ ²⁻	dCl ⁻	Sum
Crystal	fall-overturn	0.71 \pm 0.22	0.01 \pm 0.04	0.06 \pm 0.06	0.04 \pm 0.06	0.62 \pm 0.23
	pre-melt	0.75 \pm 0.24	0.02 \pm 0.02	0.04 \pm 0.04	0.04 \pm 0.05	0.70 \pm 0.18
Emerald	fall-overturn	0.58 \pm 0.30	0.27 \pm 0.13	0.04 \pm 0.04	0.03 \pm 0.05	0.78 \pm 0.24
	pre-melt	0.84 \pm 0.13	0.07 \pm 0.10	0.02 \pm 0.04	0.09 \pm 0.04	0.80 \pm 0.13
Lost	fall-overturn	1.29 \pm 0.49	0.00 \pm 0.06	0.08 \pm 0.12	0.21 \pm 0.26	1.00 \pm 0.24
	pre-melt	1.16 \pm 0.19	0.00 \pm 0.00	0.09 \pm 0.05	0.11 \pm 0.08	0.96 \pm 0.08
Pear	fall-overturn	0.44 \pm 0.48	0.20 \pm 0.20	0.04 \pm 0.05	0.08 \pm 0.07	0.60 \pm 0.48
	pre-melt	0.83 \pm 0.25	0.04 \pm 0.22	0.04 \pm 0.04	0.08 \pm 0.06	0.74 \pm 0.12
Ruby	fall-overturn	0.30 \pm 0.13	0.22 \pm 0.10	0.05 \pm 0.06	0.01 \pm 0.02	0.56 \pm 0.10
	pre-melt	0.84 \pm 0.24	0.04 \pm 0.10	0.02 \pm 0.06	0.02 \pm 0.05	0.84 \pm 0.12
Spuller	fall-overturn	0.96 \pm 0.08	0.04 \pm 0.03	0.11 \pm 0.06	0.01 \pm 0.04	0.88 \pm 0.18
	pre-melt	1.12 \pm 0.11	0.01 \pm 0.06	0.17 \pm 0.10	0.02 \pm 0.01	0.92 \pm 0.09
Topaz	fall-overturn	1.27 \pm 1.63	0.01 \pm 0.24	0.33 \pm 0.35	0.03 \pm 0.21	0.91 \pm 1.05
	pre-melt	1.16 \pm 0.12	0.02 \pm 0.06	0.10 \pm 0.04	0.08 \pm 0.01	0.96 \pm 0.10

Table I-8. Percent of the snowmelt ANC depression caused by dilution (decrease in base cations) and by acidification (increase in acid anions); results are shown by water year and as an overall average for the individual study catchment. Superposition scales the ANC vs. time relationship during snowmelt to that for SBC; scaled ANC decreases greater than the SBC depression are attributed to acidification. The less accurate % difference estimate is derived by comparing the relative magnitudes of the maximum ANC and SBC depressions. Some percentages (*) were not computed due to insufficient chemical samples.

Catchment	Water Year.	by % differences		by superposition	
		% dilution	% acidification	% dilution	% acidification
Crystal	88	46	54	80	20
	90	69	31	76	24
	91	71	29	62	38
	92	62	38	67	33
	93	68	32	94	6
	average	69	31	76	24
Emerald	84	45	55	68	32
	85	78	22	74	26
	86	54	46	76	24
	87	35	65	61	39
	88	80	20	*	*
	90	64	36	68	32
	91	79	21	68	32
	92	65	35	63	37
	93	80	20	73	27
	94	59	41	60	40
average	64	36	68	32	
Lost	90	91	9	89	11
	91	87	13	91	9
	92	96	4	90	10
	93	97	3	94	6
	average	93	7	91	9
Pear	87	48	52	77	23
	88	54	46	*	*
	89	92	8	*	*
	91	72	28	66	34
	92	82	18	67	33
	93	82	18	72	28
	average	65	35	71	30
Ruby	87	109	-9	*	*
	88	46	54	*	*
	89	118	-18	*	*
	90	70	30	74	26
	91	52	48	60	40
	92	56	44	69	31
	93	75	25	79	21
	94	74	26	73	27
average	73	27	71	29	
Spuller	90	93	7	97	3
	91	90	10	92	8
	92	88	12	88	12
	93	98	2	97	3
	94	89	11	91	9
average	92	8	93	7	
Topaz	87	93	7	*	*
	88	92	8	*	*
	90	94	6	82	18
	91	105	-5	91	9
	92	100	0	90	10
	93	86	14	96	4
average	95	5	90	10	

Table I-9. Base-flow SBC/ANC ratios (R) for the study lakes. The ratio and the square of the correlation coefficient (r^2) were determined from a zero-intercept regression using base-flow samples (late fall to the beginning-of-snowmelt) for all the years of study at the individual lakes, i.e., $SBC = m \times ANC$. Some ratios (*) were not computed due to insufficient chemical samples.

Lake	SBC/ANC ratio from lake samples			SBC/ANC ratio from outflow samples		
	Ratio	r^2	SE	Ratio	r^2	SE
Crystal	1.11	0.39	0.008	1.16	0.36	0.028
Emerald	1.26	0.44	0.009	1.30	0.77	0.021
Lost	1.28	0.76	0.033	*	*	*
Pear	1.26	0.51	0.018	1.34	.080	0.028
Ruby	1.16	0.52	0.021	1.15	0.81	0.017
Spuller	1.18	0.92	0.013	1.27	0.96	0.015
Topaz	1.20	0.87	0.025	1.21	0.88	0.028

Table I-10. Average index and episodic (minimum ANC) anion concentrations (\pm 95% confidence intervals), in $\mu\text{Eq}\cdot\text{L}^{-1}$, for the study catchments. Spuller Lake exhibits high pre-melt sulfate concentrations due to appreciable groundwater flows influenced by sulfide mineral weathering. The nitrate peak typically occurs before the maximum ANC depression and mean values for peak nitrate concentrations are also shown.

Acid Anion	Lakes Included	Fall overturn	Pre-melt	Episode	Peak
Cl^-	all	2.89 ± 0.32	3.97 ± 0.31	2.21 ± 0.21	*
NO_3^-	all	0.54 ± 0.19	2.65 ± 0.59	2.84 ± 0.81	7.25 ± 1.32
SO_4^{2-}	all	7.16 ± 0.69	9.20 ± 1.18	6.38 ± 0.57	*
	w/o Spuller	*	7.55 ± 0.43	*	*
	Spuller	*	24.29 ± 1.18	*	*

Table I-11. ANC predictions for the study lakes using the acidification model (a revised version of the Eshleman et al., 1995, model) for depositional increases in both nitrate and sulfate of 50, 100 and 150 percent. The 0/0 model represents present-day deposition; the 50/50 model represents an increase in atmospheric deposition of both nitrate and sulfate of 50%, etc. Estimates of minimum episodic ANC (ANC_{min}) and pre-melt ANC (ANC_{pm}) are shown for each lake and scenario. The ANC_{min} values in parenthesis are measured ANC minimums; all concentrations are in $\mu\text{Eq}\cdot\text{L}^{-1}$. High lake, the only episodically acidified lake ($ANC < 0$) documented in the Sierra Nevada (Stoddard, 1995) is included for comparison.

Lake	Model: (% nitrate increase)/(% sulfate increase)							
	0/0		50/50		100/100		150/150	
	ANC_{pm}	ANC_{min}	ANC_{pm}	ANC_{min}	ANC_{pm}	ANC_{min}	ANC_{pm}	ANC_{min}
Crystal	78	45 (59)	76	41	73	36	71	31
Emerald	41	18 (16)	39	14	36	9	34	4
Lost	52	26 (17)	50	22	47	17	45	12
Pear	32	12 (16)	30	7	27	2	25	-3
Ruby	80	47 (45)	78	42	75	37	73	32
Spuller	104	64 (29)	102	60	99	55	97	50
Topaz	58	31 (28)	56	26	53	21	51	16
High	11	-4 (-1)	9	-8	6	-13	4	-18

Figure Captions

- Figure I-1. Map of California with study locations.
- Figure I-2. Map of Upper Marble Fork of the Kaweah River (Tokopah Valley).
- Figure I-3. Hypsographic curve and winter ice-depths from Crystal Lake.
- Figure I-4. Time-series of temperature and oxygen from Crystal Lake.
- Figure I-5. Topographic map of the Crystal Lake watershed. Scale and contour intervals are shown on map.
- Figure I-6. Vegetation map of the Crystal Lake watershed. Key to classifications and scale is shown on map.
- Figure I-7. Soil map of the Crystal Lake watershed. Key to classifications and scale is shown on map.
- Figure I-8. Hypsographic curve and winter ice-depths from Emerald Lake.
- Figure I-9. Time-series of temperature and oxygen from Emerald Lake.
- Figure I-10. Hypsographic curve and winter ice-depths from Lost Lake.
- Figure I-11. Time-series of temperature and oxygen from Lost Lake.
- Figure I-12. Topographic map of the Lost Lake watershed. Scale and contour intervals are shown on map.
- Figure I-13. Vegetation map of the Lost Lake watershed. Key to classifications and scale is shown on map.
- Figure I-14. Soil map of the Lost Lake watershed. Key to classifications and scale is shown on map.
- Figure I-15. Hypsographic curve and winter ice-depths from Pear Lake.
- Figure I-16. Time-series of temperature and oxygen from Pear Lake.
- Figure I-17. Topographic map of the Pear Lake watershed. Scale and contour intervals are shown on map.
- Figure I-18. Vegetation map of the Pear Lake watershed. Key to classifications and scale is shown on map.
- Figure I-19. Soil map of the Pear Lake watershed. Key to classifications and scale is shown on map.
- Figure I-20. Hypsographic curve and winter ice-depths from Ruby Lake.
- Figure I-21. Time-series of temperature and oxygen from Ruby Lake.
- Figure I-22. Topographic map of the Ruby Lake watershed. Scale and contour intervals are shown on map.
- Figure I-23. Vegetation map of the Ruby Lake watershed. Key to classifications and scale is shown on map.
- Figure I-24. Soil map of the Ruby Lake watershed.
- Figure I-25. Hypsographic curve and winter ice-depths from Spuller Lake

- Figure I-26. Time-series of temperature and oxygen from Spuller Lake
- Figure I-27. Topographic map of the Spuller Lake watershed. Scale and contour intervals are shown on map.
- Figure I-28. Vegetation map of the Spuller Lake watershed. Key to classifications and scale is shown on map.
- Figure I-29. Soil map of the Spuller Lake watershed.
- Figure I-30. Hypsographic curve and winter ice-depths from Topaz Lake.
- Figure I-31. Time-series of temperature and oxygen from Topaz Lake.
- Figure I-32. Topographic map of the Topaz Lake watershed. Scale and contour intervals are shown on map.
- Figure I-33. Vegetation map of the Topaz Lake watershed. Key to classifications and scale is shown on map.
- Figure I-34. Soil map of the Topaz Lake watershed. Key to classifications and scale is shown on map.
- Figure I-35. Frequency histograms of % Ion Difference and theoretical/measured conductance for lake and stream samples.
- Figure I-36. Scatter-plot of theoretical conductance/ measured conductance vs % Ion Difference, and histogram of difference between cations and anions in lake and stream samples.
- Figure I-37. Outflow discharge and pH in the Crystal Lake watershed during the snowmelt periods of 1990 through 1993. Solid lines are discharge and solid lines with circles are outflow chemistry (symbols denote individual chemical samples).
- Figure I-38. Outflow discharge and pH in the Emerald Lake watershed during the snowmelt periods of 1990 through 1994. Solid lines are discharge and solid lines with circles or * are outflow chemistry (symbols denote individual chemical samples). During 1993 and 1994, samples were collected in two ways: ISCO sampler (denoted with o) and by hand (grabs samples denoted by *).
- Figure I-39. Outflow discharge and pH in the Lost Lake watershed during the snowmelt periods of 1990 through 1993. Solid lines are discharge and solid lines with circles are outflow chemistry (symbols denote individual chemical samples).
- Figure I-40. Outflow discharge and pH in the Upper Marble Fork watershed during the snowmelt periods of 1993 and 1994. Solid lines are discharge and solid lines with circles are outflow chemistry (symbols denote individual chemical samples).
- Figure I-41. Outflow discharge and pH in the Pear Lake watershed during the snowmelt periods of 1990 through 1993. Solid lines are discharge and solid lines with circles are outflow chemistry (symbols denote individual chemical samples).
- Figure I-42. Outflow discharge and pH in the Ruby Lake watershed during the snowmelt periods of 1990 through 1993. Solid lines are discharge and solid lines with circles are outflow chemistry (symbols denote individual chemical samples).
- Figure I-43. Outflow discharge and pH in the Spuller Lake watershed during the snowmelt periods of 1990 through 1993. Solid lines are discharge and solid lines with circles are outflow chemistry (symbols denote individual chemical samples).

- Figure I-44. Outflow discharge and pH in the Topaz Lake watershed during the snowmelt periods of 1990 through 1993. Solid lines are discharge and solid lines with circles are outflow chemistry (symbols denote individual chemical samples).
- Figure I-45. Outflow discharge and ANC in the Crystal Lake watershed during the snowmelt periods of 1990 through 1993. Solid lines are discharge and solid lines with circles are outflow chemistry (symbols denote individual chemical samples).
- Figure I-46. Outflow discharge and ANC in the Emerald Lake watershed during the snowmelt periods of 1990 through 1994. Solid lines are discharge and solid lines with circles or * are outflow chemistry (symbols denote individual chemical samples).
- Figure I-47. Outflow discharge and ANC in the Lost Lake watershed during the snowmelt periods of 1990 through 1993. Solid lines are discharge and solid lines with circles are outflow chemistry (symbols denote individual chemical samples).
- Figure I-48. Outflow discharge and ANC in the Upper Marble Fork watershed during the snowmelt periods of 1993 and 1994. Solid lines are discharge and solid lines with circles are outflow chemistry (symbols denote individual chemical samples).
- Figure I-49. Outflow discharge and ANC in the Pear Lake watershed during the snowmelt periods of 1990 through 1993. Solid lines are discharge and solid lines with circles are outflow chemistry (symbols denote individual chemical samples).
- Figure I-50. Outflow discharge and ANC in the Ruby Lake watershed during the snowmelt periods of 1990 through 1993. Solid lines are discharge and solid lines with circles are outflow chemistry (symbols denote individual chemical samples).
- Figure I-51. Outflow discharge and ANC in the Spuller Lake watershed during the snowmelt periods of 1990 through 1993. Solid lines are discharge and solid lines with circles are outflow chemistry (symbols denote individual chemical samples).
- Figure I-52. Outflow discharge and ANC in the Topaz Lake watershed during the snowmelt periods of 1990 through 1993. Solid lines are discharge and solid lines with circles are outflow chemistry (symbols denote individual chemical samples).
- Figure I-53. Outflow discharge and nitrate in the Crystal Lake watershed during the snowmelt periods of 1990 through 1993. Solid lines are discharge and solid lines with circles are outflow chemistry (symbols denote individual chemical samples).
- Figure I-54. Outflow discharge and nitrate in the Emerald Lake watershed during the snowmelt periods of 1990 through 1994. Solid lines are discharge and solid lines with circles or * are outflow chemistry (symbols denote individual chemical samples).
- Figure I-55. Outflow discharge and nitrate in the Lost Lake watershed during the snowmelt periods of 1990 through 1993. Solid lines are discharge and solid lines with circles are outflow chemistry (symbols denote individual chemical samples).
- Figure I-56. Outflow discharge and nitrate in the Upper Marble Fork watershed during the snowmelt periods of 1993 and 1994. Solid lines are discharge and solid lines with circles are outflow chemistry (symbols denote individual chemical samples).
- Figure I-57. Outflow discharge and nitrate in the Pear Lake watershed during the snowmelt periods of 1990 through 1993. Solid lines are discharge and solid lines with circles are outflow chemistry (symbols denote individual chemical samples).

- Figure I-58. Outflow discharge and nitrate in the Ruby Lake watershed during the snowmelt periods of 1990 through 1993. Solid lines are discharge and solid lines with circles are outflow chemistry (symbols denote individual chemical samples).
- Figure I-59. Outflow discharge and nitrate in the Spuller Lake watershed during the snowmelt periods of 1990 through 1993. Solid lines are discharge and solid lines with circles are outflow chemistry (symbols denote individual chemical samples).
- Figure I-60. Outflow discharge and nitrate in the Topaz Lake watershed during the snowmelt periods of 1990 through 1993. Solid lines are discharge and solid lines with circles are outflow chemistry (symbols denote individual chemical samples).
- Figure I-61. Outflow discharge and sulfate in the Crystal Lake watershed during the snowmelt periods of 1990 through 1993. Solid lines are discharge and solid lines with circles are outflow chemistry (symbols denote individual chemical samples).
- Figure I-62. Outflow discharge and sulfate in the Emerald Lake watershed during the snowmelt periods of 1990 through 1994. Solid lines are discharge and solid lines with circles or * are outflow chemistry (symbols denote individual chemical samples).
- Figure I-63. Outflow discharge and sulfate in the Lost Lake watershed during the snowmelt periods of 1990 through 1993. Solid lines are discharge and solid lines with circles are outflow chemistry (symbols denote individual chemical samples).
- Figure I-64. Outflow discharge and sulfate in the Upper Marble Fork watershed during the snowmelt periods of 1993 and 1994. Solid lines are discharge and solid lines with circles are outflow chemistry (symbols denote individual chemical samples).
- Figure I-65. Outflow discharge and sulfate in the Pear Lake watershed during the snowmelt periods of 1990 through 1993. Solid lines are discharge and solid lines with circles are outflow chemistry (symbols denote individual chemical samples).
- Figure I-66. Outflow discharge and sulfate in the Ruby Lake watershed during the snowmelt periods of 1990 through 1993. Solid lines are discharge and solid lines with circles are outflow chemistry (symbols denote individual chemical samples).
- Figure I-67. Outflow discharge and sulfate in the Spuller Lake watershed during the snowmelt periods of 1990 through 1993. Solid lines are discharge and solid lines with circles are outflow chemistry (symbols denote individual chemical samples).
- Figure I-68. Outflow discharge and sulfate in the Topaz Lake watershed during the snowmelt periods of 1990 through 1993. Solid lines are discharge and solid lines with circles are outflow chemistry (symbols denote individual chemical samples).
- Figure I-69. Outflow discharge and the sum of calcium, magnesium, sodium and potassium in the Crystal Lake watershed during the snowmelt periods of 1990 through 1993. Solid lines are discharge and solid lines with circles are outflow chemistry (symbols denote individual chemical samples).
- Figure I-70. Outflow discharge and the sum of calcium, magnesium, sodium and potassium in the Emerald Lake watershed during the snowmelt periods of 1990 through 1994. Solid lines are discharge and solid lines with circles or * are outflow chemistry (symbols denote individual chemical samples).

- Figure I-71. Outflow discharge and the sum of calcium, magnesium, sodium and potassium in the Lost Lake watershed during the snowmelt periods of 1990 through 1993. Solid lines are discharge and solid lines with circles are outflow chemistry (symbols denote individual chemical samples).
- Figure I-72. Outflow discharge and the sum of calcium, magnesium, sodium and potassium in the Upper Marble Fork watershed during the snowmelt periods of 1993 and 1994. Solid lines are discharge and solid lines with circles are outflow chemistry (symbols denote individual chemical samples).
- Figure I-73. Outflow discharge and the sum of calcium, magnesium, sodium and potassium in the Pear Lake watershed during the snowmelt periods of 1990 through 1993. Solid lines are discharge and solid lines with circles are outflow chemistry (symbols denote individual chemical samples).
- Figure I-74. Outflow discharge and the sum of calcium, magnesium, sodium and potassium in the Ruby Lake watershed during the snowmelt periods of 1990 through 1993. Solid lines are discharge and solid lines with circles are outflow chemistry (symbols denote individual chemical samples).
- Figure I-75. Outflow discharge and the sum of calcium, magnesium, sodium and potassium in the Spuller Lake watershed during the snowmelt periods of 1990 through 1993. Solid lines are discharge and solid lines with circles are outflow chemistry (symbols denote individual chemical samples).
- Figure I-76. Outflow discharge and the sum of calcium, magnesium, sodium and potassium in the Topaz Lake watershed during the snowmelt periods of 1990 through 1993. Solid lines are discharge and solid lines with circles are outflow chemistry (symbols denote individual chemical samples).
- Figure I-77. Outflow discharge and silicate in the Crystal Lake watershed during the snowmelt periods of 1990 through 1993. Solid lines are discharge and solid lines with circles are outflow chemistry (symbols denote individual chemical samples).
- Figure I-78. Outflow discharge and silicate in the Emerald Lake watershed during the snowmelt periods of 1990 through 1994. Solid lines are discharge and solid lines with circles or * are outflow chemistry (symbols denote individual chemical samples).
- Figure I-79. Outflow discharge and silicate in the Lost Lake watershed during the snowmelt periods of 1990 through 1993. Solid lines are discharge and solid lines with circles are outflow chemistry (symbols denote individual chemical samples).
- Figure I-80. Outflow discharge and silicate in the Upper Marble Fork watershed during the snowmelt periods of 1993 and 1994. Solid lines are discharge and solid lines with circles are outflow chemistry (symbols denote individual chemical samples).
- Figure I-81. Outflow discharge and silicate in the Pear Lake watershed during the snowmelt periods of 1990 through 1993. Solid lines are discharge and solid lines with circles are outflow chemistry (symbols denote individual chemical samples).
- Figure I-82. Outflow discharge and silicate in the Ruby Lake watershed during the snowmelt periods of 1990 through 1993. Solid lines are discharge and solid lines with circles are outflow chemistry (symbols denote individual chemical samples).

- Figure I-83. Outflow discharge and silicate in the Spuller Lake watershed during the snowmelt periods of 1990 through 1993. Solid lines are discharge and solid lines with circles are outflow chemistry (symbols denote individual chemical samples).
- Figure I-84. Outflow discharge and silicate in the Topaz Lake watershed during the snowmelt periods of 1990 through 1993. Solid lines are discharge and solid lines with circles are outflow chemistry (symbols denote individual chemical samples).
- Figure I-85. Generalized patterns of solute concentration during snowmelt runoff period. Solid lines are concentration, dashed lines are generalized discharge. Y-axes show relative solute concentration without scale. X-axes simulate the period of snowmelt which typically begins in April and continues through July.
- Figure I-86. Time-series of outflow pH and ANC from the Crystal Lake watershed, 1990-1993.
- Figure I-87. Time-series of outflow nitrate and sulfate from the Crystal Lake watershed, 1990-1993.
- Figure I-88. Time-series of outflow sum of base cations and silicate from the Crystal Lake watershed, 1990-1993.
- Figure I-89. Time-series of outflow pH and ANC from the Emerald Lake watershed, 1983-1994.
- Figure I-90. Time-series of outflow nitrate and sulfate from the Emerald Lake watershed, 1983-1994.
- Figure I-91. Time series of outflow chloride and ammonium from the Emerald Lake watershed, 1983-1994.
- Figure I-92. Time-series of outflow sum of base cations and silicate from the Emerald Lake watershed, 1983-1994.
- Figure I-93. Time-series of outflow pH and ANC from the Lost Lake watershed, 1990-1993.
- Figure I-94. Time-series of outflow nitrate and sulfate from the Lost Lake watershed, 1990-1993.
- Figure I-95. Time-series of outflow sum of base cations and silicate from the Lost Lake watershed, 1990-1993.
- Figure I-96. Time-series of outflow pH and ANC from the Pear Lake watershed, 1987-1994.
- Figure I-97. Time-series of outflow nitrate and sulfate from the Pear Lake watershed, 1987-1994.
- Figure I-98. Time-series of outflow sum of base cations and silicate from the Pear Lake watershed, 1987-1994.
- Figure I-99. Time-series of outflow pH and ANC from the Ruby Lake watershed, 1987-1994.
- Figure I-100. Time-series of outflow nitrate and sulfate from the Ruby Lake watershed, 1987-1994.
- Figure I-101. Time-series of outflow sum of base cations and silicate from the Ruby Lake watershed, 1987-1994.
- Figure I-102. Time-series of outflow pH and ANC from the Spuller Lake watershed, 1990-1994.
- Figure I-103. Time-series of outflow nitrate and sulfate from the Spuller Lake watershed, 1990-1994.

- Figure I-104. Time-series of outflow sum of base cations and silicate from the Spuller Lake watershed, 1990-1994.
- Figure I-105. Time-series of outflow pH and ANC from the Topaz Lake watershed, 1987-1994.
- Figure I-106. Time-series of outflow nitrate and sulfate from the Topaz Lake watershed, 1987-1994.
- Figure I-107. Time-series of outflow sum of base cations and silicate from the Topaz Lake watershed, 1987-1994.
- Figure I-108. Time-series of volume-weighted mean pH and ANC in Crystal Lake, 1986 - 1994.
- Figure I-109. Time-series of volume-weighted mean nitrate and sulfate in Crystal Lake, 1986-1994.
- Figure I-110. Time-series of volume-weighted mean chloride and specific conductance in Crystal Lake, 1986-1994.
- Figure I-111. Time-series of volume-weighted mean sum of base cations and silicate in Crystal Lake, 1986-1994.
- Figure I-112. Time-series of volume-weighted mean pH and ANC in Emerald Lake, 1982 - 1994.
- Figure I-113. Time-series of volume-weighted mean nitrate and sulfate in Emerald Lake, 1982-1994.
- Figure I-114. Time-series of volume-weighted mean chloride and specific conductance in Emerald Lake, 1982-1994.
- Figure I-115. Time-series of volume-weighted mean sum of base cations and silicate in Emerald Lake, 1982-1994.
- Figure I-116. Time-series of volume-weighted mean pH and ANC in Lost Lake, 1989 - 1993.
- Figure I-117. Time-series of volume-weighted mean nitrate and sulfate in Lost Lake, 1989-1993.
- Figure I-118. Time-series of volume-weighted mean chloride and specific conductance in Lost Lake, 1989-1993.
- Figure I-119. Time-series of volume-weighted mean sum of base cations and silicate in Lost Lake, 1989-1993.
- Figure I-120. Time-series of volume-weighted mean pH and ANC in Pear Lake, 1986 - 1993.
- Figure I-121. Time-series of volume-weighted mean nitrate and sulfate in Pear Lake, 1986-1993.
- Figure I-122. Time-series of volume-weighted mean chloride and specific conductance in Pear Lake, 1986-1993.
- Figure I-123. Time-series of volume-weighted mean sum of base cations and silicate in Pear Lake, 1986-1993.
- Figure I-124. Time-series of volume-weighted mean pH and ANC in Ruby Lake, 1986 - 1994.
- Figure I-125. Time-series of volume-weighted mean nitrate and sulfate in Ruby Lake, 1986-1994.
- Figure I-126. Time-series of volume-weighted mean chloride and specific conductance in Ruby Lake, 1986-1994.

- Figure I-127. Time-series of volume-weighted mean sum of base cations and silicate in Ruby Lake, 1986-1994.
- Figure I-128. Time-series of volume-weighted mean pH and ANC in Spuller Lake, 1989 - 1993.
- Figure I-129. Time-series of volume-weighted mean nitrate and sulfate in Spuller Lake, 1989-1993.
- Figure I-130. Time-series of volume-weighted mean chloride and specific conductance in Spuller Lake, 1989-1993.
- Figure I-131. Time-series of volume-weighted mean sum of base cations and silicate in Spuller Lake, 1989-1993.
- Figure I-132. Time-series of volume-weighted mean pH and ANC in Topaz Lake, 1986 - 1994.
- Figure I-133. Time-series of volume-weighted mean nitrate and sulfate in Topaz Lake, 1986-1994.
- Figure I-134. Time-series of volume-weighted mean chloride and specific conductance in Topaz Lake, 1986-1994.
- Figure I-135. Time-series of volume-weighted mean sum of base cations and silicate in Topaz Lake, 1986-1994.
- Figure I-136. ANC time-series from Treasure, Gem, Upper Gaylor and Granite lakes (Eastern Sierra Nevada), 1981-1995. Lakes were sampled in the autumn after lake mixing.
- Figure I-137. ANC time-series from Heather, Upper Mosquito, Crystal (Mineral King) and Emerald lakes (Western Sierra Nevada), 1981-1995. Lakes were sampled in the autumn after lake mixing.
- Figure I-138. pH time-series from Treasure, Gem, Upper Gaylor and Granite lakes (Eastern Sierra Nevada), 1981-1995. Lakes were sampled in the autumn after lake mixing.
- Figure I-139. pH time-series from Heather, Upper Mosquito, Crystal (Mineral King) and Emerald lakes (Western Sierra Nevada), 1981-1995. Lakes were sampled in the autumn after lake mixing.
- Figure I-140. The variation of nitrate, sulfate and ANC with time at the outflows of (a) Emerald Lake and (b) Spuller Lake. At Emerald, nitrate and sulfate play equal roles in depressing ANC during the first half of snowmelt and sulfate is dominant during the latter half; at minimum ANC sulfate is the more important anion. At Spuller, where there is a weathering source of sulfate (iron sulfide), sulfate is always dominant.
- Figure I-141. Superposition analysis: a comparison between acidification at Spuller (left-hand side) and Emerald (right-hand) in 1993. Panels (a) and (b) show the variation in the SBC/ANC ratio over the year, the solid line indicates the average base flow SBC/ANC ratio (R) for all years of data. Panels (c) and (d) illustrate the superposition of the SBC and modified (multiplied by R) ANC relationships with time; acidification occurred whenever the $R \cdot \text{ANC}$ curve dipped below that for SBC, i.e., an ANC depression greater than the measured base cation dilution. Panels (e) and (f) show the variation in the total depression flux and the fraction caused by acidification (3% at Spuller, 24% at Emerald).

- Figure I-142. A comparison of the percentage (%) of total ANC depression caused by base cation (SBC) dilution calculated by superposition vs. values calculated from percent differences in the SBC and ANC depressions: (a) annual values and (b) average annual values using all years of data.
- Figure I-143. (a) Minimum episodic ANC is plotted against fall-overturn ANC for the study catchments and for other lake data from Melack et al. (1982), Melack et al. (1985) and Melack and Setaro (1986). Panel (b) is an expanded view of the lower ANC region. The regression line shown in both figures was developed solely from study catchment data (excluding Spuller; Equation 7). Data that did not fit the model are shown as hollow squares (Spuller and 2 other high dilution lakes).
- Figure I-144. Minimum ANC vs. pre-melt ANC for the wet water year of 1993 and the drought years of 1990, 1992 and 1994. The respective regression equations are $ANC_{min} = 0.54 ANC_{pm} - 4.8$ (Equation 9) and $ANC_{min} = 0.80 ANC_{pm} - 11.8$ (Equation 10). The difference between the equations, while only significant at $p = 0.10$, suggests that wet years may have a reduced acidification impact on low ANC lakes. The lower wet-year slope is consistent with the expectation of a greater "new-water" contribution; the higher wet-year intercept indicates a lower new-water acidity. This suggests a more-or-less finite catchment source of anions as the major contributor to acidification in the Sierra Nevada, e.g., the flushing out of anions in soil by dilute snowmelt.
- Figure I-145. The Eshleman et al. model applied to the study lakes. The model estimates the fraction of the ANC depression caused by increased nitrate (a) and decreased base cation concentrations (b). More exactly, the R values on the y-axis are the increase in nitrate or the decrease in SBC divided by the sum of the nitrate increase and SBC decrease, i.e., only nitrate is assumed to play a role in acidification. Pre-melt ANC is used as the index value and calculated annual and average catchment R values are both shown. The heavy shaded lines represent results from the Eshleman et al. Adirondack model; the increased importance of dilution in the Sierra Nevada is evident.
- Figure I-146. The Eshleman et al. (1995) model revised as an "acidification" model to estimate the percent of ANC depression caused by (a) acidification and (b) base cation dilution. Average catchment values were derived from superposition analysis or percent difference estimates (Table I-9). The model uses "effective" concentrations of episodic nitrate and sulfate to more accurately portray the influence of these acid anions on ANC depression. Data from High and Treasure lakes (Stoddard, 1995) are included with study catchment data in the figure. The shaded lines represent the change in the relative influences of acidification and dilution caused by a 150 % increase in acid deposition above current levels (the 150/150 prediction scenario).
- Figure I-147. Histogram of the number of Sierra Nevada lakes in various ANC classes for present and future fall-overturn ANC (a) and minimum snowmelt ANC (b). Lakes with $ANC > 100$ have been omitted. The estimated number of lakes in the Sierra Nevada is 2119. Future values are from the 150/150 prediction model, i.e., a 150 % increase in acid deposition. The 150/150 model predicted that 290 lakes will become acidic (i.e., $ANC < 0$) during snowmelt. The present-day model estimates that no lakes are currently episodically acidified. However, the model's standard error allows for up to 24 of the lowest ANC lakes to currently have minimum ANC's less than or equal to zero.

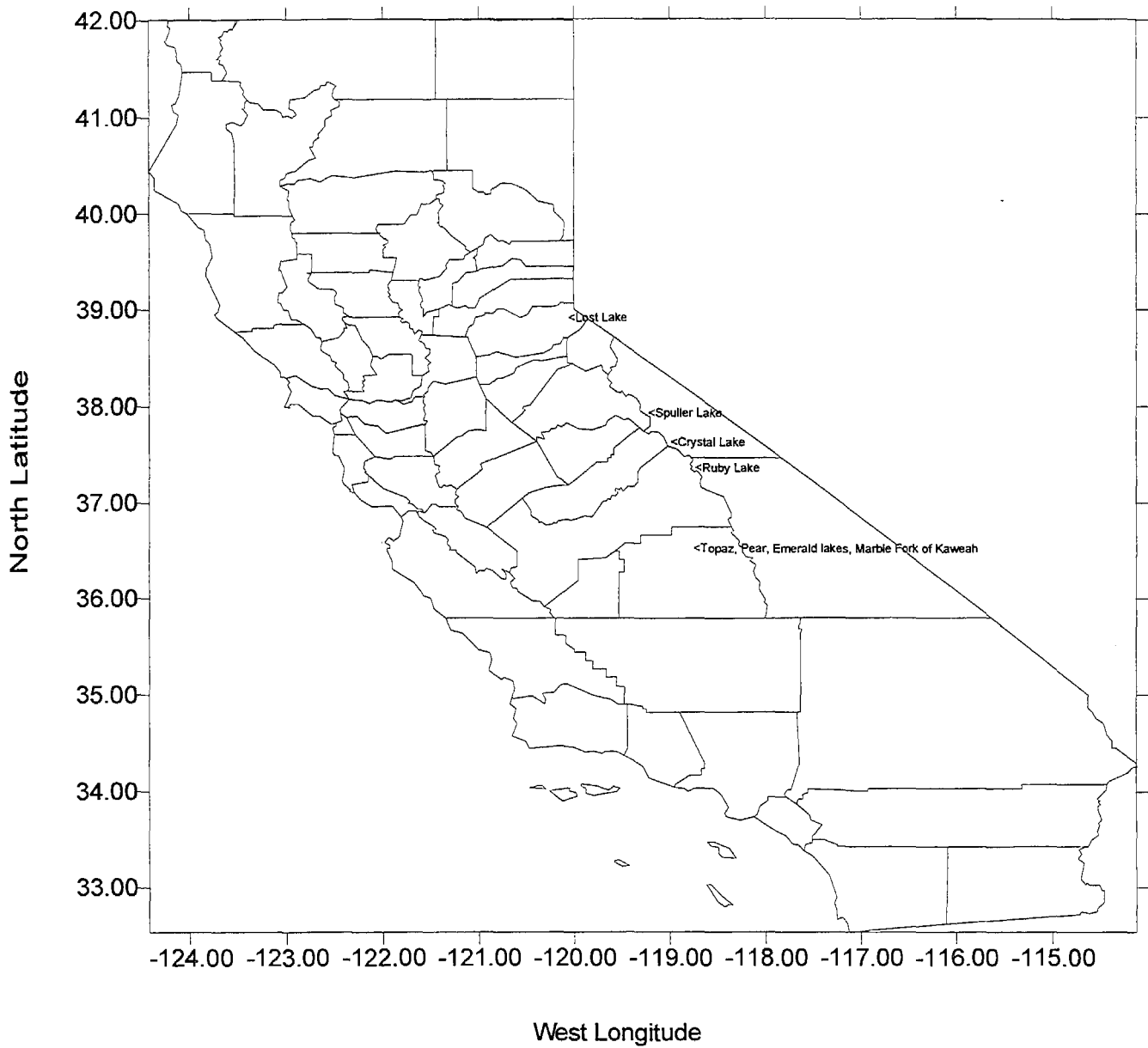


Figure I-1. Map of California (counties delineated) and locations of study sites.

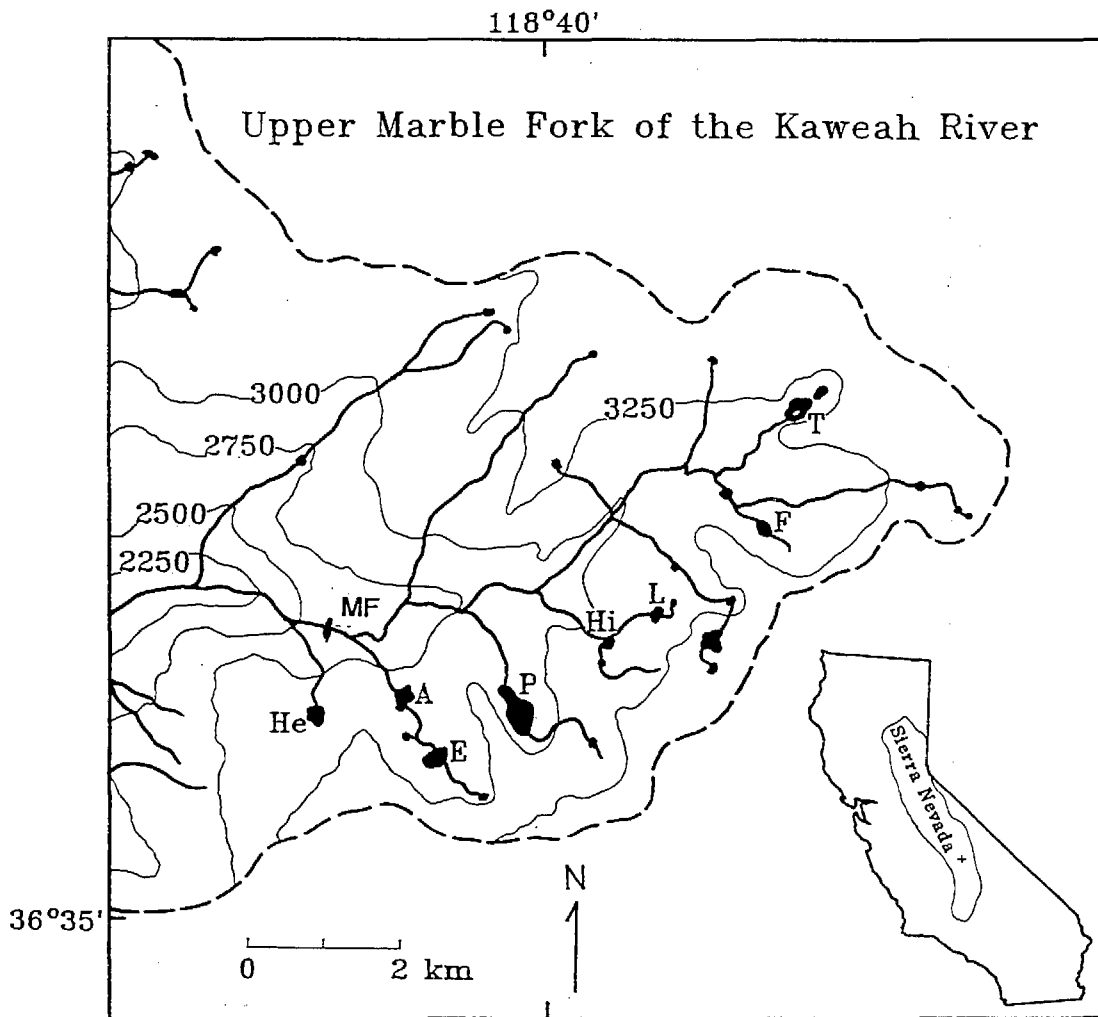
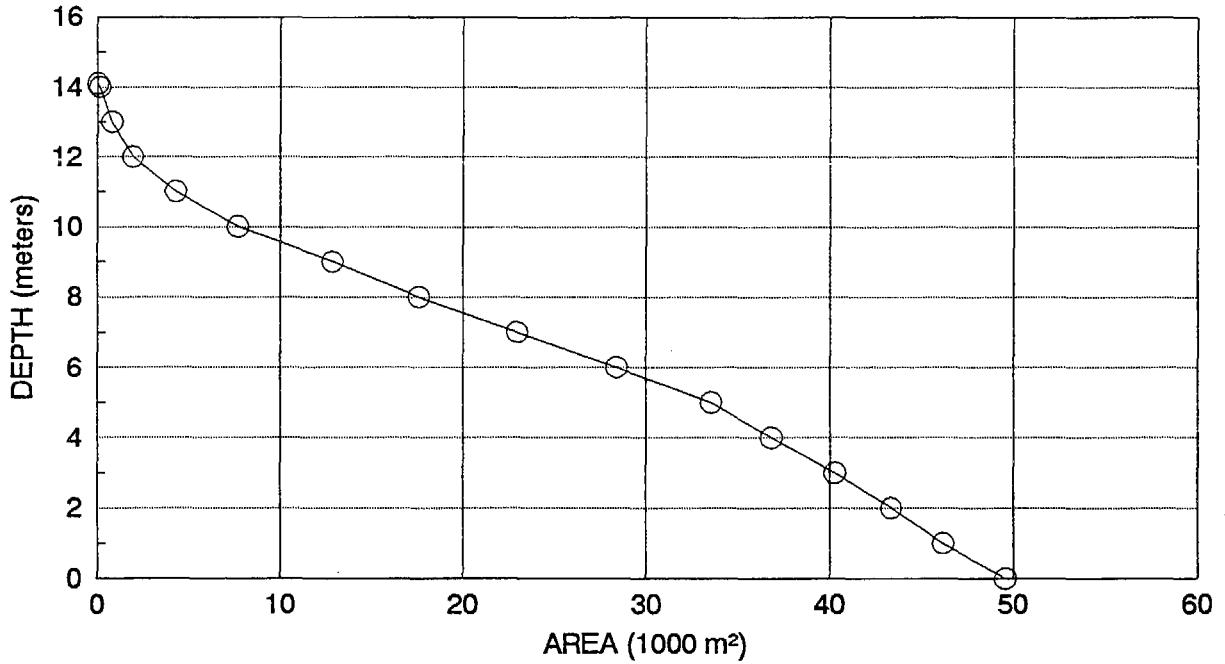


Figure I-2. Map of Upper Marble Fork of Kaweah River, Sequoia National Park. Elevation contours are meters. Site names are abbreviated as follows: E - Emerald Lake, A - Aster Lake, He - Heather Lake, P - Pear Lake, Hi - Hidden Lake, L - Lyness Lake, F - Frog Lake, T - Topaz Lake, MF - Marble Fork Gauging Station.

CRYSTAL LAKE
HYPSOGRAPHIC CURVE



VOLUME = 324,000 CUBIC METERS

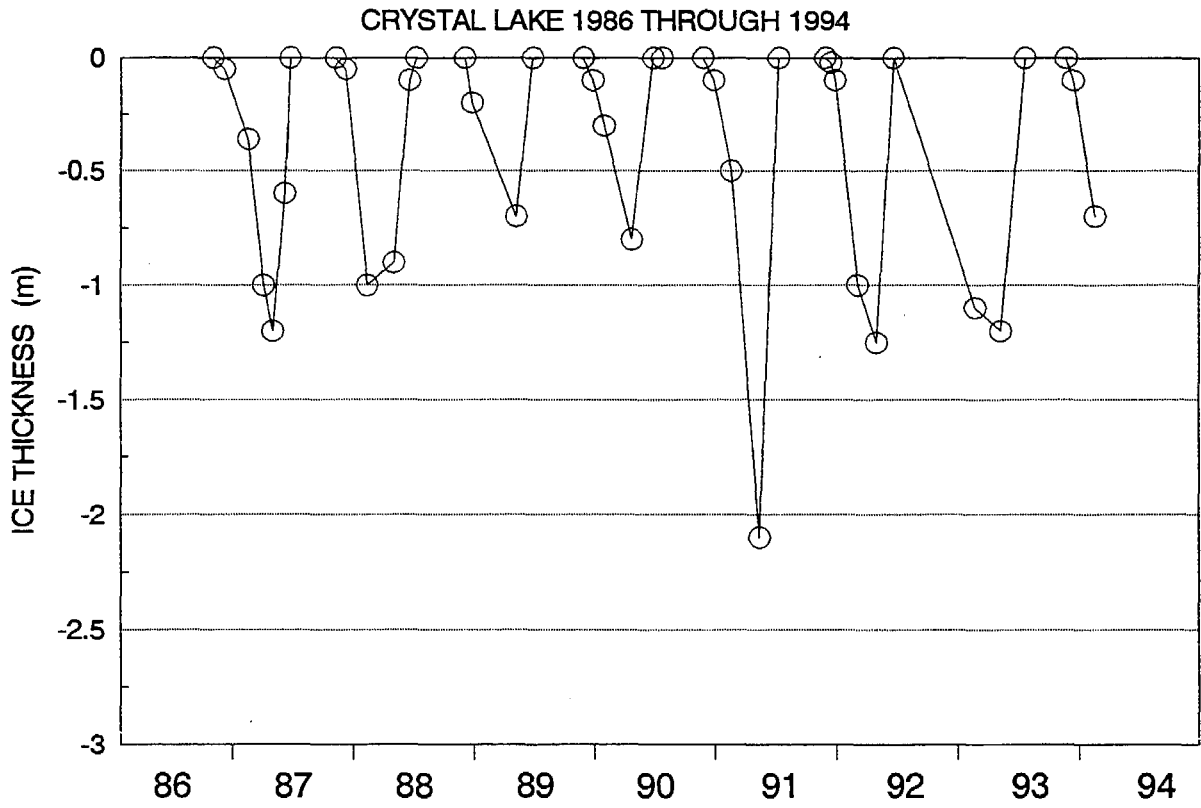
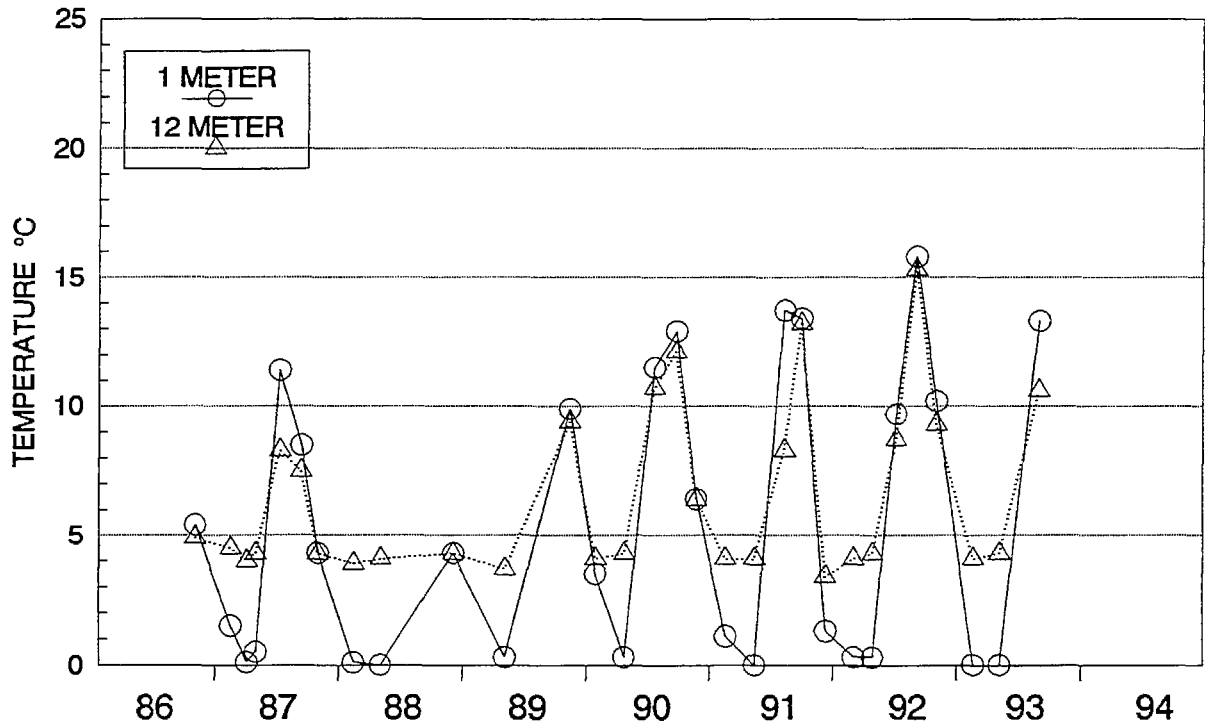


Figure I-3

CRYSTAL LAKE
1986 THROUGH 1993



CRYSTAL LAKE
1986 THROUGH 1993

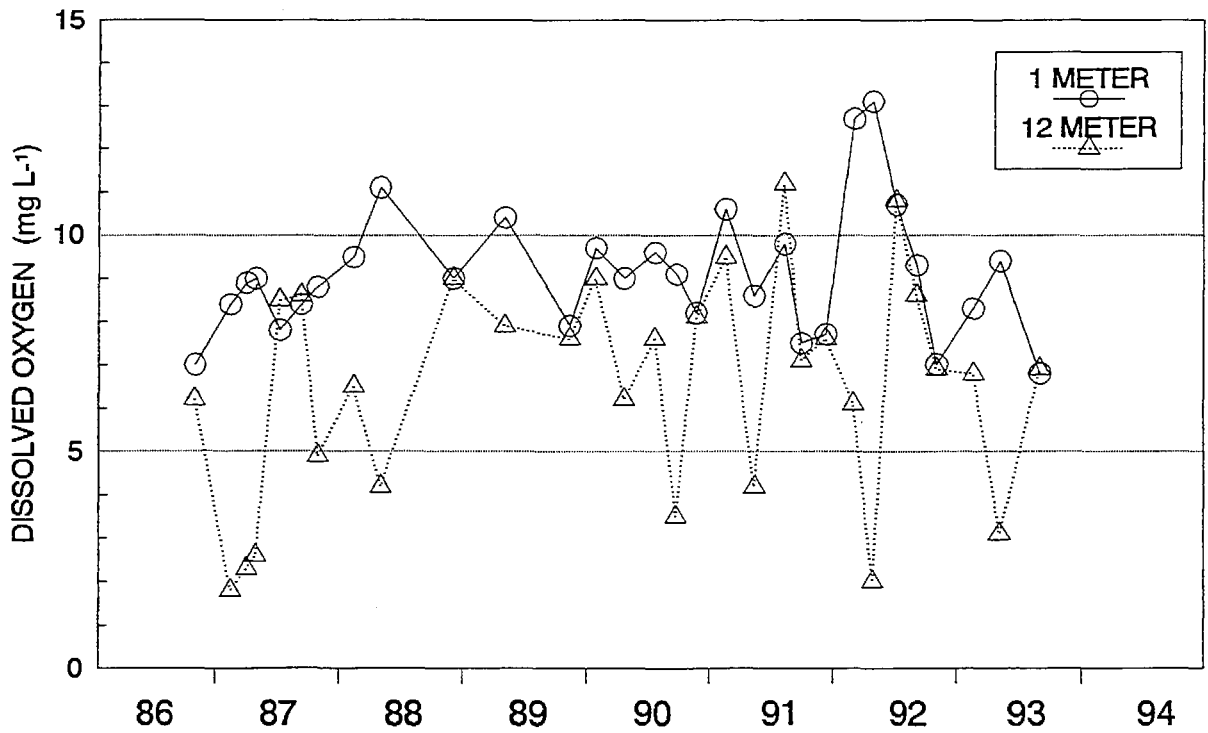
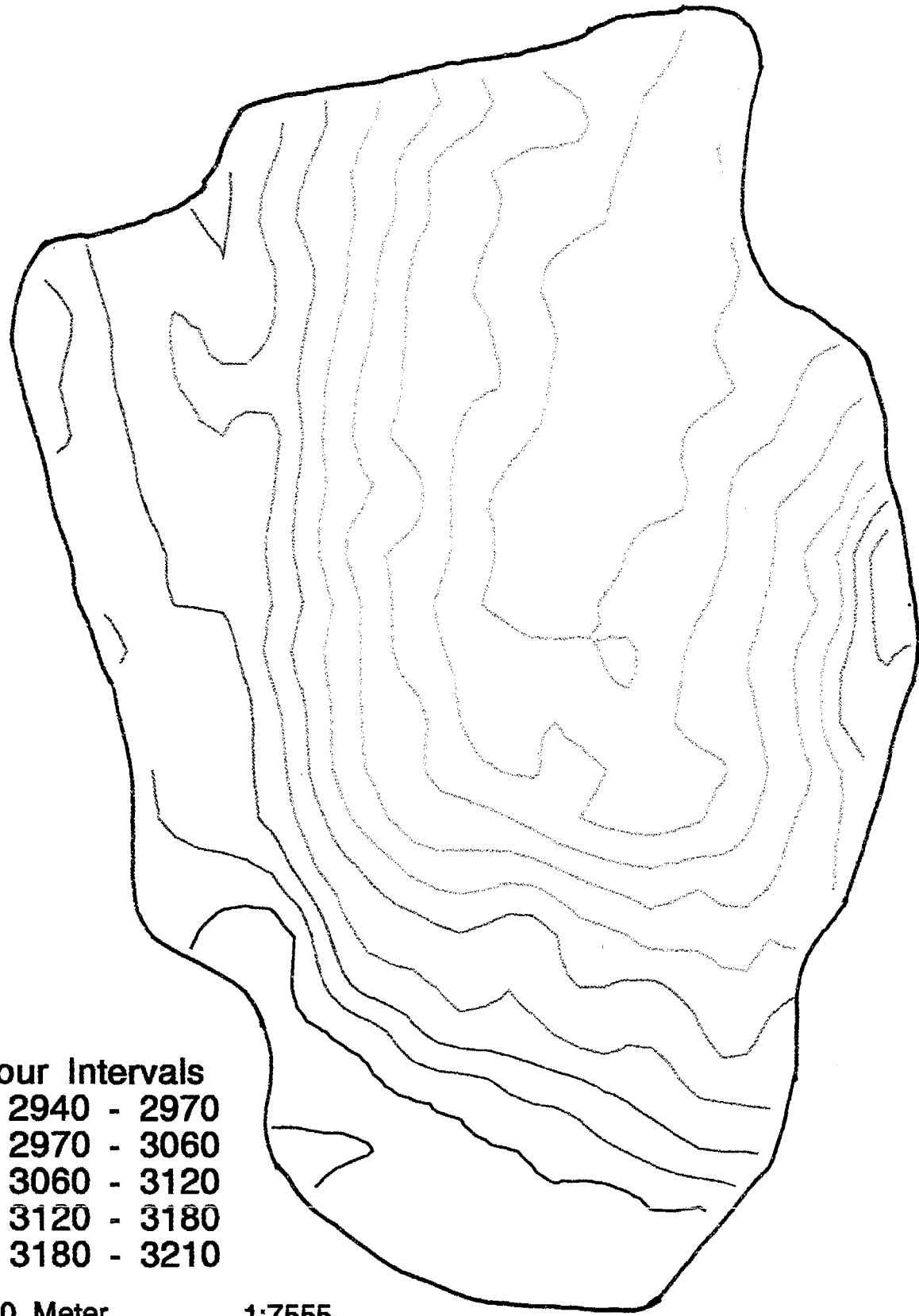


Figure I-4

Crystal Lake Digital Elevation Map



- Contour Intervals**
-  2940 - 2970
 -  2970 - 3060
 -  3060 - 3120
 -  3120 - 3180
 -  3180 - 3210

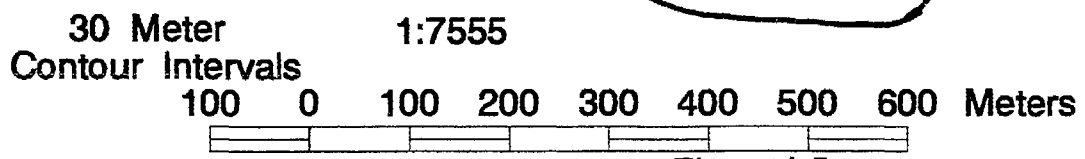


Figure I-5

Crystal Lake Vegetation Cover



100 0 100 200 300 400 500 600 Meters

Figure I-6

Crystal Lake: Soil Types

Soil

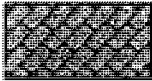
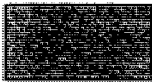
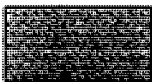
	RO	Rock Outcrop
	RR	Rocky Riparian Soil Complex
	RVB	Rock Outcrop and Volcanic Brown Soils
	T	Talus
	VB	Volcanic Brown Soils
	VBR	Volcanic Brown Soil and Rock
	VBS	Volcanic Brown Soil and Scree
	VBT	Volcanic Brown Soil and Talus
	VMM	Volcanic Moist Meadow Soils
	VST	Volcanic Scree and Talus
	VWM	Volcanic Wet Meadow Soils
	W	Water

Figure I-7

Crystal Lake Soil Coverage



1:7545

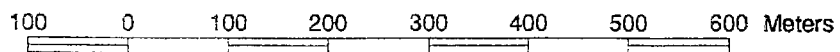
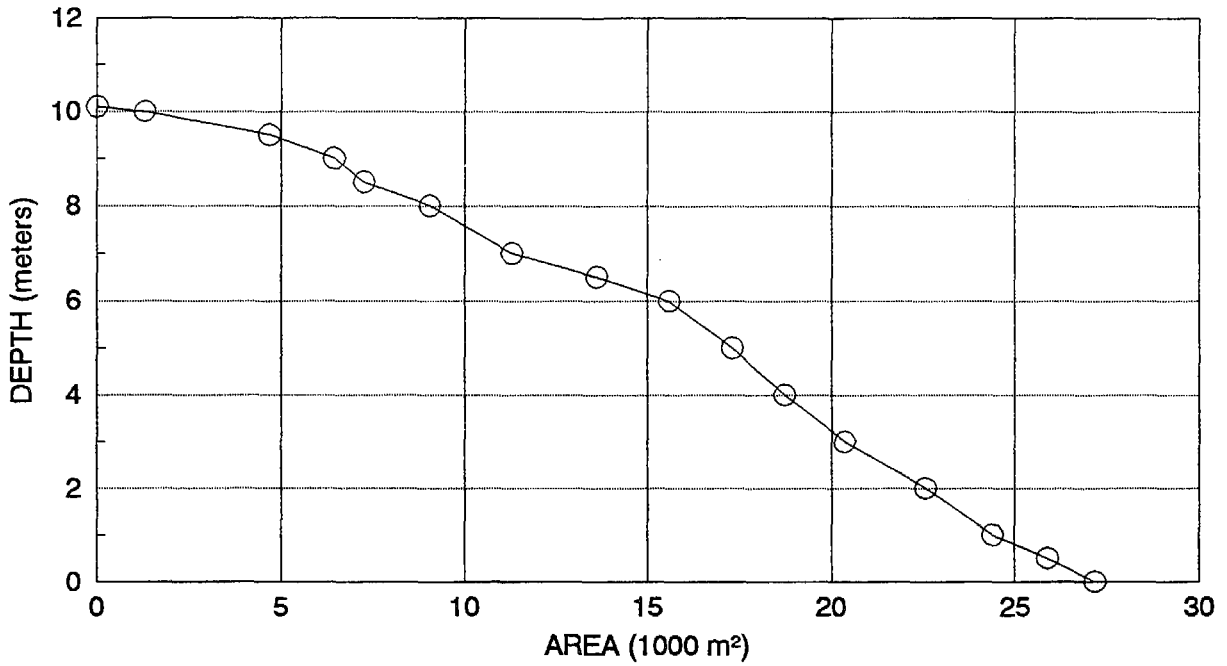


Figure I-7 cont.

EMERALD LAKE
HYPSOGRAPHIC CURVE



VOLUME = 162,000 CUBIC METERS

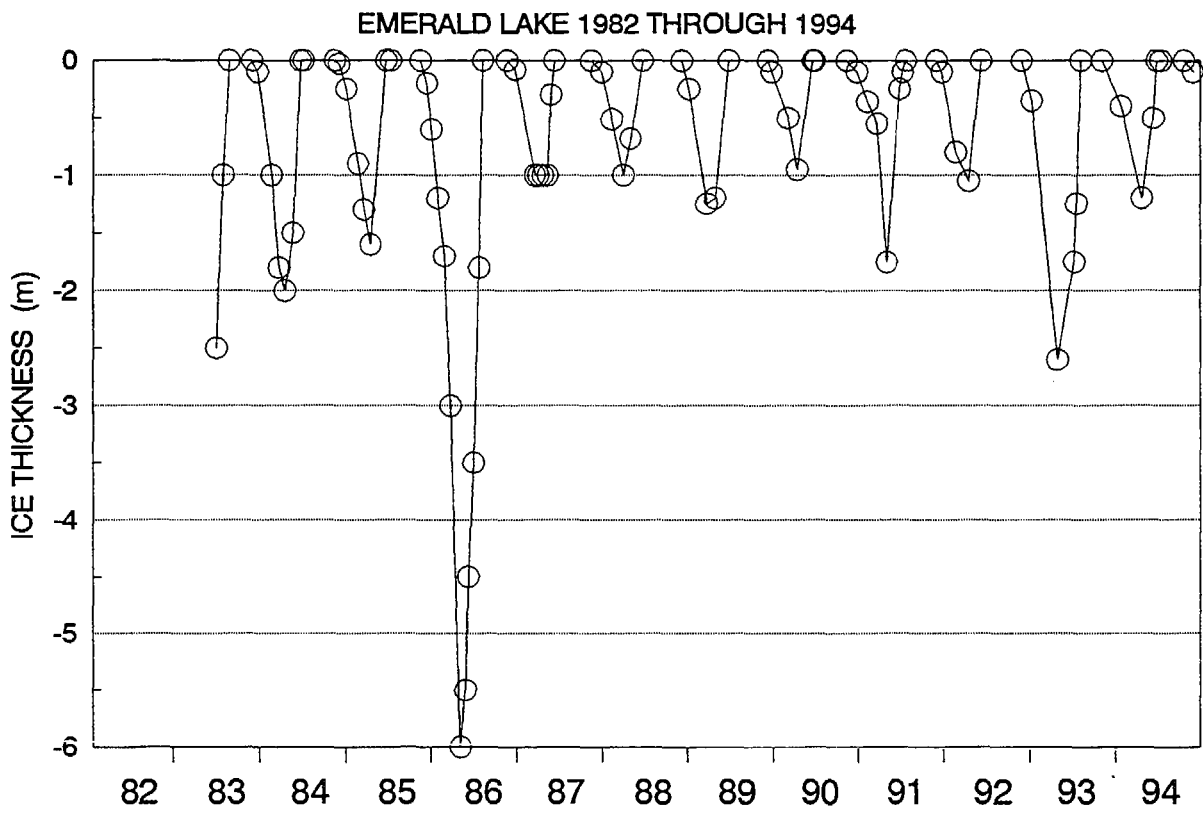
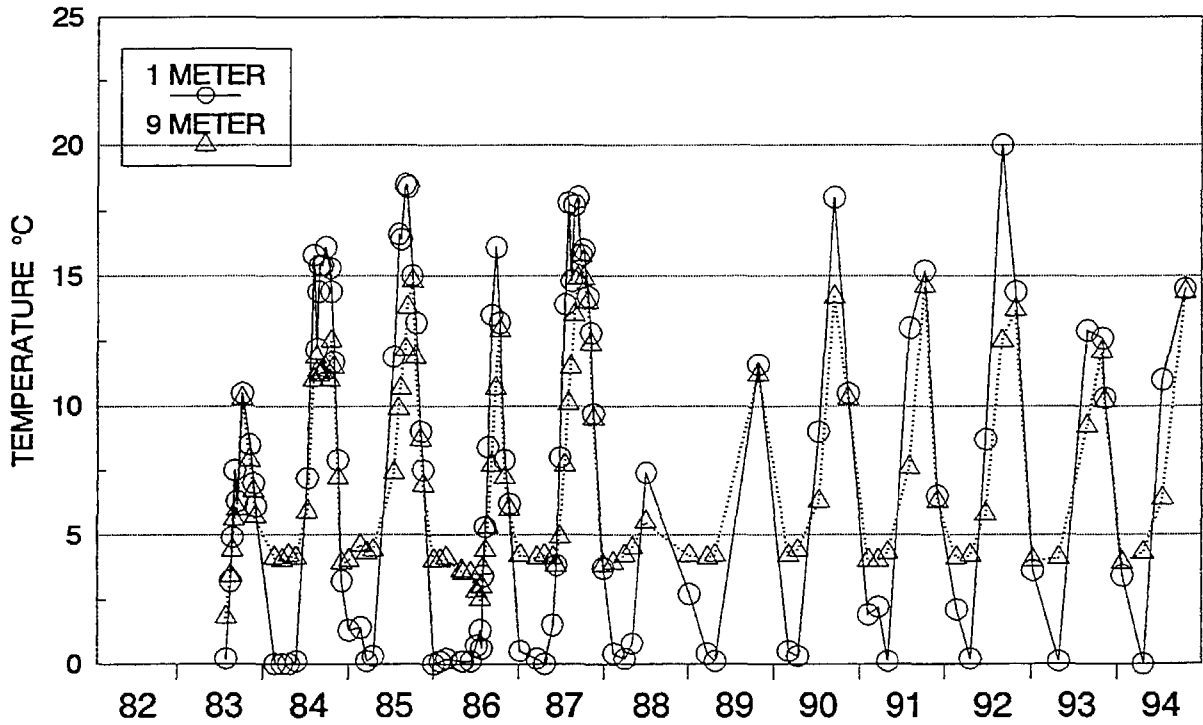


Figure I-8

EMERALD LAKE
1983 THROUGH 1994



EMERALD LAKE
1983 THROUGH 1994

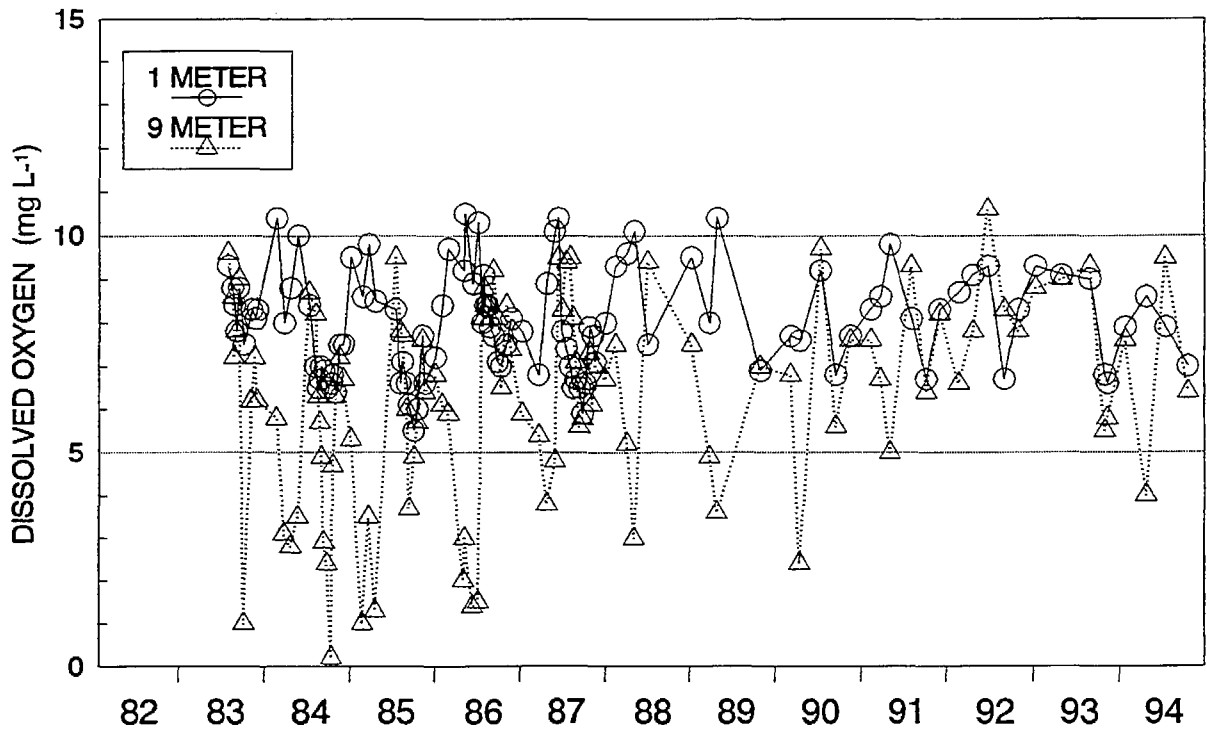
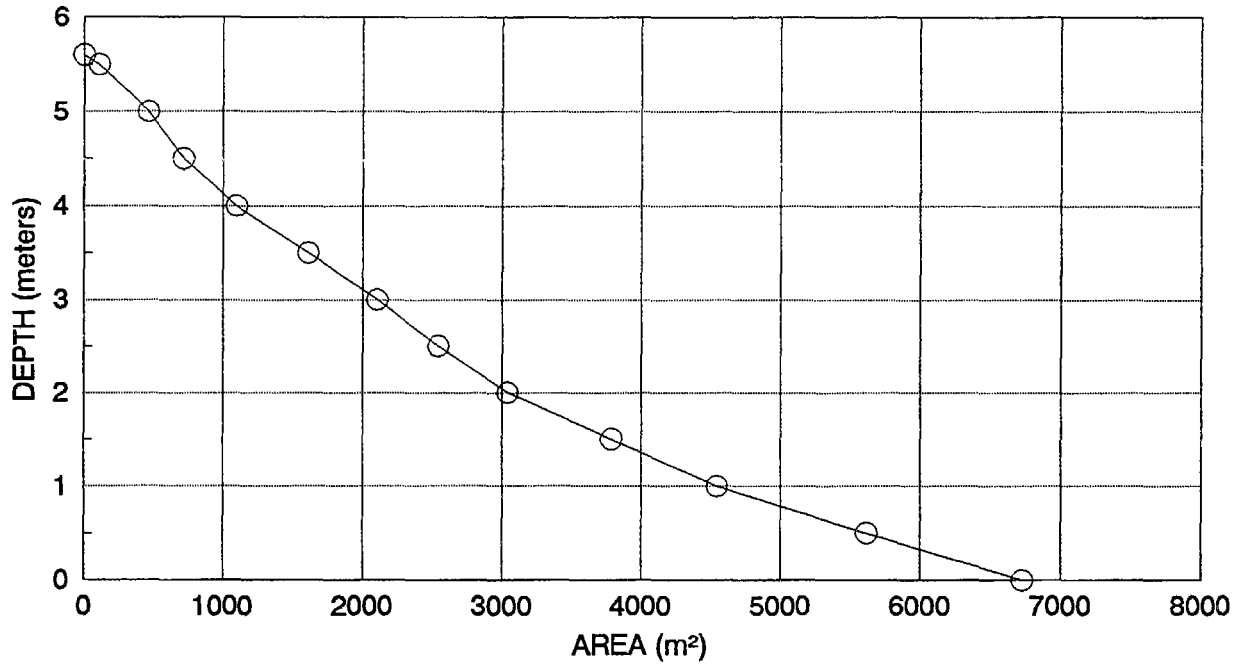


Figure I-9

LOST LAKE
HYPSOGRAPHIC CURVE



VOLUME = 12,500 CUBIC METERS

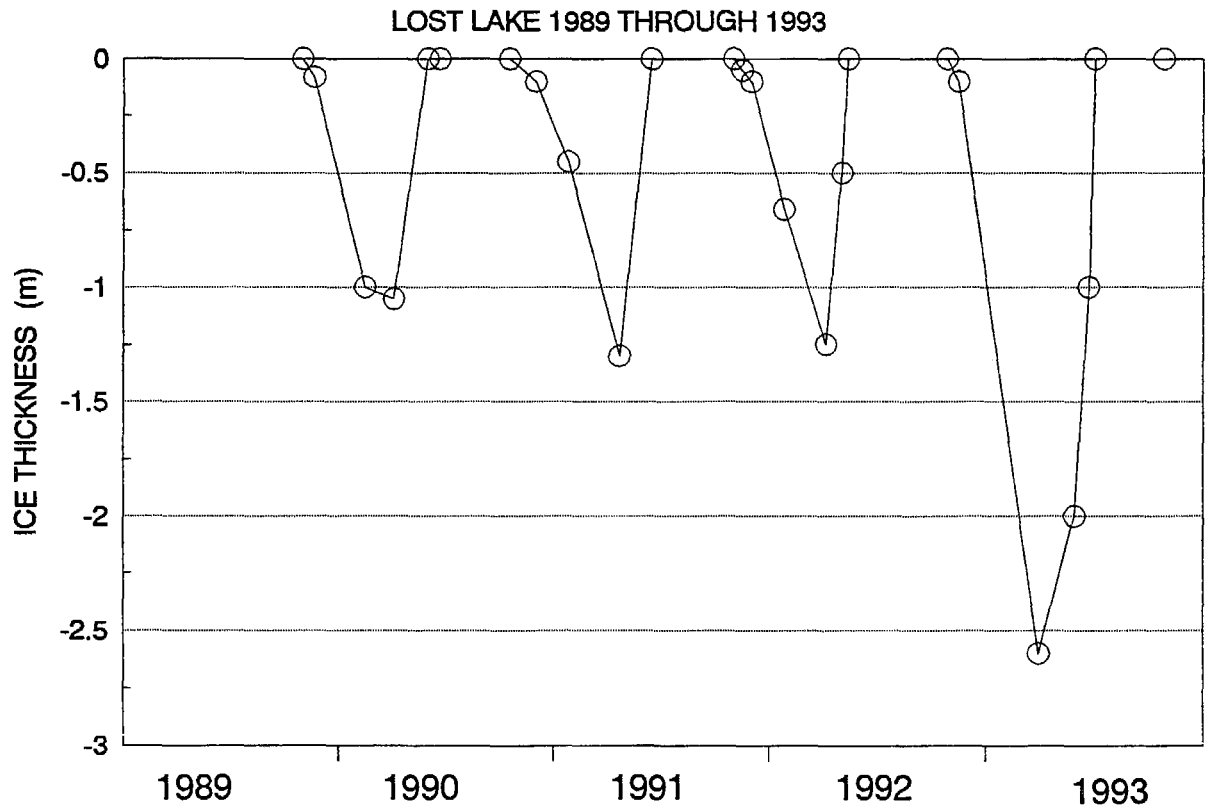
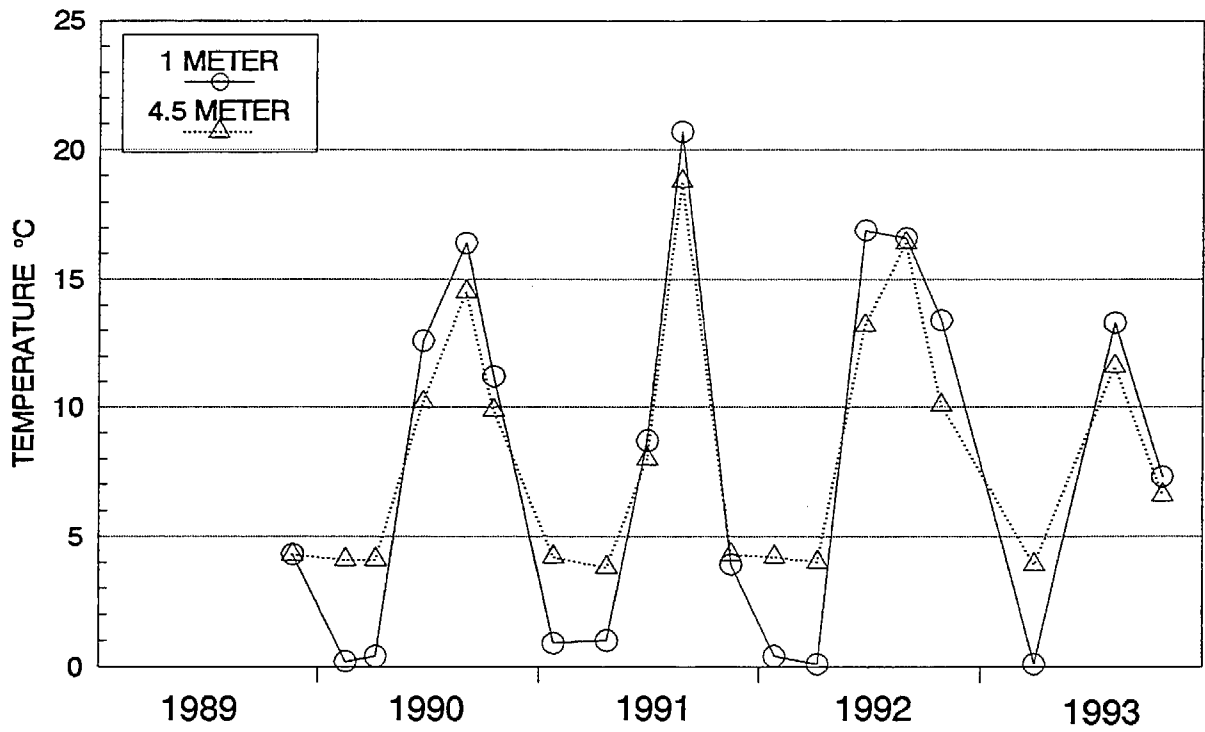


Figure I-10

LOST LAKE
1989 THROUGH 1993



LOST LAKE
1989 THROUGH 1993

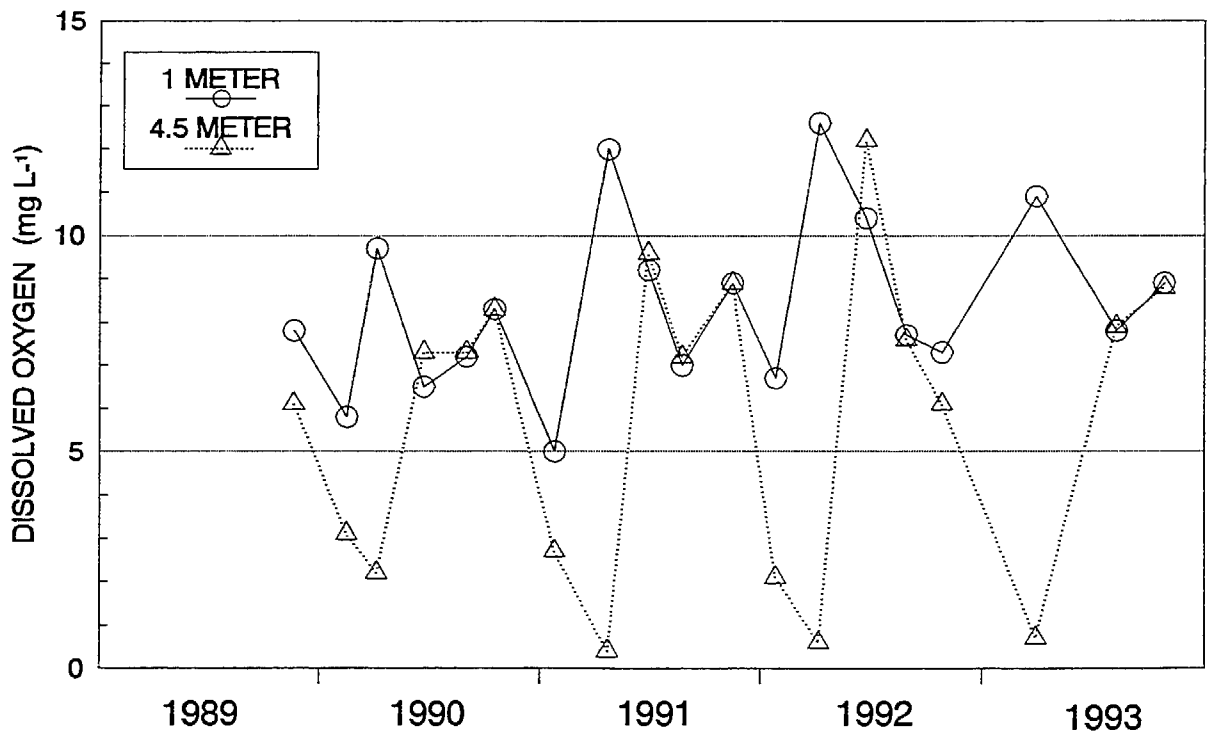
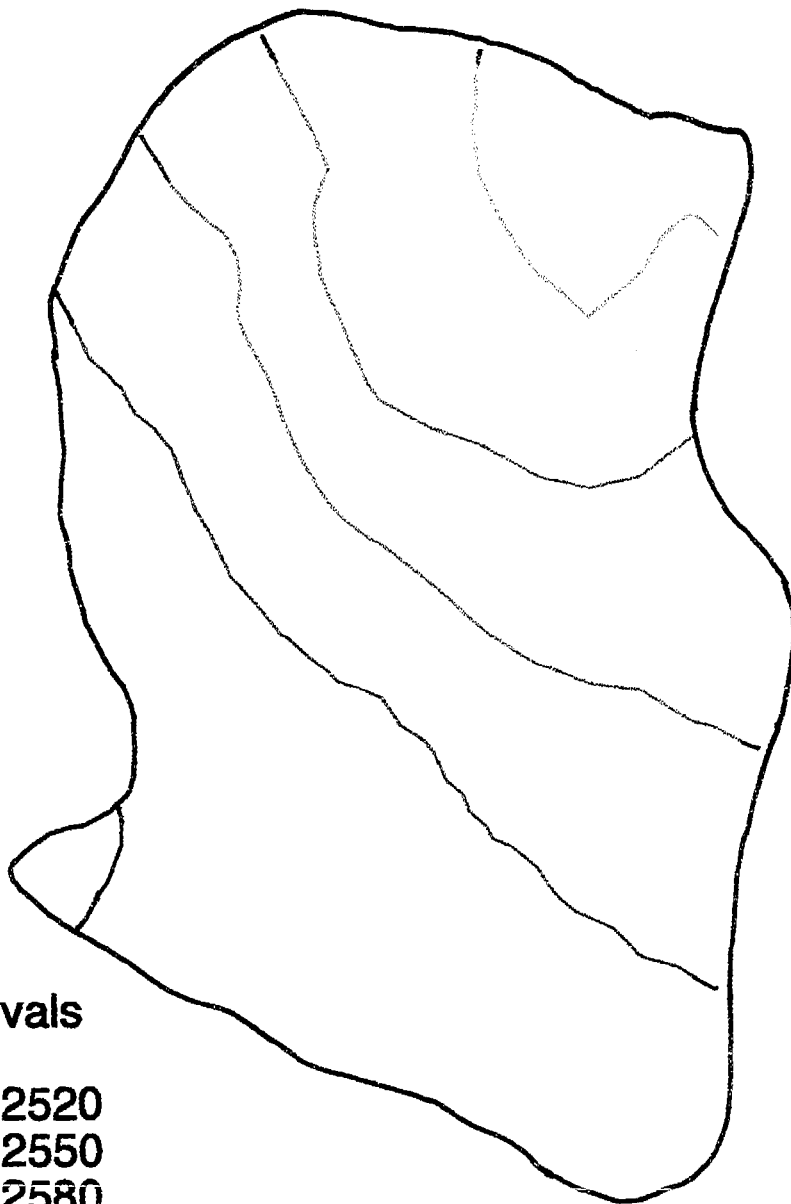
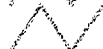
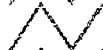


Figure I-11

Lost Lake Digital Elevation Map



Contour Intervals

-  2490
-  2490 - 2520
-  2520 - 2550
-  2550 - 2580
-  2580 - 2610

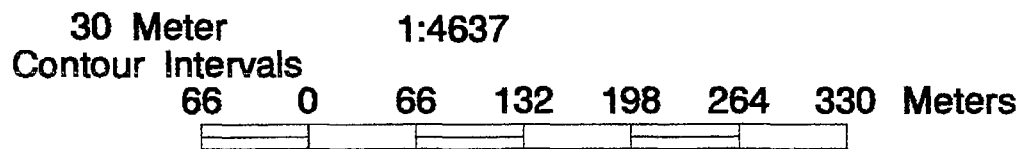
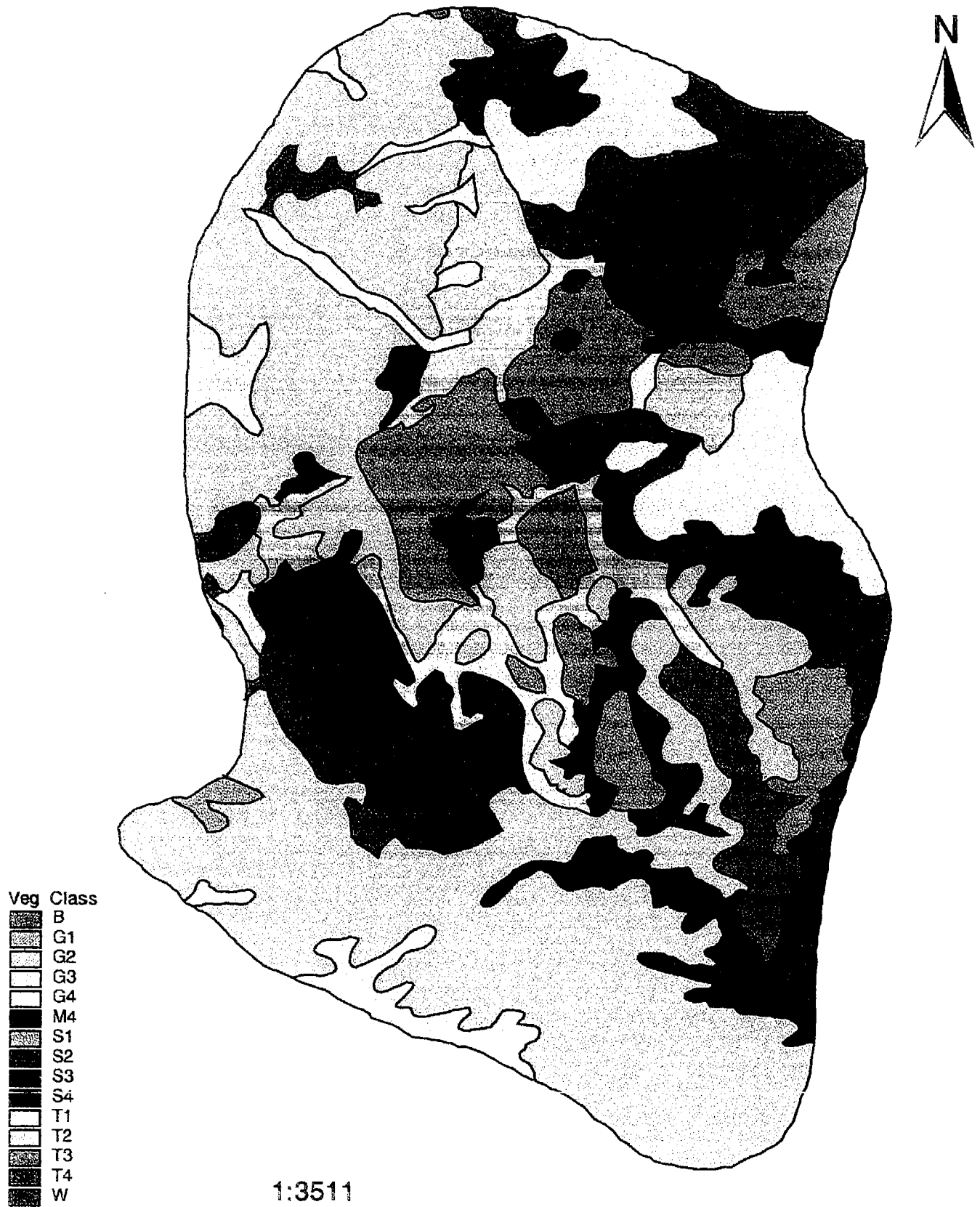


Figure I-12

Lost Lake Vegetation Cover

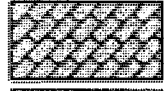
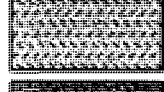
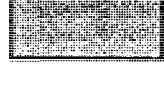


50 0 50 100 150 200 250 Meters

Figure I-13

Lost Lake: Soil Types

Soil

	BC	Alpine Brown Soil-Meadow Complex
	BrR	Alpine Brown Soils and Rock
	MMC	Moist Meadow Soil Complex
	RO	Rock Outcrop
	ROB	Rock Outcrop and Alpine Brown Soils
	RR	Rocky Riparian Soil Complex
	RRT	Rocky Riparian Soil and Talus Complex
	T	Talus
	TB	Talus and Alpine Brown Soils
	TR	Talus and Rubble
	TRB	Talus, Rubble and Alpine Brown Soils
	W	Water
	WM	Wet Meadow Soils

Lost Lake Soil Coverage

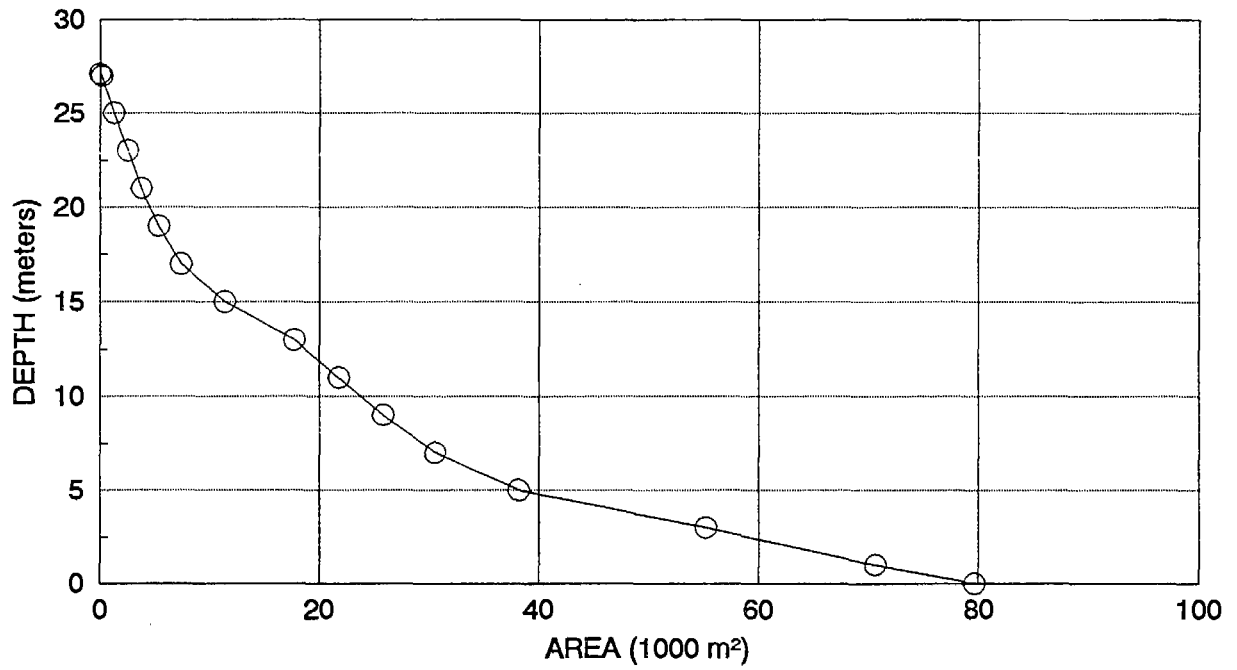


1:3511

50 0 50 100 150 200 250 Meters

Figure I-14 cont.

PEAR LAKE
HYPSOGRAPHIC CURVE



VOLUME = 591,000 CUBIC METERS

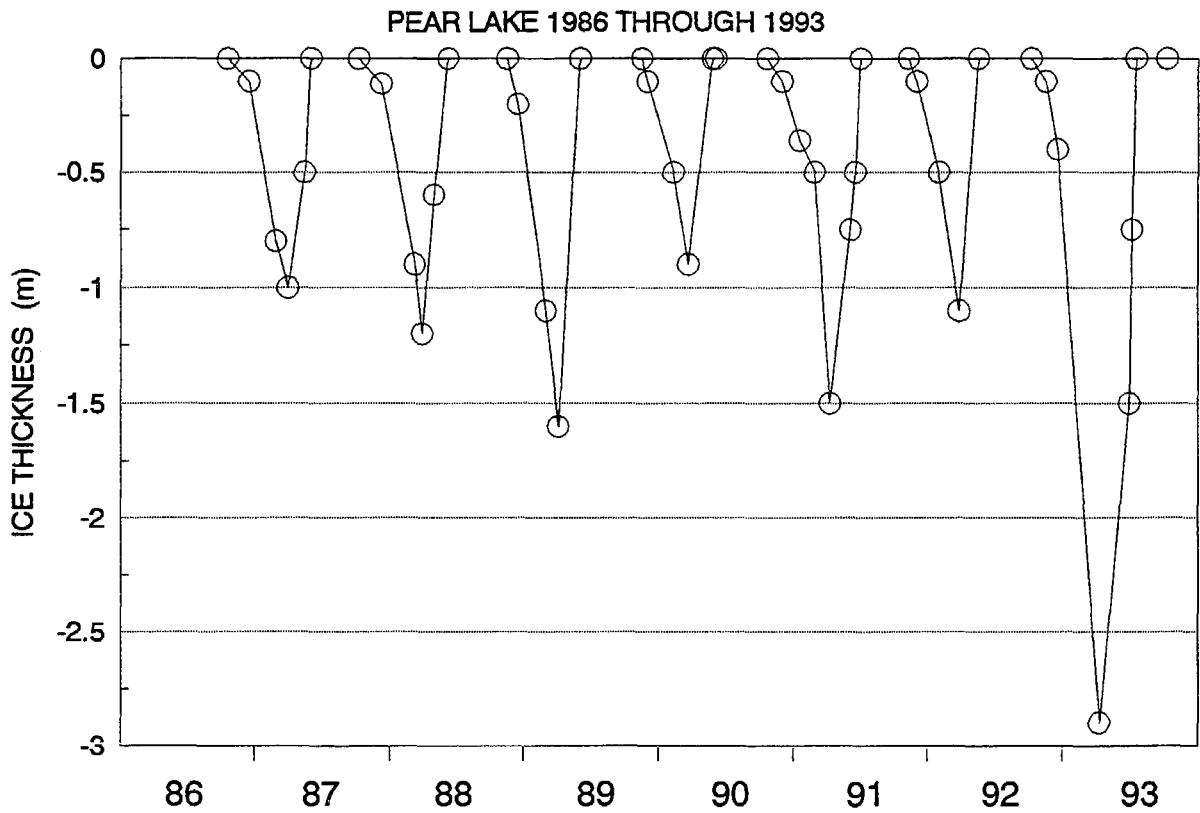
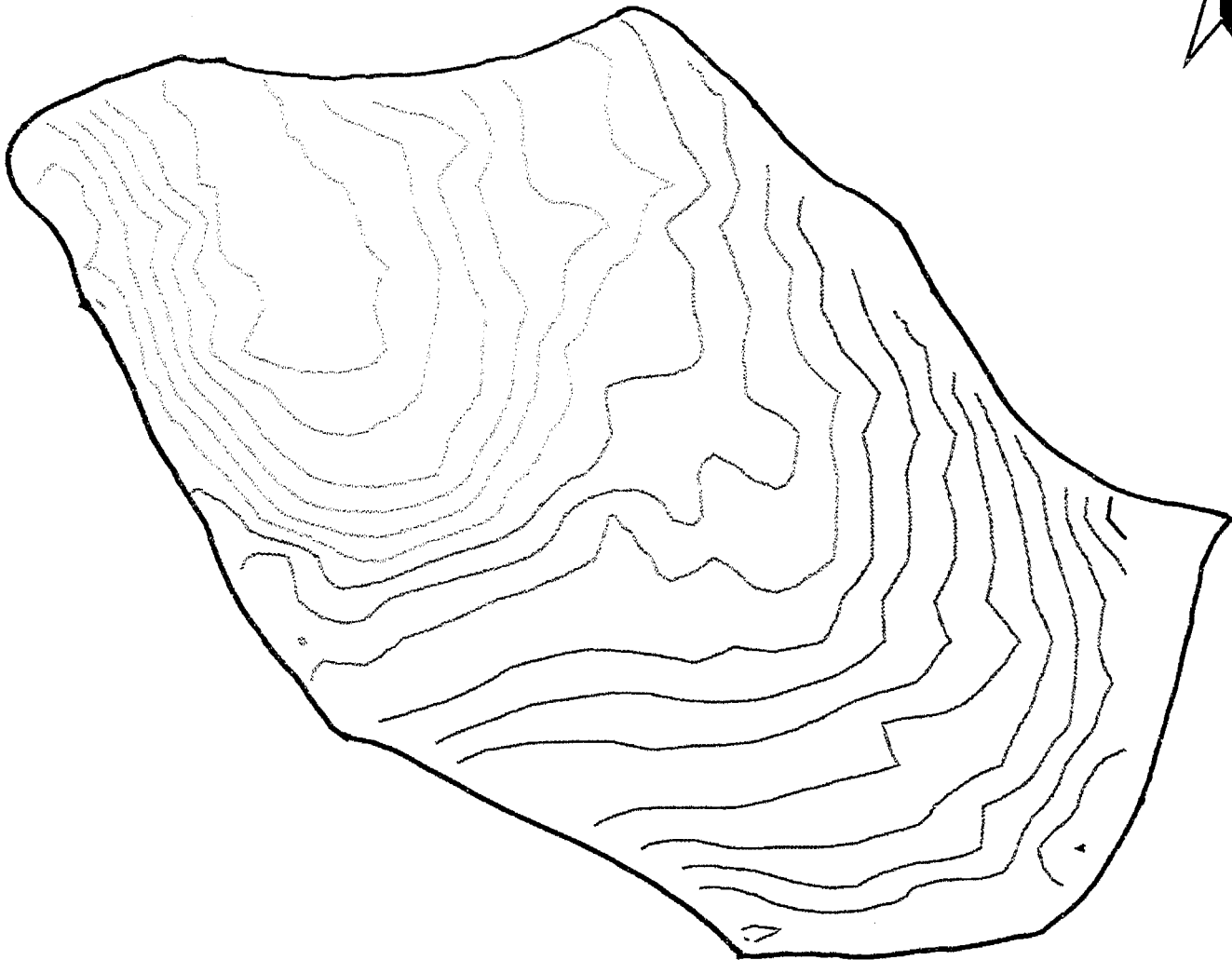


Figure I-15

Pear Lake Digital Elevation Map



Contour Intervals

-  2910 - 3060
-  3060 - 3150
-  3150 - 3240
-  3240 - 3390
-  3390 - 3420

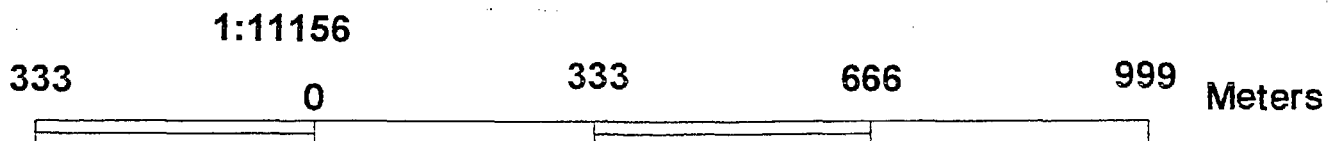
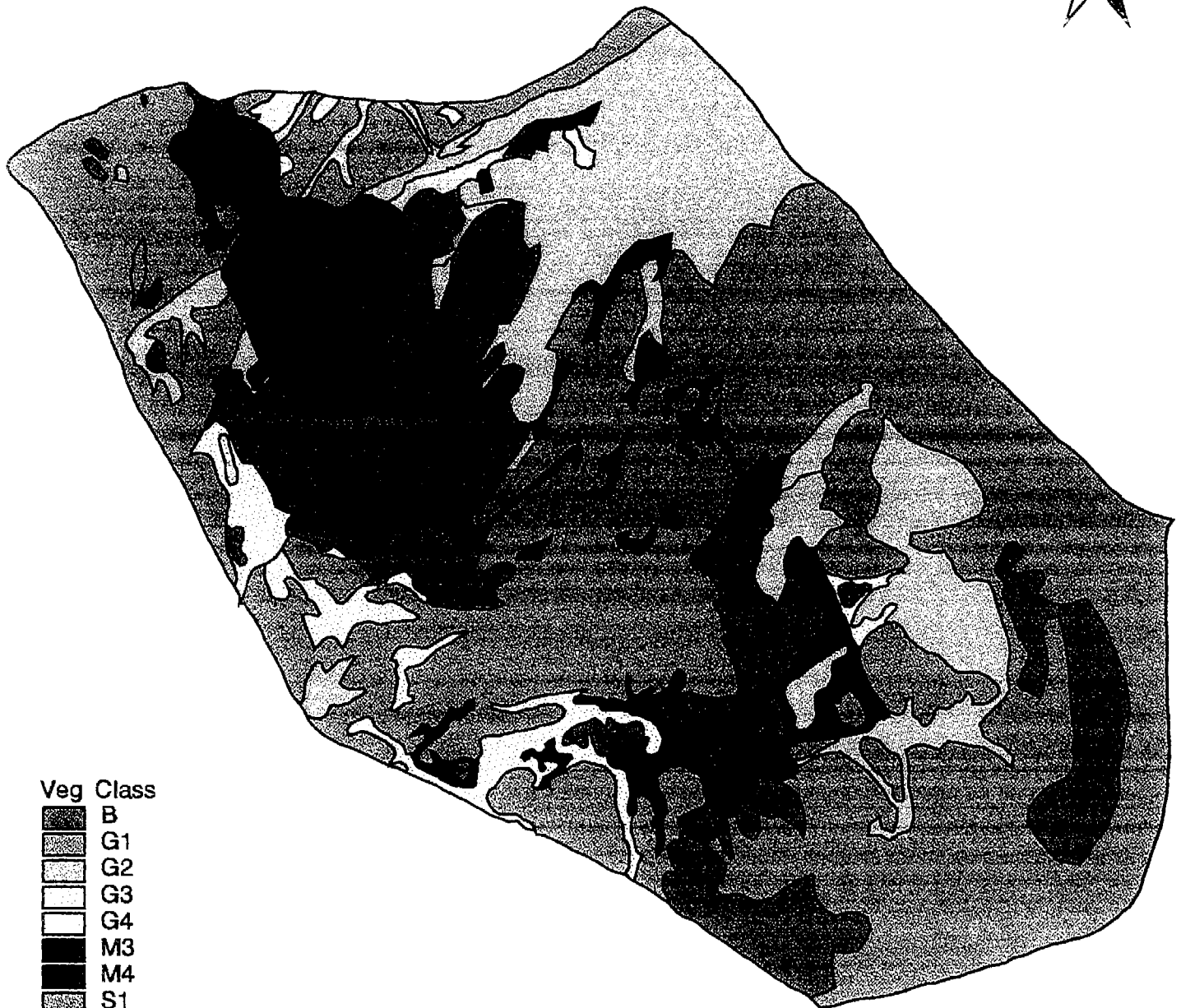


Figure I-17

Pear Lake Vegetation Cover



Veg Class
B
G1
G2
G3
G4
M3
M4
S1
S2
S3
S4
T1
T2
T3
T4
W

1:11156

333

0

333

666

999

Meters

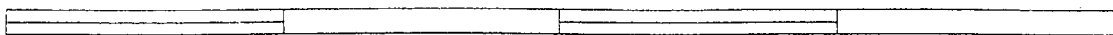


Figure I-18

Pear Lake: Soil Types

Soil

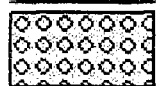
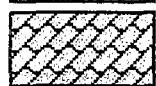
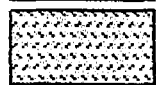
	BC	Alpine Brown Soil-Meadow Complex
	BL	Boulders
	BT	Alpine Brown Soils and Talus
	BrR	Alpine Brown Soils and Rock
	MMC	Moist Meadow Soil Complex
	RO	Rock Outcrop
	ROB	Rock Outcrop and Alpine Brown Soils
	RR	Rocky Riparian Soil Complex
	RRT	Rocky Riparian Soil and Talus Complex
	T	Talus
	TB	Talus and Alpine Brown Soils
	TS	Talus and Scree
	W	Water
	WMC	Wet Meadow Soil Complex

Figure I-19

Pear Lake Soil Coverage

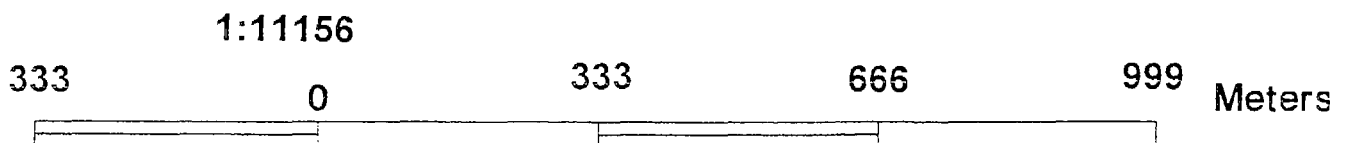
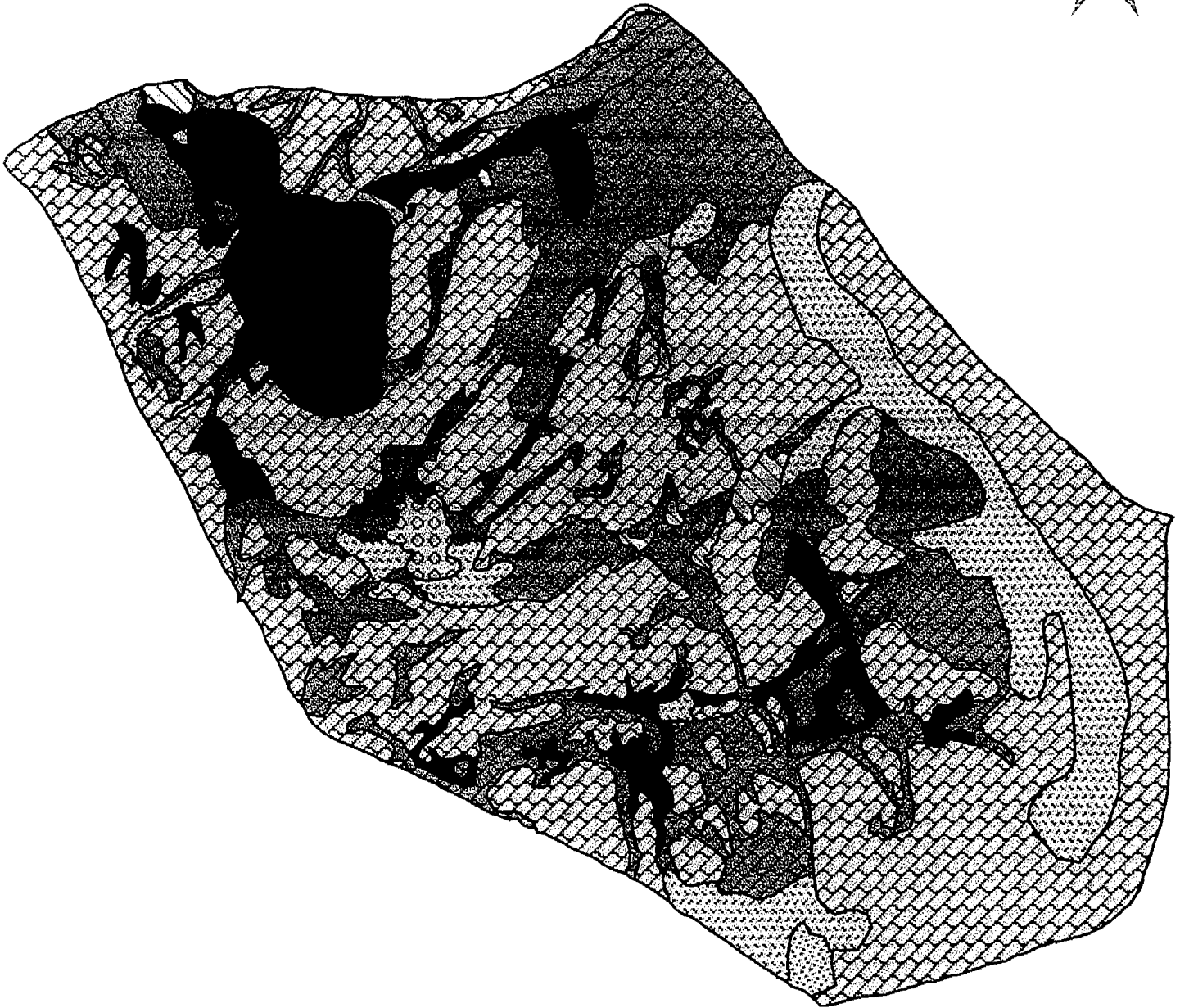
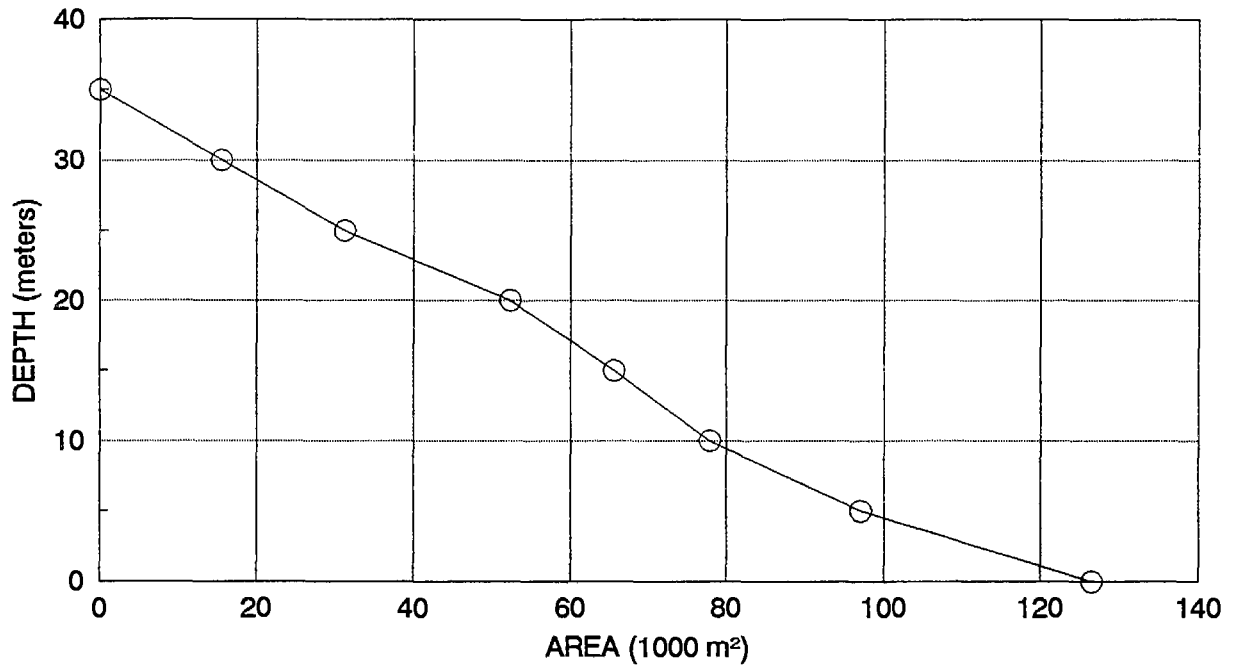


Figure I-19 cont.

RUBY LAKE
HYPSOGRAPHIC CURVE



VOLUME = 2,080,000 CUBIC METERS

RUBY LAKE 1986 THROUGH 1994

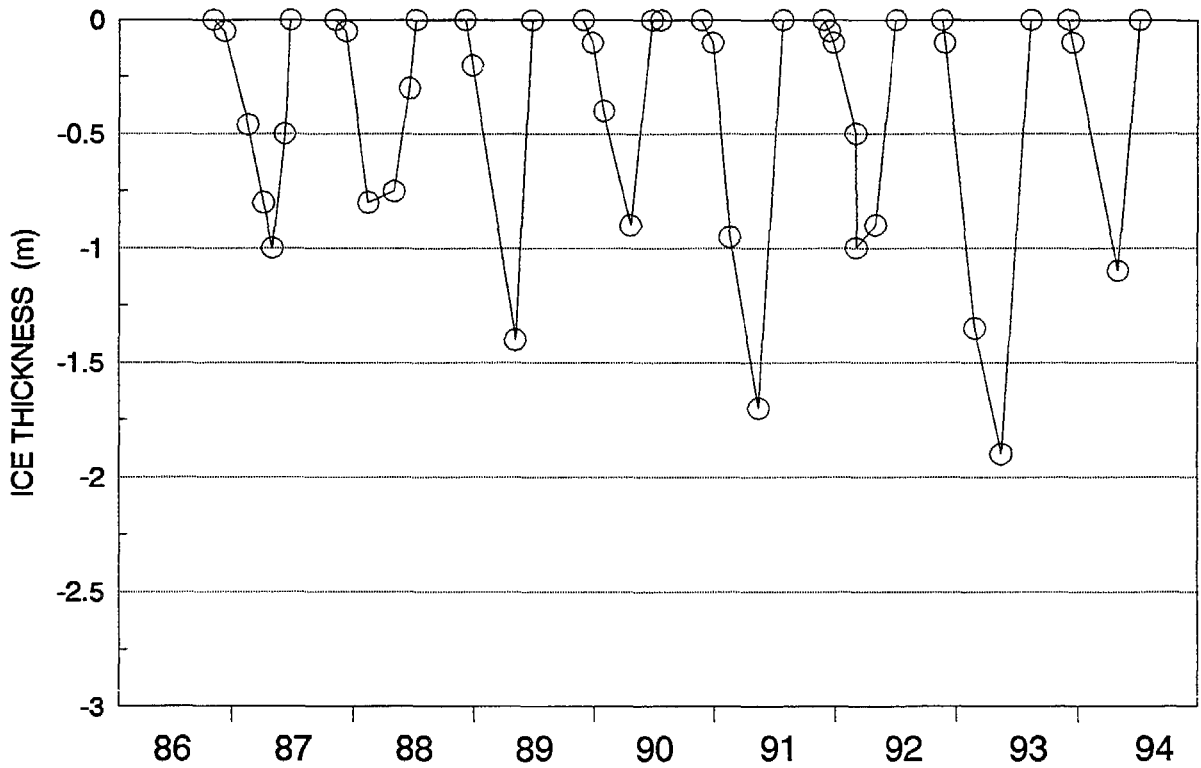
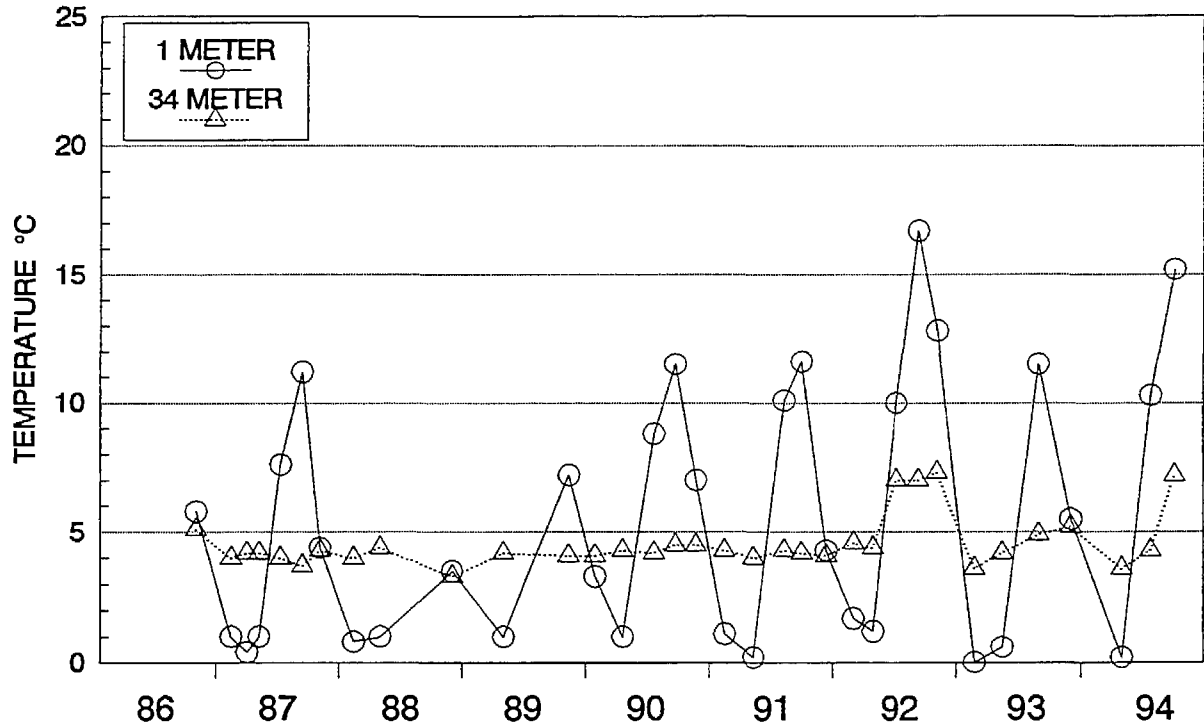


Figure I-20

RUBY LAKE
1986 THROUGH 1994



RUBY LAKE
1986 THROUGH 1994

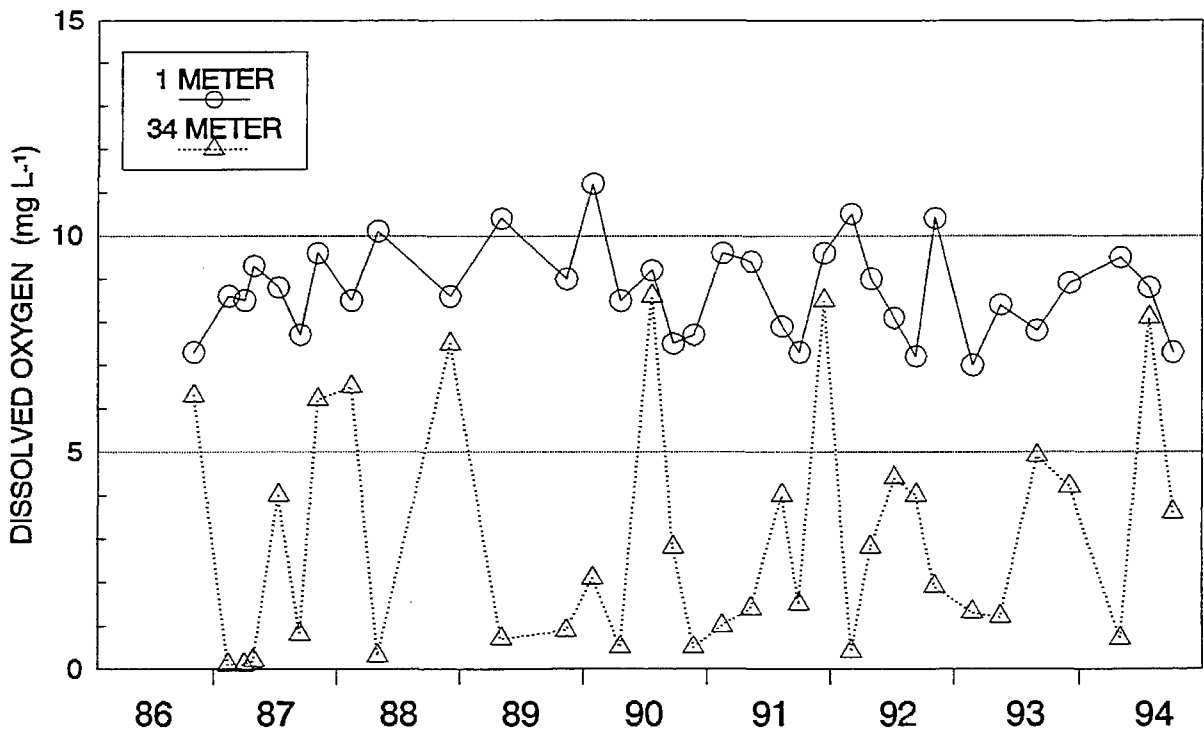


Figure I-21

Ruby Lake Digital Elevation Map



Contour Intervals

	3390 - 3630
	3630 - 3780
	3780 - 3900
	3900 - 3960
	3960 - 4140

30 Meter
Contour Intervals

1:22930

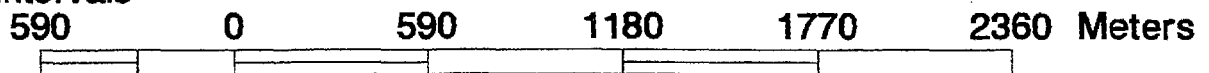


Figure I-22

Ruby Lake Vegetation Cover

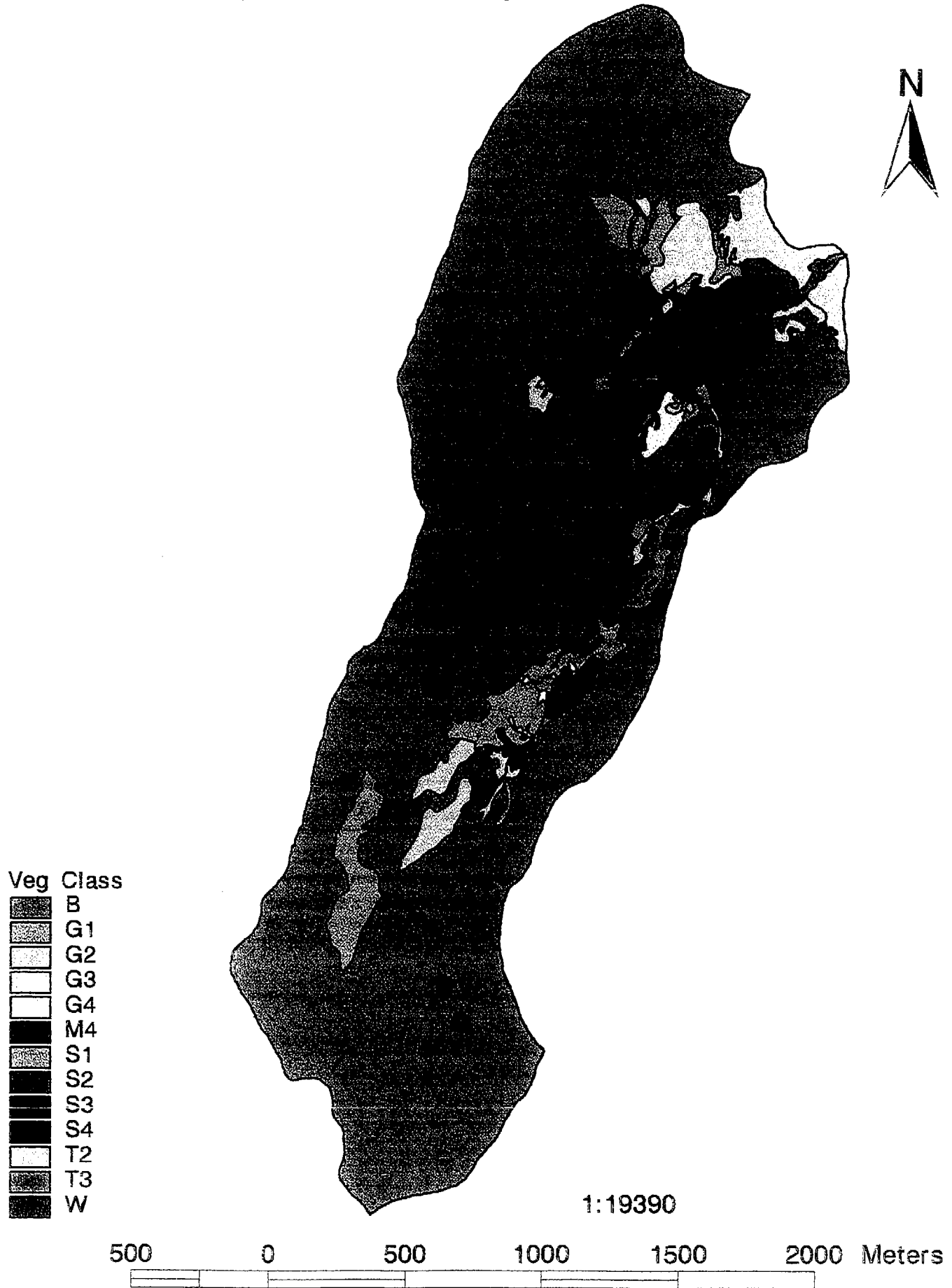
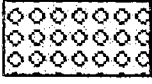
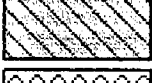
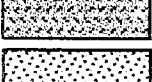


Figure I-23

Ruby Lake: Soil Types

Soil

	BC	Alpine Brown Soil-Meadow Complex
	BL	Boulders
	BLB	Boulders and Alpine Brown Soils
	BT	Alpine Brown Soils and Talus
	Br	Alpine Brown Soils
	BrR	Alpine Brown Soils and Rock
	BrS	Alpine Brown Soils and Scree
	MMC	Moist Meadow Soil Complex
	RG	Rock covered Glaciers
	RO	Rock Outcrop
	ROB	Rock Outcrop and Alpine Brown Soils
	RR	Rocky Riparian Soil Complex
	RRT	Rocky Riparian Soil and Talus Complex
	T	Talus
	TB	Talus and Alpine Brown Soils
	TS	Talus and Scree
	W	Water

Ruby Lake Soil Coverage

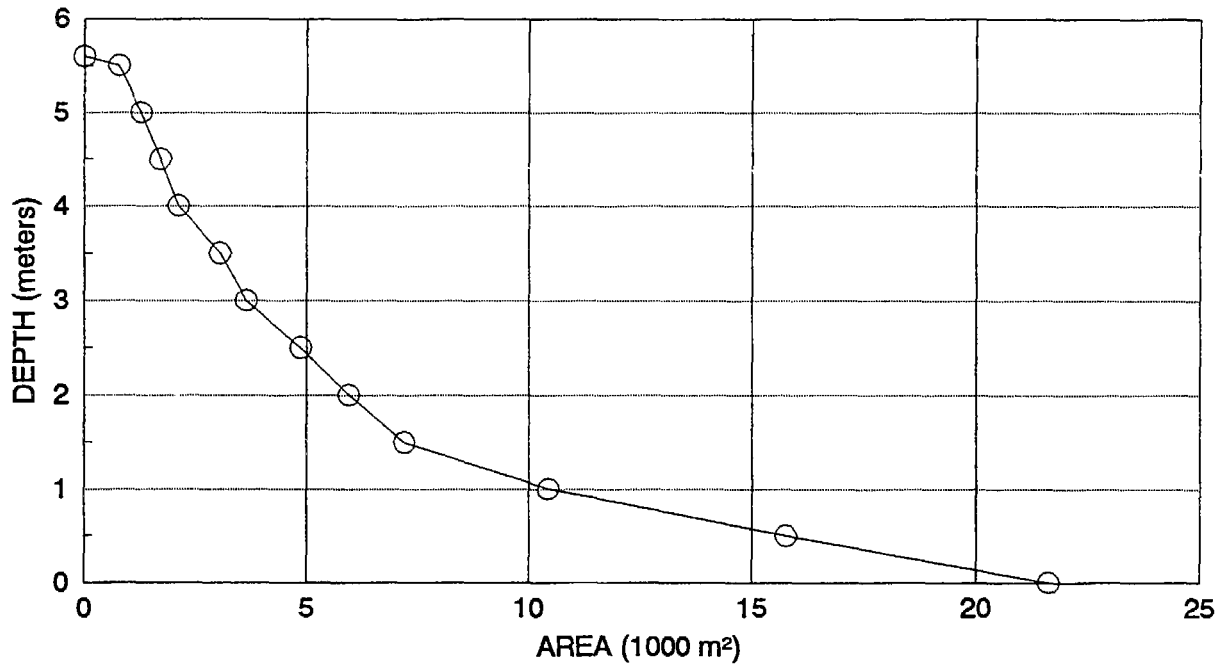


1:19376

500 0 500 1000 1500 2000 Meters

Figure I-24 cont.

SPULLER LAKE
HYPSOGRAPHIC CURVE



VOLUME = 34,700 CUBIC METERS

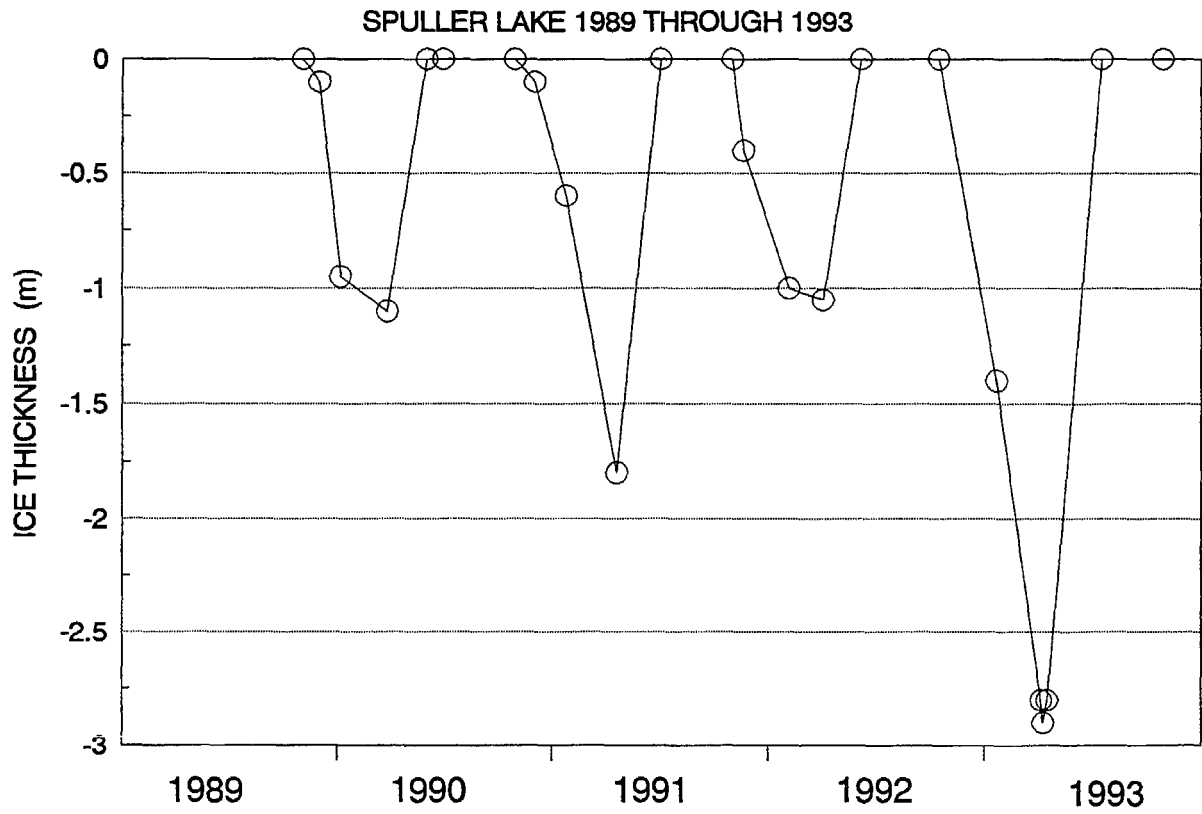
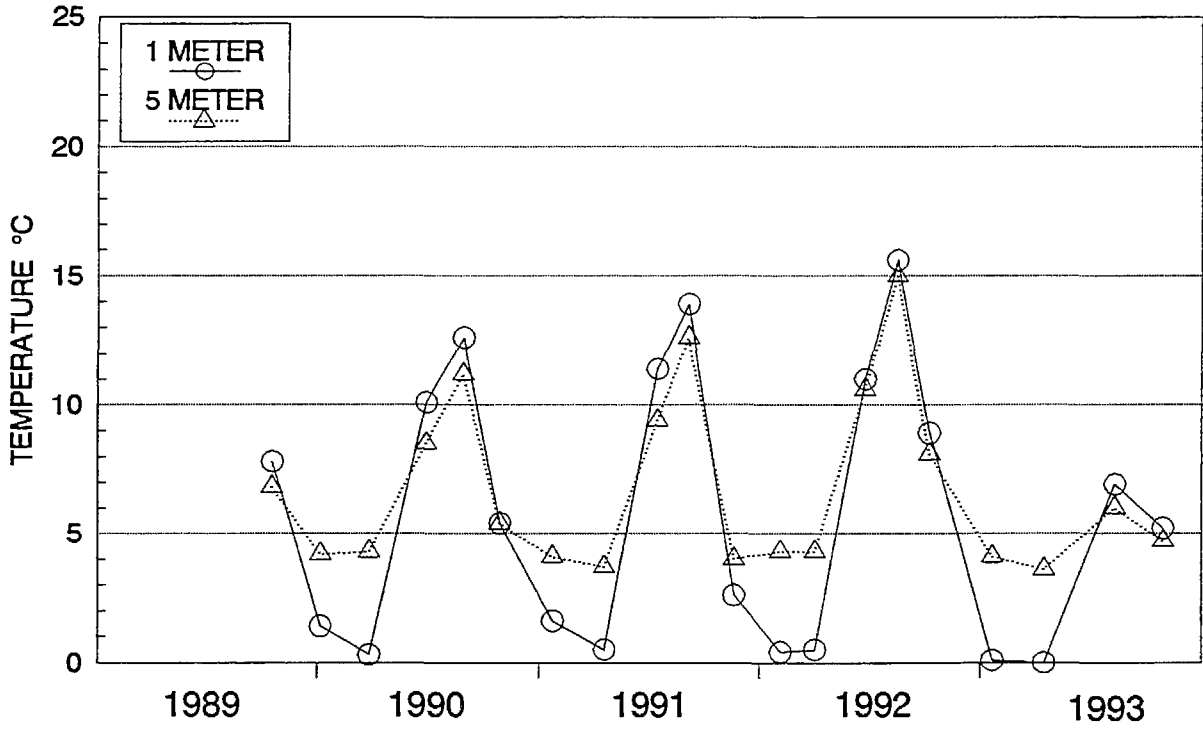


Figure I-25

SPULLER LAKE
1989 THROUGH 1993



SPULLER LAKE
1989 THROUGH 1993

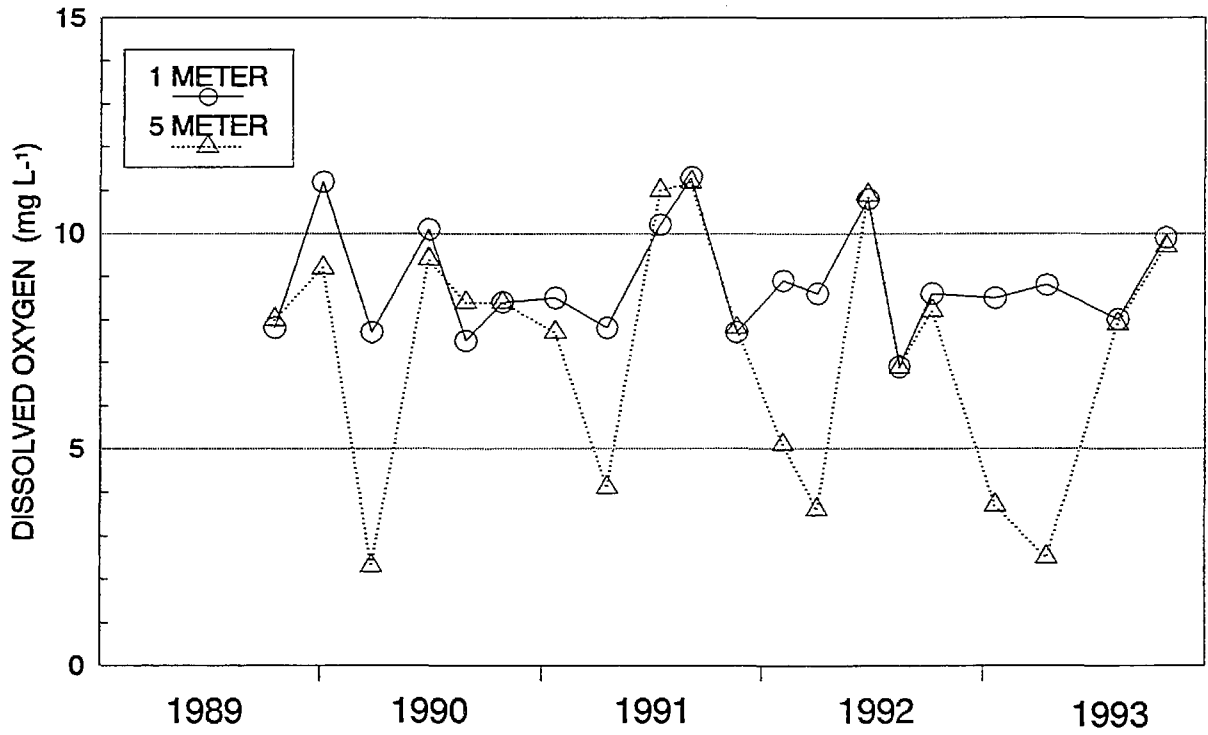


Figure I-26

Spuller Lake Digital Elevation Map

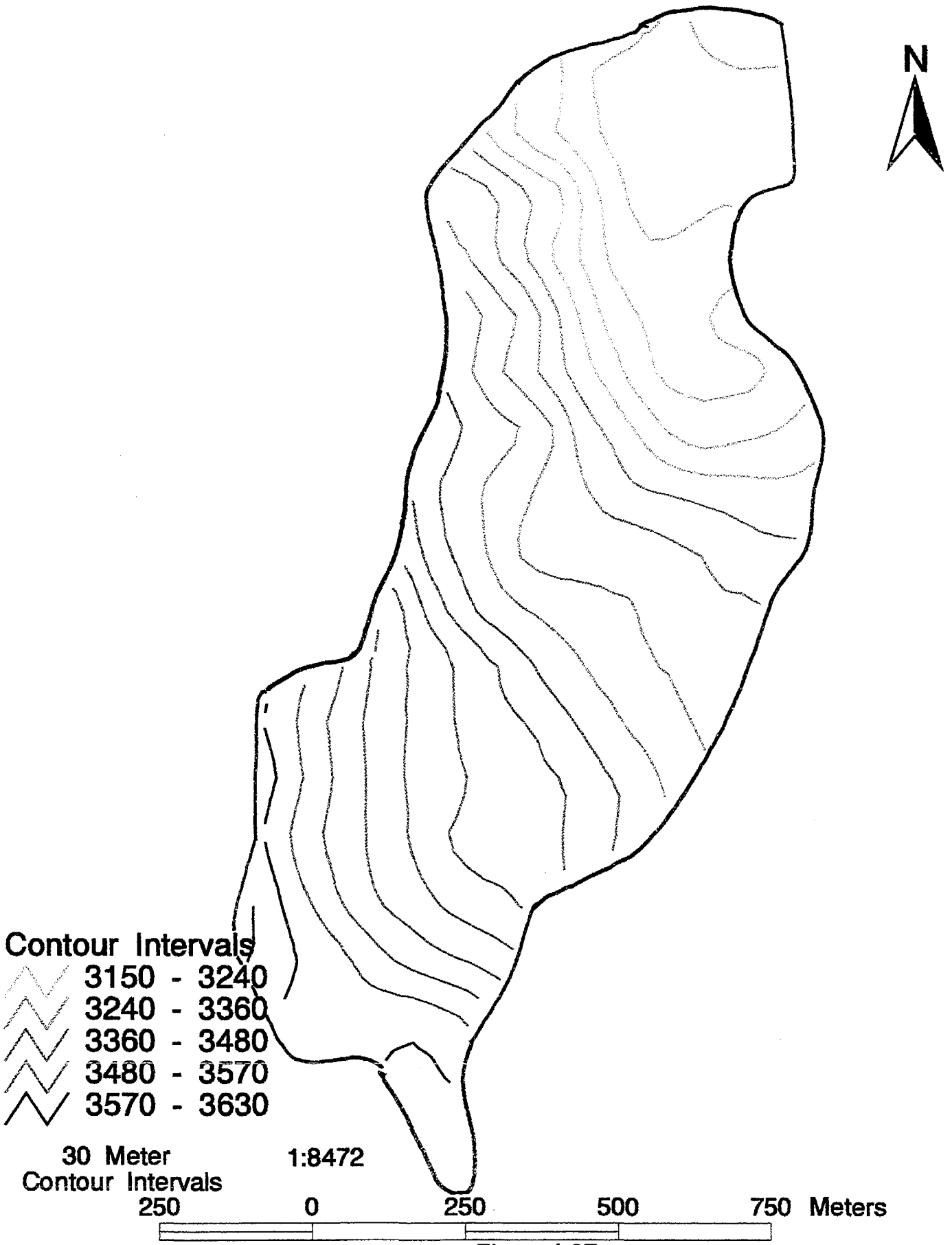


Figure I-27

Spuller Lake Vegetation Cover

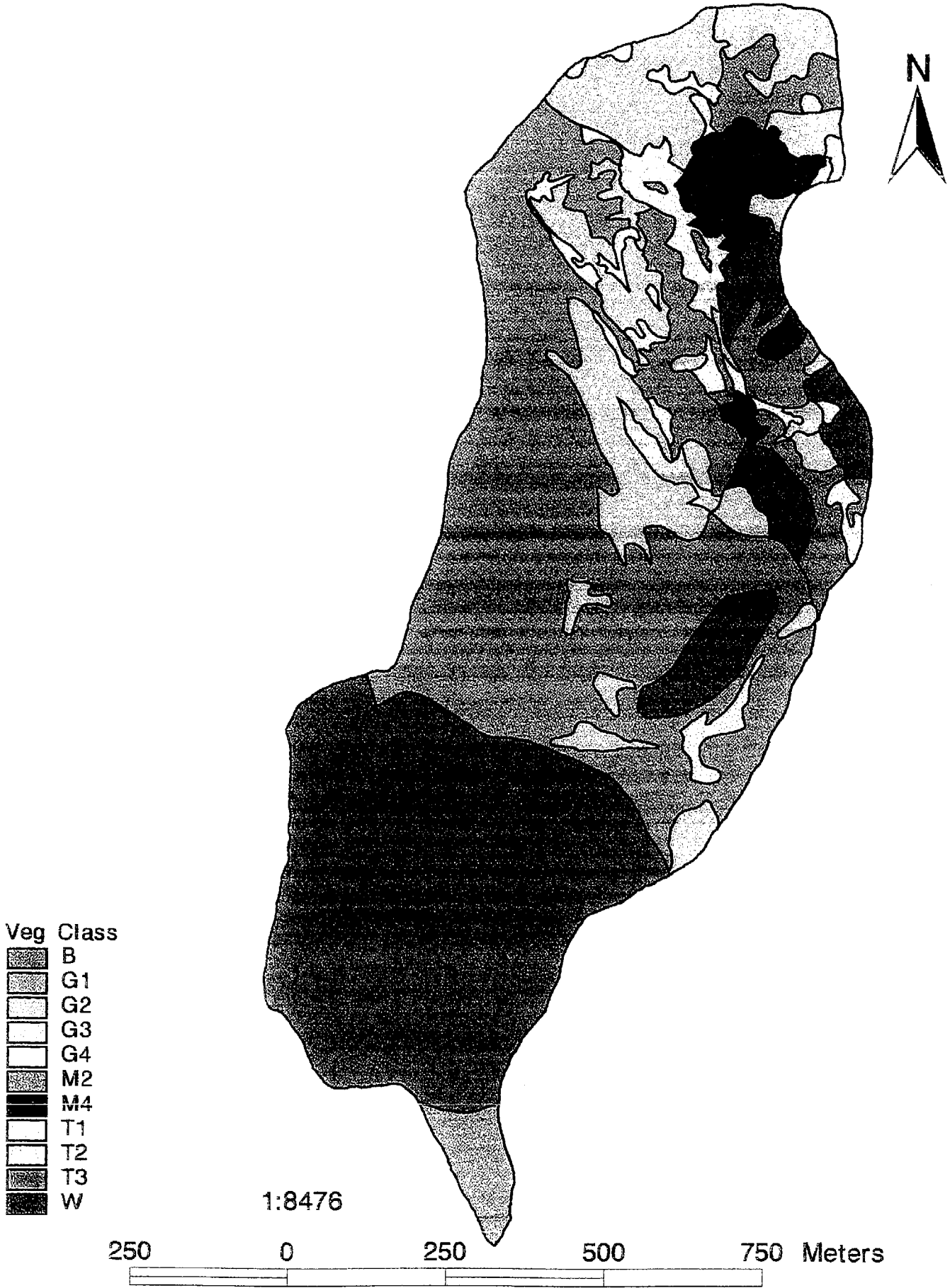
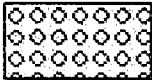
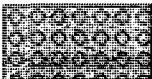
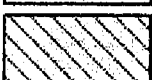


Figure I-28

Spuller Lake: Soil Types

Soil

	BC	Alpine Brown Soil-Meadow Complex
	BL	Boulders
	BLB	Boulders and Alpine Brown Soils
	BT	Alpine Brown Soils and Talus
	Br	Alpine Brown Soils
	BrR	Alpine Brown Soils and Rock
	BrS	Alpine Brown Soils and Scree
	MM	Moist Meadow Soils
	MMC	Moist Meadow Soil Complex
	RO	Rock Outcrop
	ROB	Rock Outcrop and Alpine Brown Soils
	RR	Rocky Riparian Soil Complex
	RRT	Rocky Riparian Soil and Talus Complex
	T	Talus
	TB	Talus and Alpine Brown Soils
	W	Water

Spuller Lake Soil Coverage

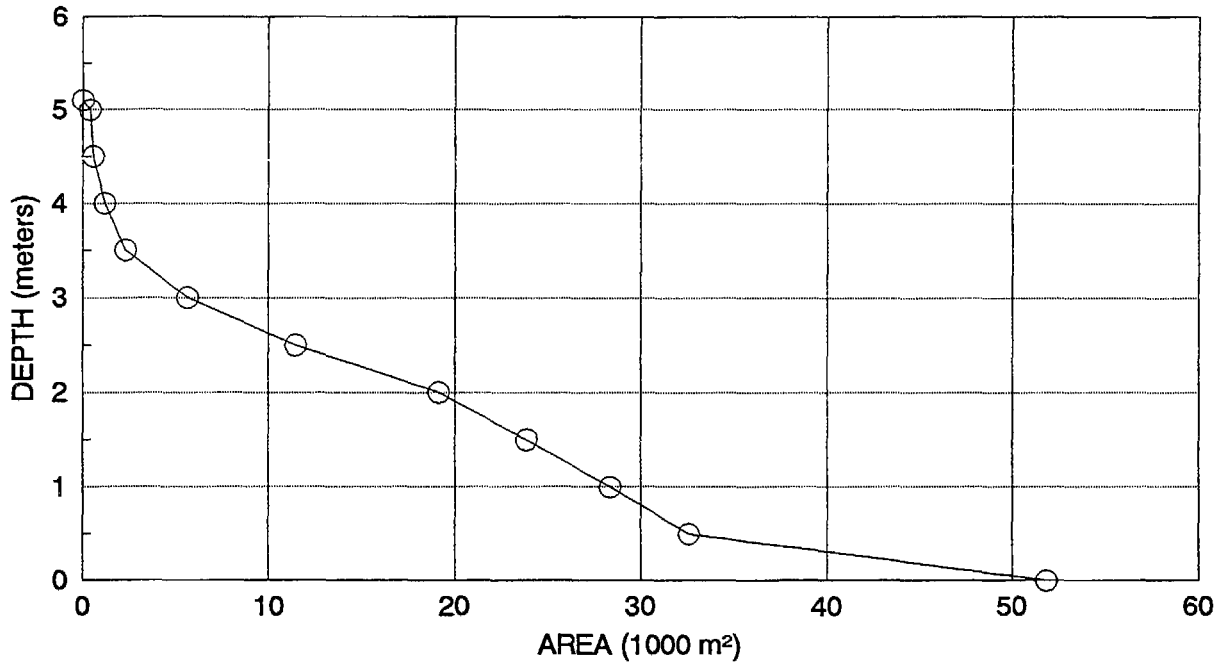


1:8476

250 0 250 500 750 Meters

Figure I-29 cont.

TOPAZ LAKE
HYPSOGRAPHIC CURVE



VOLUME = 76,900

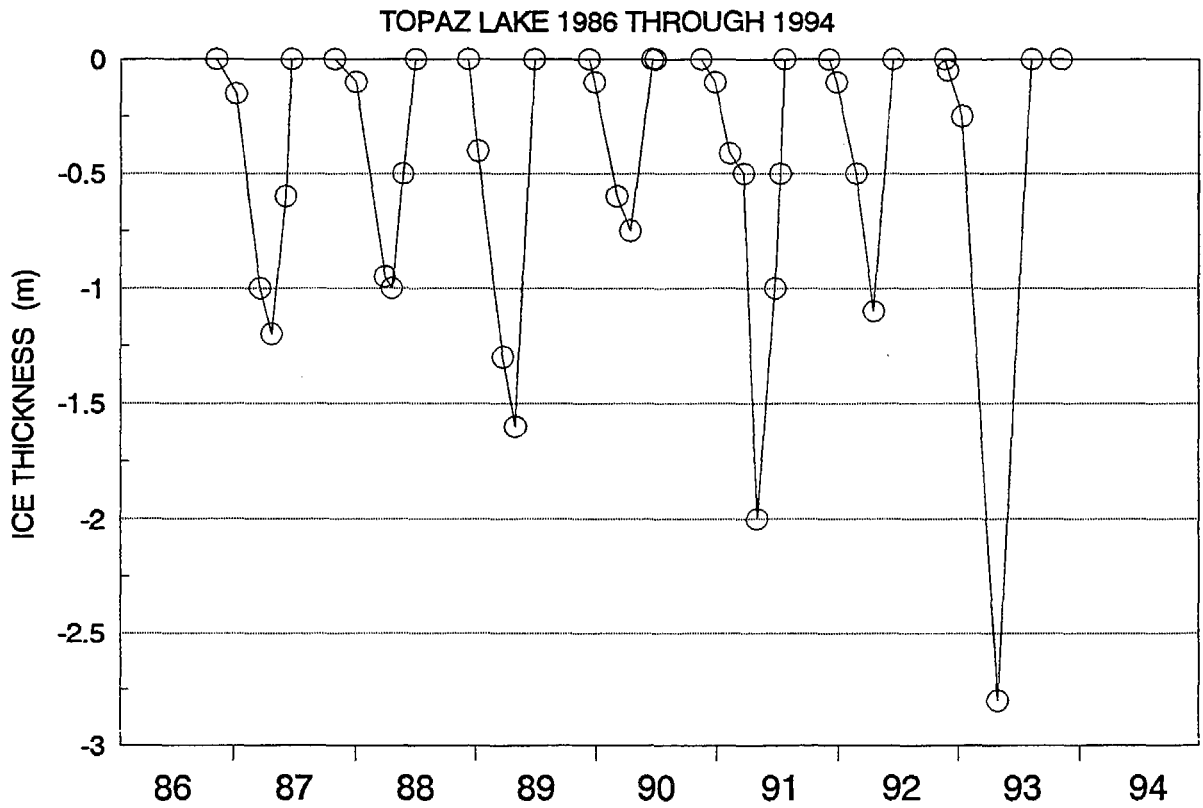
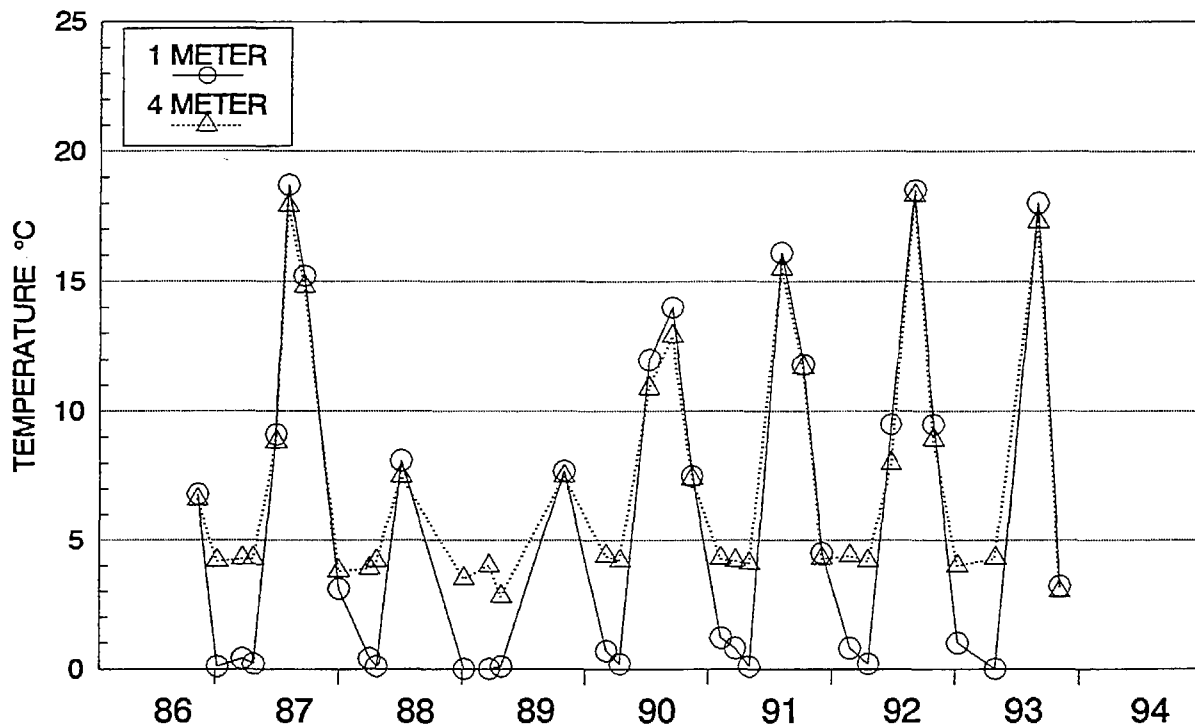


Figure I-30

TOPAZ LAKE
1986 THROUGH 1994



TOPAZ LAKE
1986 THROUGH 1994

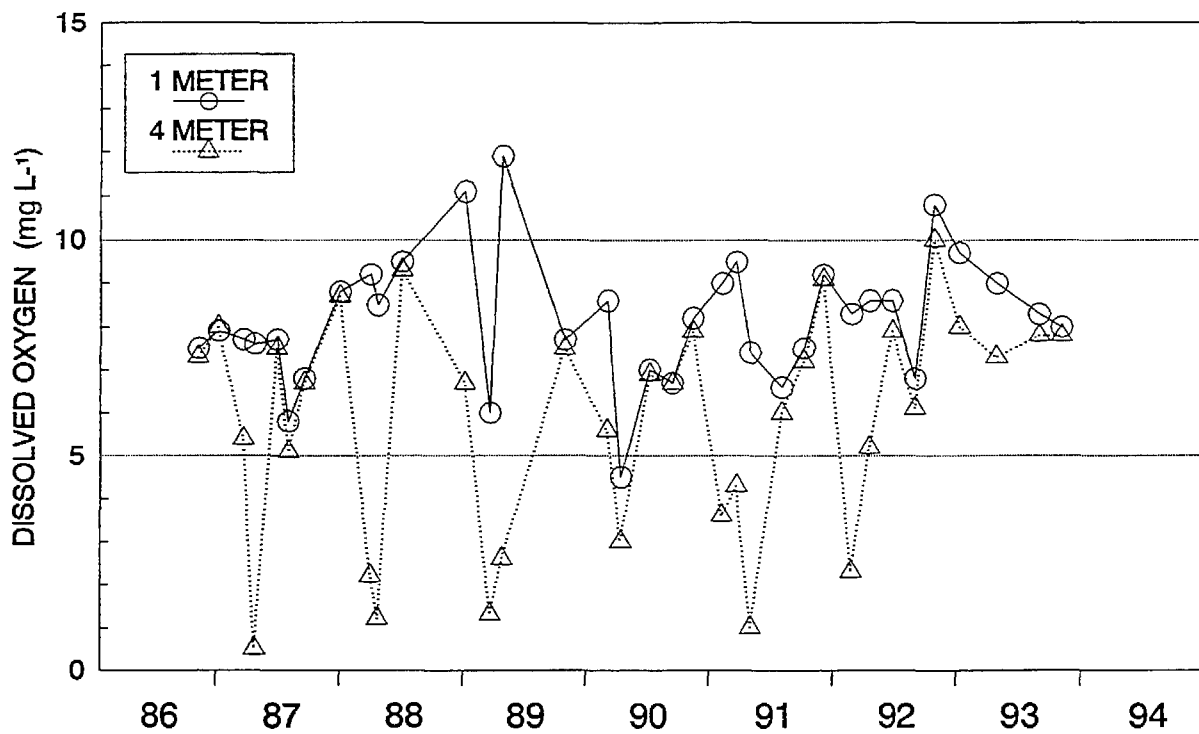
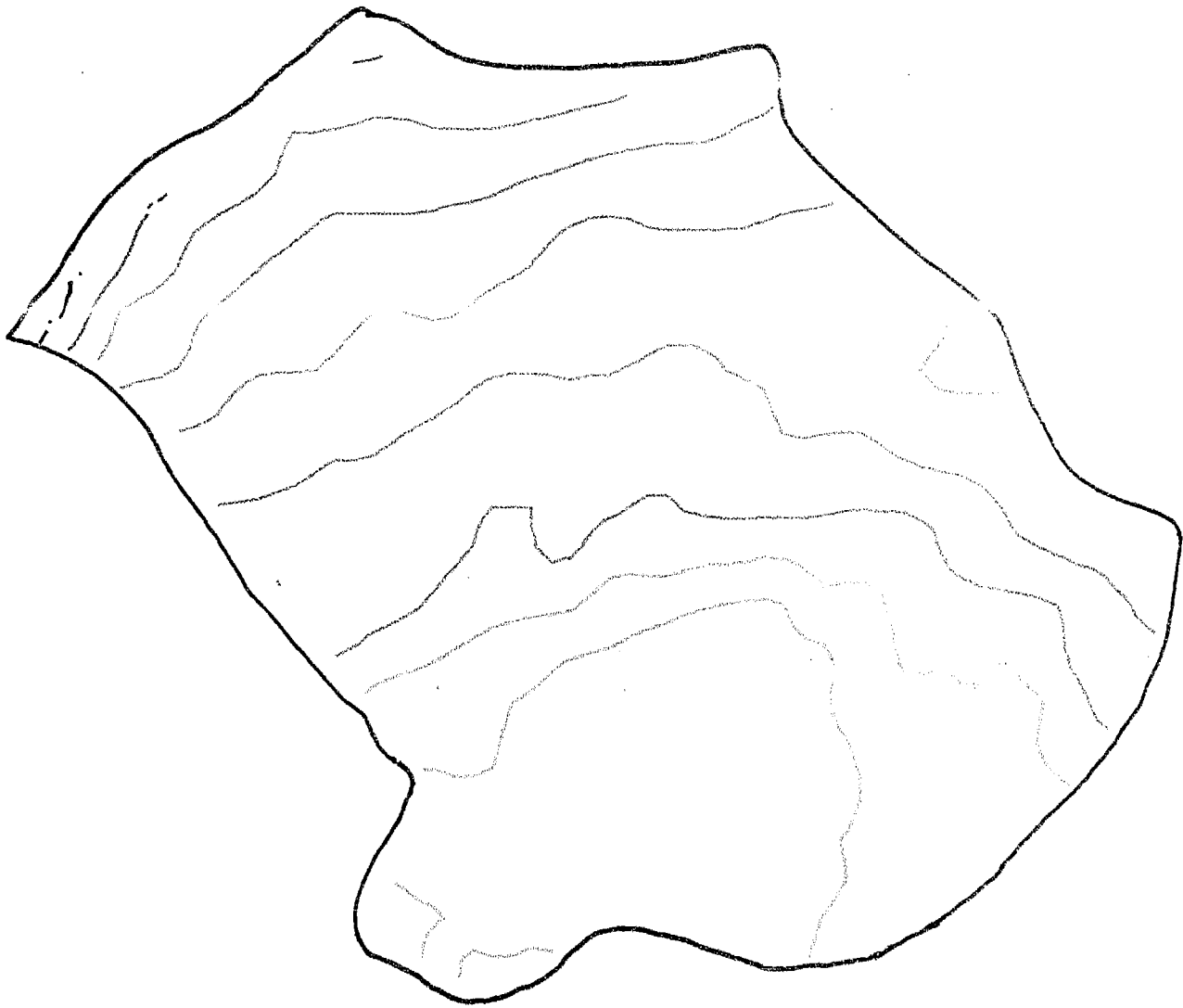


Figure I-31

Topaz Lake Digital Elevation Map



- Contour Interval**
-  3210 - 3270
 -  3270 - 3360
 -  3360 - 3420
 -  3420 - 3450
 -  3450 - 3480

30 Meter
Contour Intervals

1:10732

290 0 290 580 870 1160 Meters

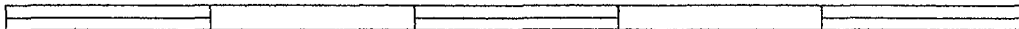
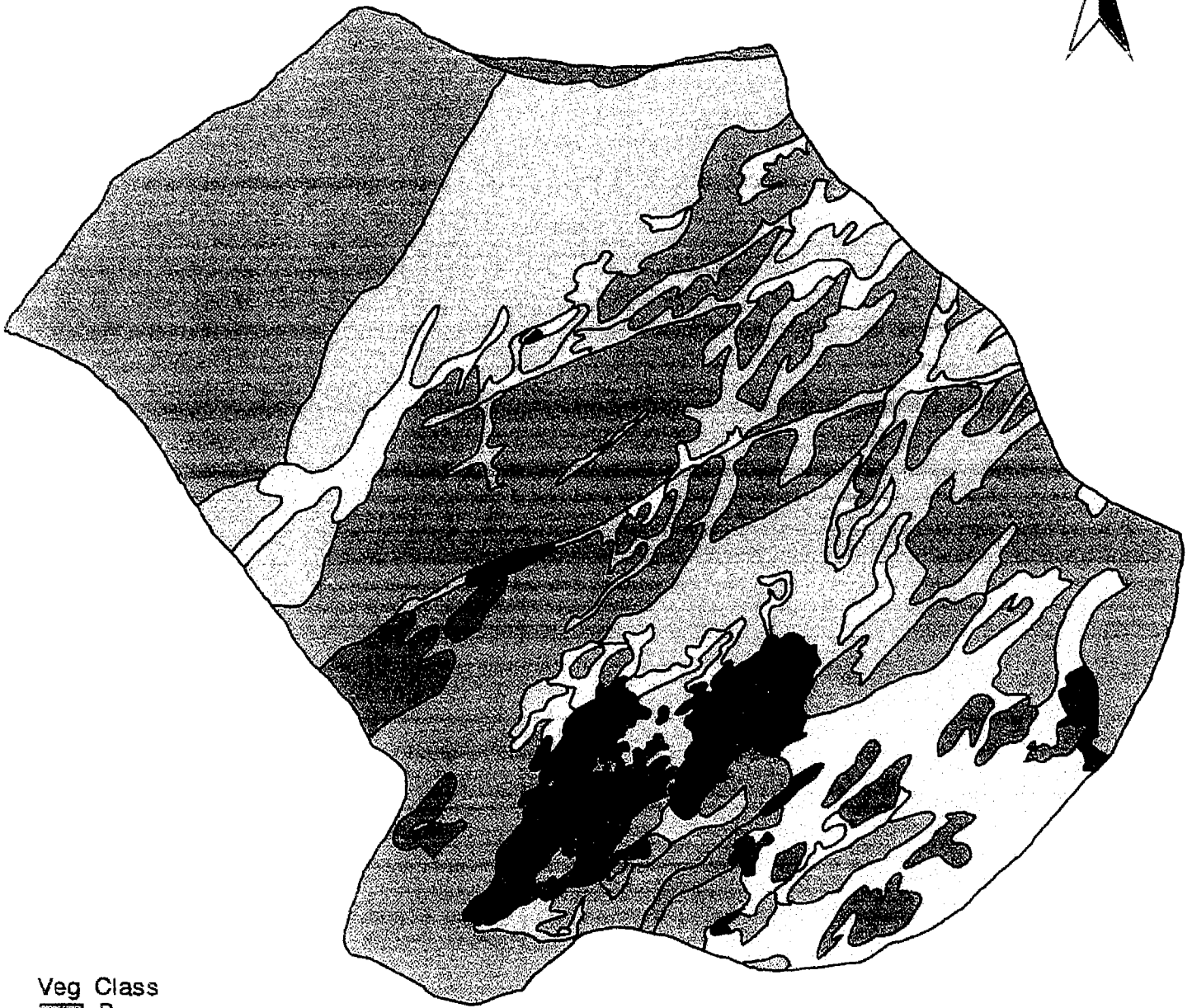


Figure I-32

Topaz Lake Vegetation Cover



Veg Class
B
G1
G2
G3
G4
M2
M3
M4
T1
W

1:9279

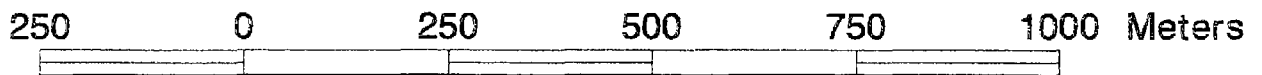


Figure I-33

Topaz Lake: Soil Types

Soil



BC

Alpine Brown Soil-Meadow Complex



Br

Alpine Brown Soils



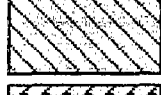
BrR

Alpine Brown Soils and Rock



MM

Moist Meadow Soils



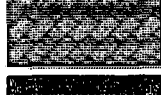
MMC

Moist Meadow Soil Complex



RO

Rock Outcrop



ROB

Rock Outcrop and Alpine Brown Soils



RR

Rocky Riparian Soil Complex



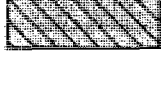
W

Water



WM

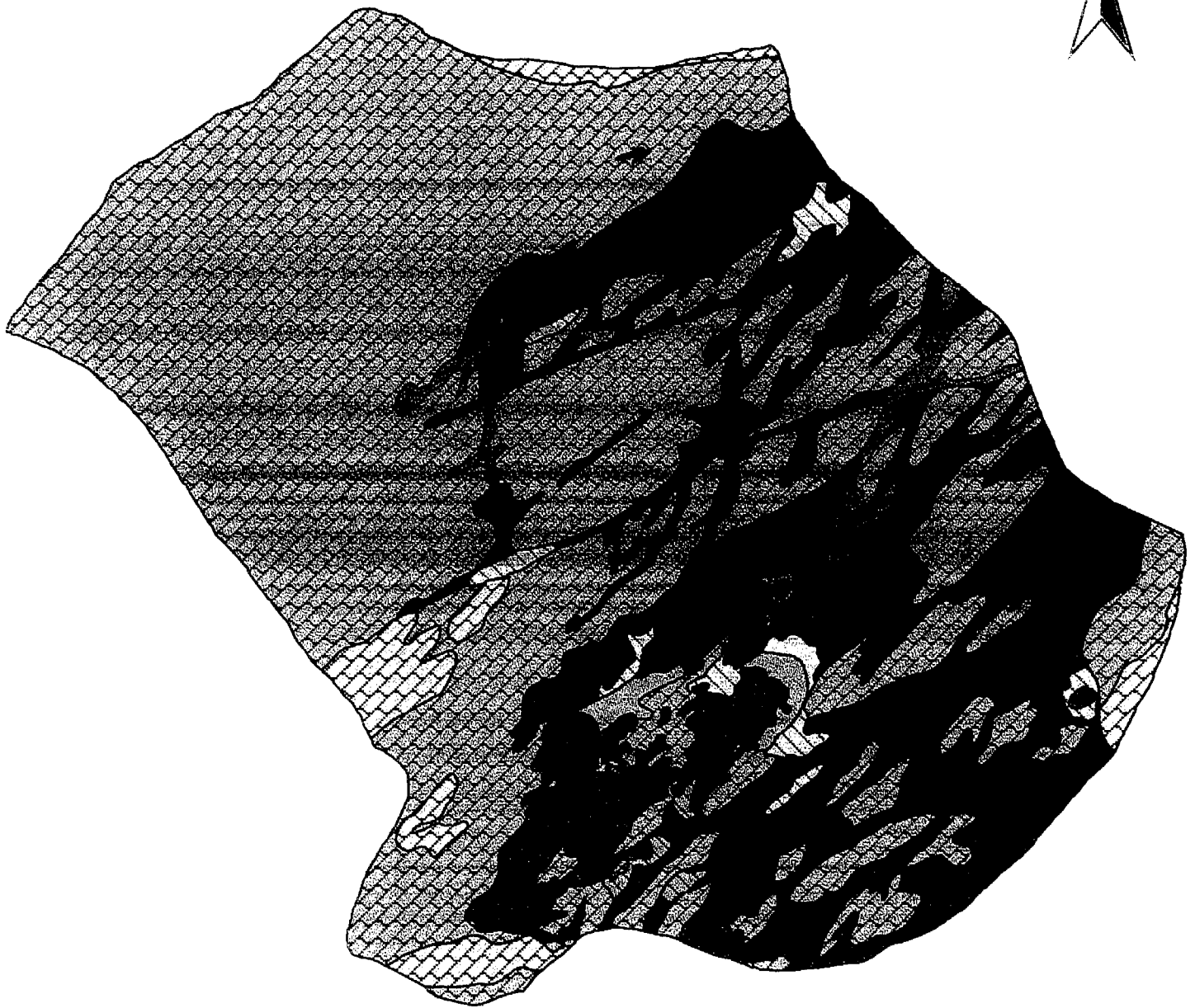
Wet Meadow Soils



WMC

Wet Meadow Soil Complex

Topaz Lake Soil Coverage

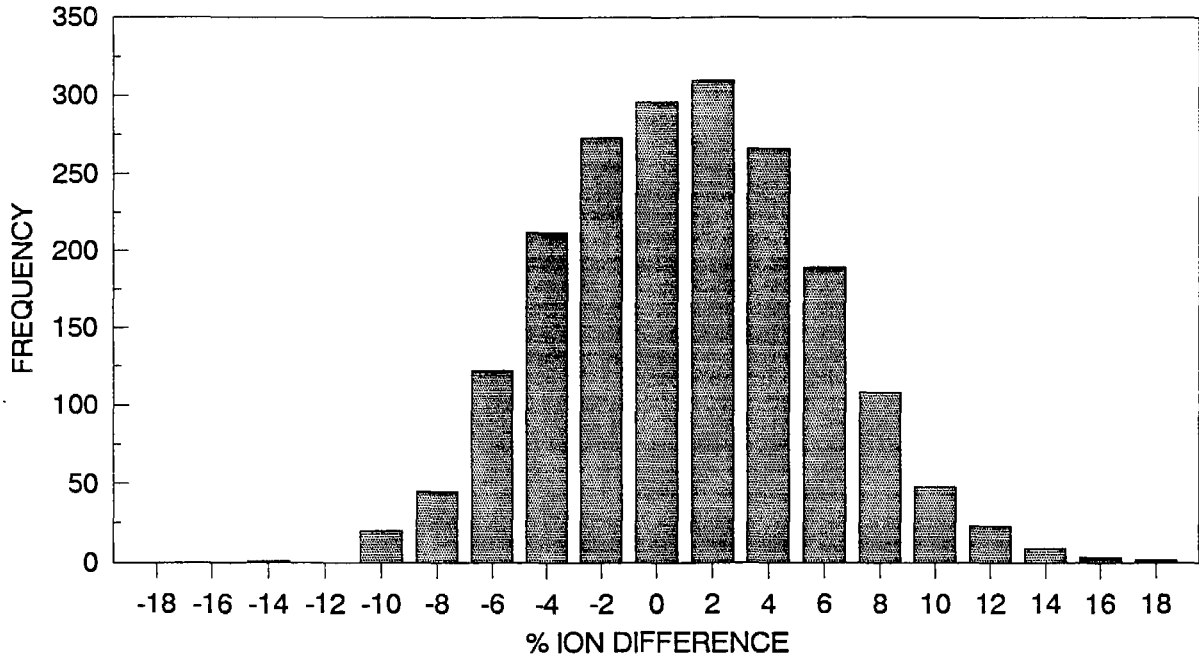


1:9279



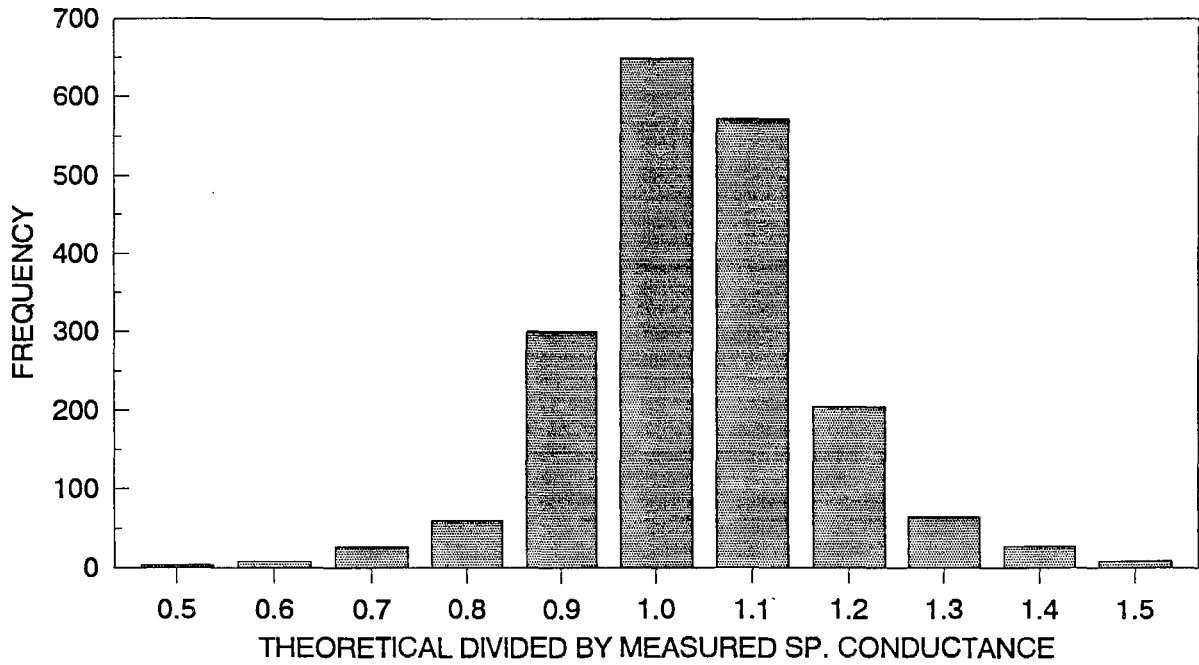
Figure I-34 cont.

LAKE AND OUTFLOW SAMPLES
1982-1994



MEAN = 0.003

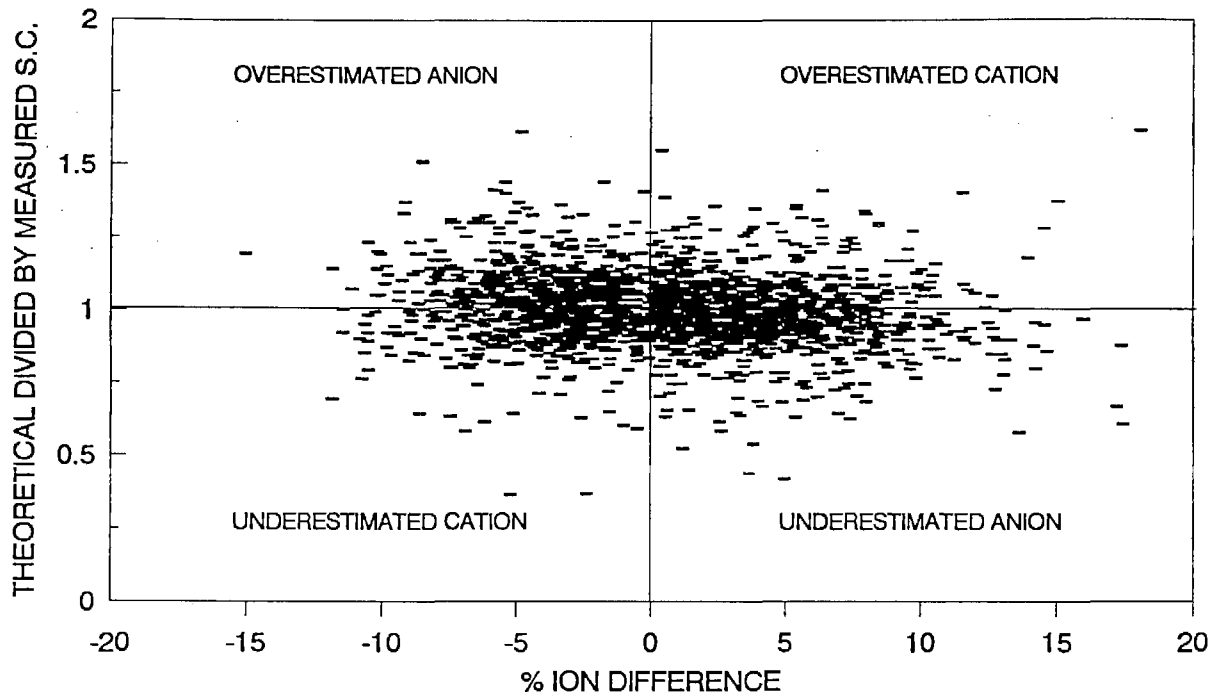
LAKE AND OUTFLOW SAMPLES
1982-1994



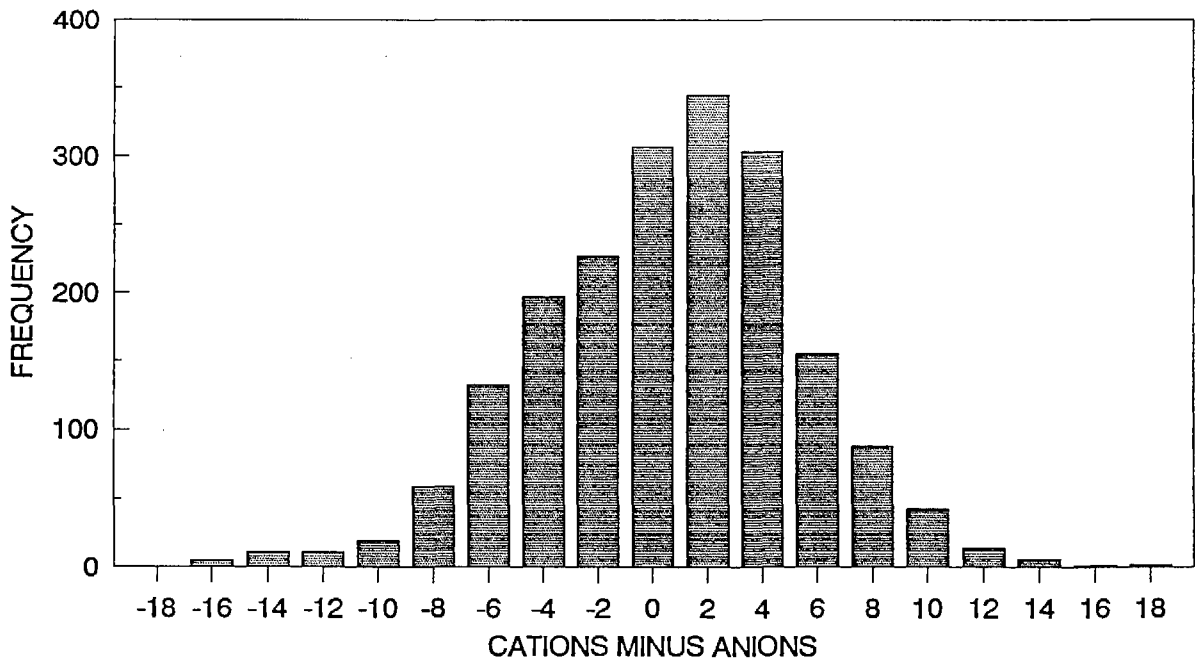
MEAN = 0.99

Figure I-35

LAKE AND OUTFLOW SAMPLES
1982-1994



LAKE AND OUTFLOW SAMPLES
1982-1994



MEAN = -0.4

Figure I-36

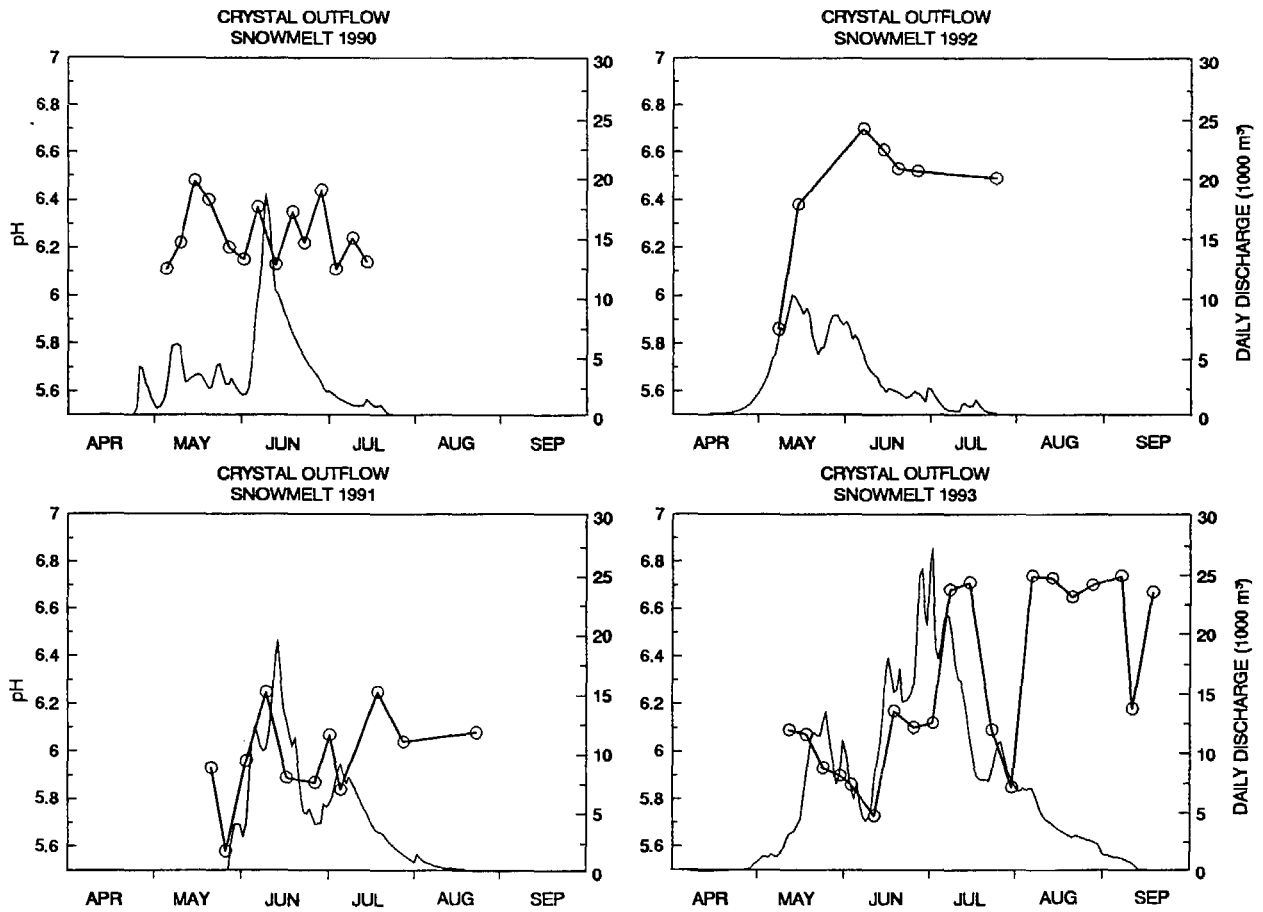


Figure I-37

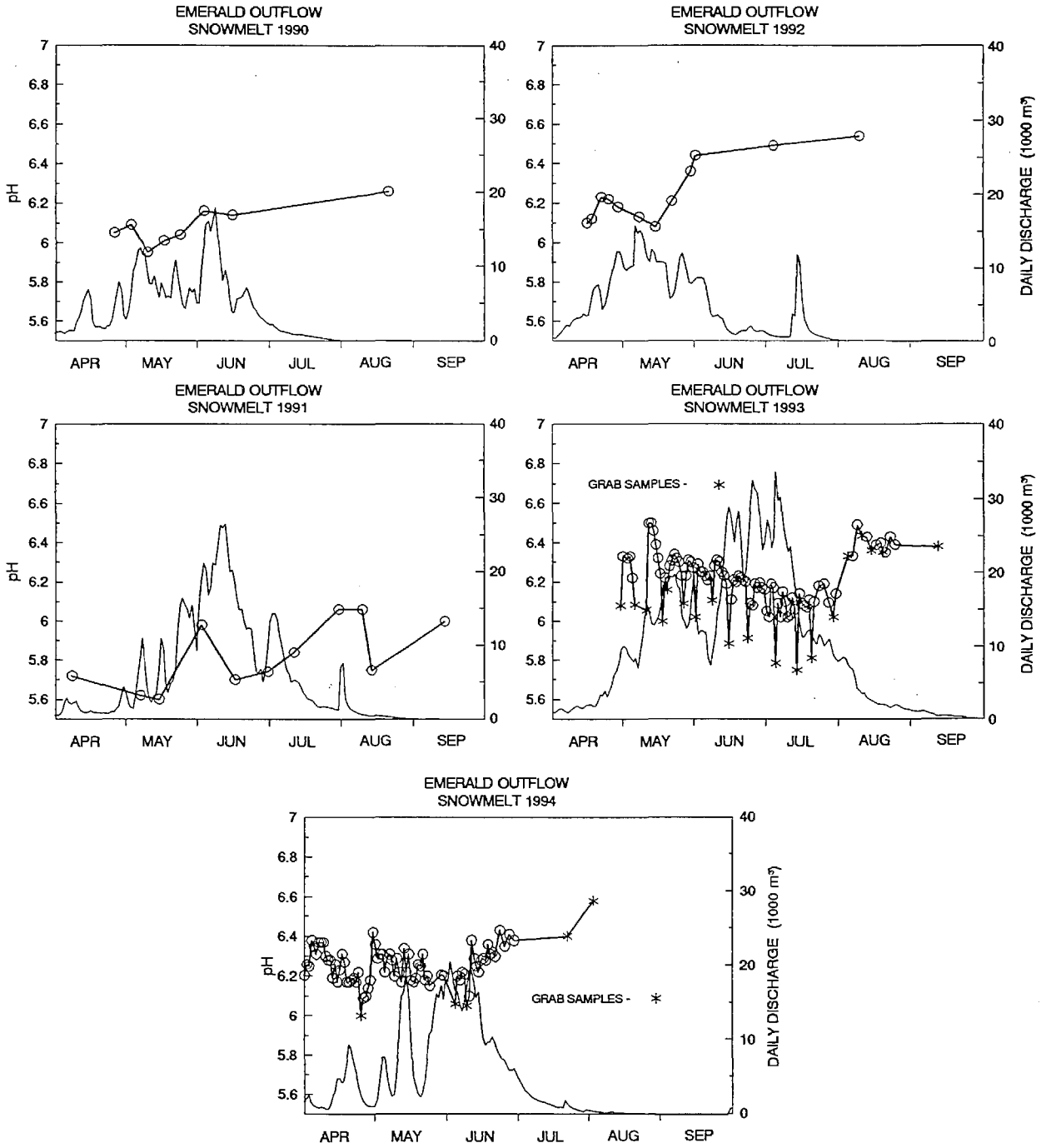


Figure I-38

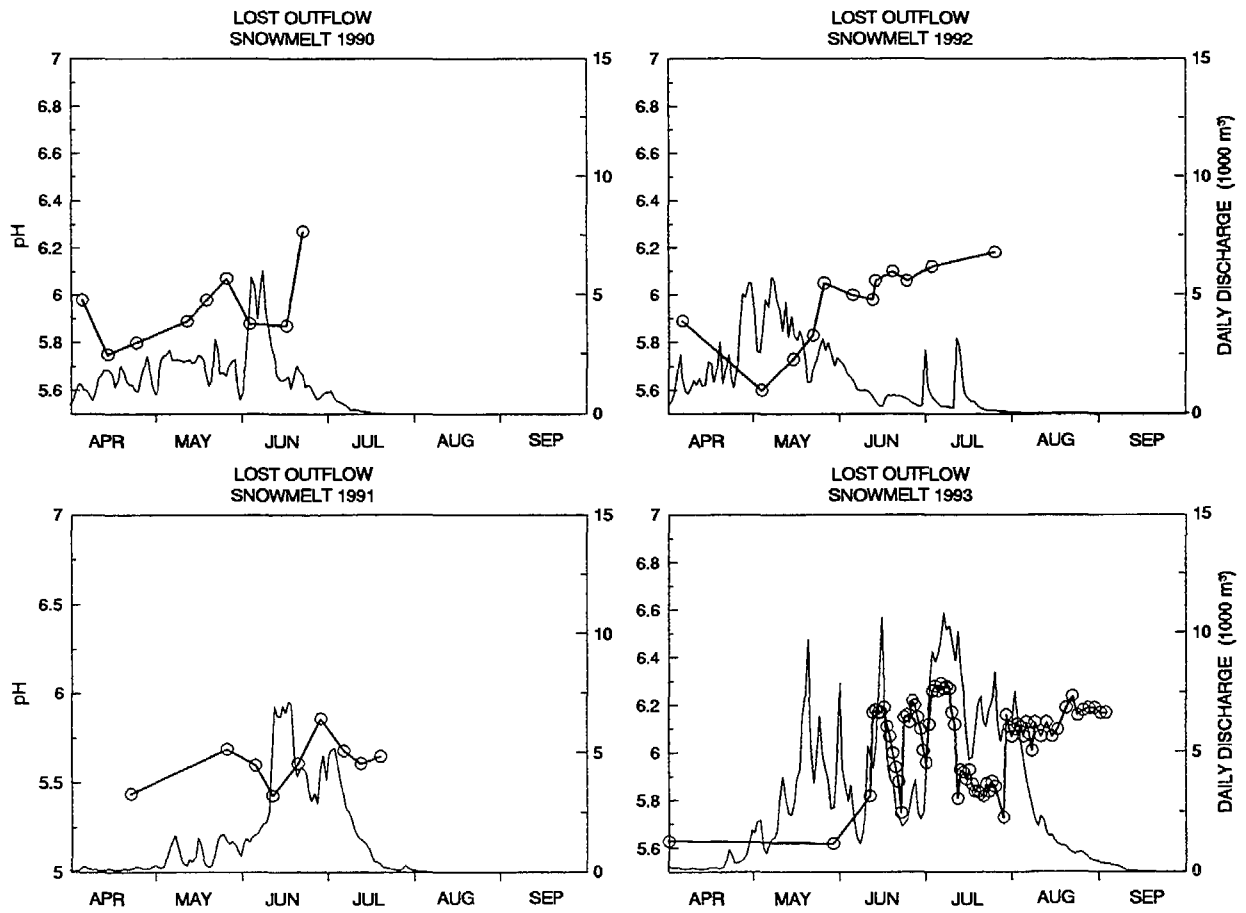
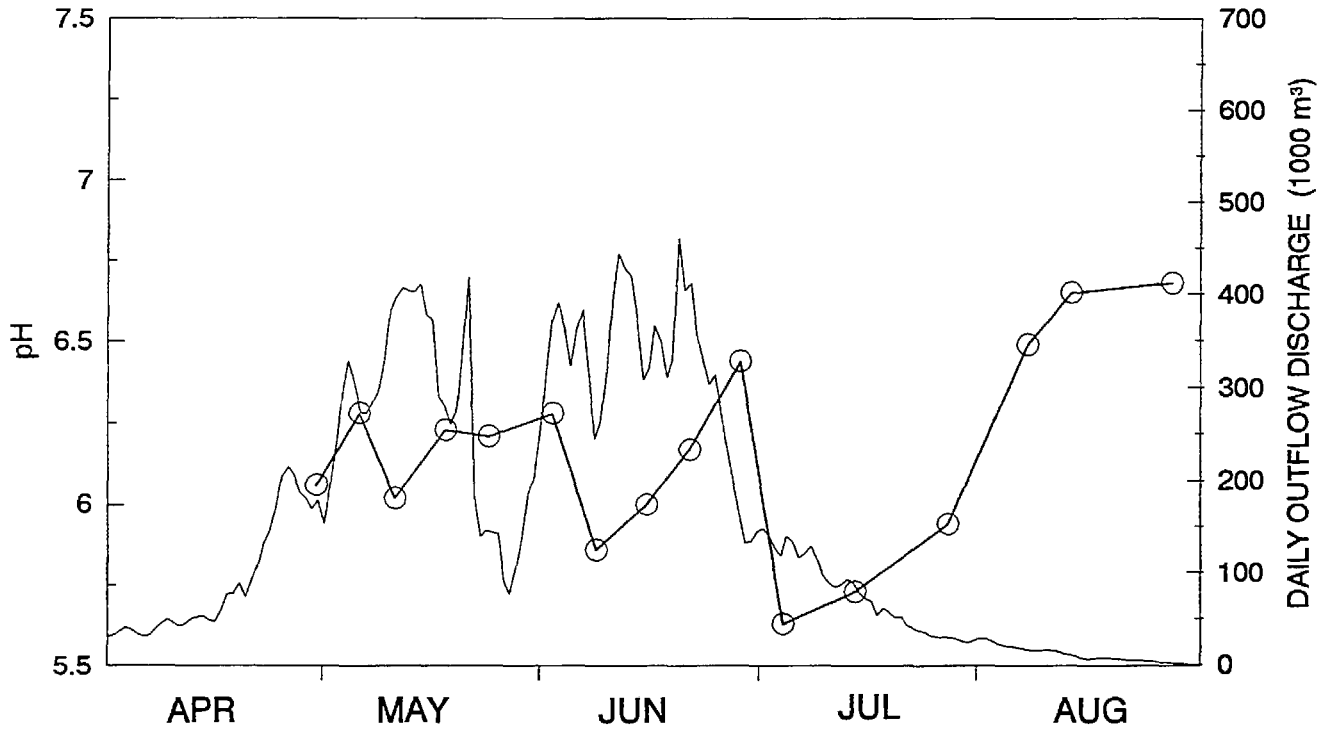


Figure I-39

MARBLE FORK OF KAWEAH
SNOWMELT 1993



MARBLE FORK OF KAWEAH
SNOWMELT 1994

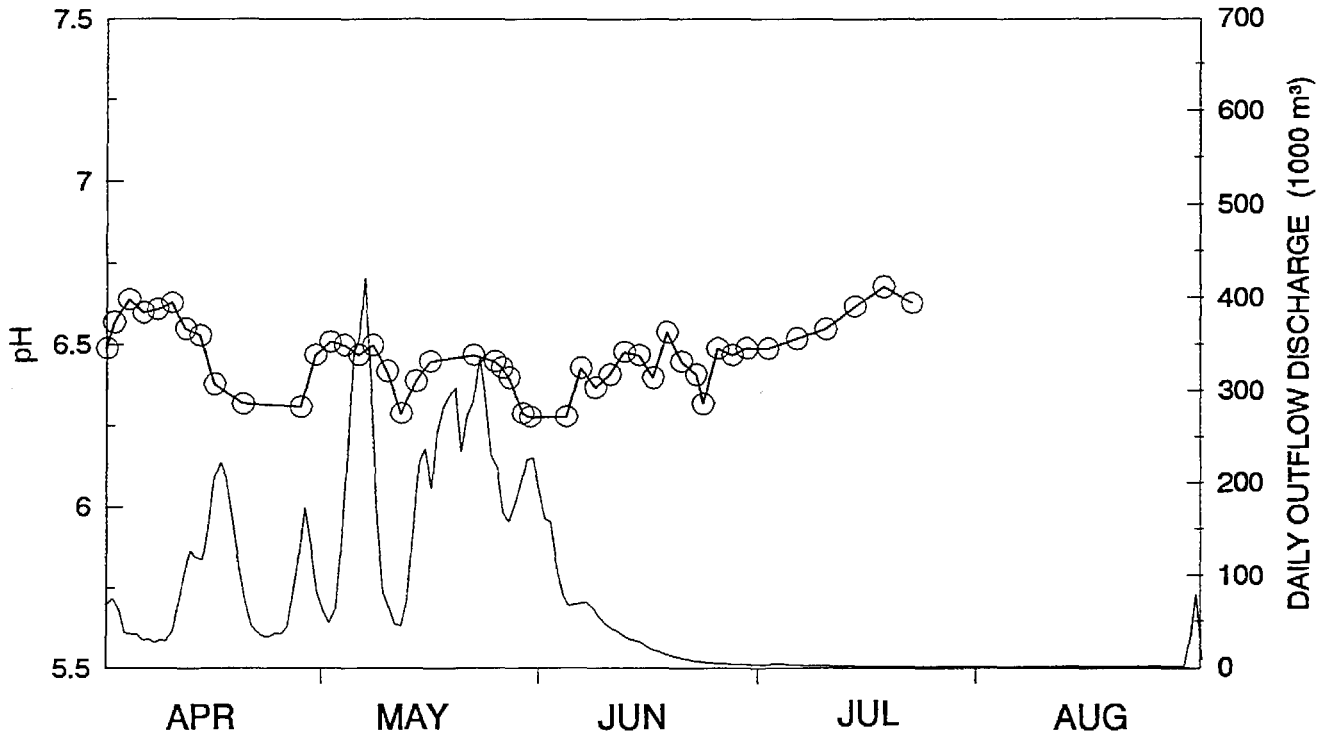


Figure I-40